

The Institute for Solid State Physics  
The University of Tokyo

# Activity Report 2023

S

S

T

# ISSP

## Activity Report 2023

Contents	Pages
Preface	1
Research Highlights	2 - 27
Joint Research Highlights	28 - 43
Progress of Facilities	44 - 51
Conferences and Workshops	52 - 61
Publications	62 - 94
Subjects of Joint Research	95 - 146



# Preface

We would like to present the annual activity report of the Institute for Solid State Physics (ISSP) for the academic year 2023. ISSP was established in 1957 as a joint usage/research institute affiliated with the University of Tokyo. In every era, we strive to lead the frontiers of condensed matter physics and materials science and contribute to the development of science and technology from a basic research perspective. In this report, we present a selection of research outcomes produced by ISSP members and other researchers from our community who participated in joint research programs.



The first section of the report includes 27 research highlights from ISSP groups, and the second section contains 14 highlights from joint research conducted by outside researchers with the assistance of ISSP members using the joint-use program. The third section details the development of the following facilities: Supercomputer Center, Neutron Science Laboratory, International MegaGauss Science Laboratory, Center of Computational Materials Science, Laser and Synchrotron Research Center, and Synchrotron Radiation Laboratory. The fourth section provides a summary of 17 conferences/workshops held by ISSP in 2023. The publication and joint-use research topics lists conclude the document.

These activities demonstrate ISSP's position as the global center of excellence in condensed matter physics and materials science and we appreciate the ongoing support and cooperation of the community to continue our activities.

October 2024

**HIROI Zenji**

Director of the Institute for Solid State Physics  
The University of Tokyo

# Research Highlights

## Metallic State of Sequence-Controlled Oligomer Conductor that Models Doped PEDOT Family

Mori and Ozaki Groups

Organic conducting materials are attracting attention because of their flexibility and solution processability, characteristics not found in inorganic semiconductors and metals which are currently the mainstream materials. Among them, conductive polymers such as doped poly(3,4-ethylenedioxythiophene) (PEDOT) are widely used organic conducting materials because of their easy solution-processability and high conductivity. However, the large molecular-weight distribution of polymers during processing causes less-crystallinity and less-accessible to atomic-level structural information and makes it difficult to elucidate the conduction mechanism and design polymers based on the crystal structure. In this study, we focused on oligomers to challenge these issues. Oligomers have high degrees of freedom in molecular design controlling three parameters (hetero-sequence, chain length, and terminal group). In addition, since oligomers possess single-crystallinity, detailed structural information can be accessible, the conduction mechanism based on crystal structures can be clarified and materials design are possibly proposed.

So far, Mori group has developed 3,4-ethylenedioxythiophene (EDOT, **O**) oligomeric salts  $n\mathbf{O}\cdot\mathbf{X}$  [1-3]. EDOT dimer salts  $2\mathbf{O}\cdot\mathbf{X}$  ( $\mathbf{X} = \text{BF}_4, \text{ClO}_4, \text{PF}_6$ ) have a relatively wide calculated bandwidth of around 1 eV [1], but are Mott insulators with 1/2-filled band structure. To deviate from the Mott insulating state and to improve the conductivity, two strategies for reducing the Coulomb repulsion ( $U_{\text{eff}}$ ) between carriers have been reported. The first is band-filling modulation from the 1/2-filled state [2]. The second strategy is the extension of conjugate length, namely elongation of oligomer length. The trimer salt  $3\mathbf{O}\cdot\text{PF}_6(\text{CH}_2\text{Cl}_2)$  has been synthesized for oligomer-length elongation, which leads the reduction of resistivity by about one order of magnitude than that of dimer salt  $2\mathbf{O}\cdot\text{PF}_6$  [3]. From the above results, the realization of high conductivity and metallic state in oligomeric organic conductors can be achieved by reducing  $U_{\text{eff}}$  through conjugate expansion, band-filling modulation, and suppressing stacking dimerization with improving dimensionality of the electronic structure.

Although conjugate-length expansion of oligomers is effective in reducing  $U_{\text{eff}}$ , it has been difficult to synthesize long-chain oligomers without introduction of solubility auxiliary groups due to instability against oxidation and solubility issues of oligomers consisting of a single EDOT unit. In this study, we utilized heterogenous units, i.e., 3,4-ethylenedithiophene / 3,4-(2',2'-dimethylpropylene-dioxy)thiophene (**S/P**), to synthesize long chain oligomers in solid state. The long-chain oligomers were designed and

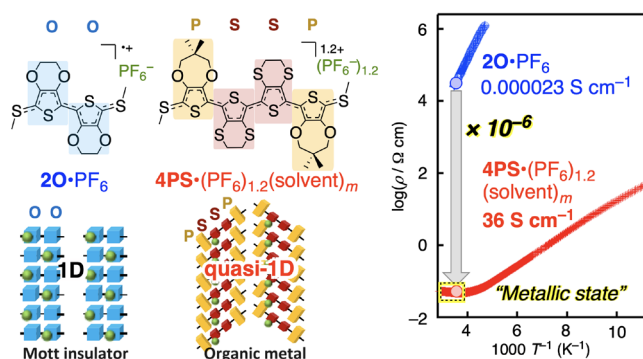


Fig. 1. Chemical structures, molecular arrangements, and temperature dependence of resistivities for doped oligomers, a Mott insulator  $2\mathbf{O}\cdot\text{PF}_6$  and metallic  $4\text{PS}\cdot(\text{PF}_6)_{1.2}(\text{solvent})_m$ , modeled the famous conductive polymer PEDOT-PSS. The resistivity of  $4\text{PS}\cdot(\text{PF}_6)_{1.2}(\text{solvent})_m$  reached  $36 \text{ S cm}^{-1}$ , which is lower by  $10^{-6}$  than that of  $2\mathbf{O}\cdot\text{PF}_6$ .

newly synthesized without the introduction of solubility-supporting groups that inhibit intermolecular interactions in solids. In the neutral 4PS (**P-S-S-P**), stability and solubility can be imparted by introducing an **S-S** structure in the center, which is a truncated and twisted structure of the conjugated system. This twisted structure is eliminated by oxidation. By introducing bulky unit **P** at both ends, dimerization is suppressed by increasing the dimensionality of the electronic structure, and band-filling modulation is achieved by creating a space where excess anions can exist (Fig. 1).

Subsequently, single crystals of  $4\text{PS}\cdot(\text{PF}_6)_{1.2}(\text{solvent})_m$  were prepared by constant-current electrochemical oxidation of tetramer donor 4PS. Band calculations show a quasi-one-dimensional band structure ( $W = 0.41 \text{ eV}$ ) with band dispersion mainly in the stacking direction, confirming the acquisition of dimensionality. The room temperature resistivity in the stacking direction is  $36 \text{ S cm}^{-1}$ , which is six orders of magnitude lower than that of  $2\mathbf{O}\cdot\text{PF}_6$ , and metallic conduction behavior is observed in the high temperature region above 280 K (Fig. 1). The IR reflection spectrum reveals a plasma edge, and the first metallic state in a single-crystalline EDOT-based oligomeric organic conductor is observed [4].

This result demonstrates that molecular arrangements and electronic functionalities in the solid state can be controlled by the type and sequence of oligomer units, which is a characteristic molecular design freedom of oligomers, and realizes a new concept in the development of conductor materials. This concept is expected to create a new trend in the development of organic conducting materials.

### References

- [1] R. Kameyama, T. Fujino, S. Dekura, M. Kawamura, T. Ozaki, and H. Mori, *Chemistry - A European Journal*, **27**, 6696 (2021).
- [2] R. Kameyama, T. Fujino, S. Dekura, S. Imajo, T. Miyamoto, H. Okamoto, and H. Mori, *J. Mater. Chem. C*, **10**, 7543 (2022).
- [3] R. Kameyama, T. Fujino, S. Dekura, and H. Mori, *Phys. Chem. Chem. Phys.* **24**, 9130(2022).

[4] K. Onozuka, T. Fujino, R. Kameyama, S. Dekura, K. Yoshimi, T. Nakamura, T. Miyamoto, T. Yamakawa, H. Okamoto, H. Sato, T. Ozaki, and H. Mori, *J. Am. Chem. Soc.*, **145**, 15152 (2023).

#### Authors

K. Onozuka, T. Fujino, R. Kameyama, S. Dekura, K. Yoshimi, T. Nakamura<sup>a</sup>, T. Miyamoto<sup>b</sup>, T. Yamakawa<sup>b</sup>, H. Okamoto<sup>b</sup>, H. Sato<sup>c</sup>, T. Ozaki, and H. Mori

<sup>a</sup>Institute for Molecular Science

<sup>b</sup>The University of Tokyo

<sup>c</sup>Rigaku Corporation

## Broken-Symmetry Quantum Hall States in Organic Dirac Fermion Systems

Osada Group

Recently, the  $\nu = 1$  quantum Hall (QH) plateau was observed in the Hall resistance of an organic conductor  $\alpha$ -(BETS)<sub>2</sub>I<sub>3</sub>, which has been known as a two-dimensional (2D) massless Dirac fermion (DF) system with finite spin-orbit coupling (SOC), under high pressure [1]. In general, the 2D DF systems show the QH effect at the LL fillings  $\nu = \pm 2, \pm 6, \pm 10, \dots$  when their Landau levels (LLs) have four-fold spin and valley degeneracy. The  $\nu = 1$  QH effect is expected only when both spin and valley degeneracy are broken in the  $N = 0$  LL. The spontaneous valley symmetry breaking is caused by the exchange interaction. We have studied the spatial order of the broken-symmetry QH states in  $\alpha$ -type organic DF systems,  $\alpha$ -(ET)<sub>2</sub>I<sub>3</sub> and  $\alpha$ -(BETS)<sub>2</sub>I<sub>3</sub>.

In order to clarify the broken-symmetry QH state of the  $\alpha$ -type organic DF system with four molecular sites (A, A', B, and C) in the unit cell, we have studied its electronic state under magnetic fields using the four-band tight-binding model including Peierls phase factors. Figure 1 shows the magnetic field dependence of the energy levels (Hofstadter butterfly) for the spinless case (no Zeeman effect and no SOC). The Chern number for each gap confirms the validity of the conventional DF picture in these materials.

The four-component envelope functions of the  $N = 0$  LL with valley degeneracy were investigated based on the Hofstadter calculation. The site-resolved probability density of the LLs is shown in Fig. 2. When the SOC is considered, it breaks the spin degeneracy of the  $N = 0$  LL and opens a spin-split gap. We can see that the degenerating  $-\mathbf{k}_0$ - and

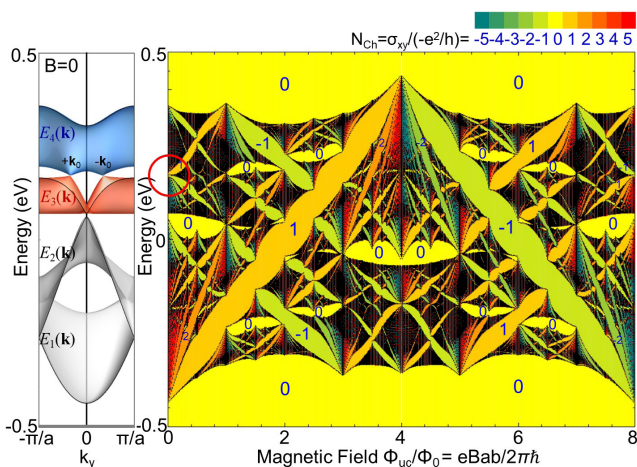


Fig. 1. (left) Band dispersion of an  $\alpha$ -type organic conductor  $\alpha$ -(ET)<sub>2</sub>I<sub>3</sub> under pressure at zero magnetic field. (right) Magnetic field dependence of energy levels (Hofstadter butterfly) in an  $\alpha$ -type organic conductor  $\alpha$ -(ET)<sub>2</sub>I<sub>3</sub> for the spinless case. The energy gap between quantized levels is colored according to the Chern number  $N_{\text{Ch}}$ .

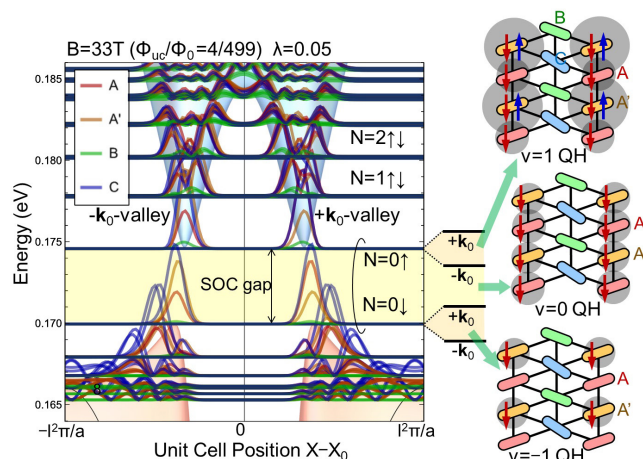


Fig. 2. (left) Probability densities of LLs under the SOC at four molecular sites of  $\alpha$ -(ET)<sub>2</sub>I<sub>3</sub> at about 33 T. Zeeman shift is not included. The zero-field gapped dispersion is also shown over them. (right) Schematics of spontaneous valley splitting of the " $N = 0 \uparrow$ " and " $N = 0 \downarrow$ " LLs and the examples of the charge and spin density patterns of the broken-symmetry  $\nu = \pm 1$  QH states when the SOC is dominant for the spin splitting.

$+\mathbf{k}_0$ -valley states have different probability weights on the A and A' molecules, which are connected by the inversion operation. This valley-site correspondence is recognized independently of the presence of the Zeeman effect or the SOC. When the spontaneous valley symmetry breaking, which is equivalent to the inversion symmetry breaking in this case, occurs due to the exchange interaction in the  $N = 0$  LLs, their valley splitting leads to the  $\nu = \pm 1$  QH effects. These broken-symmetry QH states are accompanied by the spatial modulation of charge and spin densities at A and A' sites in a unit cell, as shown in the right panel of Fig. 2.

In graphene, which is the typical 2D DF system, the broken-symmetry QH states, especially the  $\nu = 0$  QH states have been intensively studied both theoretically and experimentally. Since graphene has the ten times larger group velocity than the  $\alpha$ -type organics, the spin splitting is almost negligible compared to the LL spacing, so that we have to consider the SU(4) symmetry breaking of the  $N = 0$  LL. In fact, various QH states, the QH ferromagnet (QHF), the canted antiferromagnet, the charge order, the Kekule distortion, etc. have been proposed as the  $\nu = 0$  QH state. On the other hand, in the  $\alpha$ -type organic DF system, the spin splitting resulting from the Zeeman effect and the SOC is sufficiently large compared to the LL spacing. The  $\nu = 0$  QH state is considered to be the QHF state without spontaneous symmetry breaking (SSB) as previously pointed out [3]. Therefore, only the  $\nu = \pm 1$  QH states are accompanied by the SSB in the organic DF system.

#### References

- [1] K. Iwata, A. Koshiba, Y. Kawasugi, R. Kato, and N. Tajima, *J. Phys. Soc. Jpn.* **92**, 053701 (2023).
- [2] T. Osada, *J. Phys. Soc. Jpn.* **93**, 034711 (2024).
- [3] T. Osada, *J. Phys. Soc. Jpn.* **84**, 053704 (2015)

#### Authors

T. Osada, T. Sekine, A. Kiswandhi, and T. Taen

# Magnetic Modulation and Thickness Dependence of Second Harmonic Generation in Two-Dimensional Multiferroic $\text{CuCrP}_2\text{S}_6$

Ideue Group

Two-dimensional van der Waals multiferroics are emerging material platforms for realizing unique magnetoelectric/ magneto-optical properties and also important building blocks for functional van der Waals devices. Although they provide a new opportunity of controlling multiferroic properties in the atomic layer limit, research on few-layer multiferroic crystals is limited and the effect of thickness dependent symmetries on multiferroic properties are less explored.

In this work, we studied the symmetries and magneto-electric responses in exfoliated samples of novel van der Waals multiferroic  $\text{CuCrP}_2\text{S}_6$  by optical second harmonic generation (SHG).

$\text{CuCrP}_2\text{S}_6$  is a layered material composed of the honeycomb lattice of distorted  $\text{CrS}_6$  octahedra and  $\text{CuS}_3$  triangles and pairs of P ions inside the honeycomb, and shows the structural and magnetic phase transition at  $T_C = 190$  K and  $T_N = 32$  K, respectively. At  $T > T_C$ , it shows centrosymmetric crystal structure with  $C2/c$  space group (Fig. 1 (c)), in which Cu ions can move and ion conductor behaviors have been reported. With decreasing the temperature, movement of Cu ions start to freeze at  $T = 190$  K and is completely settle down at  $T = 145$  K, which cause the structural transition to the non-centrosymmetric phase with  $Pc$  space group (Fig. 1 (b)). Below  $T < T_N$ , A-type antiferromagnetic order develops, in which spins of  $\text{Cr}^{3+}$  align along the  $a$ -axis (Fig. 1 (a)). Because both the spatial inversion symmetry and time-reversal symmetry are broken,  $\text{CuCrP}_2\text{S}_6$  shows the magnetoelectric effect in this low-temperature phase.

Figures 1 (d)-(e) show the polarization-resolved SHG

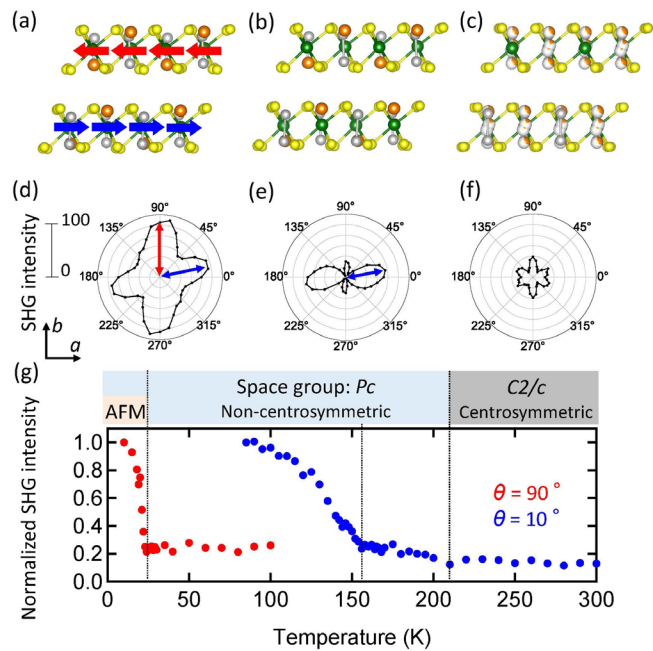


Fig. 1. (a-c) Crystal and magnetic structures of  $\text{CuCrP}_2\text{S}_6$  at  $T < T_N$  (a),  $T_N < T < T_C$  (b), and  $T_C < T$  (c). (d-f) Polarization-resolved SHG patterns in  $\text{CuCrP}_2\text{S}_6$  at  $T = 5$  K (d),  $T = 100$  K (e), and  $T = 300$  K (f). (g) Temperature dependence of SHG intensity along the polarization angle  $\theta = 10^\circ$  and  $90^\circ$ . AFM indicates antiferromagnetic phase.

patterns at  $T = 5$  K (Fig. 1 (d)),  $T = 100$  K (Fig. 1 (e)), and  $T = 300$  K (Fig. 1 (f)), respectively. At  $T = 300$  K, small SHG signal has been observed (Fig. 1 (f)), which can be attributed to the surface or electric quadrupole terms. In the intermediate temperature region, SHG intensity along the  $a$ -axis is enhanced (Fig. 1 (e)). Since inversion symmetry is broken in this phase, electric dipole term of SHG is allowed and this additional component is generated in the SHG. In the antiferromagnetic phase, SHG intensity along the  $b$ -axis is also developed (Fig. 1 (d)), which can be explained by the magnetic dipole term. In Fig. 1 (g), we plot the temperature dependence of the SHG intensity along the polarization angle  $\theta = 10^\circ$  and  $90^\circ$ . Here,  $\theta = 0^\circ$  is defined as  $a$ -axis. This temperature variation clearly indicates that SHG intensity along the  $a$ -axis ( $b$ -axis) originating from electric dipole (magnetic dipole) term reflect the structural (magnetic) phase transition in  $\text{CuCrP}_2\text{S}_6$ .

In order to understand the effect of magnetoelectric properties on SHG, we measured SHG under the magnetic field. Figure 2 (a) (red) shows the SHG pattern under the magnetic field ( $B = 1.2$  T) at  $T = 5$  K. The magnetic field is applied to the  $b$ -axis. SHG pattern changes dramatically, showing the large enhancement along the  $a$ -axis. In  $\text{CuCrP}_2\text{S}_6$ , the application of the magnetic field along the  $b$ -axis will generate the electric polarization along the  $a$ -axis due to the magnetoelectric effect. This electric polarization induced by the magnetoelectric effect is considered to generate a large SHG. Furthermore, the thickness dependence of the SHG induced by the magnetoelectric effect was investigated. Figure 2 (b) shows the SHG patterns under magnetic field ( $B = 1.2$  T) along the  $b$ -axis for samples of various thicknesses. For thicker samples, the SHG pattern is mirror symmetric with respect to the  $a$ -axis. This is because that bulk sample has the glide symmetry with respect to the  $ac$ -plane. However, as the thickness is reduced, this glide symmetry is lost, resulting in modulation of the SHG pattern. These results indicate that symmetry change by thinning can modulate the magnetoelectric effect in two-dimensional van der Waals multiferroics.

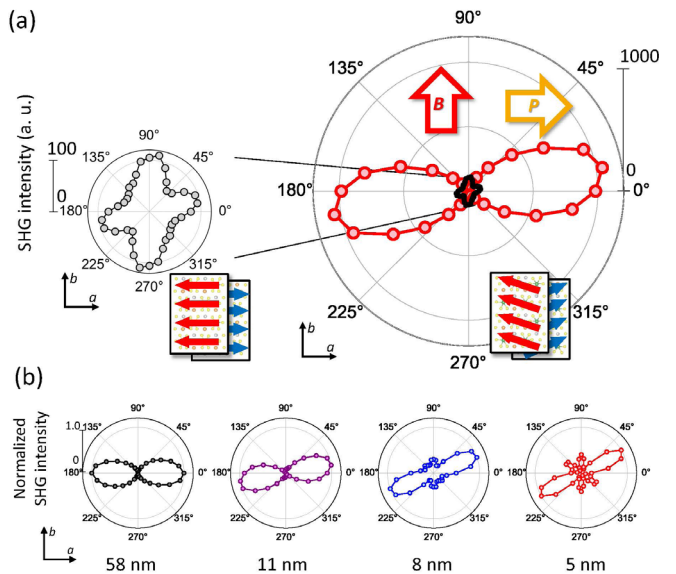


Fig. 2. (a) Polarization-resolved SHG patterns in  $\text{CuCrP}_2\text{S}_6$  under the magnetic field ( $B = 1.2$  T) along the  $b$  axis (red). SHG measured under zero magnetic field (black) is also shown. Insets show the schematics of magnetic structures and directions of the magnetic field and electric polarization induced by the magnetoelectric effect. (b) Thickness dependent SHG patterns under the magnetic field ( $B = 1.2$  T) along the  $b$ -axis. All the data were measured at  $T = 5$  K.

In summary, we have observed magnetic modulation and its thickness dependence of SHG in CuCrP<sub>2</sub>S<sub>6</sub>. This work clarifies the unique magnetoelectric properties in CuCrP<sub>2</sub>S<sub>6</sub> and also provide a new design principle of two dimensional multiferroics.

#### Reference

[1] S. Aoki, Y. Dong, Z. Wang, X. S. W. Huang, Y. M. Itahashi, N. Ogawa, T. Ideue, and Y. Iwasa, *Advanced Materials* **36**, 2312781 (2024).

#### Authors

S. Aoki<sup>a</sup>, Y. Dong<sup>a</sup>, Z. Wang<sup>b</sup>, X. S. W. Huang<sup>a</sup>, Y. M. Itahashi<sup>a</sup>, N. Ogawa<sup>b</sup>, T. Ideue<sup>a</sup>, and Y. Iwasa<sup>a,b</sup>

<sup>a</sup>The University of Tokyo

<sup>b</sup>RIKEN Center of Emergent Matter Science (CEMS)

## Chirality-Induced Phonon-Spin Conversion at an Interface

Kato Group

Chirality has been an important concept not only in high-energy physics but also in solid state physics for long time. The chirality in materials has attracted much attention after the discovery of chirality-induced spin selectivity (CISS) in DNA and peptides [1]. Indeed, the discovery of CISS has stimulated many theoretical and experimental studies on spin-related phenomena in chiral materials since it may reveal a way of developing spintronic devices without using heavy elements.

Recently, thermal phonon transport in a chiral crystal,  $\alpha$ -quartz (SiO<sub>2</sub>), induces spin current into an adjacent normal metal [2] as shown schematically in Fig. 1 (a). This observation is quite remarkable since  $\alpha$ -quartz is nonmagnetic and includes no heavy elements, which induce spin-orbit interactions. While this CISS phenomenon due to phonon transport is naively explained by angular momentum transfer from chiral motion of nuclei to spins of conduction electrons, its microscopic origin remains unanswered because of the lack of understanding of the microscopic description underlying interfacial phonon-spin conversion.

The key idea to solve this problem is reconsideration on microscopic spin-phonon coupling. Usually, it is derived from energy change of electrons induced by lattice displacement in combination with the spin-orbit interaction. In our work [3], we focused on a previously overlooked mechanism derived from the gyromagnetic effect [4], considering the coupling between local microrotations and electron

spins. The gyromagnetic effect has been studied originally as the interconversion phenomenon between spin and macroscopic mechanical rotation. We have now extended it to microscopic rotation, revealing a nontrivial spin-phonon coupling. Starting with a microscopic model for a bilayer system composed of a normal metal and chiral insulator, we derived the effective Hamiltonian describing the interfacial coupling between the electron spins and chiral phonons due to the spin-microrotation coupling. In our study, chirality is characterized by time-reversal symmetry and lack of the parity(mirror) symmetry with respect to spatial inversion. This feature is reflected by splitting of the phonon dispersion  $\omega_{q\lambda}$  as schematically shown in Fig. 1(b), where  $q$  is the wavenumber and  $\lambda = \pm$  is the chirality of phonons. When the phonons propagate along the chiral axis, their energy becomes different ( $\omega_{q+} \neq \omega_{q-}$ ) due to the chirality of the crystal. The phonon dispersion lacks the parity symmetry ( $\omega_{q\lambda} \neq \omega_{-q\lambda}$ ), while it keeps the time-reversal symmetry ( $\omega_{q\lambda} = \omega_{-q\bar{\lambda}}$ ) where  $\bar{\lambda} = \mp$  indicates the chirality opposite to  $\lambda$ .

By treating this interfacial coupling perturbatively, we formulated the spin current injected from the chiral insulator into the normal metal. The results suggest that an imbalanced distribution among the chiral phonon modes, e.g., due to a temperature gradient, drives the interfacial spin current into the normal metal. By a simplified calculation assuming the relaxation time approximation, the spin current into the normal metal is obtained as

$$I_s^z \propto \sum_{q(q_z > 0)} q_z^2 \frac{\partial}{\partial q_z} (\omega_{q+}^4 - \omega_{q-}^4) \left( -\frac{\partial_z T}{T} \right)$$

Combining this result with chiral property of phonons described above, we can show that nonzero spin current is generated across the interface only for chiral insulators.

Our findings clearly illustrate the microscopic origin of the spin current generation by chiral phonons without the spin-orbit interaction and may lead to a breakthrough in the development of spintronic devices without heavy elements.

#### References

- [1] J. Fransson, *Isr. J. Chem.* **62**, e202200046 (2022).
- [2] K. Ohe et al., *Phys. Rev. Lett.* **132**, 056302 (2024).
- [3] T. Funato, M. Matsuo, and T. Kato, *Phys. Rev. Lett.* **132**, 236201 (2024).
- [4] G. G. Scott, *Rev. Mod. Phys.* **34**, 102 (1962).

#### Authors

T. Funato<sup>a,b</sup>, M. Matsuo<sup>b,c,d</sup>, and T. Kato

<sup>a</sup>Keio University

<sup>b</sup>University of Chinese Academy of Sciences

<sup>c</sup>Japan Atomic Energy Agency

<sup>d</sup>RIKEN Center for Emergent Matter Science (CEMS)

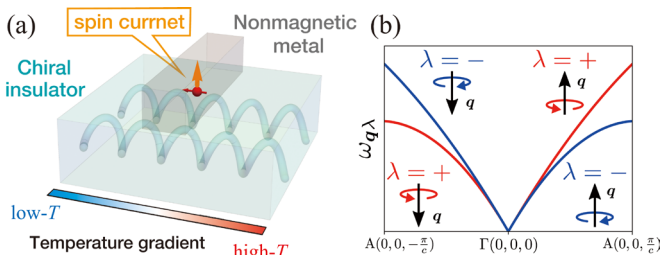


Fig. 1. (a) Schematic setup. Heat current in the chiral insulator generates a spin current in the normal metal through an interface. The generated spin current can be observed by a voltage in the NM induced by the inverse spin Hall effect. (b) Schematic illustration of energy dispersion splitting for chiral phonons. The red and blue lines represent the energy of the right-handed ( $\lambda = +$ ) and left-handed ( $\lambda = -$ ) chiral phonon modes, respectively.

## Gapless Detection of Broadband Terahertz Pulses Using a Metal Surface in Air Based on Field Induced Second-Harmonic Generation

Yoshinobu and Matsunaga Groups

Terahertz (THz) time-domain spectroscopy has been attracting much attention in many research areas such as imaging, molecular spectroscopy, and solid-state physics because the energy covers various elementary excitations in solids and molecules. Various methods for detecting the phase-locked THz electric field have been developed,

such as electro-optic (EO) sampling and photoconductive antennas. Because most of these detection methods use insulating solid crystals, phonon absorptions and the phase matching condition in the crystals largely disturb the time-domain waveform of the THz pulse, particularly between 5 and 15 THz. To realize a gapless detection for broadband THz pulses, Air-Biased Coherent Detection (ABCD) has been utilized; it is based on the interference between the THz electric field-induced second harmonic (TFISH) light from air molecules and an electric-field-induced second harmonic light by the electrodes with high bias voltage above 1 kV. Recently, to reduce the voltage value, Solid-State-Biased Coherent Detection (SSBCD) using insulators such as silica or diamond instead of air was developed; however, it still requires sub-kV bias and microfabrication processes. Therefore, a much simpler geometry for gapless broadband THz pulse detection is highly demanded.

We have developed a new detection method, termed as Air-Metal Coherent Detection (AMCD), where we utilize a metal surface instead of the bias voltage in ABCD. The schematic of our experimental setup is depicted in Fig. 1(a). Second-harmonic generation (SHG) light from a Pt surface in air under broadband THz pulse irradiation was investigated. An output of the Ti:sapphire regenerative amplifier was divided into two beams for THz generation and for a near-infrared pulse as a fundamental light of SHG lights. Here, the THz pulse was generated from the two-color laser-induced air plasma filamentation, and we confirmed its broad bandwidth up to at least several tens of THz by using mid-infrared-sensitive power meters. Both P-polarized pulses were collinearly focused on the Pt surface in air, and THz pulse-modulated SHG intensity  $\Delta I_{2\omega}$  was measured by a photomultiplier tube. The time profile of  $\Delta I_{2\omega}$  and the amplitude spectrum obtained by fast Fourier transform of the time trace were shown in Figs. 1(b) and 1(c), respectively. For comparison, the spectrum evaluated by using a conventional EO sampling method with a GaP crystal is also added in Fig. 1(c). The spectrum evaluated by EO sampling (red) was restricted only below 7 THz due to the phonon resonances and phase-matching conditions in the GaP crystal. By clear contrast, the spectrum obtained from the time trace of  $\Delta I_{2\omega}$  measurement (blue) detected the broadband frequency components without gaps. Because the THz field inside the metal is sufficiently weak, the TFISH generation in the metal

is negligible. As a result, the effect of phonons is absent for the  $\Delta I_{2\omega}$  measurements, enabling a gapless detection of broadband THz pulses in the region of 0.2–20 THz as shown in Fig. 1(c). We also confirmed that this method works well even with a gold mirror instead of the Pt surface.

In this study, a new gapless detection method was developed for broadband THz pulses by using a metal surface in air without any high voltage electrodes. The present AMCD method does not suffer from phonons or phase matching in insulating solid-state optics and does not require any power supply, bias voltage, or fabrication process, but offers a simple and gapless sampling method for broadband THz pulses.

#### References

S. Tanaka, Y. Murotani, S. A. Sato, T. Fujimoto, T. Matsuda, N. Kanda, R. Matsunaga, and J. Yoshinobu, *Appl. Phys. Lett.*, **122**, 251101 (2023).

#### Authors

S. Tanaka, Y. Murotani, S. A. Sato<sup>a</sup>, T. Fujimoto, T. Matsuda, N. Kanda, R. Matsunaga, and J. Yoshinobu  
<sup>a</sup>Tsukuba University

## Fabrication of Orientation-Controlled Orthoferrite Films

Lippmaa and Nakatsuji Groups

YFeO<sub>3</sub> is an orthorhombic antiferromagnet with a distorted pseudocubic perovskite structure. The spins are slightly canted, giving the material a small spontaneous residual magnetic moment. Single crystals of YFeO<sub>3</sub> have been shown to have a magnon decay length of several hundred nm. As the spin ordering temperature is about 640 K and YFeO<sub>3</sub> has no spin-flop transitions below the ordering temperature, it can be a useful material for designing room-temperature antiferromagnetic spintronic devices. The choice of suitable antiferromagnets is small, with most experimental work focusing on hematite  $\alpha$ -Fe<sub>2</sub>O<sub>3</sub>. However, device design generally requires thin films and it is known for  $\alpha$ -Fe<sub>2</sub>O<sub>3</sub> that the magnon decay length in a thin film is much shorter than in a single crystal. In Fe<sub>2</sub>O<sub>3</sub>, this reduction of the decay length may be related to the small grain size and high defect density, which is an intrinsic problem with iron oxides due to the existence of multiple crystalline phases with the same nominal film composition. Compared to hematite, the orthoferrite phase is more stable and it should thus be possible to fabricate films with single-crystal-like quality, at least in terms of the magnetic structure. In particular, large magnetic domains are desirable with few grain boundaries. However, when orthorhombic films are grown on common cubic substrates, such as SrTiO<sub>3</sub>, the film would spontaneously form various twinned structures due to the unequal lengths of the pseudocubic in-plane axes of the film. We have successfully grown YFeO<sub>3</sub> films with large magnetic domains and a well-defined in-plane orientation of the crystallographic axes by using an orthorhombic NdGaO<sub>3</sub> substrate. The (110) surface of a NdGaO<sub>3</sub> crystal has a tetragonal in-plane unit cell, which can work as a growth template for a fully-strained epitaxial film, ensuring that the orthorhombic *c*-axis is in the plane of the film and that there are no 90° in-plane twin boundaries. To achieve such growth, the substrate has to have an atomically flat surface. The substrates were therefore annealed in air at 1000°C to

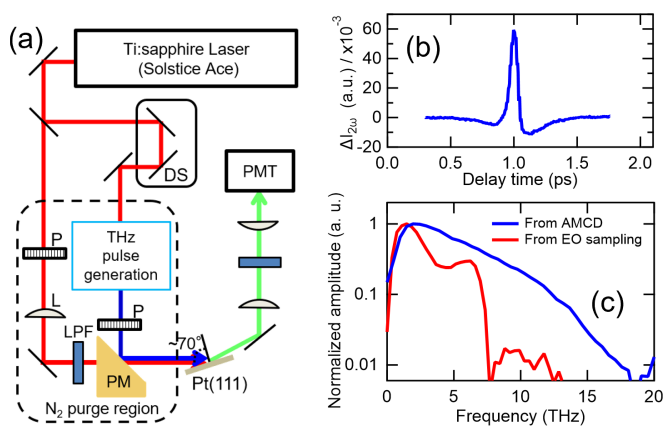


Fig. 1 (a) Schematic illustration of the experimental setup. (b) The time profile of  $\Delta I_{2\omega}$  measured for the Pt single crystal using the broadband THz pulse. (c) The blue line corresponds to the amplitude spectra obtained by fast Fourier transformation of the time trace of (b). As a reference, the amplitude spectrum detected by the EO sampling method with the GaP crystal was added as the red line.

# Coupled Electron-Proton Transfer Dynamics in Electrochemical Media

Sugino Group

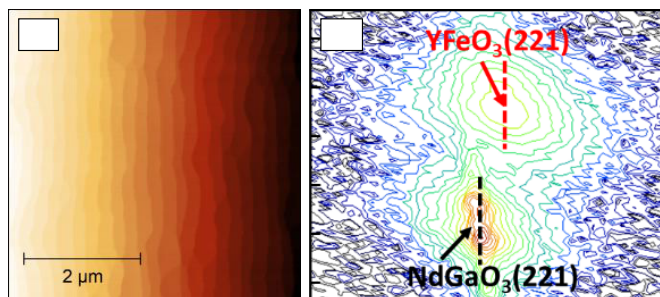


Fig. 1. Atomic force microscope image of a YFeO<sub>3</sub> film surface. A defect-free step-and-terrace surface was observed over large length scales. X-ray reciprocal space mapping of a YFeO<sub>3</sub> film on a NdGaO<sub>3</sub> substrate shows that the film does not contain twin domains.

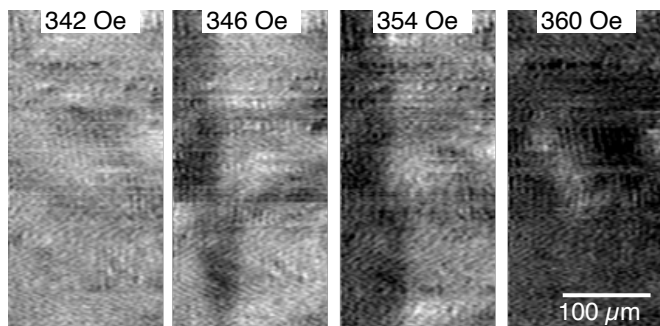


Fig. 2. MOKE imaging of the direction switching of the weak residual magnetic moment of a YFeO<sub>3</sub> film during a gradual increase of an external magnetic field. The magnetic domain size appears to be larger than 100 μm.

obtain a step-and-terrace NdGaO<sub>3</sub>(110) surface. The YFeO<sub>3</sub> films grown by pulsed laser deposition also exhibited a clean long-range step-and-terrace morphology (Fig. 1a), indicating that the films did not have 90° twin grain boundaries. The structural quality was confirmed through x-ray reciprocal space mapping (Fig. 1b), which showed that the films did not have a multi-domain structure. The magnetic ordering temperature of the films was verified to be close to 640 K by measuring the small residual ferromagnetic component of the canted spin structure. Hysteresis loops associated with the switching of the spontaneous residual magnetic moment were only observed when the magnetic field was applied in the plane of the film along the YFeO<sub>3</sub> *c*-axis. The magnetic domain size was analyzed by magneto-optic Kerr rotation (MOKE) imaging. By slowly increasing the magnitude of the applied field, a gradual domain formation and domain wall movement could be observed in a narrow field range of 342 to 360 Oe (Fig. 2). The MOKE imaging showed that the magnetic domain size was on the scale of 100 μm or more. The magnon decay length in single crystals has been shown to be on the order of 0.5 μm, which means that for the purpose of device design, the films can be considered to have a single-domain structure. The well-ordered flat surface of the films provides a good starting point for constructing devices with very well defined interfaces. The YFeO<sub>3</sub> films can be easily combined with various oxide ferromagnets, such as (La,Sr)MnO<sub>3</sub> or metal layers.

## Reference

[1] C. Wang, M. Lippmaa, and S. Nakatsuji, *J. Appl. Phys.* **135**, 113901 (2024).

## Authors

C. Wang, M. Lippmaa, and S. Nakatsuji

Protons couple with water molecules in solution to form a hydronium ion (H<sub>3</sub>O<sup>+</sup>(aq)), which is sometimes regarded as a small polaron. At low voltages, instead, they prefer to combine with an electron near the electrode and are adsorbed thereon as a neutral species (H<sup>0</sup>(ads)). This is a prototypical electrochemical reaction called Volmer step. This change in the proton state is called coupled electron-proton transfer dynamics; its microscopic elucidation, however, has long been a challenge of theoreticians. A few decades ago, Schmickler modeled it by adding solvent phonons coupled harmonically with protons to a surface adsorption model called Newns-Anderson model. The resulting Newns-Anderson-Schmickler model, consisting of a hydrogen atom, electrons in electrode, and solution, has been regarded as one of the standard models for the electrochemical step.

It is found that the terms added to consider the solvation effect can be apparently removed by applying the Lang-Firsov transformation, often used in studying polaron dynamics. This technique allows us to apply the non-equilibrium approaches so far developed for the Newns-Anderson model. Based on this recognition, we provided an analytical expression for the Volmer dynamics and revealed the non-adiabaticity caused by the moving hydrated protons, i.e. the deviation from the adiabatic Born-Oppenheimer (BO) state [1]. This is an extension of our previous work on the Volmer dynamics based on first-principles BO dynamic simulation [2] although the model used therein has been greatly simplified in the present Schmickler model. Importantly, however, it is possible for the model to consider the energy dissipation channels; (a) electron-hole excitation in the electrode or the electronic friction channel, and (b) vibrational excitation in the solvents. The former channel opens mainly when the proton affinity level aligns with the Fermi level and is increasingly important as the velocity of the proton increases, while the latter channel is constantly active under the conditions we have assumed. Our solution to

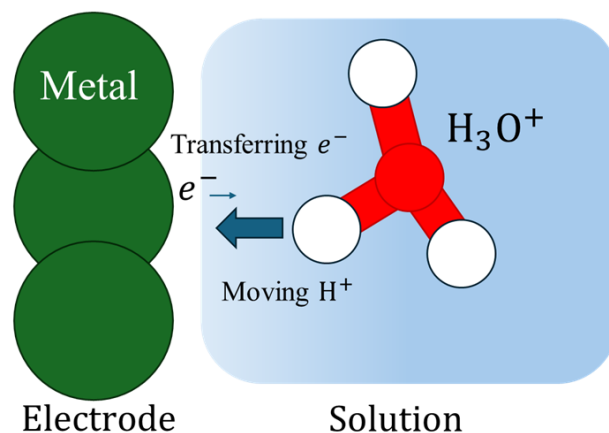


Fig. 1. Electrode-solution interface. Green circles represent the atoms constituting the electrode, and the red and white circles represent, respectively, the oxygen and hydrogen atoms constituting the hydronium ion. The hydrogen atom nearest to the electrode is moving towards the electrode, and this motion is coupled to transfer of an electron in the electrode. The Newns-Anderson-Schmickler model represent the coupled proton-electron transfer dynamics, for which an analytical solution has been provided in our research.

the time-dependent News-Anderson-Schmickler model can be used to explain qualitatively the experiments regarding how the reaction rate depends on the electrode potential. The solution can also be used to show how the kinetic energy of the hydrated protons is dissipated into the dissipation channels, which should be important for the chemical-to-electric energy conversion efficiency. As far as we know, the two channels have not been studied together although each of them has been studied separately; the electrode problem thus provides a novel target for non-equilibrium statistical physicists.

Our simulation is currently based on assumed trajectories of the proton although the trajectory can be assumed only for fast-moving protons; in the present case, however, protons are moderately accelerated in the electric double layer, possibly on the order of several tens of meV. In the future step, therefore, the trajectory will be determined by solving the proton's equation of motion considering self-consistently the two dissipation channels as described above. We will consider in addition the quantum effect of protons, such as tunneling and interference, that may play a role as discussed in the literature. Those are the target of our long-term project "Establishing a Quantum Theory of Electrodes". Our study has enabled us to take an important step in this direction.

#### References

- [1] E. F. Arguelles and O. Sugino, *J. Chem. Phys.* **160**, 144102 (2024).  
 [2] M. Otani, I. Hamada, O. Sugino, Y. Morikawa, Y. Okamoto, and T. Ikeshoji, *J. Phys. Soc. Jpn.* **77**, 024802 (2008).

#### Authors

E. F. Arguelles and O. Sugino

## Extremely Large Magnetoresistance in Multipolar Kondo System $\text{PrTi}_2\text{Al}_{20}$

Nakatsuji Group

The multipolar Kondo systems  $\text{Pr}(\text{Ti}, \text{V})_2\text{Al}_{20}$  provide unprecedented opportunities to design new quantum phases and functionalities beyond the spin-only paradigm. They host a nonmagnetic crystal-electric-field ground state in which the magnetic dipole moment is absent while higher-order quadrupolar and octopolar moments are active; the substantial Kondo entanglement between these multipolar moments and the conduction electron sea serves as the root for strange

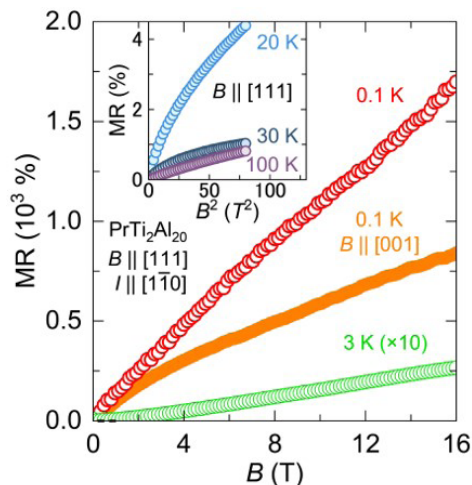


Fig. 1. Transverse magnetoresistance (MR) curves of  $\text{PrTi}_2\text{Al}_{20}$  obtained at various temperatures. While conventional  $B^2$  behavior is observed at high  $T$  (inset), unsaturated quasi linear MR is observed at low  $T$  up to 16 T (main panel).

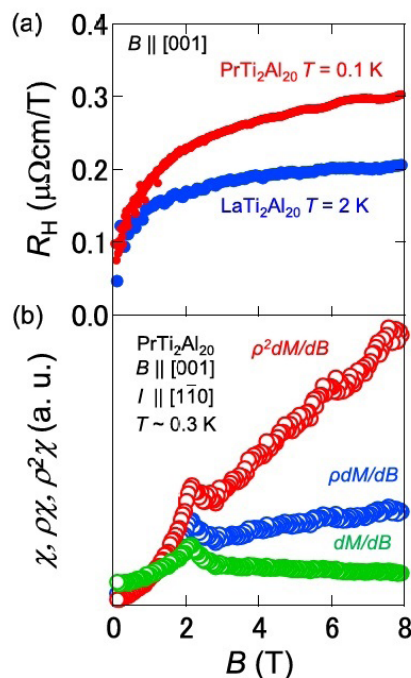


Fig. 2. Low- $T$  Hall coefficient  $R_H$  (a) and  $\chi$ ,  $\chi\rho$  and  $\chi\rho^2$  (b) as a function of  $B$ .  $R_H$  cannot be scaled by either  $\chi$ ,  $\chi\rho$  and  $\chi\rho^2$ , indicating the anomalous Hall component associated with the magnetization is negligibly small.

metal behavior, quantum criticality, and exotic superconductivity observed in these systems. Here, we discover extremely large magnetoresistance (XMR) exceeding  $\sim 10^3\%$  in the pure ferroquadrupolar ordered state of  $\text{PrTi}_2\text{Al}_{20}$  and identify the key role of Fermi surface topology in generating this XMR. Large magnetoresistance lays the foundation for various technological applications; a well-known example is the magnetic field sensor based on giant magnetoresistance (GMR). Our findings demonstrate that a multipolar ordered state, without involving spin degrees of freedom, can realize large magnetoresistance. These findings provide essential insights that may facilitate revealing unified mechanisms behind large magnetotransport phenomena and thereby widen the material platforms for their applications.

#### Reference

- [1] T. Isomae, A. Sakai, M. Fu, T. Taniguchi, M. Takigawa, and S. Nakatsuji, *Phys. Rev. Research* **6**, 013009 (2024).

#### Authors

T. Isomae, A. Sakai<sup>a</sup>, M. Fu<sup>a</sup>, T. Taniguchi<sup>b</sup>, M. Takigawa, and S. Nakatsuji

<sup>a</sup>The University of Tokyo

<sup>b</sup>Institute for Materials Research, Tohoku University

## Giant Anomalous Nernst Effect in Polycrystalline Thin Films of $\text{Co}_2\text{MnGa}$

Nakatsuji Group

$\text{Co}_2\text{MnGa}$  is a Heusler compound that exhibits the largest anomalous Nernst effect at room temperature. This effect arises from its topological band structure, namely, the Weyl cone. Previously, the large anomalous Nernst effects in thin films of  $\text{Co}_2\text{MnGa}$  were obtained via epitaxial growth using a single-crystal substrate or an interface with an easily crystallized material such as AlN. Here, by improving the deposition process, we have succeeded in obtaining the anomalous Nernst effect of  $-5.4 \mu\text{V/K}$  in  $\text{Co}_2\text{MnGa}$



# X-Ray Magnetic Circular Dichroism Study of Enhanced Interfacial Perpendicular Magnetic Anisotropy in LiF-Inserted Fe/MgO Interface

Miwa Group

Fe(CoB)/MgO interfaces are crucial for spintronics applications such as magnetoresistive random access memories (MRAMs) due to their giant tunneling magnetoresistance (TMR) effect and strong interfacial perpendicular magnetic anisotropy (PMA). Strong PMA is key to shrinking the size of magnetic cells while keeping thermal stability intact, and improving PMA is one of the most significant challenges in MRAM development.

Recently, Nozaki *et al.* demonstrated that inserting an ultrathin LiF layer between the MgO and Fe layers significantly boosts interfacial PMA while preserving or even enhancing TMR ratio [1]. Although this discovery is promising, the cause of the enhancement remains elusive, and clarifying its origin is of great importance for further improvements in PMA. For such purpose, we conduct x-ray magnetic circular dichroism (XMCD) measurements on Fe/LiF/MgO multilayers [2].

The Fe/LiF/MgO structures were grown on single-crystalline MgO (001) substrates using molecular beam epitaxy. The sample structure is illustrated in Fig. 1(a). XMCD measurements were conducted at the BL-16A beamline in the Photon Factory.

Figure 1(b) presents an out-of-plane magnetic hysteresis loop measured with the magneto-optical Kerr effect. The loops are perfectly square, indicating that the Fe/LiF/MgO multilayers exhibit PMA. The coercive field becomes larger with LiF thickness up to 0.4 nm but slightly declines when the LiF layer reaches 0.6 nm, in agreement with the previous study [1]. This suggests that PMA energy increases with LiF insertion.

To uncover the origin of the enhanced PMA, we measured XMCD spectra with both out-of-plane and nearly in-plane (70°) magnetic fields. Figure 2(a) compares the XMCD spectra for samples without LiF and with a 0.4-nm-thick LiF layer. The XMCD spectra are normalized to the Fe  $L_2$ -edge maxima. The XMCD spectra consists of broad single peak for each  $L_3$  and  $L_2$  edge, confirming the absence of Fe oxides or fluorides at the interface. The intensity of the XMCD is stronger for the out-of-plane magnetic fields than for the in-plane magnetic fields. This intensity anisotropy becomes more pronounced with LiF insertion, indicating that the orbital magnetic moment becomes more anisotropic.

To be more quantitative, we estimated spin and orbital magnetic moments using XMCD sum rules. Figure 2(b)

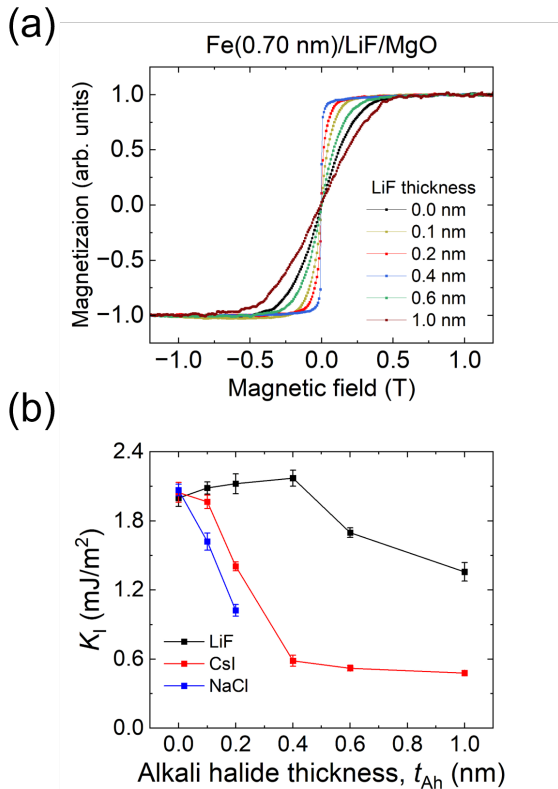


Fig. 2. (a) LiF thickness dependence of the normalized magnetization curves for the Fe 0.7-nm region. (b) Interfacial magnetic anisotropy energies as a function of alkali halide thickness for the LiF, CsI, and NaCl samples.

anisotropy energies as a function of alkali halide thickness for the LiF, CsI, and NaCl samples are shown in Fig. 2(b). For the LiF sample, the  $K_1$  slightly increases in the 0–0.4-nm regions but starts to decrease in the 0.4–1.0-nm regions. It is suggested that the high electronegativity of F is beneficial for interfacial PMA probably because of the weaker Fe-F hybridization and stronger electron localization at the interface. For the CsI and NaCl cases, the interfacial PMA decreases monotonically with CsI or NaCl thickness. Despite their strong spin-orbit interactions, the finite magnetic dead layers suggest an intermixing of the alkali halide and Fe layers, which contributes to the interfacial PMA degradation.

In summary, we studied the effect of alkali halide insertions on magnetic anisotropy at the Fe/MgO interface, and our study shall serve as a guiding principle for designing a new dielectric layer to achieve stronger PMA in ultrathin Fe films.

## References

- [1] T. Nozaki, T. Nozaki, T. Yamamoto, M. Konoto, A. Sugihara, K. Yakushiji, H. Kubota, A. Fukushima, and S. Yuasa, *NPG Asia Mater.* **14**, 5 (2022).
- [2] S. Sakamoto, T. Nozaki, S. Yuasa, K. Amemiya, and S. Miwa, *Phys. Rev. B* **106**, 174410 (2022).
- [3] J. Chen, S. Sakamoto, H. Kosaki, and S. Miwa, *Phys. Rev. B* **107**, 094420 (2023).

## Authors

J. Chen, S. Sakamoto, H. Kosaki, and S. Miwa

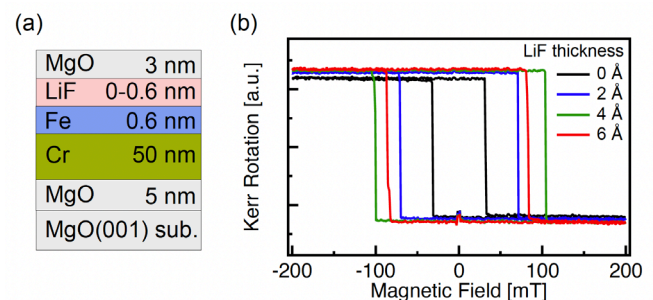


Fig. 1. (a) Schematic sample structure. (b) Hysteresis curves measured using magneto-optical Kerr effect.

# Influence of Alkali-Fluoride Insertion Layers on the Perpendicular Magnetic Anisotropy at the Fe/MgO Interface

Miwa Group

Fe/MgO-based systems have attracted significant attention because of their strong perpendicular magnetic anisotropy (PMA) and giant tunneling magnetoresistance (TMR). Recently, it was reported that an ultrathin LiF layer insertion at the Fe/MgO interface could enhance the interfacial PMA while maintaining the TMR ratio [1, 2], and the following study showed that inserting other alkali-halide layers, such as NaCl and CsI, degrades the interfacial PMA [3]. Such findings suggest the importance of the strong electronegativity of fluorine atoms. However, since LiF has better lattice matching with Fe than MgO ( $a_{\text{LiF}} = 0.403$  nm,  $a_{\text{MgO}} = 0.421$  nm,  $\sqrt{2}a_{\text{Fe}} = 0.405$  nm), it remains unclear whether the presence of fluorine atoms on the Fe atoms or the improved lattice matching between Fe and LiF layers contributes more significantly to the PMA enhancement. In this study, we insert an ultrathin NaF layer with suboptimal lattice matching to Fe at the Fe/MgO interface and characterize the PMA energy to disentangle the effects of strong electronegativity and lattice matching [4]. NaF, LiF, and MgO share the same NaCl-type crystal structure with lattice constants of 0.462, 0.403, and 0.421 nm, respectively.

The schematic of the multilayer structure is shown in Fig. 1(a). The multilayers consist of single-crystalline MgO (001) substrate/MgO (5 nm)/V (30 nm)/Fe (0.3–0.9 nm)/NaF (0–1 nm)/MgO (5 nm)/SiO<sub>2</sub> (5 nm). We performed reflection high-energy electron diffraction (RHEED) measurements to examine the surface crystallinity. The RHEED images of the 0.6-nm-thick Fe layer,

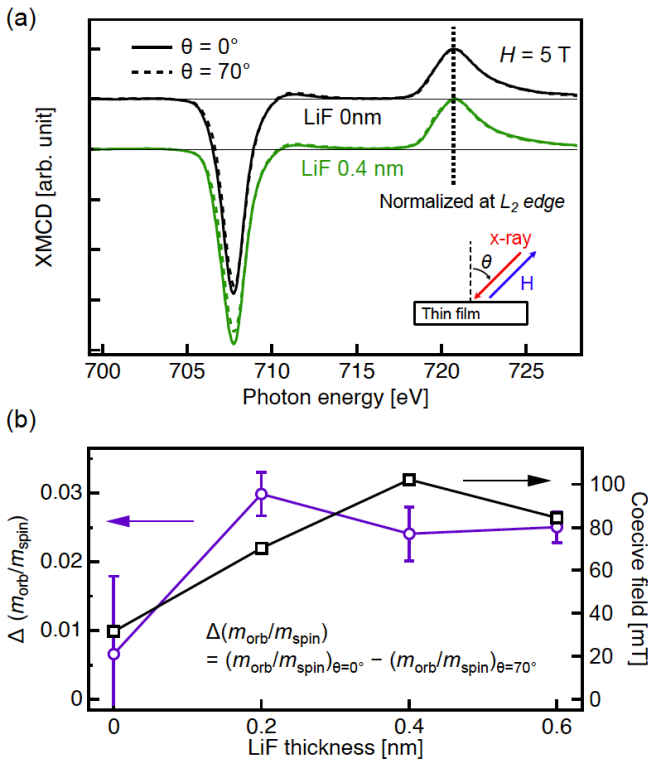


Fig. 2. (a) X-ray magnetic circular dichroism spectra for the samples without LiF and with 0.4-nm-thick LiF, measured with out-of-plane ( $\theta = 0^\circ$ ) and nearly in-plane ( $\theta = 70^\circ$ ) magnetic fields. The measurement geometry is depicted in the inset. (b) Anisotropy in the ratio of the Fe orbital magnetic moment to the Fe spin magnetic moment as a function of LiF thickness. The coercive fields are also plotted for comparison.

shows the obtained anisotropy of the orbital to spin magnetic moment ratio, defined as  $\Delta(m_{\text{orb}}/m_{\text{spin}}) = (m_{\text{orb}}/m_{\text{spin}})_{\theta=0^\circ} - (m_{\text{orb}}/m_{\text{spin}})_{\theta=70^\circ}$ . This anisotropy increases with LiF thickness. This strengthened orbital moment anisotropy is consistent with the PMA enhancement because the PMA energy is proportional to the orbital moment anisotropy in the simplest approximation. Indeed, the coercive fields behave similarly to the orbital moment anisotropy, as displayed in Fig. 2(b). The  $\Delta(m_{\text{orb}}/m_{\text{spin}})$  values seem saturated at the LiF thickness of 0.2 nm, the origin of which may be attributed to the fact that the Fe layer is almost fully covered by a monolayer of LiF ( $\sim 0.2$  nm).

We infer that the enhancement of the orbital moment anisotropy arises from the more robust interfacial electron localization and electron-electron correlation, due to the highly ionic nature of LiF and weak Fe-F hybridization, or from improved interface quality with fewer defects.

## References

- [1] T. Nozaki, T. Nozaki, T. Yamamoto, M. Konoto, A. Sugihara, K. Yakushiji, H. Kubota, A. Fukushima, and S. Yuasa, NPG Asia Materials **14**, 5 (2022).
- [2] S. Sakamoto, T. Nozaki, S. Yuasa, K. Amemiya, and S. Miwa, Phys. Rev. B **106**, 174410 (2022).

## Authors

S. Sakamoto, T. Nozaki<sup>a</sup>, S. Yuasa<sup>a</sup>, K. Amemiya<sup>b</sup>, and S. Miwa<sup>a</sup>  
<sup>a</sup>AIST  
<sup>b</sup>KEK

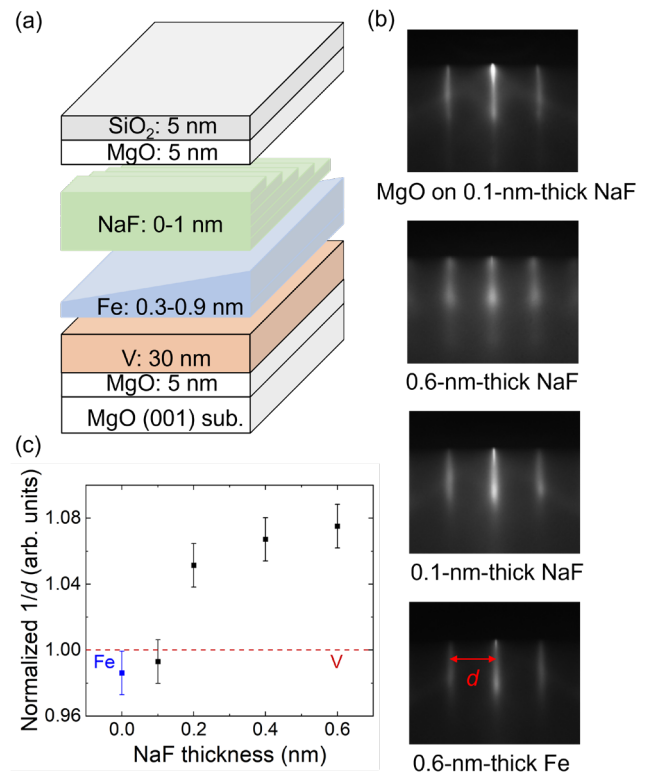


Fig. 1. (a) Schematic of the multilayers. (b) RHEED patterns of the multilayers: 0.66-nm-thick Fe layer, 0.1- and 0.6-nm-thick NaF layers, and MgO overlayer on 0.1-nm-thick NaF layer. (c) Normalized reciprocal of the distance between streaks ( $1/d$ ) in V, Fe, and NaF epilayers obtained from pixel analysis.

0.1- and 0.6-nm-thick NaF layers, and the corresponding MgO cap layer on the 0.1-nm-thick NaF layer, are shown in Fig. 1(b), respectively. The sharp streaks observed in the RHEED pattern indicate the well-epitaxial deposition of each layer.

To evaluate the lattice matching properties, we estimated the in-plane lattice constants of the NaF with various thicknesses by measuring the distance between the streaks in the RHEED patterns [represented as  $d$  in Fig. 1(b)]. As the in-plane lattice constant is inversely proportional to  $d$ , we plotted  $1/d$  values for the Fe and NaF layers normalized to that for the V layer in Fig. 1(c). The lattice constant of the Fe underlayer is plotted in blue at a NaF thickness of 0 nm. The  $1/d$  value remained constant with a 0.1-nm-thick NaF insertion but drastically increased when the NaF thickness exceeded 0.1 nm. The in-plane lattice constant of the 0.6-nm-thick NaF layer is estimated as  $\sim 0.323$  nm, approaching its unconstrained bulk lattice constant ( $a_{\text{NaF}}/\sqrt{2} = 0.327$  nm). These results indicate that a NaF layer epitaxially forms islands on the Fe layer when the NaF layer is thinner than a monolayer. However, for thicker NaF layer insertions, accumulated internal stress overcomes the epitaxial stress and creates interfacial defects, and therefore, the lattice constant approaches the bulk lattice constant.

The magnetic properties were characterized by polar magneto-optical Kerr effect (polar-MOKE) measurement. The magnetic dead layer thickness of the NaF sample and the compared LiF sample are shown in Fig. 2(a). The dead layer exhibits robustness after LiF insertion and remains unchanged with a 0.1-nm-thick NaF insertion. However, it drastically increases as the NaF thickness becomes thicker, suggesting interlayer mixing between NaF and Fe layers. We estimated the magnetic anisotropy energies from magnetization curves and extracted the interfacial magnetic anisotropy from the fitting. The interfacial magnetic anisotropy energies ( $K_I$ ) of NaF and the compared LiF samples are shown in Fig. 2(b). The 0.1-nm-thick NaF insertion shows a slight enhancement of  $K_I$  which is similar to the LiF case, except for the critical thickness difference probably originating from

the difference in lattice matching conditions. Despite the suboptimal lattice matching, the  $K_I$  enhancement in the Fe/NaF interface underscores the importance of fluorine atoms on the Fe atoms.

In summary, we have investigated the influence of NaF insertion on magnetic anisotropy at the Fe/MgO interface to disentangle the effects of fluorine electron negativity and lattice matching. Our result deepens the understanding of the effects of fluorine insertion on magnetic anisotropy at the Fe/MgO interface.

## References

- [1] T. Nozaki, T. Nozaki, T. Yamamoto, M. Konoto, A. Sugihara, K. Yakushiji, H. Kubota, A. Fukushima, and S. Yuasa, *NPG Asia Mater.* **14**, 5 (2022).
- [2] S. Sakamoto, T. Nozaki, S. Yuasa, K. Amemiya, and S. Miwa, *Phys. Rev. B* **106**, 174410 (2022).
- [3] J. Chen, S. Sakamoto, H. Kosaki, and S. Miwa, *Phys. Rev. B* **107**, 094420 (2023).
- [4] J. Chen, S. Sakamoto, and S. Miwa, *Phys. Rev. B* **109**, 064413 (2024).

## Authors

J. Chen, S. Sakamoto, and S. Miwa

# Pressure-Induced Superconductivity in Polycrystalline $\text{La}_3\text{Ni}_2\text{O}_{7-\delta}$

Uwatoko Group

High- $T_c$  superconductors have been at the forefront of scientific exploration due to their immense potential for transformative technological applications. The groundbreaking discovery of high- $T_c$  cuprates, where superconductivity (SC) emerges through doping Mott insulators with strong electron correlations, has motivated numerous endeavors in the past decades to unveil its mechanism and to find more superconducting families with high  $T_c$ . Through sharing striking structural and electronic similarities with cuprates, the nickelates with  $\text{Ni}^+(3d^9)$  electron configuration offer a tantalizing avenue for uncovering new high- $T_c$  superconductors. However, SC was not experimentally realized in nickelates until 2019, when the infinite-layer  $\text{Nd}_{1-x}\text{Sr}_x\text{NiO}_2$  thin films were found to show SC with  $T_c \approx 9\text{--}15$  K [1]. Since then, considerable dedication has been directed toward finding more nickelate superconductors with higher  $T_c$ .

Recently, Sun et al. reported the signature of high-temperature SC in  $\text{La}_3\text{Ni}_2\text{O}_7$  crystals with  $T_c$  up to 80 K at pressures above 14 GPa [2]. In contrast to the infinite-layer  $\text{Nd}_{1-x}\text{Sr}_x\text{NiO}_2$ ,  $\text{La}_3\text{Ni}_2\text{O}_7$  exhibits an exceptionally unique electronic configuration with the nominal oxidation state of  $\text{Ni}^{2.5+}$  as a mixed valence state of  $\text{Ni}^{2+}(3d^8)$  and  $\text{Ni}^{3+}(3d^7)$ . According to the structural study under high pressure, a structural phase transition from the orthorhombic  $Amam$  to  $Fmmm$  space group occurs at about 10-15 GPa, where the interlayer Ni-O-Ni bond angle changes from  $168^\circ$  to  $180^\circ$  [2]. Subsequent high-pressure studies on  $\text{La}_3\text{Ni}_2\text{O}_7$  crystals confirmed the presence of a zero-resistance state under better hydrostatic pressure conditions, yet revealed also some issues related with sample-dependent behaviors that remain unclear so far [3,4]. Such a remarkably high  $T_c$  has immediately ignited widespread theoretical investigations on the mechanism of high- $T_c$  SC. The significance of interlayer exchange between the  $d_{z^2}$  orbitals and intra-layer hybridization of the  $d_{z^2}$  and  $d_{x^2-y^2}$  orbitals on the nearest neighbor sites has received substantial attention. In contrast to the extensive

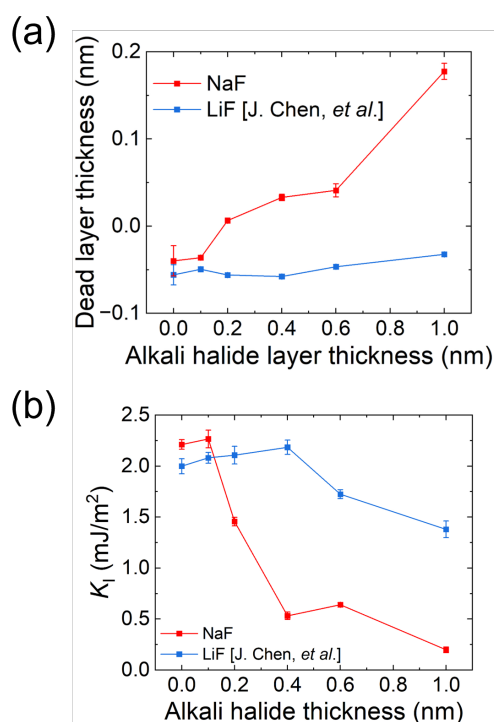


Fig. 2. NaF and LiF thickness dependence of the (a) dead layer and (b) interfacial magnetic anisotropy energies ( $K_I$ ).

theoretical investigations, experimental progress appears to have lagged behind, presumably due to the challenges associated with obtaining high-quality  $\text{La}_3\text{Ni}_2\text{O}_7$  single crystals with controlled and homogeneous stoichiometry. Depending on the post-annealing process, the oxygen content of  $\text{La}_3\text{Ni}_2\text{O}_7$  can vary from  $\text{O}_{6.35}$  to  $\text{O}_{7.05}$ . In addition, other competitive Ruddlesden-Popper phases are easily formed in the crystals grown using the optical image floating-zone furnace under moderate oxygen pressures. It thus becomes an important issue to perform a comprehensive study on the samples with well-controlled quality. Additionally, an open question remains concerning whether superconductivity can be achieved in  $\text{La}_3\text{Ni}_2\text{O}_7$  polycrystalline samples subjected to high pressure. Therefore, we are motivated to prepare phase-pure polycrystalline  $\text{La}_3\text{Ni}_2\text{O}_{7-\delta}$  samples in which oxygen content and chemical homogeneity can be easily controlled, and then to study the pressure effects on its

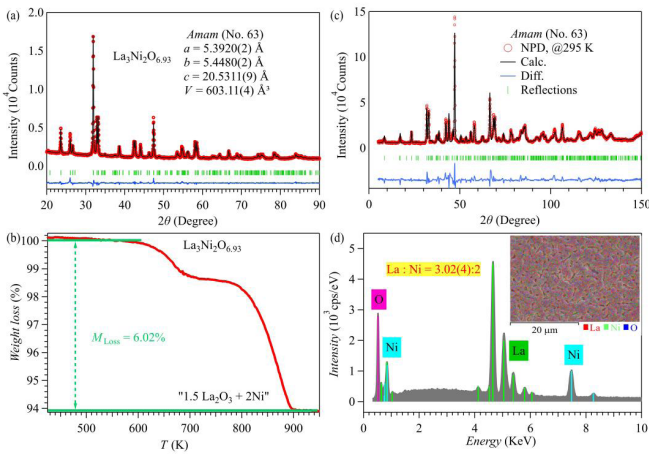


Fig. 1. (a) Rietveld refinements on the room temperature XRD pattern of  $\text{La}_3\text{Ni}_2\text{O}_{7-\delta}$ . The obtained lattice parameters are shown in the figure. The bottom marks and line correspond to the calculated Bragg diffraction positions and the difference between observed and calculated data, respectively. (b) Thermogravimetric curves for  $\text{La}_3\text{Ni}_2\text{O}_{7-\delta}$  in 10%  $\text{H}_2/\text{Ar}$ . (c) Rietveld refinements on the NPD pattern of  $\text{La}_3\text{Ni}_2\text{O}_{7-\delta}$ . (d) The SEM-EDS elemental mapping of  $\text{La}_3\text{Ni}_2\text{O}_{7-\delta}$ .

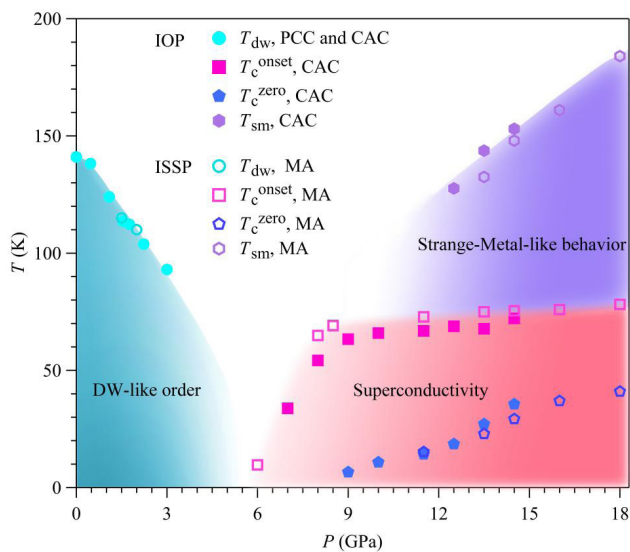


Fig. 2. The T-P phase diagram of the  $\text{La}_3\text{Ni}_2\text{O}_{6.93}$  polycrystalline. The solid and open circles represent the DW-like transition measured at various pressures using PCC, CAC and MA. The solid and open squares and pentagons represent the onset and zero-resistance superconducting transition temperatures determined from the present measurements in CAC and MA. The solid and open hexagon represent the critical temperature for the strange-metal-like behavior, above which the (T) curve deviates from linearity.

electrical transport properties under high pressure.

In this work [5], we synthesized high-quality  $\text{La}_3\text{Ni}_2\text{O}_{7-\delta}$  ( $\delta \approx 0.07$ ) polycrystalline samples by using the sol-gel method without post-annealing under high oxygen pressure (Fig. 1), and then measured temperature-dependent resistivity under various hydrostatic pressures up to 18 GPa by using the cubic anvil and two-stage multi-anvil apparatus. We find that the density-wave-like anomaly in resistivity is progressively suppressed with increasing pressure and the resistivity drop corresponding to the onset of superconductivity emerges at pressure as low as 6 GPa. Zero resistivity is achieved at 9 GPa below  $T_c^{\text{zero}} \approx 6.6$  K, which increases quickly with pressure to 41 K at 18 GPa. However, the diamagnetic response was not detected in the ac magnetic susceptibility measurements up to 15 GPa, indicating a filamentary nature of the observed superconductivity in the studied pressure range. The constructed T-P phase diagram (Fig. 2) reveals an intimate relationship between superconductivity, density-wave-like order, and the strange-metal-like behaviors. The observation of zero resistance state in the polycrystalline  $\text{La}_3\text{Ni}_2\text{O}_{7-\delta}$  samples under high pressures not only corroborates the recent report of superconductivity in the pressurized  $\text{La}_3\text{Ni}_2\text{O}_{7-\delta}$  crystals but also facilitates further studies on this emerging family of nickelate high- $T_c$  superconductors.

## References

- [1] D. Li *et al.* and H. Y. Hwang, *Nature* **572**, 624 (2019).
- [2] H. L. Sun *et al.*, *Nature* **621**, 493 (2023).
- [3] Y. Zhang *et al.*, *Nature Physics* (to be published).
- [4] J. Hou *et al.*, *Chin. Phys. Lett.* **40**, 117302 (2023).
- [5] G. Wang *et al.*, *Phys. Rev. X* **14**, 011040 (2024).

## Authors

G. Wang<sup>a</sup>, N. N. Wang<sup>a</sup>, X. L. Shen<sup>a</sup>, Y. Uwatoko, and J.-G. Cheng<sup>a</sup>  
<sup>a</sup>Institute of Physics Chinese Academy of Sciences

## Investigation of the Atomic Coordinates of $\text{CeNiC}_2$ under Pressure: Switching of the Ce-Ce First Nearest Neighbor Direction

Uwatoko Group

$\text{CeNiC}_2$  is notable for its unique properties, including heavy fermion behavior and multiple magnetic orderings. As the temperature decreases,  $\text{CeNiC}_2$  undergoes an incommensurate antiferromagnetic transition (ICAF) at  $T_{\text{ICAF}} \sim 20$  K, followed by a commensurate antiferromagnetic transition at  $T_{\text{CAF}} \sim 10$  K, and ferromagnetic ordering below 2.2 K.  $T_{\text{ICAF}}$  increases with pressure, reaching a maximum around 7 GPa. Beyond 11 GPa, the ICAF order is suppressed, and a SC dome with a maximum  $T_c \sim 3.5$  K appears. This SC state has a large upper critical field,  $H_{c2}(0) \sim 18$  T, nearly three times the Pauli paramagnetic limiting field, indicating an unconventional nature of the SC state.  $\text{CeNiC}_2$  has the highest  $T_c$  among Ce-based heavy fermion superconductors [1]. In NCS superconductors, antisymmetric spin-orbit coupling can occur due to the lack of inversion symmetry, favoring spin-triplet Cooper pairing with large  $H_{c2}(0)$ . Also, NCS superconductors can host a mix of spin-triplet and singlet pairing. While  $\text{CeNiC}_2$  has an NCS crystal structure at ambient pressure, it is unclear if this structure is maintained across the pressure range where the SC state appears. Subtle variations in interatomic distances under pressure can significantly affect the magnetic and electronic properties of heavy

fermion materials. However, obtaining precise structural information under pressure is essential for understanding CeNiC<sub>2</sub>'s properties, although challenging. This study investigates the effect of pressure on CeNiC<sub>2</sub>'s atomic coordinates using single crystal X-ray diffraction (XRD) measurements at room temperature up to 18.6 GPa.

High-quality single crystals of CeNiC<sub>2</sub> were grown using the Czochralski pulling method in an Argon gas environment, with high-purity Ce, Ni, and C atoms. Single crystal X-ray diffraction at 293(2) K was conducted using a Rigaku XtaLab MicroMax007 HFMR with Mo-K $\alpha$  radiation and a HyPix6000 diffractometer. The crystal structure was solved using Olex2 with SHELXT 2018/2 and refined with SHELXL 2018/3. High-pressure experiments utilized a diamond anvil cell (DAC) with a 300  $\mu$ m culet size. A CeNiC<sub>2</sub> single crystal (~100  $\mu$ m) was loaded into the DAC with a ruby pressure manometer, and a 4:1 methanol-ethanol mixture served as the pressure transmitting medium.

Figure 1(b) shows the normalized unit-cell parameters and unit-cell volume of CeNiC<sub>2</sub> in the pressure range from 0 to 18.6 GPa. The normalized unit-cell parameters show anisotropic compressibility under pressure; the length of the a-axis decreases at a much faster rate compared to the b- and c-axes. The compressibility of the a-axis ( $k_a = d(a/a_0)/dP = -3.70 \times 10^{-3}$ ) is the highest, whereas the b-axis is the lowest ( $k_b = d(b/b_0)/dP = -1.39 \times 10^{-3} \text{ GPa}^{-1}$ ). The unit-cell parameters decrease linearly with pressure, showing no structural phase transition. Compressibility is anisotropic, with the a-axis compressing fastest. The bulk modulus  $B_0$  is  $\sim 134 \pm 3 \text{ GPa}$  with  $B_0' = 0.75 \pm 0.05$ .

The anisotropic compressibility of CeNiC<sub>2</sub>, with higher compressibility along the a-axis than along the b- and c-axes, likely causes this behavior. The stiffness of the NiC<sub>2</sub> layer, attributed to strong C-C bonds and Ni-C interactions in the bc plane, hinders compression along these axes. This results in different responses of interatomic distances under pressure. Similar effects on magnetic exchange interactions have been observed in other CeT<sub>2</sub>X<sub>2</sub> compounds, like CeRh<sub>2</sub>Ge<sub>2</sub> and CeCu<sub>2</sub>Ge<sub>2</sub>, where interatomic distances govern the c-f interaction strength.

Figures 2(a), (b) and (c) show the interatomic distances between Ce-Ce, Ni-Ni and Ni-Ce atoms. Atomic coordinates

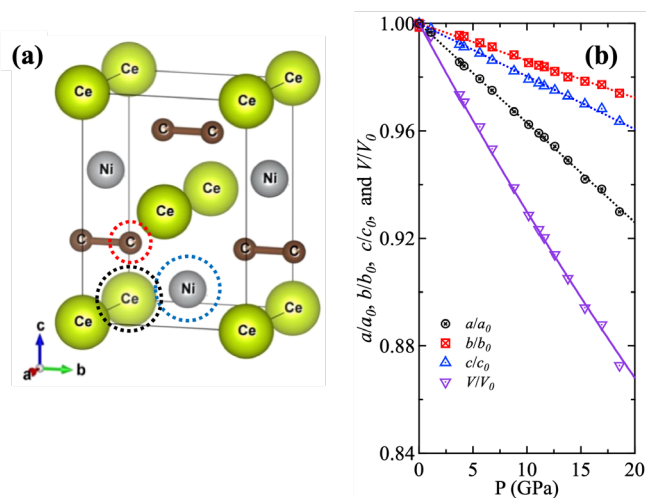


Fig. 1. (a) The positions of C, Ni, and Ce atoms in the unit cell are illustrated with red, blue, and black dashed circles, respectively. (b) The pressure dependence of normalized lattice parameters and unit cell volume. The error bars are smaller than the symbols. The dashed lines are the linear fittings to the pressure dependence of the lattice parameters used for estimating the compressibility. The solid line represents a fit of the Birch-Murnaghan equation of state to the normalized unit cell volume [2].

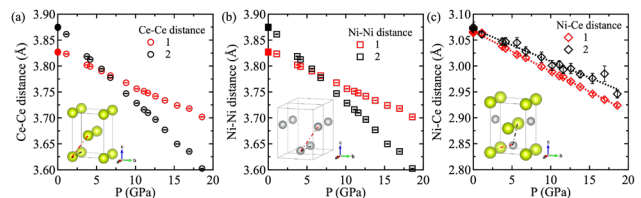


Fig. 2. The pressure dependence of interatomic distances between the (a) Ce-Ce atom, (b) Ni-Ni atom, and (c) Ni-Ce atom is illustrated. The dashed lines in (c) represent the linear fitting results. The red and black dot-dashed lines in the inset illustrate the direction of interatomic distances 1 and 2 in the unit cell. The solid symbol shows the ambient condition data [2].

of Ce, Ni, and C, and interatomic distances were measured under pressure, revealing changes primarily in the y-coordinate of C and the C-C bond length, especially around 7 GPa. The interatomic distances between Ce-Ce, Ni-Ni, Ni-Ce, and C-C exhibit notable changes with pressure, indicating anisotropic compressibility and bond length variations, particularly highlighting the unique behavior of C-C and C-Ni bonds around 7 GPa.

Nonmonotonic pressure dependencies in C-C, C-Ni, and C-Ce distances, particularly around 7 GPa, indicate anomalies that may result from increased Ce-Ce interaction along the a-axis penetrating the NiC<sub>2</sub> layer. These findings highlight the intricate relationship between pressure, atomic distances, and magnetic properties in CeNiC<sub>2</sub>, providing critical insights into the behavior of heavy fermion materials. As shown in Fig. 2 the first and second nearest neighbor directions of Ce-Ce and Ni-Ni atoms interchange around 7 GPa, with nonmonotonic pressure dependence observed for interatomic distances between C-Ce, C-Ni, and C-C atoms at this pressure. Increasing pressure causes these distances to decrease and become equal around 7 GPa. Above this pressure, the FNN and SNN directions interchange; the FNN aligns along the a-axis, and the SNN lies in the bc-plane. This interchange correlates with the weakening of incommensurate antiferromagnetic (ICAF) order and the emergence of the Kondo effect above 7 GPa, suggesting increased interplanar Ce-Ce interaction influences the spin structure of CeNiC<sub>2</sub> [2].

In summary, we investigated the crystal structure of CeNiC<sub>2</sub> from 0 to 18.6 GPa by using single crystal X-ray diffraction with a laboratory X-ray source. Our results reveal a large Bulk modulus  $\sim 134 \text{ GPa}$  and anisotropic linear compressibility following the relationship  $|k_a| > |k_c| > |k_b|$ . Although, we do not detect any signature of structural phase transition, the direction of FNN and SNN between the Ce-Ce and Ni-Ni atoms interchanges near the pressure where the antiferromagnetic ordering temperature reaches a maximum in the pressure temperature phase diagram of CeNiC<sub>2</sub>. Our results suggest that the direction of nearest neighbors interchange might play a key role in the suppression of magnetic order and the enhancement of the Kondo effect.

## References

- [1] S. Katano, H. Nakagawa, K. Matsubayashi, Y. Uwatoko, H. Soeda, T. Tomita, and H. Takahashi, Phys. Rev. B **90**, 220508 (2014).
- [2] H. Ma, D. Bhoi, J. Gouchi, H. Sato, T. Shigeoka, J.-G. Cheng, and Y. Uwatoko, Phys. Rev. B **108**, 064435 (2023).

## Authors

H. Ma, D. Bhoi, J. Gouchi, H. Sato<sup>a</sup>, T. Shigeoka<sup>b</sup>, J.-G. Cheng<sup>c</sup>, and Y. Uwatoko

<sup>a</sup>Rigaku Corporation

<sup>b</sup>Yamaguchi University

<sup>c</sup>Chinese Academy of Science

# Dynamics in Active Cyclic Potts Model

## Noguchi Group

Spatiotemporal patterns, such as traveling waves, have been observed in nonequilibrium active systems. Many phenomena are well-captured by a description in terms of nonlinear but deterministic partial differential equations. However, noise effects are not understood so far. We focused on the effects of thermal fluctuations, since they are significant on a molecular scale.

We simulated the nonequilibrium dynamics of a Potts model with three cyclic states ( $s = 0, 1, \text{ and } 2$ ) [1]. The neighboring sites of the same states have an attraction to induce a phase separation between different states, and they have a cyclic state-energy-difference in the rock–paper–scissors manner. Both forward and backward flips are considered by the Monte Carlo method. It is a model system for chemical reactions on a catalytic surface or molecular transport through a membrane. For the reaction case, the three states are reactant, product, and unoccupied sites. For the transport case, the molecule can bind to both surfaces and flip between these two states. For one cycle, a reaction proceeds in bulk in the former case, and a molecule is transported across the membrane in the latter case. In this study, we consider the cyclically symmetric condition, i.e., the self-energy difference of the successive states is constant as  $\varepsilon_0 - \varepsilon_1 = \varepsilon_1 - \varepsilon_2 = \varepsilon_2 - \varepsilon_0 = h$ . This model can be tuned from thermal-equilibrium to far-from-equilibrium conditions and corresponds to the standard Potts model at  $h = 0$ .

We found two dynamic modes: homogeneous cycling mode and spiral wave mode. At a low cycling energy  $h$  between two states, the homogeneous dominant states cyclically change as  $s = 0 \rightarrow 1 \rightarrow 2 \rightarrow 0$  via nucleation and growth, as shown in Fig. 1(a). In contrast, spiral waves are formed at high energy  $h$ , as shown in Fig. 1(b). The waves are generated from the contacts of three states and rotate around them. The homogeneous cycling mode is newly found in this study, whereas the spiral waves have been

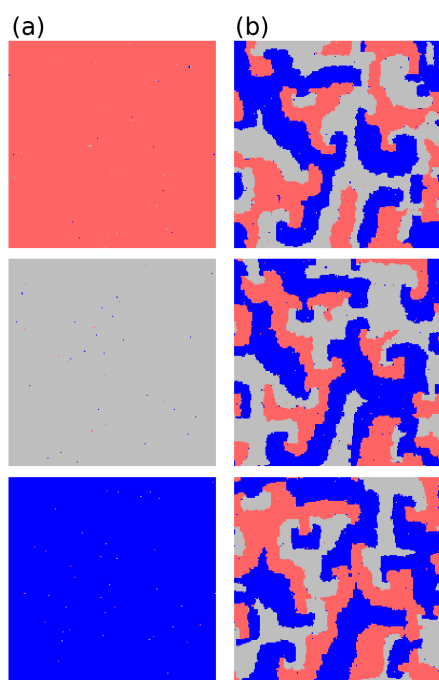


Fig. 1. Sequential snapshots of active cyclic Potts model. (a) Homogeneous cycling mode at  $h = 0.8$ . (b) Spiral wave mode at  $h = 1.1$ . The states,  $s = 0, 1$  and  $2$ , are displayed in gray, blue, and red colors, respectively.

reported in continuum models and other lattice models.

For large systems, a discontinuous transition occurs from these cyclic homogeneous phases to spiral waves, while the opposite transition is absent. Conversely, these two modes can temporally coexist for small systems, and the ratio of the two modes continuously changes with increasing  $h$ . The transition from the homogeneous cycling to spiral wave modes occurs by the nucleation of the third state during the domain growth, i.e., it is determined by the competition of the nucleation and growth. The opposite transition from the spiral wave to homogeneous cycling modes occurs through the stochastic disappearance of three-state contacts. With increasing system size, the former transition rate increases, but the latter rate exponentially decreases. The transition character is changed by these size dependencies.

## Reference

[1] H. Noguchi, F. van Wijland, and J.-B. Fournier, *J. Chem. Phys.* **161**, 025101 (2024).

## Author

H. Noguchi

# A New Superconductor Family with Various Magnetic Elements

## Okamoto Group

There is a complex relationship between superconductivity, where the electrical resistance of a material becomes completely zero at low temperatures, and magnetism, which is the property of a material as a magnet. Generally, superconductivity is destroyed by strong magnetism, so superconductivity does not often appear in materials containing magnetic elements such as iron. In rare cases, however, materials containing magnetic elements exhibit unconventional superconductivity with very high critical temperature or unusual properties that cannot be explained within the framework of existing theories. Uncovering the complex relationship between superconductivity and magnetism may be important for the realization of room-temperature superconductivity. The discovery of unique superconductors is essential for elucidating this relationship.

We discovered that the ternary telluride series  $\text{Sc}_6M\text{Te}_2$  is a unique family of  $d$ -electron superconductors incorporating various magnetic elements [1].  $\text{Sc}_6M\text{Te}_2$  compounds with  $M = \text{Mn, Fe, Co, Ni, Ru, Rh, Os, and Ir}$  have been synthesized and reported to crystallize in the hexagonal  $\text{Zr}_6\text{CoAl}_2$ -type structure, but their physical properties have not been reported thus far [2,3]. A characteristic point of this crystal structure is the fact that the  $M$  atoms are trigonal prismatic coordinated by six Sc atoms and form one-dimensional chains along the  $c$  axis, as shown in Fig. 1(a). Polycrystalline samples of  $\text{Sc}_6M\text{Te}_2$  with various transition metal  $M$  were synthesized by the arc-melting method and the bulk superconducting transitions in seven  $M$  cases were confirmed based on the electrical resistivity, magnetization, and heat capacity measurements on the obtained polycrystalline samples. A  $\text{Sc}_6\text{FeTe}_2$  sample is shown in the lower right panel of Fig. 1(a).

Figure 1(b) shows the electrical resistivity at low temperatures for various  $M$  cases. The seven  $M$  cases except for  $M = \text{Mn}$ , the resistivity shows a sharp drop to zero above 2 K. They also show large diamagnetic signal and clear heat

**Authors**

Y. Shinoda<sup>a</sup>, Y. Okamoto, Y. Yamakawa<sup>a</sup>, H. Matsumoto, D. Hirai<sup>a</sup>, and K. Takenaka<sup>a</sup>

<sup>a</sup>Nagoya University

## Dynamics of Acetonitrile Absorbed in a Metal–Organic Framework MIL-101 with Mg-Ion Conduction

Yamamuro Group

MIL-101 is a kind of Metal–Organic Framework (MOF), which contains numerous pores and attracts great attention for various applications, e.g., gas reservoirs, filters, reaction fields, ionic conductors, etc. Recently, the group of Prof. Sadakiyo (our collaborator and visiting professor of ISSP) discovered that MIL-101 containing Mg(TFSI)<sub>2</sub> (TFSI: Bis(trifluoromethanesulfonyl)imide) exhibits superionic conductivity of around 10<sup>-3</sup> S cm<sup>-1</sup> after absorbing acetonitrile (AN) vapor [1]. This discovery may contribute to the development of Mg-ion batteries, which are promising candidates for non-lithium-ion solid-state batteries.

To clarify the effect of AN on Mg-ion conduction, we conducted a quasielastic neutron scattering (QENS) experiment using AGNES at JRR-3 and DNA at J-PARC for three samples: bulk AN, MIL-101 with absorbed AN (AN-MOF) and MIL-101 with absorbed AN and Mg(TFSI)<sub>2</sub> (AN-Mg-MOF). The QENS spectra observed by AGNES and DNA were Fourier transformed into intermediate scattering functions  $I(Q,t)$ s and smoothly joined as shown in Fig. 1. As shown in Fig. 2, the  $I(Q,t)$  of bulk AN is fitted well by a single Kohlrausch-Williams-Watts (KWW) function as ordinary  $\alpha$  relaxations of molecular liquids, while those of AN-MOF and AN-Mg-MOF by the sum of a KWW function, a constant (elastic component) which corresponds to the stationary hydrogen atoms in MIL-101, and an exponential function which may correspond to a methyl rotation decoupled from the  $\alpha$ -relaxation.

To investigate the  $\alpha$ -relaxation expressed by the KWW function, we examine the  $Q^2$ -dependence of the inverse of

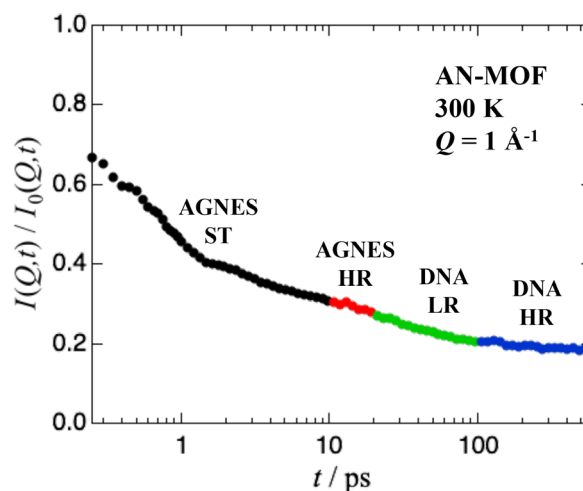


Fig. 1. Intermediate scattering functions of AN-MOF obtained from the Fourier transformation of the QENS data at  $T = 300$  K and  $Q = 1 \text{ \AA}^{-1}$ . The  $I(Q,t)$  data from the standard (ST) and high-resolution (HR) modes of AGNES and the low-resolution (LR) and high-resolution (HR) modes of DNA are smoothly joined.

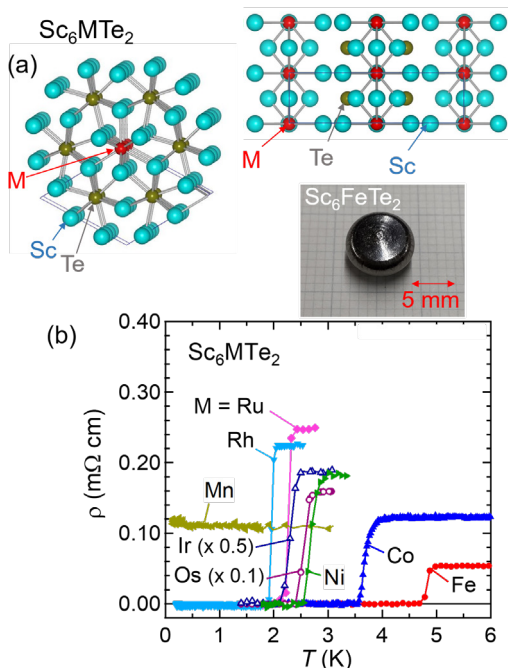


Fig. 1. (a) Crystal structure of  $\text{Sc}_6\text{MTe}_2$ . The lower right panel shows a polycrystalline sample of  $\text{Sc}_6\text{FeTe}_2$  synthesized by the arc-melting method. (b) Temperature dependence of electrical resistivity of  $\text{Sc}_6\text{MTe}_2$  polycrystalline samples.

capacity jump, indicating the bulk superconducting transition occurs in them. A characteristic feature of the superconductivity in  $\text{Sc}_6\text{MTe}_2$  is the  $M$  dependence of the superconducting transition temperature  $T_c$ . Four compounds with  $M = 4d$  and  $5d$  elements displayed almost the same  $T_c$  of approximately 2 K, but those with  $M = 3d$  elements displayed higher values and increased in the order of Ni, Co, and Fe. Therefore,  $\text{Sc}_6\text{FeTe}_2$  showed the highest  $T_c$  of 4.7 K.

These results strongly suggest that the  $3d$  electrons of  $M$  atoms play an important role in realizing the superconductivity in this system. First principles calculations indicate the presence of significant contribution of Fe  $3d$  orbitals at the Fermi energy, which most likely enhance the  $T_c$  of  $\text{Sc}_6\text{FeTe}_2$ . The heat capacity data of  $\text{Sc}_6\text{FeTe}_2$  indicate that the electronic specific heat in  $\text{Sc}_6\text{FeTe}_2$  is strongly enhanced by some reason. At present, the origin of this enhancement is still unclear, but it might be interesting if the strong electron correlation of Fe  $3d$  electron plays an important role in this enhancement.

Another important point of this  $\text{Sc}_6\text{MTe}_2$  family is that all of Sc,  $M$ , and Te sites can be replaced by various elements and physical properties of almost all of them have not been investigated thus far. In fact, following  $\text{Sc}_6\text{MTe}_2$ , we recently discovered superconductivity in a Zr analogues  $\text{Zr}_6\text{MTe}_2$  [4]. The  $T_c$  values in  $\text{Zr}_6\text{MTe}_2$  is much lower than those for  $\text{Sc}_6\text{MTe}_2$ , but the highest  $T_c$  was realized in  $\text{Zr}_6\text{FeTe}_2$  as in the case of  $\text{Sc}_6\text{MTe}_2$ .  $\text{Zr}_6\text{FeSb}_2$  is also found to show superconductivity at 1.3 K [5]. It is expected that more new superconductors will be found in this family and the future research on this family will contribute to a complete understanding of the relationship between superconductivity and magnetic elements.

**References**

- [1] Y. Shinoda, Y. Okamoto, Y. Yamakawa, H. Matsumoto, D. Hirai, and K. Takenaka, J. Phys. Soc. Jpn. **92**, 103701 (2023).
- [2] P. A. Maggard and J. D. Corbett, Inorg. Chem. **39**, 4143 (2000).
- [3] L. Chen and J. D. Corbett, Inorg. Chem. **43**, 436 (2004).
- [4] H. Matsumoto, Y. Yamakawa, R. Okuma, D. Nishio-Hamane, and Y. Okamoto, J. Phys. Soc. Jpn. **93**, 023705 (2024).
- [5] R. Matsumoto, E. Murakami, R. Oishi, S. Ramakrishnan, A. Ikeda,

# Field Control of Quasiparticle Decay in a Quantum Antiferromagnet

Masuda Group

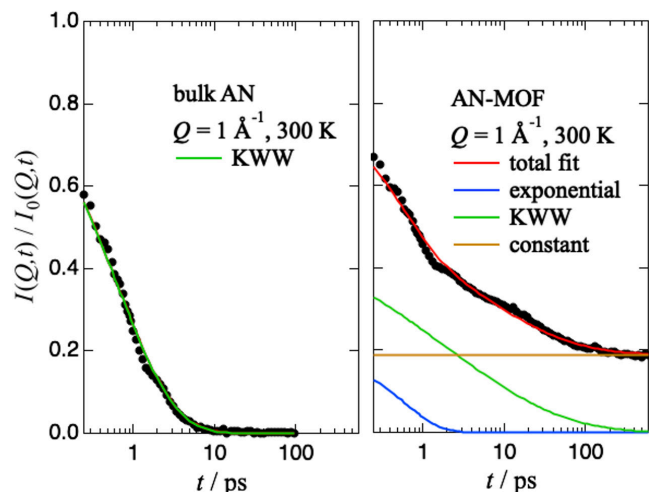


Fig. 2. Fitting of the intermediate scattering functions of bulk AN and AN-MOF at  $T = 300$  K and  $Q = 1 \text{ \AA}^{-1}$ .

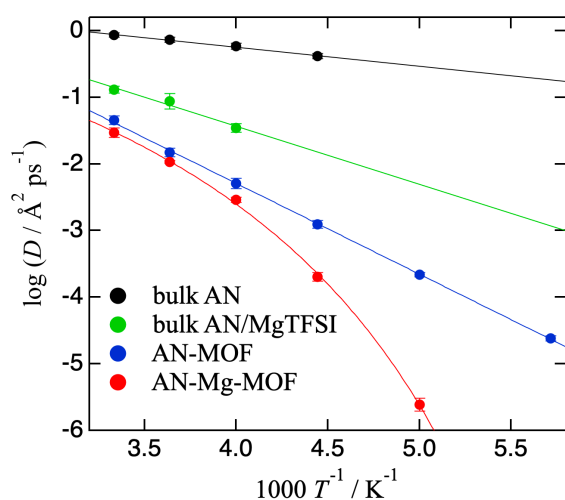


Fig. 3. Fitting of the Arrhenius plots of the diffusion constants of bulk AN, bulk AN/Mg(TFSI)<sub>2</sub>, AN-MOF, and AN-Mg-MOF.

the average relaxation time  $\langle \tau \rangle^{-1}$ . The plots for bulk AN and AN-MOF show continuous diffusion ( $\langle \tau \rangle^{-1} = DQ^2$ ,  $D$ : diffusion constant), whereas that for AN-Mg-MOF is represented by the jump-diffusion model ( $\langle \tau \rangle^{-1} = DQ^2/(1 + \tau_0 DQ^2)$ ,  $\tau_0$ : mean residence time). This jump may be related to the connection/disconnection process of AN molecules to  $\text{Mg}^{2+}$ . Figure 3 displays the Arrhenius plots of  $D$  comparing the three samples. The plots for bulk AN and AN-MOF are classified to Arrhenius type, while that for AN-Mg-MOF is non-Arrhenius type. This may be because AN molecules coordinate to  $\text{Mg}^{2+}$  ions and the number of the coordinated AN molecules increases as temperature is lowered. The diffusion constants become smaller in order of bulk AN, AN-MOF and AN-Mg-MOF, indicating that the diffusion of AN is hindered by the pore walls of MIL-101 and further by  $\text{Mg}^{2+}$  ions. The mean jump distance  $\langle l \rangle$  was calculated by  $\langle l \rangle = (6D\tau_0)^{1/2}$  to be  $1.6 \text{ \AA}$ . The results shown above should provide important information to clarify the mechanism of  $\text{Mg}^{2+}$  conduction.

## Reference

[1] Y. Yoshida *et al.*, *J. Am. Chem. Soc.* **144**, 8669 (2022).

## Authors

S. Sato, H. Akiba, Y. Ohmasa, and O. Yamamuro

The concept of a quasiparticle has been successful in explaining various types of low-energy excitations in many-body systems including charge, spin, and lattice. Using a spectroscopic approach, a weakly coupled quasiparticle with a long lifetime can be probed as a well-defined excitation, allowing identification of the effective Hamiltonian and basic understanding of the system. Momentum-resolved spectroscopy has permitted investigations into the intricate structure of spectra, revealing the effect of quasiparticle interactions that results in the renormalization of the dispersion and instability of the quasiparticle.

The microscopic phenomena in the spectra affect bulk properties of materials. In the thermoelectric material PbTe, the interaction between longitudinal acoustic and transverse optical modes (here, the quasiparticles are phonons) induces the decay and overdamping of the former phonon in the low energy region, leading to low conductivity of thermal current [1]. The instability of the quasiparticle is key for the current to exist in bulk property.

Two examples illustrate that the instability of the quasiparticle is changed by the interaction between the one-quasiparticle and two-quasiparticle continuum [2]. An example for a case of the strong interaction is found in the longitudinal sound wave, phonon, in superfluid  $^4\text{He}$  [3]. The spectrum in low energy exhibits a local minimum with energy  $\Delta$ , called a roton, for which qualitative behavior is explained by Feynman and Cohen (FC) harmonic dispersion. However, the spectrum does not exceed a critical energy of  $2\Delta$ , which is the lower boundary of the two-phonon continuum. The strong interaction between the one-phonon and continuum pushes one-phonon energy downwards, and the one-phonon stays at  $2\Delta$  outside the continuum. On the FC dispersion beyond the critical energy, the bare one-phonon decays into a pair of rotons, and a remnant of one-phonon which is ascribed to the bound state of two-phonon was observed. The phenomenon is considered universal in bosonic systems and has also been observed in a spin-gap antiferromagnet  $\text{BiCu}_2\text{PO}_6$  [4].

An example for the weak interaction is found in a two-dimensional quantum magnet, piperazinium hexachlorodocuprate (PHCC) [3]. This case is simple; the quasiparticle decays in the continuum, and a remnant one-magnon is probed as a broad excitation. The conjecture which this work tests is that if one tunes the interaction between a quasiparticle and the continuum in an identical material by applying external field, would the quasiparticle decay behavior change?

This study [5] examines magnon decay in a triangular lattice quantum antiferromagnet  $\text{RbFeCl}_3$ . Magnetism of  $\text{Fe}^{2+}$  ion surrounded by  $\text{Cl}^-$  octahedra with trigonal distortion is effectively described by an  $S = 1$  spin with strong easy-plane anisotropy.  $\text{Fe}^{2+}$  ions form a one-dimensional ferromagnetic chain along the crystallographic  $c$ -axis, and the interchain interaction in the triangular lattice in the  $ab$ -plane is antiferromagnetic. At low temperatures the compound exhibits a non-collinear  $120^\circ$  structure due to the frustration. The spectrum was qualitatively similar to that of the pressure-induced ordered state in the isostructural compound  $\text{CsFeCl}_3$  near the quantum critical point (QCP) [6], which cannot be explained by standard linear spin wave

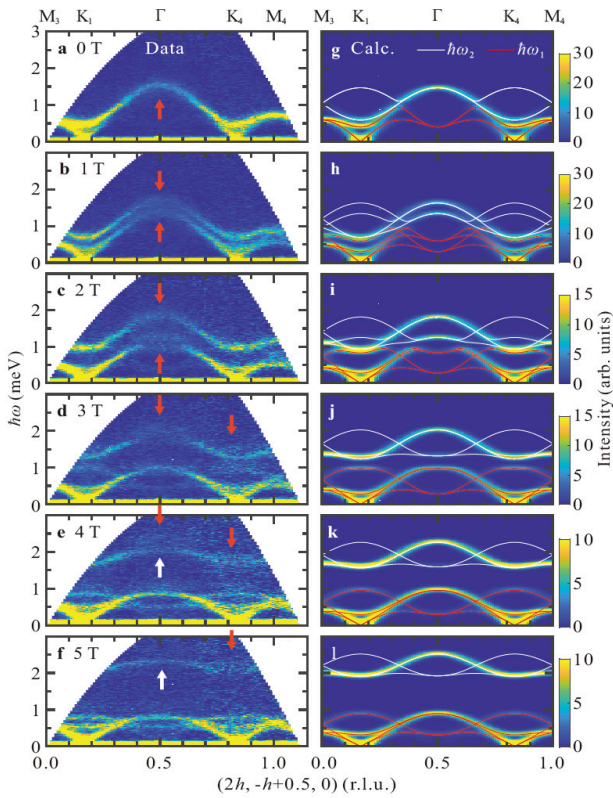


Fig. 1. False color map of inelastic neutron scattering (INS) spectra and calculated two-magnon density of state in RbFeCl<sub>3</sub>. **a-f**: Magnetic field ( $H \parallel c$ -axis) dependences of false color maps for observed (**a-f**) and calculated (**g-l**) INS spectra. Red arrows in **a-f** indicate broadening linewidth. White arrows in **e** and **f** indicate magnons avoiding decay. White and red solid curves in **g-l** are one-magnon dispersion relations of  $\hbar\omega_1$  and  $\hbar\omega_2$  modes calculated using linear extended spin wave theory (LESW) using the best fit parameters. The calculated spectra are convoluted by the instrumental resolution.

theory. Instead, the strong hybridization of the transverse and longitudinal fluctuations resulting from the non-collinear magnetic structure renormalizes the magnetic excitation, as explained by the linear extended spin wave theory (LESW) [3]. Because a non-collinear magnetic structure is realized near the QCP and the excitation is strongly hybridized with longitudinal fluctuation, the magnon decay is anticipated in wide four-dimensional momentum-energy space. Furthermore, gapless behavior and a large dispersion perpendicular to the triangular lattice yield a two-magnon continuum covering the whole region of one-magnon excitation.

In this study, we performed inelastic neutron scattering (INS) measurements in the magnetic field on RbFeCl<sub>3</sub> to study the magnon decay and the interaction between single magnons and the two-magnon continuum. We observed a simple magnon decay in a low field where the interaction is small and a magnon avoiding decay in high field where the interaction was large as shown in Fig. 1. Thus, we succeeded in controlling the magnon decay using the field. In contrast with the avoided phonon decay in superfluid <sup>4</sup>He and magnons in magnetic materials previously reported [2,4], the phenomenon was observed in the presence of a two-quasi-particle continuum, indicating that the phenomenon is not limited to outside the continuum, but also occurs inside.

#### References

- [1] O. Delaire, J. Ma, K. Marty, A. F. May, M. A. McGuire, M. H. Du, D. J. Singh, A. Podlesnyak, G. Ehlers, M. D. Lumsden, and B. C. Sales, *Nat. Mater.* **10**, 614 (2011).
- [2] R. Verresen, R. Moessner, and F. Pollmann, *Nat. Phys.* **15**, 750 (2019).
- [3] M. B. Stone, I. A. Zaliznyak, T. Hong, C.L. Broholm, and D. H. Reich, *Nature (London)* **440**, 187 (2006).

- [4] K. W. Plumb, K. Hwang, Y. Qiu, L. W. Harriger, G. E. Granroth, A. I. Kolesnikov, G. J. Shu, F. C. Chou, C. Rüegg, Y. B. Kim, and Y.-J. Kim, *Nat. Phys.* **12**, 224 (2016).
- [5] S. Hasegawa, H. Kikuchi, S. Asai, Z. Wei, B. Winn, G. Sala, S. Itoh, and T. Masuda, *Nat Commun* **15**, 125 (2024).
- [6] S. Hayashida, M. Matsumoto, M. Hagiwara, N. Kurita, H. Tanaka, S. Itoh, T. Hong, M. Soda, Y. Uwatoko, and T. Masuda, *Sci. Adv.* **5**, eaaw5639 (2019).

#### Authors

S. Hasegawa, H. Kikuchi, S. Asai, Z. Wei, B. Winn<sup>a</sup>, G. Sala<sup>a</sup>, S. Itoh<sup>b</sup>, and T. Masuda,

<sup>a</sup>Oak Ridge National Laboratory

<sup>b</sup>KEK

## Single-q and Multi-q Magnetic Orders in the Collinear Commensurate Antiferromagnet CeRh<sub>2</sub>Si<sub>2</sub>

Nakajima Group

Since the discovery of magnetic skyrmion lattice (SkL) in MnSi[1], magnetic orders described by multiple magnetic modulation wave vectors ( $q$ -vectors), which are referred to as multi- $q$  magnetic orders, have been attracting remarkable attention. In the early stage of the magnetic skyrmion studies, the Dzyaloshinskii-Moriya (DM) arising from the broken inversion symmetry of the crystal structure was considered to be one of the most important ingredients for realizing the SkL states. Thus, non-centrosymmetric magnets were intensively investigated. This trend has changed since the discovery of the SkL state with a large topological Hall effect in Gd<sub>2</sub>PdSi<sub>3</sub> [2], which has the centrosymmetric crystal structure. It was also theoretically pointed out that the biquadratic interaction term derived from the perturbative expansion for the Kondo lattice Hamiltonian can stabilize a variety of multi- $q$  states even in centrosymmetric systems [3]. In the present study, we applied this model to the centrosymmetric collinear-commensurate antiferromagnet CeRh<sub>2</sub>Si<sub>2</sub> [4].

CeRh<sub>2</sub>Si<sub>2</sub> has a ThCr<sub>2</sub>Si<sub>2</sub>-type centrosymmetric tetragonal crystal structure and is known to have two antiferromagnetic phases at low temperatures in zero magnetic field [5]. Both magnetic phases are characterized by commensurate  $q$ -vectors. Specifically, the high-temperature phase (AF1) has a single  $q$ -vector of  $q = (1/2, 1/2, 0)$ . This  $q$ -vector breaks the fourfold rotational symmetry of the crystal structure, and thus results in two magnetic domains characterized by  $q = (1/2, 1/2, 0)$  and  $(1/2, -1/2, 0)$ . On the other hand, the low-temperature phase (AF2) is characterized by four  $q$ -vectors of  $q = (1/2, 1/2, 0)$ ,  $(1/2, -1/2, 0)$ ,  $(1/2, 1/2, 1/2)$ , and  $(1/2, -1/2, 1/2)$ . In contrast to the AF1 phase, AF2 phase was reported to be a multi- $q$  phase, i.e., the magnetic structure is described by a superposition of the four magnetic modulations. This means that the AF2 phase retrieves the fourfold rotational symmetry of the crystal, although it was lost in the high-temperature AF1 phase. This distinct change in symmetry should be seen in bulk properties such as magnetization, resistivity etc. as well as the neutron diffraction intensities. However, they were not observed because the AF1 phase exhibits a multi-domain state, in which the two single- $q$  magnetic domains coexist. The intrinsic anisotropy of the magnetic order and associated physical properties were not macroscopically observed.

We thus applied a weak uniaxial stress to a single crystal of CeRh<sub>2</sub>Si<sub>2</sub>, and performed magnetization, resistivity and neutron diffraction measurements. The direction of the

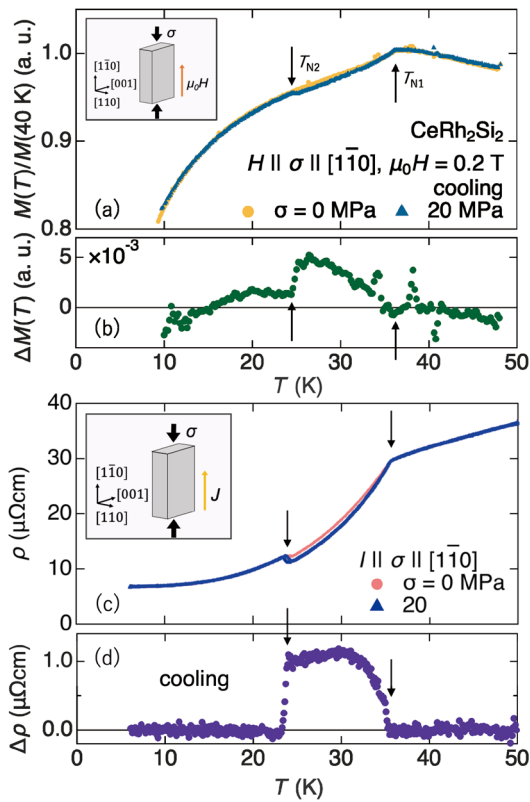


Fig. 1. (a) Temperature dependence of magnetization  $M$  at  $\mu_0 H = 0.2$  T and  $\sigma = 0, 20$  MPa.  $M \parallel H \parallel \sigma \parallel [1-10]$ .  $M$  is normalized by  $M$  at 40 K. (b) Temperature dependence of the difference of magnetization  $\Delta M$ . (c) Temperature dependence of resistivity  $\rho$  at  $\mu_0 H = 0$  T and  $\sigma = 0, 20$  MPa. Electric current  $I$  is applied along  $\sigma \parallel [1-10]$ . (d) Temperature dependence of the difference of resistivity  $\Delta \rho$ . The measurements were performed under cooling condition. A schematic of the geometry for each measurement are shown in inset. Black arrows indicate ordering temperature. This figure is taken from Ref. 4.

uniaxial stress was selected to be the  $[1-10]$  direction of the crystal to lift the degeneracy between the two magnetic domains. In Fig. 1, we show temperature variations of magnetization and resistivity measured at ambient pressure and under uniaxial stress of 20 MPa. In both the measurements, the applications of the uniaxial stress induced the difference in magnetization and resistivity only in the AF1 phase. We also performed neutron diffraction measurements with uniaxial stress. We measured temperature variations of the magnetic Bragg peaks at  $(1/2, 1/2, 0)$  and  $(1/2, 1/2, 1)$ , which correspond to the two  $q$ -vectors of  $(1/2, 1/2, 0)$  and  $(1/2, -1/2, 0)$  respectively. Similarly to the magnetization and resistivity measurements with the uniaxial stress, we observed significant uniaxial-stress dependence of the intensity only in the AF1 phase. Specifically, the magnetic scattering corresponding to the  $q$ -vector of  $(1/2, -1/2, 0)$  completely suppressed by the application of uniaxial stress, demonstrating that the system exhibits a single-domain AF1 phase under uniaxial stress. Interestingly, the magnetic Bragg peak at  $(1/2, 1/2, 1)$  reappeared in the AF2 phase even in the finite uniaxial stress. In addition, the temperature dependence of the magnetic peak at  $(1/2, 1/2, 1/2)$ , which is characteristic of the AF2 phase, was not affected by the uniaxial stress. These observations mean that the AF2 phase indeed has the multi- $q$  magnetic order with fourfold symmetry. This is also consistent with the fact that the bulk properties of the AF2 phase are insensitive to the uniaxial stress. We also performed neutron inelastic scattering experiments and determined the exchange interactions between the magnetic moments. We calculated the exchange energies for the AF1

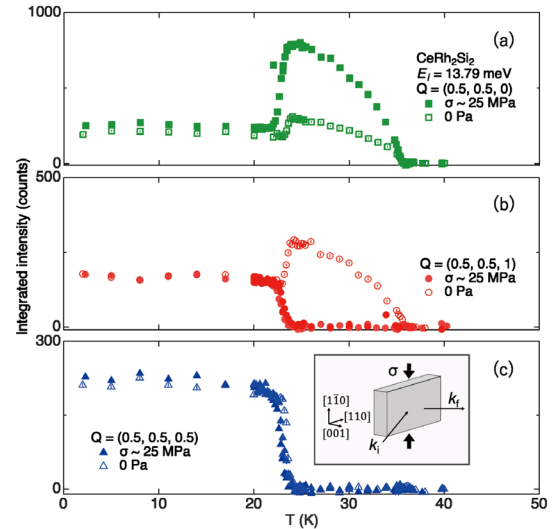


Fig. 2. Temperature dependence of integrated intensity at  $\sigma = 0$  and  $\sim 25$  MPa at  $Q =$  (a)  $(1/2, 1/2, 0)$ , (b)  $(1/2, 1/2, 1)$ , and (c)  $(1/2, 1/2, 1/2)$ , respectively. Open (closed) symbols are the data at  $\sigma = 0$  Pa ( $\sim 25$  MPa). The experimental geometry is shown in inset of (c).  $k_i$  and  $k_f$  indicate the incident and reflection neutron, respectively.

and AF2 phases and found that they are equal. By introducing the biquadratic interaction term mentioned above, the degeneracy is lifted, and the multi- $q$  state is stabilized as the ground state. The present results demonstrated that the biquadratic term, which was originally introduced to explain the SkLs in centrosymmetric magnets, is also applicable to collinear commensurate multi- $q$  orders. We also emphasize here that an application of uniaxial stress is quite useful to investigate magnetic materials exhibiting both single- $q$  and multi- $q$  orders.

## References

- [1] S. Mühlbauer *et al.*, Science **323**, 915 (2009).
- [2] T. Kurumaji *et al.*, Science **365**, 914 (2019).
- [3] S. Hayami *et al.*, Phys. Rev. B **95**, 224424 (2017).
- [4] H. Saito *et al.*, Phys. Rev. B **108**, 094440 (2023).
- [5] S. Kawarazaki *et al.*, Phys. Rev. B **61**, 4167 (2000).

## Authors

H. Saito, F. Kon<sup>a</sup>, H. Hidaka<sup>a</sup>, H. Amitsuka<sup>a</sup>, C. Kwanghee<sup>b</sup>, M. Hagihala<sup>b</sup>, T. Kamiyama<sup>b</sup>, S. Itoh<sup>b</sup>, and T. Nakajima<sup>a</sup>  
<sup>a</sup>Hokkaido University  
<sup>b</sup>KEK-IMSS

## Stiff and Tough Ion Gels for Electrolyte Membranes of Flexible Batteries

Mayumi Group

Gel electrolytes consist of polymer network and ion-conductive liquids as solvent. Due to their flexibility, they have been applied for electrolyte membranes of flexible Li ion batteries that can be attached to our skin or clothing. Electrolyte membranes require a high elastic modulus to prevent Li metal crystals from growing at the electrode surface during charging and discharging, causing a short circuit in the batteries. Previous research has reported that the formation of lithium metal crystal is suppressed for electrolyte membranes with an elastic modulus of 10 MPa or more. In addition, to prevent crack growth during repeated deformation of flexible batteries, gel electrolyte membranes need to exhibit high fracture toughness. For conventional gel electrolytes, polymer crystallization was used to increase stiffness. However, hard gel electrolytes tend to become

# Hyperoctagon Cobalt Oxalate MOF as a Platform for Kitaev Spin Liquid Physics

Kindo, Yamashita, and Yamaura Groups

Water becomes vapor or ice when the temperature changes. In the same way, spins change the state and exhibit various magnetic properties when the environment such as temperature and magnetic field changes. Generally, at sufficiently low temperatures, the orientation of the spins aligns like a solid. On the other hand, a state where the spins are not ordered down to the lowest temperatures, despite the presence of sizable interactions between the spins to order their orientations, can be viewed as a liquid state that does not solidify. Such a state is called a quantum spin liquid and has attracted condensed matter physicists as a new state of matter. The most promising theoretical model for realizing a quantum spin liquid state is the honeycomb lattice model proposed by Kitaev [1]. A worldwide research competition involving both physics and chemistry communities is underway to create a material that realizes the Kitaev's honeycomb model. Thus far, simple inorganic compounds with a two-dimensional honeycomb lattice and their derivatives have been studied exhaustively. On the other hand, it has been pointed out that there are small number of variations of materials and the effect of disorder can be problematic in the layered compounds. Therefore, the development of materials from a new perspective has been desired.

We focus on a three-dimensional honeycomb lattice called a hyperoctagonal lattice realized in a Metal Organic Framework (MOF), which has been studied as an ionic conductor previously. In this MOF, metal ions are linked by the oxalic acid molecules to form a three-dimensional network. A similar situation was theoretically studied in 2017 by M. Yamada, H. Fujita, and M. Oshikawa in the Institute for Solid State Physics at the University of Tokyo, who proposed the realization of a quantum spin liquid [2]. However, no experimental studies have been conducted to date. We selected cobalt as the magnetic element because the effect of the spin-orbit coupling is prominent. We synthesized the crystals of the MOF and investigated the magnetic properties down to low temperatures and in the strong magnetic fields [3].

Our experiments revealed that the MOF with a hyperoctagonal lattice exhibits various spin states as the temperature and magnetic field change. In particular, as the temperature is lowered, a peculiar intermediate temperature state where the spins are not ordered appears, despite the fact that interactions between spins are active. Interestingly, the entropy of the spin is released by about a half around the intermediate temperature region, which is similar to the behavior expected in the theory. This interesting magnetic property should be attributed to the unique cobalt network connected

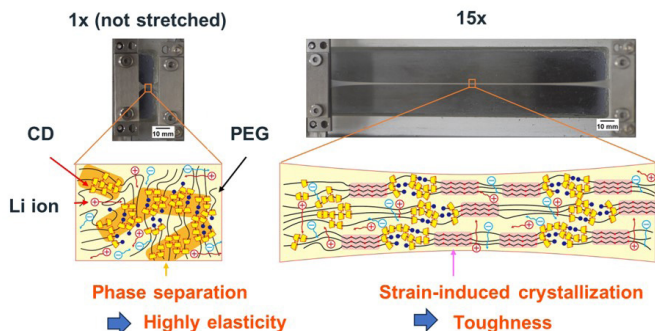


Fig. 1. Phase-separation and strain-induced crystallization of stiff and tough gel electrolyte

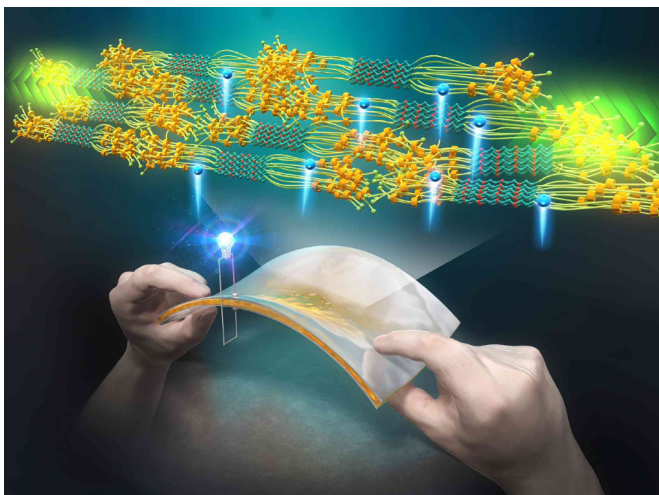


Fig. 2. Schematic illustration of flexible battery containing a stiff and tough gel electrolyte membrane.

brittle, and it has been difficult to achieve both stiffness and toughness. Although various high-strength gel electrolytes have been developed, no gel electrolytes achieved high elastic modulus (over 10 MPa) and fracture toughness. In our laboratory, by combining phase separation and strain-induced crystallization, we have succeeded in developing a gel electrolyte that exhibit a high elastic modulus of over 10 MPa and high toughness of about 100 MJ/m<sup>3</sup> (Fig. 1) [1]. When our gel electrolyte is deformed, stretched polymer chains form crystals, which improves the mechanical toughness [2]. To homogenize chain deformation in the gel electrolytes, we used slide-ring (SR) network in which polymer chains are connected by ring molecules. The ring molecules of the SR network are aggregated to form a hard continuous phase, which resulted in a high elastic modulus (70 MPa). Our gel electrolytes are sufficiently stiff to prevent short circuits during charging and discharging of the batteries, and are also tough enough to withstand repeated deformation, which leads to improved durability of flexible batteries (Fig. 2).

## References

- [1] K. Hashimoto, T. Shiwaku, H. Aoki, H. Yokoyama, K. Mayumi, and K. Ito, *Sci. Adv.* **9**, eadi8505 (2023).
- [2] C. Liu, N. Morimoto, L. Jiang, S. Kawahara, T. Noritomi, H. Yokoyama, K. Mayumi, and K. Ito, *Science* **372**, 1078 (2021).

## Author

K. Mayumi

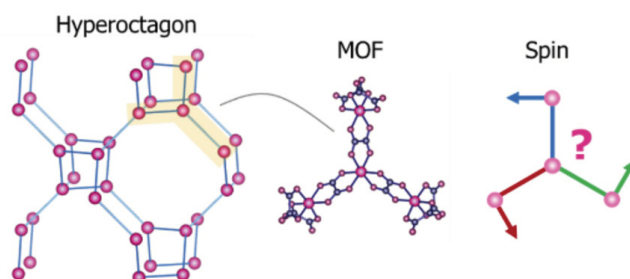


Fig. 1. (Left) Hyperoctagon lattice in the cobalt oxalate MOF. (Right) Image of the quantum spin liquid state.

by the oxalic acid molecules, which generates the magnetic interactions to align the spins in different directions for each bonding direction of the hyperoctagon lattice.

It has been proposed that the properties of the quantum spin liquids can be used to perform quantum computation. Our results represent a totally new direction in the development of materials that can be the platform for the quantum computation. The development of MOFs is expected to accelerate the development of materials of the research area.

#### References

- [1] A. Kitaev, *Ann. Phys. (Amsterdam)* **321**, 2 (2006).
- [2] M. G. Yamada, H. Fujita, and M. Oshikawa, *Phys. Rev. Lett.* **119**, 057202 (2017).
- [3] H. Ishikawa, S. Imajo, H. Takeda, M. Kakegawa, M. Yamashita, J. Yamaura, and K. Kindo, *Phys. Rev. Lett.* **132**, 156702 (2024).

#### Authors

H. Ishikawa, S. Imajo, H. Takeda, M. Kakegawa, M. Yamashita, J. Yamaura, and K. Kindo

## Quantum Liquid-Quantum Liquid Transition in a Strong Magnetic Field

### Kindo and Tokunaga Groups

In recent years, quantum liquids of quasiparticles, which are disordered states by quantum fluctuations, has attracted much attention. The similarities and differences between quantum and classical liquids are an interesting topic. In the case of classical liquids, the absence of order typically suggests the existence of only a single liquid phase. However, some anomalous molecules, such as H<sub>2</sub>O, which have locally stable structures, exhibit multiple liquid phases, and liquid-liquid phase transitions have been observed. Due to the involvement of various degrees of freedom in liquid-liquid transitions, its complete understanding is still elusive. For quantum liquids, it has not even been clear whether a quantum liquid state can exhibit athermal transition to a distinctly different quantum liquid state.

We have investigated the organic charge-transfer complex, TTF-QBr<sub>3</sub>I (tetrathiafulvalene-2-iodo-3,5,6-tri-bromo-*p*-benzoquinone) that simultaneously exhibits ferroelectric and spin-Peierls (FSP) transition at 5.6 K. As the one-dimensional alternate stack of ionic TTF (cation) and QBr<sub>3</sub>I (anion) molecules, spin solitons are excited as topological defects in the FSP ordered state, as shown in Fig. 1. Our earlier research in zero magnetic field [1] demonstrated that spin solitons traverse potential barriers by quantum tunneling even at extremely low temperatures. In this study [2], we performed magnetization, dielectric property, and ultrasound measurements of this salt in pulsed high magnetic fields. Given the density and dynamics of spin

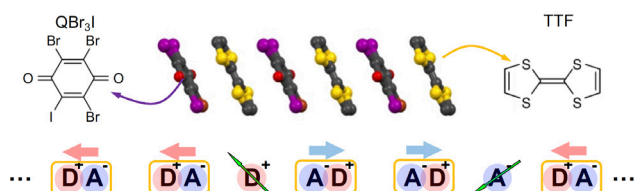


Fig. 1. Schematic illustration of one-dimensional chain of TTF and QBr<sub>3</sub>I molecules and creation of spin solitons at the domain walls in the ferroelectric spin-Peierls (FSP) state. Green arrows represent spins, while the site colors indicate the ion type (red: cation, blue: anion). Thick arrows show the electric polarization of the dimers.

solitons, we demonstrated that these solitons can be regarded as a quantum liquid at zero field. TTF-QBr<sub>3</sub>I positions near the quantum critical point in its electronic phase diagram, and the FSP state is strongly influenced by strong quantum fluctuations. We revealed that the quantum liquidity originates from the developed quantum fluctuations.

When a strong magnetic field of 40 T is applied, an anomaly was observed in all measured physical quantities, indicating the emergence of an additional FSP state. In the case of a conventional spin-Peierls state, the strong Zeeman effect leads to a transition to an incommensurate state with an emergent distortion wave vector, known as the soliton-lattice state. Given this analogy, the solidification of solitons due to the lattice formation would be expected. Nevertheless, our results suggested that the presence of the strong quantum fluctuations in TTF-QBr<sub>3</sub>I preclude the formation of such a soliton lattice, causing the dense solitons to remain in a quantum-mechanically melted state even in high magnetic fields. Namely, the observed transition indicates the realization of a quantum liquid-quantum liquid transition of topological particles by the application of a strong magnetic field.

Even in classical liquids, since liquid-liquid phase transitions appear only in anomalous systems, their origins are still mysterious. In this study, we have for the first time discovered the phenomenon where quasiparticles drifting quantum mechanically undergo a phase transition from one quantum liquid state to another under the influence of a magnetic field. This discovery not only represents a novel phenomenon but also holds potential to contribute to the understanding of classical liquids.

#### References

- [1] S. Imajo, A. Miyake, R. Kurihara, M. Tokunaga, K. Kindo, S. Horiuchi, and F. Kagawa, *Phys. Rev. B* **103**, L201117 (2021).
- [2] S. Imajo, A. Miyake, R. Kurihara, M. Tokunaga, K. Kindo, S. Horiuchi, and F. Kagawa, *Phys. Rev. Lett.* **132**, 096601 (2024).

#### Authors

S. Imajo, A. Miyake<sup>a</sup>, R. Kurihara<sup>b</sup>, M. Tokunaga, K. Kindo, S. Horiuchi<sup>c</sup>, and F. Kagawa<sup>d,e</sup>

<sup>a</sup>Tohoku University

<sup>b</sup>Tokyo University of Science

<sup>c</sup>AIST

<sup>d</sup>Tokyo Institute of Technology

<sup>e</sup>RIKEN CEMS

## Discovery of superconductivity in La<sub>2</sub>IOs<sub>2</sub> with 5d Honeycomb Lattice

### Kindo Group

5d transition metal compounds have gained considerable interest in the condensed matter community in the last decade. The combination of strong spin-orbit coupling and Coulomb interactions may stabilize a Mott insulating state with nontrivial ground states such as a quantum spin liquid on the honeycomb lattice. In metallic compounds, the spin-orbit coupling and electron-electron interactions may cause a Fermi surface instability that gives rise to various electronic orders and exotic superconductivity.

We focus on the intermetallic compound La<sub>2</sub>IOs<sub>2</sub> with Gd<sub>2</sub>IFe<sub>2</sub>-type, which is known as the intermediate between cluster compounds and intermetallic phases. The crystal structure (Fig. 1) features a two-dimensional slab made of a transition-metal-centered trigonal prism of lanthanum, where

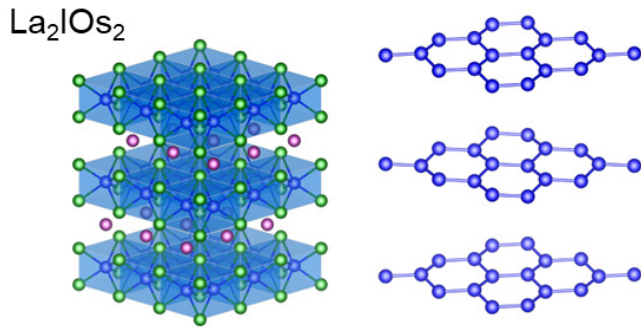


Fig. 1. Crystal structure of  $\text{La}_2\text{IOs}_2$  (left) and the honeycomb lattice of Os (right).

the Os form the honeycomb network. We have prepared the pure polycrystalline and  $\sim 100 \mu\text{m}$  size single crystal samples of  $\text{La}_2\text{IOs}_2$  and investigate its physical properties by the resistivity, torque, and specific heat measurements.

We have demonstrated the bulk superconductivity at  $T_c = 12 \text{ K}$  in  $\text{La}_2\text{IOs}_2$  by the physical property measurements. Despite the heavy constituent elements, which are generally unfavorable for a phonon mediated mechanism,  $T_c$  is the highest among lanthanoid iodides made of lighter elements such as  $\text{La}_2\text{IRu}_2$  with  $T_c = 4.8 \text{ K}$ . Moreover, electronic anomalies are observed at 60 K and 30 K, which are similar to those observed in isostructural  $\text{La}_2\text{IRu}_2$  at 140 K and 85 K, pointing to the presence of the common electronic instability inherent to the  $\text{Gd}_2\text{IFe}_2$ -type crystal structure. We consider the fluctuations relevant to the electronic instability enhances the superconductivity in  $\text{La}_2\text{IOs}_2$ , while this point should be clarified in the future work. Furthermore, we observed that the superconductivity is robust against the magnetic field especially when the magnetic field is applied parallel to the honeycomb layer. We observed zero resistivity at least up to 12 T and the estimated upper critical field is around 40 T.

Our discovery indicates that  $\text{La}_2\text{IOs}_2$  is a layered  $5d$  electron system providing a platform to investigate the interplay between the electronic anomaly, superconductivity, and strong magnetic field. Further investigations to understand the superconducting pairing mechanism and the origin of the unusual properties are ongoing. Besides the interest from the physical perspective, our first-principles electronic structure calculations reveal the effective valence of Os is  $-1$ , indicating the Os is anionic. Examples of transition metal anions in solids are limited to a few intermetallic compounds including platinum or gold. Exploring the  $d$ -electron physical properties of relative compounds with anionic transition metals are also of interest.

#### References

[1] H. Ishikawa, T. Yajima, D. Nishio-Hamane, S. Imajo, K. Kindo, and M. Kawamura, Phys. Rev. Materials 7, 054804 (2023)

#### Authors

H. Ishikawa, T. Yajima, D. Nishio-Hamane, S. Imajo, K. Kindo, M. Kawamura<sup>a</sup>

<sup>a</sup>Information Technology Center, University of Tokyo

## Possible Intermediate Quantum Spin Liquid Phase in $\alpha\text{-RuCl}_3$ under High Magnetic Fields up to 100 T

Y. Matsuda and Kindo Group

Quantum spin liquid (QSL) constitutes a topological state of matter in frustrated magnets, where the constituent spins remain disordered even down to absolute zero temperature and share long-range quantum entanglement. Due to the lack of rigorous QSL ground states, such ultra quantum spin states are less well-understood in systems in more than one spatial dimension before Alexei Kitaev introduced the renowned honeycomb model with bond-dependent exchange.

The  $4d$  spin-orbit magnet  $\alpha\text{-RuCl}_3$  has been widely accepted as a prime candidate for Kitaev material. This compound is now believed to be described by the  $K\text{-}J\text{-}\Gamma\text{-}\Gamma'$  effective model that includes the Heisenberg  $J(1, 3)$ , Kitaev exchange  $K$ , and the symmetric off-diagonal exchange terms. The Kitaev interaction originates from chlorine-mediated exchange through edge-shared octahedra arranged on a honeycomb lattice. Similar to most of Kitaev candidate, additional non-Kitaev terms, unfortunately, stabilize a zigzag antiferromagnetic order below  $T_N \approx 7 \text{ K}$  in the compound. Given that, a natural approach to realizing the Kitaev QSL is to suppress the zigzag order by applying magnetic fields to the compound.

Recently, the theoretical studies point out an interesting two-transition scenario with a field-induced intermediate QSL phase under the out-of-plane magnetic field [1], which is later confirmed by a large Kitaev-term spin Hamiltonian also based on the  $K\text{-}J\text{-}\Gamma\text{-}\Gamma'$  model [2]. With the precise model parameters determined from fitting the experimental thermodynamics data, they theoretically reproduced the suppression of zigzag order under the 7-T in-plane field, and find a gapless QSL phase located between two out-of-plane transition fields that are about 35 T and of 100-T class, respectively. However, because theoretical studies predict very high critical fields—where  $H_c^l \approx 32.5 \text{ T}$  and  $H_c^h$  is in 100-T range—they are challenging to observe experimentally.

In this work, we report the magnetization ( $M$ ) process of  $\alpha\text{-RuCl}_3$  by applying magnetic fields ( $H$ ) in various

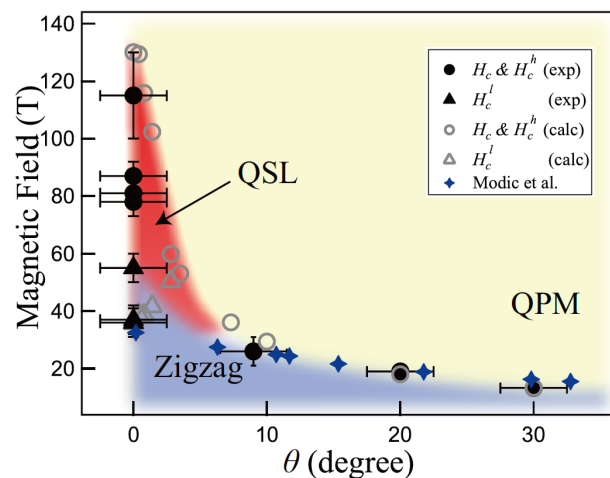


Fig. 1. The field-angle phase diagram that summarizes the values of transition fields determined from both the experimental (black solid markers) and the calculated (grey open ones)  $H_c$ ,  $H_c^l$  and  $H_c^h$ . We also plot the low-field results (blue stars) taken from ref. [3] as a supplement. The zigzag antiferromagnetic, quantum paramagnetic (QPM), and the quantum spin liquid (QSL) phases are indicated. Here,  $H_c$  denotes the critical field from zigzag order to the QPM state,  $H_c^l$  indicates the transition from zigzag order to the QSL phase, and  $H_c^h$  represents the critical field from the QSL to the QPM state.

directions within the honeycomb plane and along the  $c^*$  axis (out-of-plane) up to 100 T, and find clear experimental evidence supporting the two-transition scenario. Here, the  $c^*$  axis is the axis perpendicular to the honeycomb plane. Under fields applied along and close to the  $c^*$  axis, an intermediate phase is found bounded by two transition fields  $H_C^l$  and  $H_C^h$ . In particular, besides the previously reported  $H_C^l \approx 32.5$  T [3], remarkably we find a second phase transition at a higher field  $H_C^h$  (higher than 83 T) [4]. Below  $H_C^h$  and above  $H_C^l$  there exists an intermediate phase, i.e. the predicted field-induced QSL phase. When the field tilts an angle from the  $c^*$  axis by  $9^\circ$ , only the transition field  $H_C$  is observed, indicating the intermediate QSL phase disappears. Accordingly, we also perform the density-matrix renormalization group (DMRG) calculations based on the previously proposed  $K$ - $J$ - $\Gamma$ - $\Gamma'$  model of  $\alpha$ - $\text{RuCl}_3$ , and find the simulated phase transitions and extended QSL phase are in agreement with experiments. Therefore, we propose a complete field-angle phase diagram (as shown in Fig. 1) and provide the experimental evidence for the field-induced QSL phase in the prominent Kitaev compound  $\alpha$ - $\text{RuCl}_3$  [4].

## References

- [1] J. S. Gordon, A. Catuneanu, E. S. Sørensen, and H.-Y. Kee, Nat. Commun. **10**, 2470 (2019).
- [2] H Li, HK Zhang, J Wang, HQ Wu, Y Gao, DW Qu, ZX Liu, SS Gong, and W Li, Nat. Commun. **12**, 4007 (2021).
- [3] K. A. Modic, Ross D. McDonald, J. P. C. Ruff, M. D. Bachmann, Y. Lai, J. C. Palmstrom, D. Graf, M. K. Chan, F. F. Balakirev, J. B. Betts, G. S. Boebinger, M. Schmidt, M. J. Lawler, D. A. Sokolov, P. J. W. Moll, B. J. Ramshaw, and A. Shekhter, Nature Physics, **17**, 240 (2021)
- [4] Peer Review File of Nature Communications, **14**(1), 5613 (2023).
- [5] X.-G. Zhou, H. Li, Y. H. Matsuda, A. Matsuo, W. Li, N. Kurita, G. Su, K. Kindo, H. Tanaka, Nature Communications, **14**, 5613 (2023).

## Authors

X.-G. Zhou, H. Li<sup>a</sup>, Y. H. Matsuda, A. Matsuo, W. Li<sup>a</sup>, N. Kurita<sup>b</sup>, G. Su<sup>a</sup>, K. Kindo, H. Tanaka<sup>b</sup>  
<sup>a</sup>Chinese Academy of Sciences  
<sup>b</sup>Tokyo Institute of Technology

# Double-Peak Specific Heat Anomaly in Quantum Oscillation

Kohama Group

Quantum oscillation phenomenon is an essential tool for understanding the electronic structure of a metal. The origin of the quantum oscillation is the Landau quantization of the carrier motion, which gives rise to a series of quantized singularities in the density of states (DOS) that cross the Fermi level. The Lifshitz–Kosevich (LK) theory has been widely used to describe the behavior of the quantum oscillation, notably to extract parameters such as the effective mass and Landé g-factor. Although the theory is remarkably successful in the most of metals over a wide range of magnetic fields and temperatures, there is growing evidence to suggest that experiment often deviates from the predicted LK behavior [1]. Although the oscillatory magnetoresistance, magnetization, and thermopower exhibit a clear departure from LK theory at the high-magnetic field limit called the quantum limit, the oscillatory behavior of the specific heat ( $C_p$ ) in the quantum limit has yet to be fully explored. In this research, we have measured  $C_p$  of graphite as a function of the magnetic field and demonstrated that the crossing of a single spin Landau level and the Fermi energy gives rise to a double-peak structure in  $C_p$ , in striking contrast to the single-

peak expected from LK theory.

When a Landau level crosses the Fermi energy, the occupation of the Landau level changes rapidly, inducing large changes in the entropy of the system, which can be probed using thermodynamic measurements, such as magnetocaloric effect (MCE) and  $C_p$ . To follow the evolution of the entropy in a metal sample, we show the MCE trace ( $1/T$ ) of the natural graphite as a function of the magnetic field taken at an initial temperature of 0.7 K (Fig. 1a). The entropy is proportional to the logarithm of the number of states within the Fermi edge, and therefore shows a maximum when a Landau level is located at the Fermi level, resulting in a series of well-defined single peaks labeled as  $N^{\pm}_{e=h}$  (see Fig. 1a). Here,  $N$  is the Landau index,  $e/h$  indicates if the Landau level originates from the electron or hole pocket, and  $\pm$  indicate the spin up/down levels. For better comparison, Fig. 1b shows background removed magnetoresistance  $\Delta R_{xx}$  at 0.5 K. These results are in stark contrast to the electronic specific heat divided by temperature  $C_{el}/T$  which is proportional to the temperature derivative of entropy (Fig. 1c). Crucially, when low-index Landau levels ( $N_{e/h} < 3$ ) cross the Fermi energy,  $C_{el}/T$  exhibits a series of double-peak structure, as indicated by the double arrows in Fig. 1c.

In order to elucidate the origin of the double-peak structure, it is necessary to consider the exact expression for the specific heat. For electronic quasiparticles,  $C_{el}/T$  is given by,  $C_{el}/T = k_B^2 \int_{-\infty}^{\infty} D(E) \left( -x^2 \frac{dF(x)}{dx} \right) dx$ , where  $F(x) = 1/(1 + e^x)$ ,  $x = E/k_B T$  and  $k_B$  is the Boltzmann constant. The specific heat depends on the convolution of the Landau level DOS  $D(E)$  and a kernel term  $-x^2 dF(x)/dx$ , which involves the first derivative of the Fermi-Dirac distribution function. Importantly, the double-peak structure in  $C_{el}/T$  originates from the temperature-dependent splitting of the double maxima in the kernel term  $-x^2 dF(x)/dx$ . In Ref. 2, we show that there is a quantitative agreement between the observed double-peak structure and calculated  $C_{el}/T$  curve.

In summary, we demonstrate that, as the quantum limit is approached in high-quality graphite, Landau levels crossing the Fermi energy give rise to single features in MCE and magnetoresistance, while simultaneously a novel double-peak structure is observed in the specific heat  $C_{el}/T$ . The

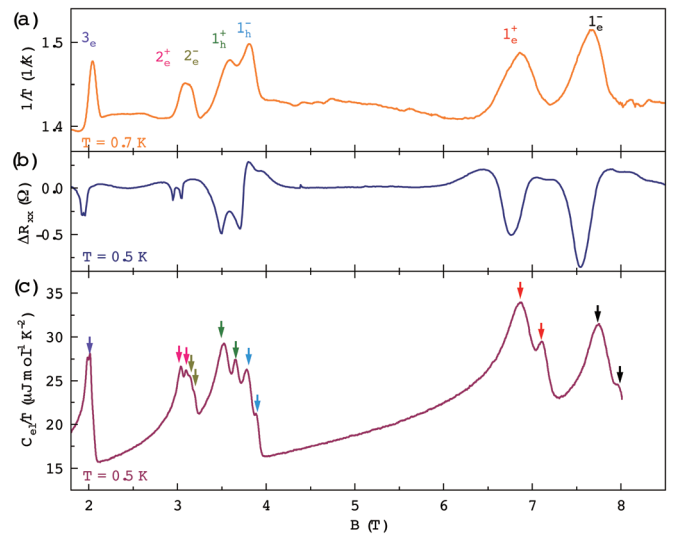


Fig. 1. Comparison of quantum oscillations in MCE, resistivity and specific heat. (a) Reciprocal temperature ( $1/T$ ) of graphite as a function of applied magnetic field in a quasi-adiabatic condition. (b) Background removed resistance as a function of magnetic field. (c) Field sweep electronic specific heat divided by temperature.

calculation based on the exact form of the free electron expression successfully reproduces the double-peak structure in specific heat. The specific heat, which depends on an integral involving the kernel term, represents a spectroscopic tuning fork of width  $4.8 k_B T$  that can be tuned at will to resonance.

## References

- [1] A. E. Datars and J. E. Sipe, Phys. Rev. B **51**, 4312 (1995).  
 [2] Z. Yang, B. Fauqué, T. Nomura, T. Shitaokoshi, S. Kim, D. Chowdhury, Z. Pribulová, J. Kačmarčík, A. Pourret, G. Knebel, D. Aoki, T. Klein, D. K. Maude, C. Marceat, and Y. Kohama, Nature Communications **14** 7006 (2023).

## Authors

Y. Kohama and Z. Yang

# Quasi-Periodic Growth of One-Dimensional Copper Boride on Cu(110)

## I. Matsuda, Hasegawa, and Oshikawa Groups

A surface, located between a vacuum and a crystal substrate, forms a unique two-dimensional (2-D) lattice. By depositing atoms on the surfaces, adsorbate overlayers grow commensurately or incommensurately with respect to the substrate 2-D lattice, depending on a balance between adsorbate-adsorbate and adsorbate-substrate interactions. Such a degree of freedom, being specific to the surface system, results in formation of exotic long-range ordered phases, so-called surface superstructures or Moiré patterns. The unique environment has recently developed new research fields, such as twistrionics, and has provided a space to examine interface materials that cannot be explored in a pure 2-D system. One of the notable findings is a long-range ordered layer of copper boride (Cu-Boride) that was grown incommensurately on the (111) surface of a *fcc* copper crystal. This was unexpected since it has been known that the bulk boron hardly forms compounds with the Group-11 elements. Structural analysis by diffraction unveiled that the 2-D copper boride on Cu(111) was composed of an alternating array of atomic boron and copper chains. This has indicated an intriguing relationship between the 2-D and 1-D atomic structures at the surface. Since the (110) surface of a *fcc* copper crystal is the well-known 1-D template in surface science, one can expect formation of a unique 1-D system at the B/Cu(110) surface.

In the present research, we experimentally examined a Cu(110) surface after boron deposition and discovered a new ordered phase,  $3 \times 1'$  by low-energy electron diffraction[1]. In the following observation by scanning tunneling microscope, we found that the  $3 \times 1'$ -B/Cu(110) surface has a 1-D atomic structure of Cu-Boride [1,2]. As shown in an STM image of the  $3 \times 1'$  phase (Fig. 1(a)), the 1-D structures grow along the  $[1\bar{1}0]$  axis, separated by trenches. The 1.1-nm trench interval corresponded to  $3a_{[001]}$ , where  $a_{[001]}$  is a size of the Cu(110) unit cell along the  $[001]$  axis. This indicates the origin of the three-fold periodicity of the  $3 \times 1'$ -B phase. The 1-D structure is composed of two types of unit lengths along the 1-D direction, one commensurate and the other incommensurate with respect to the substrate lattice. A Fourier transform spectrum shows apparent signals that are ascribed to the two wavenumber units,  $a$  and  $b$ , along the 1-D direction. In the regular crystal, the number of a rank is mathematically equal to the number of dimensions of the

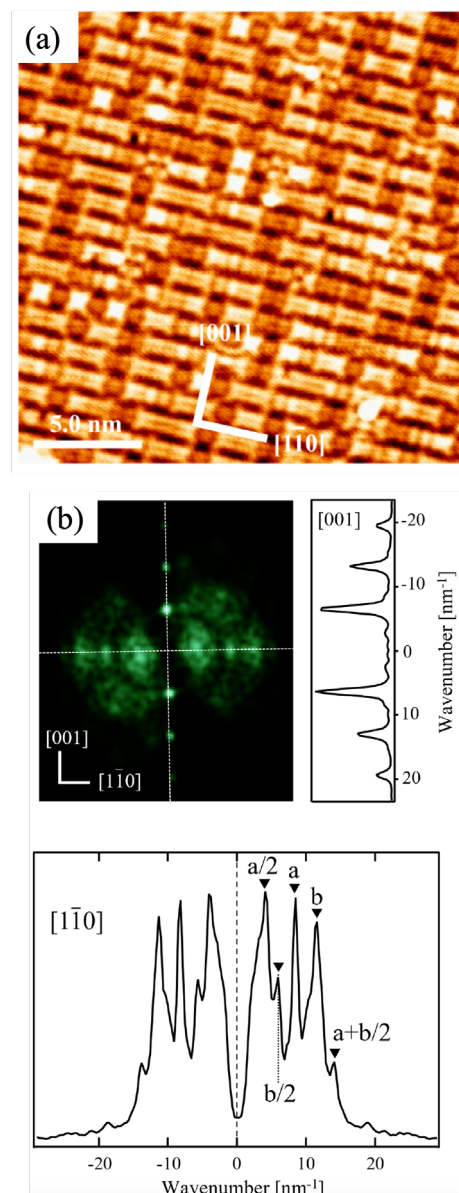


Fig. 1. Quasi-periodic 1-D structure in the B/Cu(110) system. (a) A scanning tunneling microscopy image ( $20 \times 20 \text{ nm}^2$ , tunneling current : 100 pA, Bias : 1.5 V). (b) The 2-D power spectrum obtained by fast Fourier transform with line profiles crossing the origin in  $[001]$  and  $[1\bar{1}0]$  direction.

structure due to its translational symmetry. When the rank is higher than the dimension of the structure, the structure is called quasi-periodic. The two vectors, given in Fig.1(b), cannot be described by one another. The existence, thus, verifies the quasi-periodicity of the 1-D system. Namely, we can designate that the B/Cu(110) surface as an array of quasi-periodic chains[2]. Such a long-range 1-D quasi-periodic surface structure has been modeled as a 1-D quasi-crystal and the structural parameters, obtained experimentally, satisfied formation conditions predicted by the theory [2]. This system provides an actual interface material to examine 1-D quasicrystals.

## References

- [1] Y. Tsujikawa, X. Zhang, M. Horio, T. Wada, M. Miyamoto, T. Sumi, F. Komori, T. Kondo, and I. Matsuda, Surf. Sci. **732**, 122282 (2023).  
 [2] Y. Tsujikawa, X. Zhang, K. Yamaguchi, M. Haze, T. Nakashima, A. Varadwaj, Y. Sato, M. Horio, Y. Hasegawa, F. Komori, M. Oshikawa, M. Kotsugi, Y. Ando, T. Kondo, and I. Matsuda, Nano Letters **24**, 1160 (2024).

## Authors

Y. Tsujikawa, I. Matsuda

# Nondestructive Visualization of Breakdown Process in Ferroelectric Capacitors Using in situ Laser-Based Photoemission Electron Microscope

Okazaki and Kobayashi Groups

HfO<sub>2</sub>-based ferroelectrics are one of the most actively developed functional materials for memory devices because of its high scalability and compatibility with complementary metal-oxide-semiconductor (CMOS) technology and with back-end-of-line (BEOL) process [1]. In HfO<sub>2</sub>-based ferroelectric devices, dielectric breakdown is a main failure origin during repeated polarization switching. Elucidation of the breakdown process may broaden the scope of applications for the ferroelectric HfO<sub>2</sub>.

*In situ* laser-based photoemission electron microscope (laser-PEEM) has emerged as a powerful technique for studying dynamic processes in materials and devices at the nanoscale. By a laser with an energy comparable to the typical work function of materials, we can observe a bulk electronic structure over the depth of 50 nm [2]. This allows to reveal the chemical-state distribution in a dielectric embedded through a top electrode, nondestructively.

This report presents nondestructive analyses of HfO<sub>2</sub>-based ferroelectric capacitors using a laser-PEEM system with an *in situ* voltage application and characterization system.

We fabricated crossbar-type HfO<sub>2</sub>-based metal-ferroelectric-metal (MFM) capacitors on an N<sup>+</sup> Si substrate as shown in Fig. 1. We used Hf<sub>0.5</sub>Zr<sub>0.5</sub>O<sub>2</sub> with 10-nm thickness as a ferroelectric layer which is sandwiched by TiN with 30-nm thickness.

Figure 2(a) shows cycling characteristics of leakage current measured in our *in situ* laser-PEEM system. The leakage current began to increase above the detection limit from  $1 \times 10^6$  cycles. Then, the leakage current reached a local maximum at  $4 \times 10^6$  cycles, which corresponds to a soft dielectric breakdown (SDB). After that, the MFM capacitor was completely metalized at  $7.4 \times 10^6$  cycles, which corresponds to hard dielectric breakdown (HDB). This leakage current behavior during the application of cycling stress has been reported as that of typical of MFM capacitors with HZO [3]. This indicates that the waveform was applied

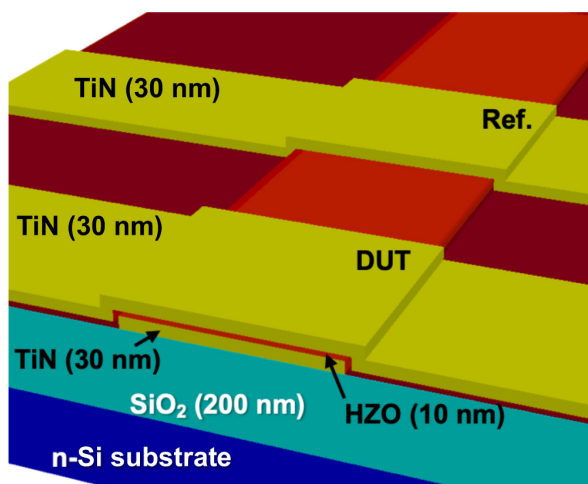


Fig. 1. Structure of the sample used for in situ laser-PEEM measurements. The values in brackets indicate the thickness of each film. DUT and Ref. indicate device under test and reference capacitor, respectively.

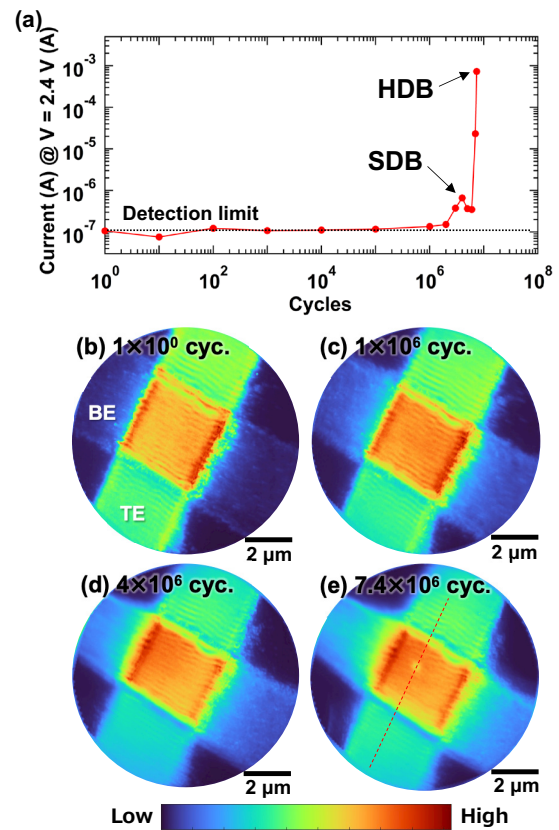


Fig. 2. Breakdown process visualized by in situ laser-PEEM. (a) Leakage current at 2.4 V on return of voltage sweep as a function of stress cycle. (b–e) Dependence of detailed PEEM images focused on the device under test on the number of cycling stresses.

to the MFM capacitor as designed in the source measure unit implemented in our PEEM system and also suggests that damages caused by laser irradiation during the image acquisitions can be regarded as negligible.

Figures 2(b)–(e) show PEEM images taken after  $1 \times 10^6$  cycle,  $1 \times 10^6$  cycles,  $4 \times 10^6$  cycles, and  $7.4 \times 10^6$  cycles, respectively. We found no significant difference between the PEEM image after 1 cycle of the square wave application and that after  $1 \times 10^6$  cycles, except for an increase in intensity from the bottom electrode (BE). However, after applying  $4 \times 10^6$  cycles, the PEEM image shows a slight increase in intensity at the corner of the MFM capacitor. From the PEEM image after HDB (Fig. 2(e)), a low-intensity spot was clearly observed near the center of the capacitor. The appearance of this spot just after the occurrence of HDB indicates that this spot is the conduction filament responsible for HDB. The result that the HDB spot was observed in the flat region is reproducible for the samples with the same dimension. This is because the electric field concentration near the edge of BE is suppressed by the voids incidentally formed at both ends of BE.

Figures 3(a) and 3(b) demonstrate that the HDB spot clearly observed by laser-PEEM is not found in the scanning electron microscope (SEM) image. This indicates that significant structural changes, such as a hillcock formation due to dielectric breakdown induced epitaxy (DBIE) of the top electrode, did not occur. It is also shown that laser-PEEM can observe changes in electronic states deeper than the probing depth of SEM. Furthermore, laser-PEEM can even investigate the electronic states in the regions where HDB and SDB have occurred. The ability to nondestructively observe not only the device topography but also the DOS distribution that dominates the functionality of materials will be indispensable for the research and development and mass

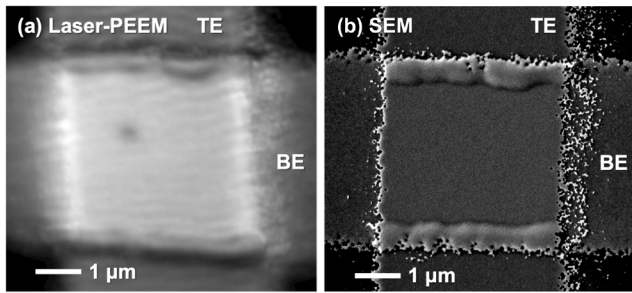


Fig. 3. Comparison of micrographs acquired by laser-PEEM and SEM. (a) PEEM micrograph after HDB, which is a magnified image of Fig. 2(e). TE and BE indicate the top and bottom electrode, respectively. (b) SEM micrograph after HDB of the sample from the *in situ* laser-PEEM experiment. The acceleration voltage was set to 4 kV.

production of devices that implement functional materials.

In summary, we have proposed *in situ* laser-PEEM as a tool for observing the breakdown process of HfO<sub>2</sub>-based MFM capacitors. We observed an increase in photoelectron intensity in a region of the MFM capacitor with the onset of SDB. This corresponds to a precursory defect enhancement of HDB, which has not been clearly observed in previous TEM studies. Furthermore, we have clearly visualized the post-HDB breakdown spot. Ability of laser-PEEM to visualize the DOS distribution will be a key technology for accelerating the control of properties of functional materials and their implementation in CMOS circuits, thereby shortening time to market.

#### References

- [1] M. H. Park, Y. H. Lee, T. Mikolajick, U. Schroeder, and C. S. Hwang, *MRS Commun.* **8**, 795 (2018).
- [2] Y. Okuda, J. Kawakita, T. Taniuchi, H. Shima, A. Shimizu, Y. Naitoh, K. Kinoshita, H. Akinaga, and S. Shin, *Jpn. J. Appl. Phys.* **59**, SGG02 (2020).
- [3] K. Y. Chen, P. H. Chen, R. W. Kao, Y. X. Lin, and Y. H. Wu, *IEEE Electron Device Lett.* **39**, 87 (2018).

#### Authors

H. Fujiwara, Y. Itoya,<sup>a</sup> M. Kobayashi,<sup>a,b</sup> C. Bareille, S. Shin,<sup>c</sup> and T. Taniuchi<sup>d,e</sup>

<sup>a</sup>Institute of Industrial Science, The University of Tokyo

<sup>b</sup>System Design Research Center (d.lab), School of Engineering, The University of Tokyo

<sup>c</sup>Office of University Professor, The University of Tokyo

<sup>d</sup>Material Innovation Research Center (MIRC), The University of Tokyo

<sup>e</sup>Department of Advanced Materials Science, Graduate School of Frontier Sciences, The University of Tokyo



# Joint Research Highlights

## Twisted Bilayer Graphene Reveals its Flat Bands under Spin Pumping

Stacking two graphene layers with a relative twist angle  $\theta$  results in a moiré superstructure which is found to host, in the vicinity of the so-called magic angle  $\theta_M 1.1^\circ$ , unconventional superconductivity and strongly correlated insulating states [1,2]. Such strong electronic correlations originate from the moiré flat bands emerging at the magic angle around the charge neutrality point. The tantalizing signature of the flat bands have been experimentally demonstrated by probing the corresponding peaks of the density of states using transport, electronic compressibility measurements, scanning tunneling microscopy (STM) and spectroscopy (STS). The direct evidence of these flat bands has been reported by angle resolved photoemission spectroscopy (ARPES). However, spectroscopic measurements on magic-angle twisted bilayer graphene (TBG) raise many technical challenges related to the need of an accurate control of the twist angle, and the necessity to have non-encapsulated samples which can degrade in air.

Recently, we proposed a noninvasive method to probe the flat bands of TBG and accurately determine the magic angle [3]. This method is based on spin pumping induced by ferromagnetic resonance, where the increase in the FMR linewidth provides insight into the spin excitations of the

nonmagnetic material adjacent to the ferromagnet. The linewidth increase is given by the Gilbert damping (GD) coefficient.

We theoretically study a planar junction of a ferromagnetic insulator (FI) and a TBG adjacent to a monolayer of transition metal dichalcogenides (TMD), as WSe<sub>2</sub> (TBG/WSe<sub>2</sub>). We show a schematic figure of a FI/TBG planar junction adjacent to WSe<sub>2</sub> under a microwave of a frequency  $\Omega$  in Fig. 1 (a). We consider the case where a microwave of a frequency  $\Omega$  is applied to this junction and focus on the twist angle dependence of the FMR linewidth. We calculated the correction to the Gilbert damping (GD) coefficient, induced by the adjacent heterostructure TBG/WSe<sub>2</sub>. We take into account the relatively strong spin-orbit interaction (SOI) induced by the WSe<sub>2</sub> in TBG.

We formulated the FMR linewidth based on the perturbation method with respect to an interfacial exchange coupling in this setup and discussed its twist angle dependence. We described the heterostructure TBG/WSe<sub>2</sub> by the continuum model including the SOI based on Ref. [4] and evaluated the increase of the effective Gilbert damping coefficient of the FMR linewidth.

In Fig. 1(b) we depicted the behavior of  $\delta\alpha_G$  as a function of the twist angle  $\theta$  for several temperatures for a clean interface. This figure shows that regardless of the temperature range,  $\delta\alpha_G$  increases by decreasing  $\theta$  but drops sharply at the magic angle, where it exhibits a relatively small peak which is smeared out at low temperature. We also discussed the case of a dirty interface and showed that the Gilbert damping correction drops at the magic angle as found in the case of a clean interface.

Our result provides an accurate determination method of the magic angle and an estimation of the SOC induced in TBG by its proximity to the TMD layer. Our proposed setup can be readily implemented regarding the state-of-the-art of the experimental realizations of spin pumping in 2D materials and TBG-based heterostructure. Our work opens the gate to a twist tunable spintronics in twisted layered heterostructures.

This project has been performed as a joint study with Sonia Haddad, who was a visiting professor of ISSP in the academic year 2022.

### References

- [1] Y. Cao *et al.*, Nature, **556**, 80 (2018).
- [2] M. Yankowitz *et al.*, Science **363**, 1059 (2019).
- [3] S. Haddad, T. Kato, J. Zhu, and L. Mandhour, Phys. Rev. B **108**, L121101 (2023).
- [4] H. S. Arora *et al.*, Nature **583**, 379 (2020).

### Authors

S. Haddad<sup>a,b</sup>, T. Kato, J. Zhu<sup>b</sup>, and L. Mandhour<sup>a</sup>  
<sup>a</sup>Université Tunis El Manar  
<sup>b</sup>Max Planck Institute for the Physics of Complex Systems

PI of Joint-use project: S. Haddad  
Host lab: Kato and Osada Groups

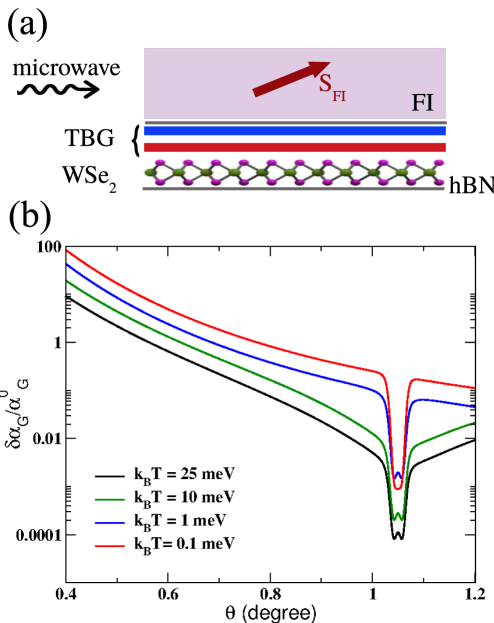


Fig. 1. (a) Schematic representation of the junction between a ferromagnetic insulator (FI) and a heterostructure of a twisted bilayer graphene (TBG) adjacent to a monolayer of WSe<sub>2</sub>. The red arrow indicates the spin orientation of the FI characterized by an average spin. The bottom line represents the boron-nitride (hBN) layers encapsulating the TBG/WSe<sub>2</sub> heterostructure. (b) Increase of the Gilbert damping coefficient,  $\delta\alpha_G$ , as a function of the twist angle at different temperature ranges.

# Element-Specific Cluster Growth on the Two-Dimensional Metal–Organic Network

Solid surfaces provide a platform to fabricate various low-dimensional structures, and the formation of surface-supported two-dimensional metal–organic networks (2D-MONs) based on supramolecular chemistry is also achieved on the substrate. Porous two-dimensional metal–organic network (2D-MON) on a substrate could capture deposited metal atoms and metal clusters growing in the pores of the 2D-MON. Growth of a metal cluster in a pore of the 2D-MON requires that the pore is a local minimum of the potential energy surface, that is, a potential well for the metal adatoms. By arranging nanometer-scale potential wells on the substrate, deposited metal atoms form metal nanoclusters spontaneously.

We investigated the growth of Ag, In, and Pd nanoclusters in the 2D-MON by scanning tunneling microscopy (STM) measurements and density functional theory (DFT) calculations, and found that the growth mechanisms of Ag, In, and Pd clusters in the 2D-MON synthesized from 1,3,5-tris(4-bromophenyl) benzene molecules on Ag(111) are different from each other. From the STM measurement, Ag and Pd clusters grow from the 2D-MON, especially two-coordinated Ag atoms in the 2D-MON. Indium clusters grow in the center of pores. Based on our DFT calculations, the total energy of an adatom in a pore depends on the position of the adatom, and the interaction of Ag and Pd adatoms with the 2D-MON is attractive. On the other hand, the interaction between an In adatom and the 2D-MON is repulsive. Since the net-charges of Ag, In, Pd adatoms on Cu(111), and two-coordinated Ag in the 2D-MON are  $-0.01e$ ,  $0.38e$ , and  $-0.14e$ , and  $0.23e$ , respectively, the electrostatic interaction between In and Pd adatoms and the 2D-MON may play a significant role. For Ag, the DFT calculation without van-der Waals correction results in repulsive interaction with the 2D-MON. We think that van-der Waals interaction plays an important role in the Ag nanocluster formation in the 2D-MON. The growth process of metal clusters is determined by the element-specific behavior of metal adatoms in the pores, taking into account the various interactions with the 2D-MON.

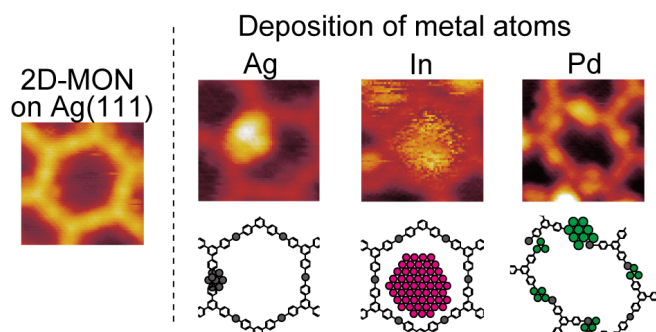


Fig. 1. (Left) An STM image of the 2D-MON on Ag(111). (Right) STM images of Ag (gray), In (red), and Pd (green) clusters on the 2D-MON/Ag(111) surface and their schematic drawings. The size of all STM images is  $4 \text{ nm} \times 4 \text{ nm}$ .

## Reference

[1] N. Tsukahara, R. Arafune, and J. Yoshinobu, *Jpn. J. Appl. Phys.* **63**, 065504 (2024).

## Authors

N. Tsukahara<sup>a</sup>, R. Arafune<sup>b</sup>, and J. Yoshinobu  
<sup>a</sup>National Institute of Technology, Gunma College.  
<sup>b</sup>National Institute for Materials Science

PI of Joint-use project: N. Tsukahara  
 Host lab: Yoshinobu Group

## Y<sub>2</sub>O<sub>3</sub> Phosphor Thin Films

When thin film materials are grown by physical vapor deposition methods, such as sputtering or pulsed laser deposition (PLD), the kinetic energy of the adatoms arriving on the film surface has a significant effect on the crystallinity and defect density of thin films. In the PLD process, the incident adatom kinetic energy can reach 100 eV or more. The kinetic energy is increased at higher ablation laser energy density (laser pulse energy) due to a larger energy transfer from the laser beam to the ablated plasma. The kinetic energy is also dependent on the temporal ablation laser pulse shape. For typical excimer gas lasers, the pulse length is 20 ns, while solid-state garnet (YAG) lasers generate around 4 ns pulses, which means that the pulse rise time is faster for YAG lasers, leading to higher plasma kinetic energies. One of the advantages of PLD is the ability to use a very broad background gas pressure range, from a typical base pressure of  $10^{-8}$  Torr to about 1 Torr. Increasing the process pressure of a background gas, such as oxygen, above 1 mTorr will increase the number of gas-phase collisions between ions in the ablation plume and the ambient gas, reducing the kinetic energy of the plume. However, high-pressure ablation also strongly reduces the growth rate, as many atoms colliding with the ambient gas are deflected from the plume and do not reach the film surface. We have developed an energy-moderated PLD technique using He as a buffer gas in the PLD chamber to reduce the kinetic energy of the plume. Due to the small mass of He, the gas-phase collisions reduce the plasma energy but do not deflect the atoms away from the plume, allowing films to be grown at the desired growth rate, but at a lower incident kinetic energy of deposited atoms, reducing the density of point defects in the film. The point defect density is a particularly serious problem for optical materials, such as phosphors,

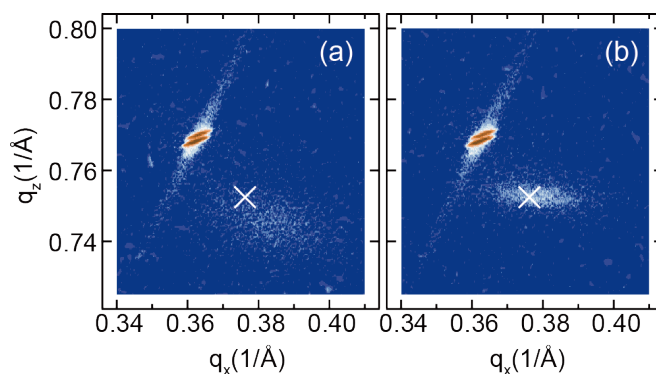


Fig. 1. X-ray reciprocal space maps of Y<sub>2</sub>O<sub>3</sub> films grown on SrTiO<sub>3</sub> at an oxygen pressure of  $10^{-4}$  Torr (a) and in a mixture of  $10^{-4}$  Torr O<sub>2</sub> and 100 mTorr He. The addition of the He buffer increased the film peak intensity, reduced the peak width, and shifted the film peak close to the expected bulk lattice parameter (marked with a white cross).

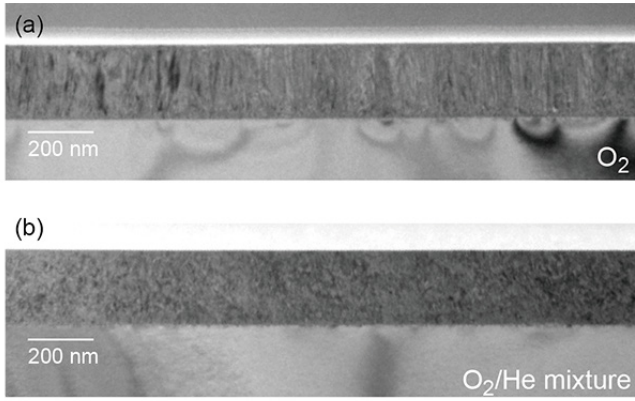


Fig. 2. Cross-sectional transmission electron microscope images of a film grown in oxygen (a), showing distinct columnar grains, and in an oxygen/helium mixture (b), showing that the grain boundaries were eliminated in the presence of the energy-moderating He buffer gas in the PLD chamber.

where defects reduce the intensity and the lifetime of the luminescence signal. We have explored the effect of plume energy moderation on the properties of PLD-grown  $\text{Y}_2\text{O}_3$  phosphors. The effect of the energy moderation can be seen in the x-ray reciprocal space maps of two films (Fig. 1), both grown at an oxygen partial pressure of  $10^{-4}$  Torr. A film grown in a conventional process (Fig. 1a) shows diffuse film scattering that is systematically shifted from the expected lattice parameter (marked with a white cross). When the PLD chamber is additionally filled to 100 mTorr with He, the film peak becomes much narrower and shifts to the expected bulk lattice parameter position, indicating that the crystalline defect density was dramatically reduced by the plume energy reduction. The microstructure change is clearly visible in cross-sectional transmission electron microscope images of films grown in a low-pressure oxygen environment and in the presence of He gas at a pressure of 100 mTorr (Fig. 2). When a  $\text{Y}_2\text{O}_3$  film was grown under conventional conditions, without the He moderator, the film formed columnar grains that extend through the thickness of the film. Such grain boundaries can effectively quench the light output of a phosphor material. This columnar structure was completely eliminated when a film was grown in a He/ $\text{O}_2$  gas mixture at a total pressure of 100 mTorr. Time-of-flight measurements indicated that the kinetic energy of the plume was reduced by a factor of about 7 at 100 mTorr of He. The reduction of the defect density of the films significantly increased the photoluminescence intensity of the Eu-doped yttria phosphor films.

#### References

[1] S. Suzuki, T. Dazai, T. Tokunaga, T. Yamamoto, R. Katoh, M. Lippmaa, and R. Takahashi, *J. Appl. Phys.* **135**, 195302 (2024).

#### Authors

S. Suzuki<sup>a</sup>, T. Dazai<sup>a</sup>, T. Tokunaga<sup>b</sup>, T. Yamamoto<sup>b</sup>, R. Katoh<sup>a</sup>, M. Lippmaa, and R. Takahashi<sup>a</sup>

<sup>a</sup>Nihon University  
<sup>b</sup>Nagoya University

PI of Joint-use project: R. Takahashi  
Host lab: Lippmaa Group

## Spin fluctuations from Bogoliubov Fermi Surfaces in the Superconducting State of S-substituted FeSe

The study of the iron-based superconductor,  $\text{FeSe}_{1-x}\text{S}_x$ , has resulted in various topics. Recently, topologically protected nodal Fermi surfaces, referred to as Bogoliubov Fermi surfaces (BFSs), have garnered much attention [1,2]. A theoretical model for  $\text{FeSe}_{1-x}\text{S}_x$  demonstrated that BFSs can manifest under the conditions of spin-orbit coupling, multi-band systems, and superconductivity with time-reversal symmetry breaking [1]. Here we report the observation of spin fluctuations originating from BFSs via  $^{77}\text{Se}$ -nuclear magnetic resonance (NMR) measurements to 100 mK [3]. We found an anomalous enhancement of low-energy spin fluctuations deep in the superconducting (SC) state for  $x = 0.18$ , which gives evidence for strong Bogoliubov quasiparticles interactions in addition to the presence of BFSs.

We performed  $^{77}\text{Se}$ -NMR measurements using a single crystal for each S-substitution level. Typical size is approximately  $1.0 \times 1.0 \times 0.5$  mm. We applied a magnetic field of 6.0 T parallel to the FeSe planes. Figure 1 shows  $1/T_1T$  below  $T_c$  for several S-substitution levels crossing the nematic quantum critical point,  $x_c \sim 0.17$ . As seen from  $^{77}\text{Se}$ -NMR spectra in Fig. 2, the double-peaks structure observed in the nematic phase disappears above  $x_c$ .  $1/T_1T$  provides a measure of low-energy spin fluctuations and is expressed as  $1/T_1T \propto \sum_{\mathbf{q}} \text{Im} \chi(\mathbf{q})$ , where  $\chi(\mathbf{q})$  is the wave-number ( $\mathbf{q}$ )-dependent susceptibility. The decrease in

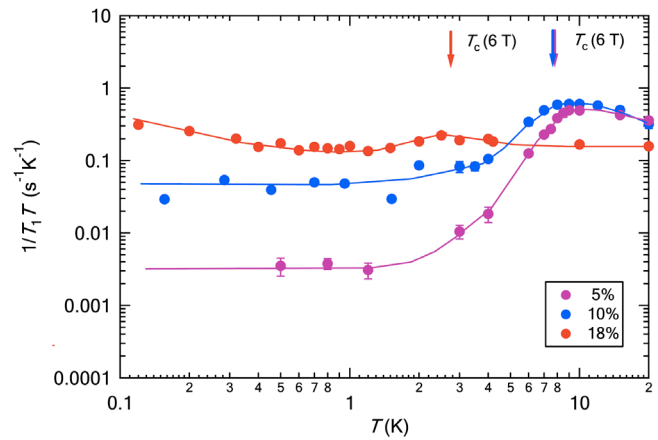


Fig. 1.  $^{77}\text{Se}$ -nuclear relaxation rate divided by temperature,  $1/T_1T$  for  $\text{FeSe}_{1-x}\text{S}_x$  ( $x = 0.05, 0.10$ , and  $0.18$ ) [3]. Arrows indicate superconducting transition temperature ( $T_c$ ) measured at 6.0 T.

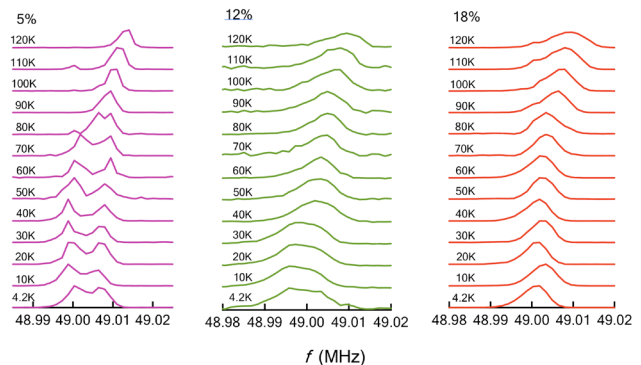


Fig. 2.  $^{77}\text{Se}$ -NMR spectra for  $x = 0.05, 0.12$ , and  $0.18$  [3]. Two peaks appearing for  $x = 0.05$  and  $0.12$  merge into a single peak with increasing S-substitution level over  $x_c (\geq 0.17)$ .

$1/T_1T$  just below  $T_c$  is due to the opening of the SC gap. In conventional clean superconductors,  $1/T_1T$  should decrease to zero with decreasing temperature. However,  $1/T_1T$  for  $x = 0.05$  and  $0.10$  became constant at low temperatures. With further substitution over  $x_c$ ,  $1/T_1T$  exhibited an upturn with decreasing temperature and the values became significantly larger than those for  $x = 0.05$  and  $0.10$ . Upturns of  $1/T_1T$  observed below and above  $T_c$  are exceedingly rare in SC systems. The behavior of  $1/T_1T = \text{constant}$  suggests a residual DOS. In most cases, the following effects may be expected: (1) the impurity effect, (2) the Volovik effect, and (3) the coexistence of SC and normal states. However, the first two cases are ruled out because the values of  $1/T_1T$  change almost one order of magnitude between  $x = 0.05$  and  $0.10$ , and the last case is also ruled out considering the high sample quality. Furthermore, the upturn of  $1/T_1T$  is difficult to be explained by these possibilities. Instead of the coexistence in real space, the coexistence in momentum space such as the formation of BFSs would be promising as shown in Fig. 3. The appearance of BFSs with two-fold rotational symmetry has been observed by laser ARPES measurements [4] and time-reversal-symmetry breaking required for the appearance of BFSs has been suggested from recent  $\mu$ SR measurements [5].

Recently, Y. Cao *et al.* theoretically calculated  $\chi(\mathbf{q})$  and  $1/T_1T$  for the ultranodal states in a minimal two-band model, where the interband non-unitary spin-triplet pairing is responsible for BFSs [6]. In this model, they assumed double hole pockets at the  $\Gamma$  point and BFSs with two-fold rotational symmetry like the schematic diagram shown in Fig. 3. By adding a Hubbard interaction in the particle-hole channel, they found that an enhancement of  $\chi(\mathbf{q})$  at low temperatures at  $\mathbf{q} \sim (0.4\pi, 0)$  connecting coherent segments/spots on the BFSs when the interaction is strong. This leads to an upturn of  $1/T_1T$  at low temperatures like experimental results of  $x = 0.18$ . In this model, the upturn can be derived based on the minimal two-band model at the  $\Gamma$  point, while the  $T$  dependence of  $1/T_1T$  below  $T_c$  is similar to that above  $T_c$ , implying that the nesting between the hole and electron pockets would be responsible for the upturn of  $1/T_1T$  below  $T_c$  [3]. It remains a future problem whether the nesting contributes to the upturn of  $1/T_1T$ .

The presence of BFSs below  $x_c$  makes it easy to comprehend  $1/T_1T = \text{constant}$ . The values of  $1/T_1T$  for  $x = 0.05$  or  $0.10$  are one or two orders of magnitude smaller than those for  $x = 0.18$ , implying that the BFSs should be much smaller

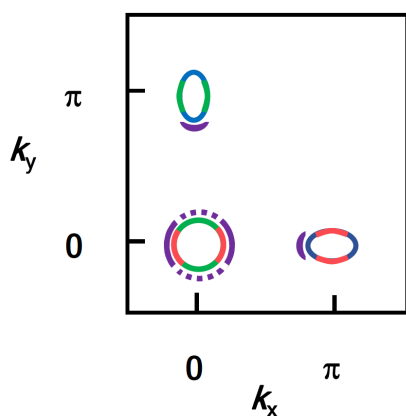


Fig. 3. Schematic diagram of two-dimensional Fermi surfaces for the tetragonal phase. The contributions from three orbitals,  $d_{xy}$ ,  $d_{yz}$  and  $d_{zx}$  are colored in blue, red, and green, respectively. Sufficiently expanded BFSs expected below  $T_c$  are colored in purple [2,6].

and the interactions should be suppressed. In such case, the upturn of  $1/T_1T$  is hardly expected and  $1/T_1T = \text{constant}$  is attributed to the scattering between a nucleus and almost free Bogoliubov quasiparticles like the Korringa relation in conventional metals. It should be noted that such relaxation process is realized not in the normal state but in the SC state. In the Korringa relation,  $1/T_1T$  is proportional to square of the DOS. The difference of  $1/T_1T$  in one order of magnitude between  $x = 0.05$  and  $0.10$  implies that the quasiparticle DOS differs almost three times between them. Our results suggest that BFSs exist even below  $x_c \sim 0.17$  and expand with increasing S-substitution level.

In conclusion, we have observed the upturn of  $1/T_1T$  deep in the SC state from  $^{77}\text{Se}$ -NMR measurements down to 100 mK. The upturn can be explained by the minimal two-band model, where the interband spin-triplet pairing is responsible for BFSs. The appearance of the upturn of  $1/T_1T$  gives evidence for strong Bogoliubov quasiparticles interactions in addition to the presence of BFSs.

## References

- [1] C. Setty, S. Bhattacharyya, Y. Cao, A. Kreisel, and P. J. Hirschfeld, *Nat. Commun.* **11**, 523 (2020).
- [2] Y. Cao, C. Setty, L. Fanfarillo, A. Kreisel, and P. J. Hirschfeld, *Phys. Rev. B* **108**, 224506 (2023).
- [3] Z. Yu, K. Nakamura, K. Inomata, X. Shen, T. Mikuri, K. Matsuura, Y. Mizukami, S. Kasahara, Y. Matsuda, T. Shibauchi, Y. Uwatoko, and N. Fujiwara, *Communications Physics* **6** (2023) 175.
- [4] T. Suzuki, A. Fukushima, S. Kasahara, K. Matsuura, M. Qiu, Y. Mizukami, K. Hashimoto, Y. Matsuda, T. Shibauchi, S. Shin, and K. Okazaki, <https://doi.org/10.21203/rs.3.rs-2224728/v1>.
- [5] K. Matsuura, *et al.*, *PNAS* **120**, e2208276120 (2023).
- [6] Y. Cao, C. Setty, A. Kreisel, L. Fanfarillo, and P. J. Hirschfeld, *Phys. Rev. B* **110**, L020503 (2024).

## Authors

Z. Yu<sup>a</sup>, K. Nakamura<sup>a</sup>, K. Inomata<sup>a</sup>, X. Shen, T. Mikuri, K. Matsuura<sup>b</sup>, Y. Mizukami<sup>b</sup>, S. Kasahara<sup>c</sup>, Y. Matsuda<sup>c</sup>, T. Shibauchi<sup>b</sup>, Y. Uwatoko and N. Fujiwara<sup>a</sup>,  
<sup>a</sup>Kyoto University  
<sup>b</sup>The University of Tokyo  
<sup>c</sup>Kyoto University

PI of Joint-use project: N. Fujiwara  
 Host lab:Uwatoko Group

## Development of a Magnetic-Susceptibility-Measurement Apparatus Used under High Pressure in Pulsed High Magnetic Fields

The combination of extreme conditions such as low temperature, high magnetic field, and high pressure provide insights into electrical and magnetic physical properties in condensed-matter materials. To date, magnetization measurements have been reported with an induction method using a non-destructive pulse magnet and a metallic piston-cylinder cell (PCC) made by Cu-Be or Ni-Cr-Al alloy under high pressure of up to 0.95 GPa in pulsed high magnetic fields of up to 50 T [1-3]. In this method, magnetization signal was detected by winding pick-up coils with approximately 100 turns around the exterior of the PCC (left panel of Fig. 1). This measurement apparatus is an effective tool for observing large abrupt transition phenomena, but the following factors may interfere with accurate measurements: (a) low sample-filling rate inside the pick-up coil, (b) extrinsic magnetization signals from the pressure cell, and (c) Joule heating caused by eddy currents in the metallic parts of the pressure cell in pulsed high magnetic fields. To deal with these problems, we have designed a new

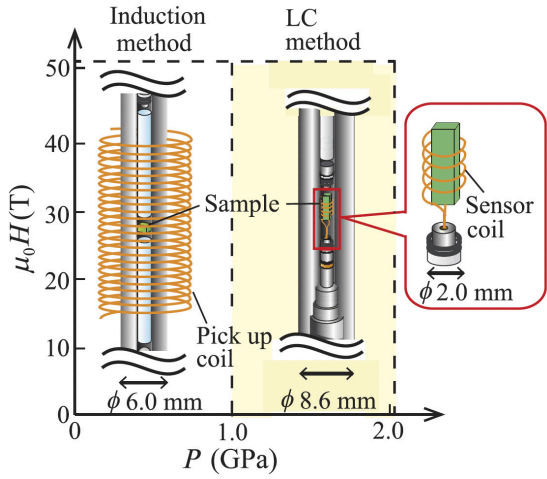


Fig. 1. Magnetic field and pressure range of magnetic-susceptibility-measurement techniques using the induction and LC methods. The schematic views below 1 GPa and above 1 GPa are the piston-cylinder cells around the sample for the induction and LC methods, respectively.

PCC in use for pulsed high magnetic fields and developed a magnetic-susceptibility-measurement apparatus using a proximity detector oscillator (PDO) under high pressures in pulsed high magnetic fields [4].

The PDO is an inductance ( $L$ )-capacitance ( $C$ ) self-resonating LC tank circuit based on a widely available proximity detector chip used in modern metal detectors [5,6]. When a magnetic insulator is put into the sensor coil, this circuit detects the change in the resonance frequency ( $\Delta f$ ) corresponding to the change in the dynamic magnetic susceptibility ( $(\Delta M/\Delta H)$ ). Hereafter, we refer to this technique as an LC method. The absolute value of  $\Delta f$  increases as the sample filling rate increases against the sensor coil. The sensor coil is typically wound only 5–30 turns with a diameter as small as 300  $\mu\text{m}$ . Therefore, the sensor coil including the sample can be inserted in the pressure cell as shown in the right panel of Fig. 1. This setting prevents the magnetization signal of the pressure cell from being superimposed to the measurement signal.

The PCC used in our magnetic-susceptibility measurements in pulsed high magnetic fields was made of Ni-Cr-Al alloy with a low conductivity and high tensile strength compared with a PCC made of Cu-Be alloy. The sensor coil is put into the PCC in this LC method, and therefore the outer diameter of the PCC can be expanded up to 8.6 mm $\phi$ , resulting in increasing the applied pressure of up to 2.10  $\pm$  0.02 GPa.

To evaluate the effect on the Joule heating at the sample position in pulsed high magnetic fields, we investigated the temperature change in the sample space using a magnetic-field and temperature-calibrated thermometer. Figure 2 shows the temperature changes at the sample position inside the PCC, starting from an initial temperature of 1.4 K, in pulsed high magnetic fields as a function of time. For the maximum field of 51 T, the temperature at the sample position remained almost 1.4 K until nearly 6.5 ms (approximately 40 T during the field-ascending process). After approximately 6.5 ms, the temperature slowly increased, reaching approximately 8 K at 40 ms (around 0 T). Since the sample is covered with a Teflon tube and immersed in Daphne 7373 as a pressure medium, the Joule heating from the metallic parts of the PCC is transmitted to the sample position with some delay.

To verify the performance of our developed magnetic-susceptibility-measurement apparatus in pulsed high

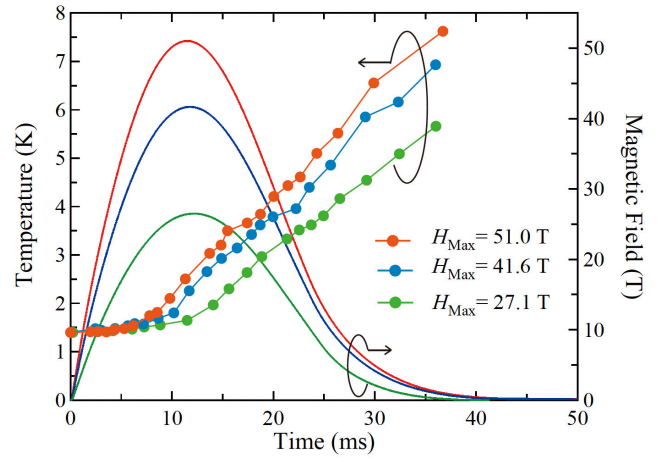


Fig. 2. Temperature change at the sample position inside the PCC starting at  $T = 1.4$  K in various maximum magnetic fields. The red, blue and green lines with filled circles represent the temperature changes inside the PCC for the cases of  $H_{\text{Max}} = 51.0$ , 41.6, and 27.1 T, respectively.

magnetic fields under high pressures, we investigated the pressure dependence of the magnetic susceptibility of  $\text{Ba}_3\text{CoSb}_2\text{O}_9$ , which is one of the typical  $S = 1/2$  triangular lattice antiferromagnets and exhibits successive phase transitions below the Néel temperature  $T_N = 3.8$  K [7]. Figure 3 shows the  $\Delta f_{\text{sub}}-H$  curve of  $\text{Ba}_3\text{CoSb}_2\text{O}_9$  for  $H \parallel ab$  plane in pulsed magnetic fields of up to 51 T under pressures of up to 1.97 GPa.  $\Delta f_{\text{sub}}$  is the frequency difference obtained by subtracting the frequency at  $T = 10$  K as background from  $\Delta f$  at 1.4 K. At ambient pressure in the PCC during the field-ascending process,  $\Delta f_{\text{sub}}-H$  curve was in good agreement with the field derivative magnetization  $dM/dH$  in a previous report [7]. Under several pressures, we also observed the anomalies at phase transition fields in the field-ascending process. In the field-descending process at ambient pressure in PCC and at 1.10 GPa,  $\Delta f_{\text{sub}}-H$  curves did not show any anomalies at phase transition fields observed in the field-ascending process owing to the temperature increase of the sample above  $T_N$ . As aforementioned,  $\Delta f_{\text{sub}}$  up to the saturation field ( $H_{\text{sat}}$ ) of approximately 32 T in the field-ascending process (Fig. 3(a)) is not affected by the increase in the sample temperature due to Joule heating. The present study demonstrated that our developed magnetic-susceptibility-measurement apparatus is a powerful tool for investigating

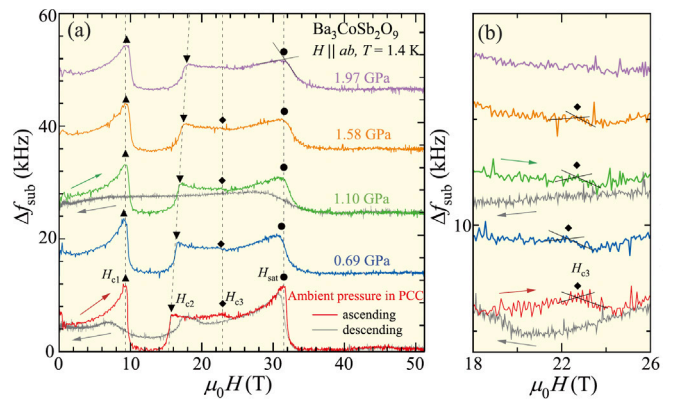


Fig. 3. (a)  $\Delta f_{\text{sub}}-H$  curves for  $H \parallel ab$  plane of  $\text{Ba}_3\text{CoSb}_2\text{O}_9$  at 1.4 K at various pressures. Gray lines show  $\Delta f_{\text{sub}}-H$  curves in the field-descending process at ambient pressure in PCC and at 1.10 GPa. Other lines are  $\Delta f_{\text{sub}}-H$  curves in the field-ascending process. The dotted lines are guidelines indicating the pressure dependence of transition fields ( $H_{c1}$ ,  $H_{c2}$ ,  $H_{c3}$  and  $H_{\text{sat}}$ ). (b) Enlarged view of the  $\Delta f_{\text{sub}}-H$  curves around 22 T. The curves in Figs. 3(a) and 3(b) are arbitrarily shifted from the ambient-pressure curve with increasing pressure for clarity.

magnetic properties of a frustrated magnet with a small spin value at low temperatures down to 1.4 K in pulsed high magnetic fields of up to 40 T under high pressures of up to 2.1 GPa. We hope that this apparatus will help us discover unconventional physical phenomena in quantum and frustrated spin systems.

## References

- [1] T. Hamamoto, K. Kindo, T. Kobayashi, Y. Uwatoko, S. Araki, R. Settai, and Y. Onuki, *Physica B* **281-282**, 64 (2000).
- [2] T. Tahara, T. Kida, Y. Narumi, T. Takeuchi, H. Nakamura, K. Miyake, K. Kindo, and M. Hagiwara, *J. Phys. Soc. Jpn.* **89**, 064711 (2020).
- [3] T. Matsunaga, T. Kida, S. Kimura, M. Hagiwara, S. Yoshida, I. Terasaki, and K. Kindo, *J. Low Temp. Phys.* **159**, 7 (2010).
- [4] K. Nihongi, T. Kida, Y. Narumi, N. Kurita, H. Tanaka, Y. Uwatoko, K. Kindo, and M. Hagiwara, *Rev. Sci. Instrum.* **94**, 113903 (2023).
- [5] M. M. Altarawneh, Ph.D. thesis, The Florida State University, 2009.
- [6] S. Ghannadzadeh, M. Coak, I. Franke, P. A. Goddard, J. Singleton, and J. L. Manson, *Rev. Sci. Instrum.* **82**, 113902 (2011).
- [7] T. Susuki, N. Kurita, T. Tanaka, H. Nojiri, A. Matsuo, K. Kindo, and H. Tanaka, *Phys. Rev. Lett.* **110**, 267201 (2013).

## Authors

K. Nihongi<sup>a</sup>, T. Kida<sup>a</sup>, Y. Narumi<sup>a</sup>, N. Kurita<sup>b</sup>, H. Tanaka<sup>b</sup>, Y. Uwatoko, K. Kindo, and M. Hagiwara<sup>a</sup>

<sup>a</sup>Osaka University

<sup>b</sup>Tokyo Institute of Technology

PI of Joint-use project: K. Nihongi

Host lab: Hagiwara, Kindo, and Uwatoko Groups

# Theoretically Predicted Collective Excitation Modes in the Quadruple-Q Magnetic Hedgehog Lattices

The Kondo-lattice magnets are recently attracting enormous research interest as hosts of rich topological magnetism. This class of magnets have localized spins coupled to itinerant electrons via exchange interactions, and the itinerant electrons mediate long-range RKKY-type interactions among the localized spins. A variety of topological magnetic textures, e.g., skyrmion crystals, meron crystals, hedgehog lattices, emerge as superpositions of multiple spin helices or spin-density waves with different wavevectors determined by the Fermi-surface nesting.

Recent intensive studies have rapidly clarified equilibrium phases and static properties of the Kondo-lattice magnets, and several new materials have been discovered and synthesized experimentally. However, their nonequilibrium properties and dynamical phenomena remain unclarified yet. Under these circumstances, we have started the research for their spin-charge dynamics and related phenomena based on large-scale numerical simulations using the supercomputer facilities in ISSP, University of Tokyo. Through these studies, we have revealed many interesting dynamical phenomena, e.g., microwave-induced magnetic topology switching [1], unexpected spin-charge segregation in the low-energy excitations of a zero-field skyrmion crystal phase [2], photoinduced magnetic phase transitions to 120-degree order [3], and peculiar collective excitation modes of hedgehog lattices [4].

Among them, the last one is the most recent achievement. Three-dimensional topological magnetic structures called magnetic hedgehog lattices (Figs. 1(a) and (b)) have been discovered recently in several itinerant magnets such as MnGe, MnSi<sub>1-x</sub>Ge<sub>x</sub> and SrFeO<sub>3</sub>. The research on magnetic hedgehog lattices to date has focused mainly on their proper-

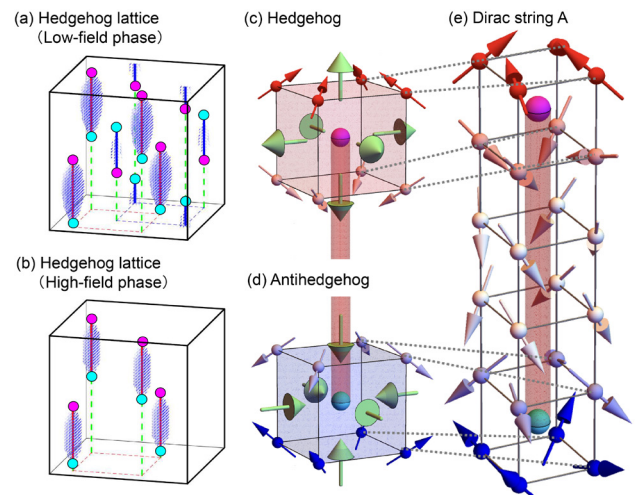


Fig. 1. (a), (b) Spatial arrangement of hedgehogs and antihedgehogs in magnetic hedgehog lattices. The magenta and cyan dots represent the hedgehogs and antihedgehogs, respectively. The lines connecting them represent Dirac strings. There are two types of Dirac strings (red line: Dirac string A, blue line: Dirac string B) with distinct magnetization winding senses. In the zero-field and low-field hedgehog lattice, both Dirac strings A and B exist (a). On the contrary, when the applied magnetic field exceeds a certain threshold value, the Dirac strings B disappear, and a hedgehog lattice with only Dirac strings A appears (b). (c), (d) Magnetization configurations (red and blue arrows) and distributions of emergent magnetic fields (green arrows) for a hedgehog and an antihedgehog. The hedgehog behaves as a source of the emergent magnetic fields, while the antihedgehog behaves as a sink of the fields. (e) Magnetization configuration of the magnetic vortex (Dirac string A) connecting the hedgehog and antihedgehog.

ties at equilibrium. On the other hand, according to the fundamentals of electromagnetism, magnetic (anti)hedgehogs, which behave as emergent (anti)monopoles, should generate emergent electric fields when they move. Therefore, clarification of their excitation dynamics will directly lead to the discovery and exploration of new emergent phenomena and device functions of topological spin textures in dynamical regimes.

Motivated by this aspect, we investigated the nature and properties of collective excitation modes expected when the quadratic- $Q$  hedgehog lattices realized in MnSi<sub>1-x</sub>Ge<sub>x</sub> and SrFeO<sub>3</sub> are irradiated by light by means of numerical simulations using a microscopic theoretical model. In the magnetic hedgehog lattices, hedgehogs (Fig. 1(c)) and antihedgehogs (Fig. 1(d)) are connected by a magnetic vortex called Dirac string (Fig. 1(e)). As shown in Fig. 1(e), the spins below the magnetic hedgehog go rotating down to the antihedgehog to form a vortex structure connecting the hedgehog and the antihedgehog. Because the rotating sense of the vortex is two-fold, there are two types of Dirac strings, which are right-handed and left-handed. Although two types of Dirac strings do not necessarily appear in a single material, in the case of the hedgehog lattices realized in MnSi<sub>1-x</sub>Ge<sub>x</sub>, there are indeed two types of Dirac strings (A and B) with different winding senses.

In the theoretical work reported in Ref. [4], we discovered that there exist three collective excitation modes (spin-wave modes) in terahertz to sub-terahertz frequency regime, which we named L1, L2 and L3 modes (Figs. 2(a) and (b)). Further analyses revealed that for the L2 and L3 modes, in-phase oscillations of the hedgehog and antihedgehog located at upper and lower ends of the Dirac string occur to exhibit translational oscillation, that is, the Dirac strings move upwards and downwards in an oscillatory manner (Figs. 2(c) and (d)). It is well-known that when a bar magnet is moved closer to or further away from a metallic coil, an

electric voltage is generated. It is interesting that the collective translational oscillations of the Dirac strings discovered here are the equivalent motion as that of the bar magnet in this case. In other words, in light-irradiated magnetic hedgehog lattices, a huge number of nano-sized bar magnets show such oscillatory motion at high frequencies of terahertz or sub-terahertz orders.

More interestingly, among the three oscillation modes, we found that the L2 mode corresponds to the oscillations of the Dirac strings B (Fig. 2(c)), while the L3 mode corresponds to those of the Dirac strings A (Fig. 2(d)). Consequently, we expect that the L2 (L3) mode vanishes when the Dirac strings B (A) disappear. In fact, application of a magnetic field can realize the selective disappearance of the Dirac strings B through inducing hedgehog-antihedgehog pair annihilations (Figs. 1(a) and (b)). We indeed observed that the L2 mode vanishes upon this field-induced annihilation

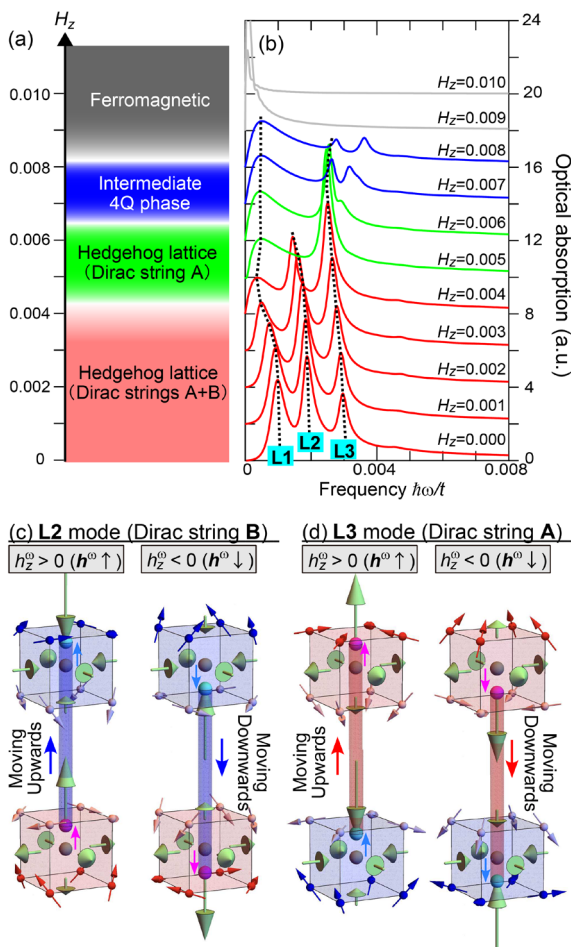


Fig. 2. (a) Phase diagram as a function of the external magnetic field  $H_z$ . At zero and low magnetic field, a hedgehog lattice with both Dirac strings A and B appears. As the magnetic field is increased, the hedgehog and antihedgehog belonging to the Dirac string B annihilate, and a phase transition occurs to a hedgehog lattice consisting of only the Dirac strings A. (b) Calculated optical absorption spectra. Three peaks correspond to collective excitation modes (named L1, L2, and L3) at the eigenfrequencies. The values of frequencies are written in normalized units, and these modes appear in a frequency range of approximately several hundred gigahertz or sub-terahertz. Looking at the L2 and L3 modes corresponding to the Dirac-string oscillations, both L2 and L3 modes appear in the low-field hedgehog-lattice phase where both Dirac strings A and B exist. On the contrary, in the high-field hedgehog-lattice phase without Dirac strings B, the L2 mode originating from the Dirac strings B disappears and only the L3 mode originating from the Dirac strings A remains. (c) Translational oscillations of the Dirac string B in the L2 mode. (d) Those of the Dirac string A in the L3 mode. The hedgehog and antihedgehog at the upper and lower ends of the string exhibit in-phase oscillations, which cause vertically translational oscillations of the strings.

of the Dirac strings B as seen in Fig. 2(b). This means that the external magnetic field can switch these collective oscillation modes, which enables us to realize on-off of the emergent electric fields and transmission of microwaves at corresponding frequencies.

Our discovery of the collective excitation modes of emergent magnetic (anti)monopoles in condensed matters is of importance from the viewpoint of fundamental science. Moreover, the discovery is expected to open the way to designing the optical/microwave device functions and spintronics functions of the three-dimensional topological magnetism that can be controlled and switched by external fields.

#### References

- [1] R. Eto and M. Mochizuki, Phys. Rev. B **104**, 104425 (2021).
- [2] R. Eto, R. Pohle, and M. Mochizuki, Phys. Rev. Lett. **129**, 017201 (2022).
- [3] T. Inoue and M. Mochizuki, Phys. Rev. B **105**, 144422 (2022).
- [4] R. Eto and M. Mochizuki, Phys. Rev. Lett. **132**, 226705 (2024).

#### Authors

M. Mochizuki<sup>a</sup>  
<sup>a</sup>Waseda University

PI of Joint-use project: M. Mochizuki  
 Host lab: Supercomputer Center

## Odd-Parity Multipole Order in the Spin-Orbit Coupled Metallic Pyrochlore $\text{Pb}_2\text{Re}_2\text{O}_7-\delta$

Transition metal compounds containing  $4d$  and  $5d$  electrons have attracted attention for their novel physical properties resulting from their strong spin-orbit interaction (SOI) [1,2]. L. Fu pointed out that SOI induces Fermi-liquid instability in metals, leading to the formation of various electronic phases, and proposed the concept of spin-orbit-coupled metals (SOCM) [3]. In SOCM, the strong SOI induces a structural phase transition with spontaneous spatial-inversion-symmetry breaking (ISB), which is associated with an unconventional odd-parity multipole ordering [4]. To date, the candidate compounds of SOCM are limited and only few of them have been experimentally verified. Progress in material development is key to reveal the diversity of electronic orders formed in SOCM and further scrutinize the physics of SOCM.

So far, many studies have focused on  $\alpha$ -pyrochlore oxide  $\text{Cd}_2\text{Re}_2\text{O}_7$  (CRO), the most investigated candidate for SOCM [4]. Three successive structural phase transitions occur in CRO; an ISB transition from the regular pyrochlore structure (phase I) to the tetragonal phase II occurs at  $T_{s1}$ ; on further cooling, transitions to an orthorhombic phase XI at  $T_{s2}$  and to the tetragonal phase III at  $T_{s3}$  occur. A theoretical work suggests that, in the phases II and III, the electronic order associated with ISB can be described by an odd-parity multipole order [3]. As depicted in Fig. 1, the displacements of Re atoms in phase II and III can be viewed as electric dipoles, certain pairs of which generate electric toroidal moments. These virtual electric toroidal moments are organized as  $x^2 - y^2$  and  $3z^2 - r^2$  configurations, respectively. Thus, the emerged electronic orders are regarded as electric toroidal quadrupole (ETQ) orders [2]. This unconventional odd-parity multipole ordering will induce ETQ-driven phenomena, such as the spin-split Fermi surface, the magneto-current effect, and nonreciprocal transport in an

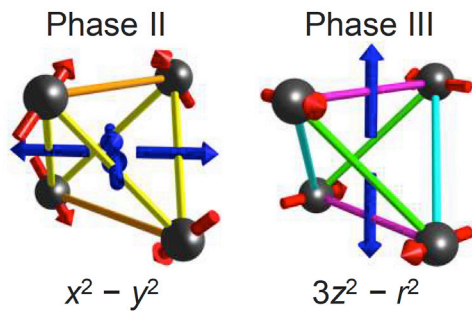


Fig. 1. Schematic figure of the deformation of Re tetrahedron in phases II and III of  $\text{Cd}_2\text{Re}_2\text{O}_7$  (CRO), with red arrows representing the displacements of Re atoms (black balls). The Re displacements generate virtual electric toroidal moments (blue arrows) of the  $x^2 - y^2$  and  $3z^2 - r^2$  types, respectively. The colors of the connecting rods between Re atoms differentiate identical bonds in each phase.

applied magnetic field.

The relevant rhenium-containing pyrochlore oxide,  $\text{Pb}_2\text{Re}_2\text{O}_{7-\delta}$  (PRO), has also been reported to exhibit an ISB phase transition from the  $\alpha$ -pyrochlore structure (phase I) to a noncentrosymmetric structure (phase II) at  $T_s = 300$  K [5,6]. Based on the ISB transition and similarity in the physical properties with CRO, PRO likely to be a SOCM. Therefore, an odd-parity multipole order may be realized. However, the crystal structure of phase II, which is crucial to identify the multipole order, is contradicting; two different structures, a cubic  $F4-3m$  and a tetragonal  $I-4m2$  structures are proposed [5,6]. Both crystal structures differ from that of CRO in the lowest temperature phase, which suggest a different multipole order is formed in PRO.

In this study, we investigated the low temperature phase of a SOCM candidate PRO by temperature-dependent synchrotron x-ray diffraction (XRD) measurements using single crystals [7]. As shown in Fig. 2, the appearance of superlattice peaks in the diffraction data of phase II indicates the violation of the  $d$ -glide plane derived extinction rule. To obtain more evidence for a lower crystal symmetry, we probed the temperature dependence of the two Bragg reflections  $(18\ 0\ 0)$  and  $(20\ 0\ 0)$  in phase I, as shown in Fig. 2 (c). Below  $T_s$ , the  $(18\ 0\ 0)$  reflection emerges upon cooling, indicating structural transition at  $T_s$ . In addition, the  $(20\ 0\ 0)$  reflection splits into two peaks (a low-angle and a high-angle peaks at an intensity ratio of approximately 2:1) demonstrating a cubic to tetragonal transition. It is noted that the  $(18\ 0\ 0)$  reflection is a single peak, not a double peak like the  $(20\ 0\ 0)$  reflection, demonstrating the presence of an additional extinction rule in phase II.

Since the phase transition at  $T_s$  is of second order, the group-subgroup relation of the space group is applied to deduce the space group of phase II. Based on the observed reflection conditions, we propose the  $I4_122$  space group for the phase II. This space group is identical to that of CRO in phase III.

The electronic order emerging in phase III of CRO is considered to be ETQ order with  $3z^2 - r^2$  component. Since the lowest temperature structure of CRO and PRO is revealed to be identical,  $3z^2 - r^2$ -type ETQ is likely formed in the phase II of PRO. Here,  $3z^2 - r^2$ -type order is selected as the ground state from the doubly degenerate  $x^2 - y^2$  and  $3z^2 - r^2$ -type ETQ orders. Electronic details about the origin of this symmetry breaking are of interest for future studies. Further comparison of the ISBs with respect to their origin and final manifestation in CRO and PRO would be useful for fundamental understanding of SOCM.

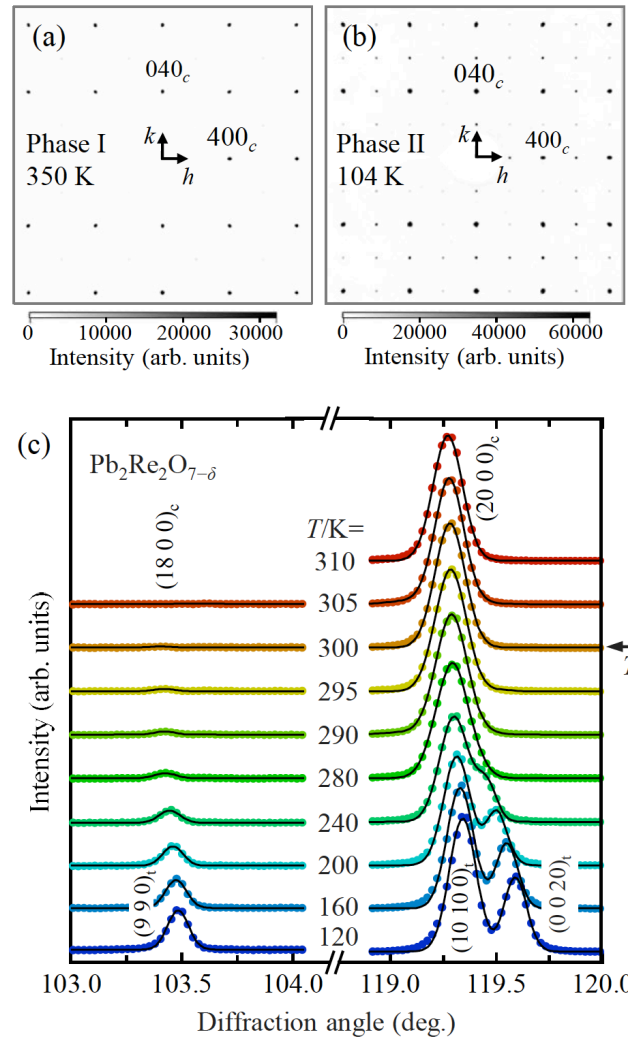


Fig. 2. Diffraction data of the  $hk0$  plane for  $\text{Pb}_2\text{Re}_2\text{O}_{7-\delta}$  (PRO) in (a) phase I and (b) II. The appearance of superlattice peaks in (b) indicates the violation of the  $d$ -glide plane derived extinction rule. (c) Temperature variation of XRD patterns near the  $(20\ 0\ 0)$  and  $(18\ 0\ 0)$  reflections of PRO. Solid black lines represent fitting curve. The transition temperature  $T_s = 300$  K is marked with an arrow.

## References

- [1] T. Takayama, J. Chaloupka, A. Smerald, G. Khaliullin, and H. Takagi, *J. Phys. Soc. Japan* **90**, 062001 (2021).
- [2] L. Fu, *Phys. Rev. Lett.* **115**, 026401 (2015).
- [3] S. Hayami, Y. Yanagi, H. Kusunose, and Y. Motome, *Phys. Rev. Lett.* **122**, 147602 (2019).
- [4] Z. Hiroi, J.-I. Yamaura, T. C. Kobayashi, Y. Matsubayashi, and D. Hirai, *J. Phys. Soc. Japan* **87**, 024702 (2018).
- [5] K. Ohgushi, J. I. Yamaura, M. Ichihara, Y. Kiuchi, T. Tayama, T. Sakakibara, H. Gotou, T. Yagi, and Y. Ueda, *Phys. Rev. B* **83**, 125103 (2011).
- [6] C. Michioka, Y. Kataoka, H. Ohta, and K. Yoshimura, *J. Phys. Condens. Matter* **23**, 445602 (2011).
- [7] Y. Nakayama, D. Hirai, H. Sagayama, K. Kojima, N. Katayama, J. Lehmann, Z. Wang, N. Ogawa, and K. Takenaka, *Phys. Rev. Mater.* **8**, 055001 (2024).

## Authors

Y. Nakayama<sup>a</sup>, D. Hirai<sup>a</sup>, H. Sagayama<sup>b</sup>, K. Kojima<sup>a</sup>, N. Katayama<sup>a</sup>, J. Lehmann<sup>c</sup>, Z. Wang<sup>c</sup>, N. Ogawa<sup>c</sup>, and K. Takenaka<sup>a</sup>  
<sup>a</sup>Nagoya University  
<sup>b</sup>KEK, <sup>c</sup>RIKEN

PI of Joint-use project: D. Hirai  
 Host lab: Hiroi and Okamoto Groups

## New Intermetallic Compounds in Sm-Fe System Alloys

High-performance neodymium-iron-boron (Nd-Fe-B) magnets are applied to various advanced electromagnetic devices, including hard disk drives, electric vehicles, and medical equipment [1]. In particular, the production of electric cars equipped with Nd-Fe-B magnet motors has significantly increased, reflecting that regulations on internal combustion engines emitting large quantities of greenhouse gases have been proposed or enacted in many countries. The continuously growing demand for high-performance Nd-Fe-B magnets has raised severe concerns over their price and availability [2]. Under such circumstances, the development of permanent magnets using the relatively abundant rare-earth element Sm has become a focus of attention. Therefore, we have continued searching for new Sm-based rare-earth intermetallic compounds.

This study chose Sm-Fe system alloys as new Sm-based rare-earth intermetallic compounds. Although only three intermetallic compounds,  $\text{Sm}_2\text{Fe}_{17}$ ,  $\text{SmFe}_3$ , and  $\text{SmFe}_2$  phases are found in the Sm-Fe phase diagram [3], the formation of new intermetallic compounds, such as  $\text{SmFe}_{12}$ ,  $\text{SmFe}_5$ , and  $\text{Sm}_5\text{Fe}_{17}$  phases, has been reported in thin film processing [4-6]. It is necessary to obtain these materials in bulk form to evaluate the magnetic properties of these phases. This study investigates the possibility of producing these new intermetallic compounds through rapid solidification processing using a melt-spinning technique. The structures and magnetic properties of the melt-spun ribbons were investigated.

Since the new intermetallic compounds are metastable, it is impossible to produce alloys with these phases using the conventional casting method. Thus, the specimens were prepared by rapid solidification processing using melt-spinning. Figure 1 shows the transmission electron microscope (TEM) micrograph of the as-quenched  $\text{SmFe}_5$  melt-spun ribbon and the corresponding selected electron diffraction pattern. The electron diffraction pattern indicates that the fine grains in the TEM micrograph were in the  $\text{SmFe}_5$  phase. This confirms that the as-quenched  $\text{SmFe}_5$  melt-spun ribbon consisted of  $\text{SmFe}_5$  fine grains. Heat treatment of the as-quenched melt-spun ribbon resulted in crystal growth of the  $\text{SmFe}_5$  grains [7]. On the other hand, the  $\text{SmFe}_{12}$  and  $\text{Sm}_5\text{Fe}_{17}$  phases were not obtained by rapid solidification processing using melt-spinning. These as-quenched melt-

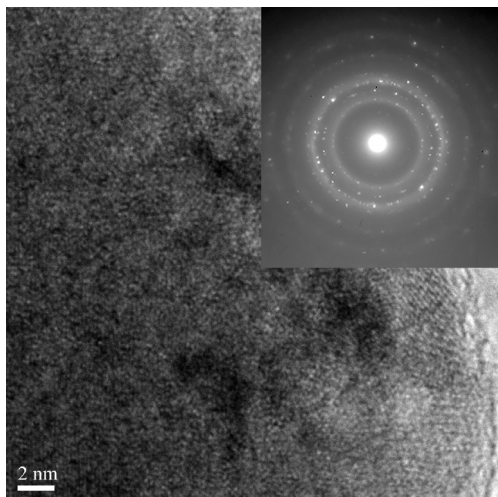


Fig. 1. TEM micrograph of the as-quenched  $\text{SmFe}_5$  melt-spun ribbon and the corresponding selected electron diffraction pattern.

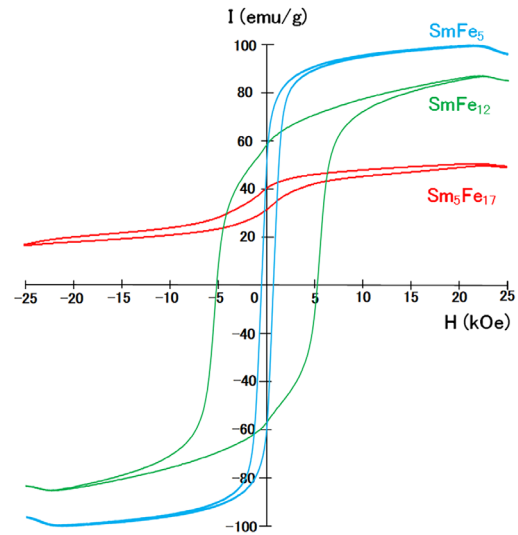


Fig. 2. Hysteresis loops of  $\text{SmFe}_{12}$ ,  $\text{SmFe}_5$ , and  $\text{Sm}_5\text{Fe}_{17}$  melt-spun ribbons. The hysteresis loops were measured by VSM with a maximum applied magnetic field of 25 kOe.

spun ribbons were amorphous. Although the  $\text{Sm}_5\text{Fe}_{17}$  phase was produced by melt-spinning followed by optimal heat treatment, the  $\text{SmFe}_{12}$  phase was not obtained by annealing the  $\text{SmFe}_{12}$  melt-spun ribbon. The  $\text{SmFe}_{12}$  phase was found to be obtained by adding small elements, such as Ti or V, to the  $\text{SmFe}_{12}$  phase.

The magnetic properties of the new intermetallic compounds were evaluated by the vibrating sample magnetometer (VSM). Figure 2 shows the typical magnetic hysteresis loops of these phases. These new intermetallic compounds exhibited hysteresis loops as magnetic materials. The  $\text{SmFe}_5$  melt-spun ribbon showed a narrow hysteresis loop with moderate coercivity, and the  $\text{SmFe}_{12}$  melt-spun ribbon showed a wide hysteresis loop with high coercivity. On the other hand, the  $\text{Sm}_5\text{Fe}_{17}$  melt-spun ribbon exhibited a minor loop, not a hysteresis loop. The coercivity of the  $\text{Sm}_5\text{Fe}_{17}$  melt-spun ribbon was extremely high, over the applied field of 25 kOe in the VSM measurement, and only the minor loop was obtained in the  $\text{Sm}_5\text{Fe}_{17}$  melt-spun ribbon.

This study obtained the new intermetallic compounds of the  $\text{SmFe}_{12}$ ,  $\text{SmFe}_5$ , and  $\text{Sm}_5\text{Fe}_{17}$  phases. However, the magnetic properties of these compounds are not yet comparable to those of high-performance Nd-Fe-B magnets. Further optimization of the annealing conditions and compositional modifications may improve the magnetization of these new intermetallic compounds.

### References

- [1] G. Bailey, N. Mancheri, and K. V. Acker, *J. Sustain. Metall.* **3**, 611 (2017).
- [2] T. Dutta, K. H. Kim, M. Uchimiya, E. E. Kwon, B. H. Jeon, A. Deep, and S. T. Yun, *Environ. Res.* **150**, 182 (2016).
- [3] K. H. J. Busschow, *J. Less-Common Met.* **25**, 131 (1971).
- [4] F. J. Cadieu, H. Hegde, R. Rani, A. Navarathna, and K. Chen, *Mater. Lett.* **11**, 284 (1991).
- [5] P. Tozmana, H. Sepehri-Amina, and K. Hono, *Scripta Mater.* **194**, 113686 (2021).
- [6] O. Yabuhara, M. Ohtake, Y. Nukaga, F. Kirino, and M. Futamoto, *J. Phys.: Conf. Ser.* **200**, 082026 (2010).
- [7] T. Saito and D. Nishio-Hamane, *AIP Advances* **10**, 015311 (2020).

### Authors

T. Saito<sup>a</sup> and D. Nishio-Hamane  
<sup>a</sup>Chiba Institute of Technology

PI of Joint-use project: T. Saito  
Host lab: Electron Microscope Section

## Structural Study of Perovskite-type RbNbO<sub>3</sub> Prepared at High Pressure

We successfully synthesized a perovskite-type RbNbO<sub>3</sub> compound by subjecting the non-perovskite RbNbO<sub>3</sub> [1,2] to high temperature (1173 K) and high pressure (4 GPa) using a cubic-type high-pressure press. We investigated the temperature dependence of crystal structure associated with dielectric properties. Based on the powder X-ray diffraction patterns collected at ISSP under the collaborative program, we determined lattice parameters of the temperature dependence of perovskite RbNbO<sub>3</sub> at 4–300 K. Our objective in this project is to discover novel ferroelectrics that are equal to or beyond BaTiO<sub>3</sub>, which is often utilized in a range of electrical devices. KNbO<sub>3</sub> is a widely recognized displacement-type ferroelectric material, and we aimed to replace the potassium (K) ion with rubidium (Rb) ion, which belong to the same group of alkali metals but have a greater ionic radius. RbNbO<sub>3</sub> has a complex quasi one-dimensional structure under normal conditions, unlike the perovskite-type structure found in KNbO<sub>3</sub>. We synthesized RbNbO<sub>3</sub> with the perovskite structure using the high pressure technique. Detailed study was published in the reference [2].

The high-pressure phase of RbNbO<sub>3</sub> at 300 K was found to have an orthorhombic cell with a perovskite-type structure. The crystal structure was determined by single-crystal X-ray diffraction analysis at Tohoku University. The space group was identified as *Amm2*, with a lattice parameter of  $a = 3.9937(2)$  Å,  $b = 5.8217(3)$  Å, and  $c = 5.8647(2)$  Å. The non-centrosymmetric space group of RbNbO<sub>3</sub> is same as that of the ferroelectric compounds BaTiO<sub>3</sub> and KNbO<sub>3</sub>. The degree of distortion in RbNbO<sub>3</sub> is more pronounced than in KNbO<sub>3</sub>, perhaps because of the larger ionic radius of Rb. The transitions from an orthorhombic structure to two sequential tetragonal phases (Tetra1 at 493 K, Tetra2 at 573 K) were observed. The perovskite framework was maintained during both phases before returning to the triclinic ambient phase at 693 K, as seen in Fig. 1. The first transition is similar to that observed in KNbO<sub>3</sub>, however the subsequent transition from the Tetra1 phase to the Tetra2 phase is distinct, characterized by elongation along the *c*-axis and a notable increase in the  $c_p/a_p$  ratio ( $c_p$  and  $a_p$  are taken with perovskite basic cell) from 1.07 to 1.43. This distortion indicates a transition that is comparable to the one observed in PbVO<sub>3</sub> [3], where the oxygen atoms of an octahedron move apart along the *c*-axis, resulting in the formation of a pyramid as shown in Fig. 1. The permittivity exhibits a

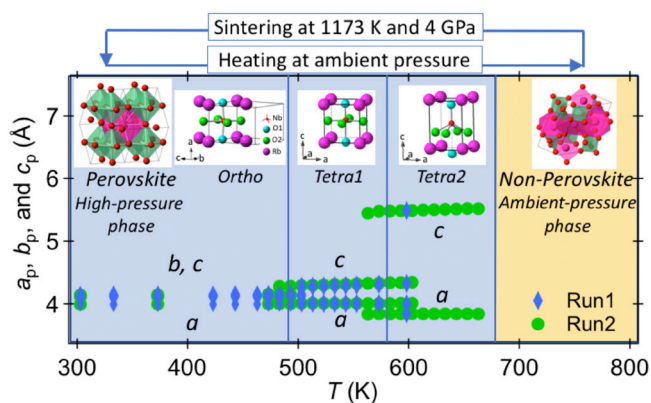


Fig. 1. Temperature dependence of crystal structure of RbNbO<sub>3</sub> at 300–800 K [2]. The lattice parameters,  $a_p$ ,  $b_p$  and  $c_p$ , are taken with perovskite basic cell. The figure was reprinted from the graphical index of Ref. 2 published by the Royal Society of Chemistry.

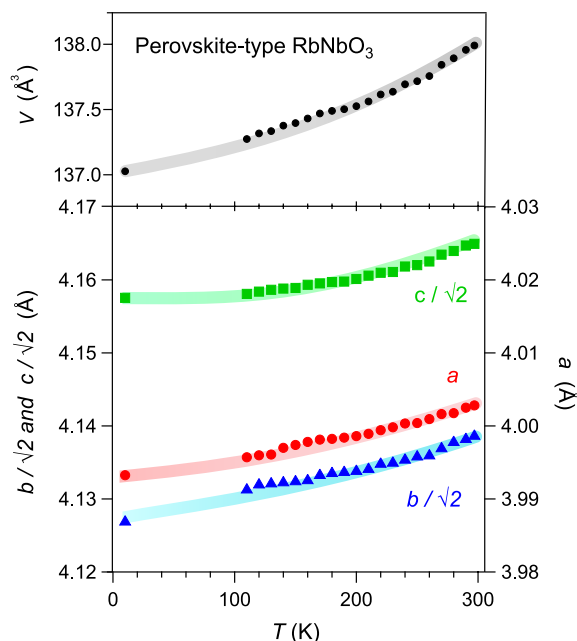


Fig. 2. Temperature dependence of lattice parameters of perovskite-type RbNbO<sub>3</sub> at 4–300 K.

discontinuous increase at the orthorhombic to tetragonal phase transition, however this enhancement is not observed for the Tetra1 and Tetra2 transitions due to the collapse of the bulk sample caused by abrupt volume expansion during the transition.

There were no observable alterations in the structure between temperatures of 4 and 300 K. The lattice parameters,  $a$ ,  $b$ ,  $c$ , and  $V$  exhibited consistent decreases with decreasing temperature, as seen in Fig. 2. A contrasting structural phase shift from orthorhombic to rhombohedral occurs at 220 K in KNbO<sub>3</sub>. This aligns with the findings reported by Fukuda *et al.* [1]. Nevertheless, the theoretical calculations regarding phase stability indicate that the orthorhombic structure with *Amm2* is the most stable phase in RbNbO<sub>3</sub>, exhibiting the lowest energy [2]. It is contrast to that the stable space group in KNbO<sub>3</sub> at low temperature is *R3m*.

In addition, we conducted thermal property measurements using a combination of thermogravimetry (TG), differential thermal analysis (DTA), and differential scanning calorimetry (DSC). Furthermore, we assessed the optical characteristics using second harmonic generation (SHG) [2]. We further synthesize a solid solution of RbNbO<sub>3</sub> and KNbO<sub>3</sub> by using the high pressure method, and investigate the structural studies with wide range of temperature. Ongoing research involves doing structural studies at various temperatures.

### References

- [1] M. Fukuda and K. Yamaura, *J. Ceram. Soc. Jpn.* **131**, 126 (2023).
- [2] A. Yamamoto, K. Murase, J. Yamaura, *et al.* *Dalton Trans.* **53**, 7044 (2024).
- [3] R. V. Shpanchenko *et al.*, *Chem. Mater.* **16**, 3267 (2004).

### Authors

A. Yamamoto<sup>a</sup>, K. Murase<sup>a</sup>, J. Yamaura, K. Sugiyam<sup>b</sup>, and T. Kawamata<sup>b</sup>  
<sup>a</sup>Shibaura-Institute of Technology  
<sup>b</sup>Tohoku University

PI of Joint-use project: Ayako Yamamoto  
 Host lab: Yamaura group and X-Ray Diffraction Section

## Implementation of Finite-Temperature Calculation in TeNeS

In quantum many-body problems, such as quantum spin systems and strongly correlated electron systems, the dimension of the Hilbert space increases exponentially with the number of spins or particles, making precise analysis of large systems difficult. The tensor network method, which is one technique to overcome such difficulties, represents quantum states as a network constructed by the contraction of small tensors, thereby reducing the effective degrees of freedom and enabling the computation of large systems. The infinite projected entangled pair state/infinite tensor product states (iPEPS/iTPS) is a tensor network that can directly represent the ground state of an infinitely large system. We are developing a tensor network library Tensor Network Solver (TeNeS) based on iPEPS/iTPS [1, 2]. TeNeS supports MPI and OpenMP hybrid parallelization, and enables us to calculate the ground states of various two-dimensional lattice models.

This year, through the support of Project for Advancement of Software Usability in Materials Science (PASUMS), we have implemented the finite-temperature calculation in TeNeS. The finite-temperature calculation is essential for the analysis of the physical properties of quantum many-body systems, such as the specific heat, and magnetization. The finite-temperature calculation is performed by the imaginary time evolution of the density matrix represented by the infinite projected entangled pair operator/infinite tensor product operator (iPEPO/iTPO) [3] (See Fig. 1). Such imaginary time evolution for iPEPO/iTPO is algorithmically similar to the ground state calculation based on iPEPS/iTPS, and we can easily implement the finite-temperature calculation in TeNeS.

In addition to the finite-temperature calculation, we also implemented the real-time evolution of a pure state using TeNeS. The algorithm of the real-time evolution is essentially the same as the imaginary time evolution. However, usually approximation based on iPEPS/iTPS becomes less accurate for longer time evolution due to the increase of quantum entanglement. Thus, real-time evolution approximated by iPEPS/iTPS is limited to short time evolution.

The finite-temperature calculation and the real-time evolution implemented in TeNeS are useful for the analysis of the physical properties of quantum many-body systems. We hope that TeNeS can enhance research in the field of quantum many-body systems.

TeNeS was developed with Yuichi Motoyama, Kazuyoshi Yoshimi, Satoshi Morita, Tatsumi Aoyama, Takeo Kato, and Naoki Kawashima.

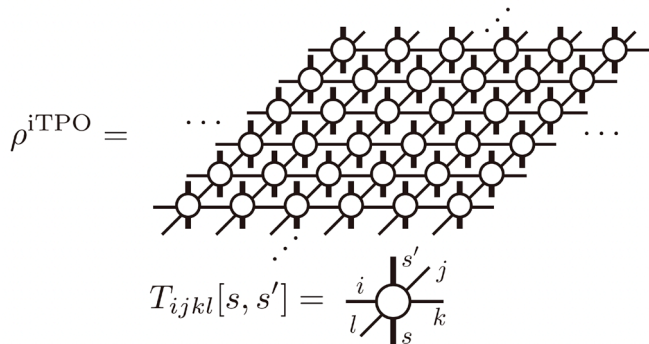


Fig. 1. Tensor network diagram of a density matrix  $\rho$  represented as an iPEPO/iTPO. Vertical open legs stand for indices of local Hilbert space.

## References

- [1] Y. Motoyama, T. Okubo, K. Yoshimi, S. Morita, T. Kato, and N. Kawashima, *Comput. Phys. Commun.* **279**, 108437 (2022).
- [2] <https://github.com/issp-center-dev/TeNeS>
- [3] A. Kshetrimayum, M. Rizzi, J. Eisert, and R. Orús, *Phys. Rev. Lett.* **122** 070502(2019).

## Author

T. OKUBO<sup>a</sup>

<sup>a</sup>Institute for Physics of Intelligence, the University of Tokyo

PI of Joint-use project: T. Okubo

Host lab: Supercomputer Center

## Magnetic Field Induced Insulator-to-Metal Mott Transition in $\lambda$ -Type Organic Conductors

The Mott transition is a key issue in condensed matter physics. Mott transitions give rise to novel physical phenomena, including unconventional superconductivity and quantum criticality. The interest in this research is the effects of the magnetic field on the Mott transition. To thoroughly investigate the effects of the magnetic field on the Mott transition, it is necessary to apply a magnetic field comparable to the energy scale of the Mott gap. However, the energy scale of the Mott gap is usually much larger than the practical limits of experimentally feasible magnetic fields. To avoid this problem, it is necessary to prepare materials near the Mott boundary region to reduce the Mott gap.

For studying the magnetic field effects on the Mott transition, we focused on  $\lambda$ -type organic conductors. Figure 1 shows the pressure-temperature ( $p$ - $T$ ) phase diagram of  $\lambda$ -type BETS salts  $\lambda$ -(BETS)<sub>2</sub>GaBr<sub>x</sub>Cl<sub>4-x</sub>, where BETS is bis(ethylenedithio)tetraselenafulvalene. It has been reported that the increase in Br content works as a negative pressure effect and that the compound with  $x \sim 0.75$  is located near the Mott boundary [1]. These indicate that by controlling the Br content  $x$ , we can access the Mott boundary region under ambient conditions, which allows us to study the magnetic field effects on the Mott transition over a wide temperature and magnetic field ranges using pulsed magnetic fields.

In this study, we performed magnetoresistance measure-

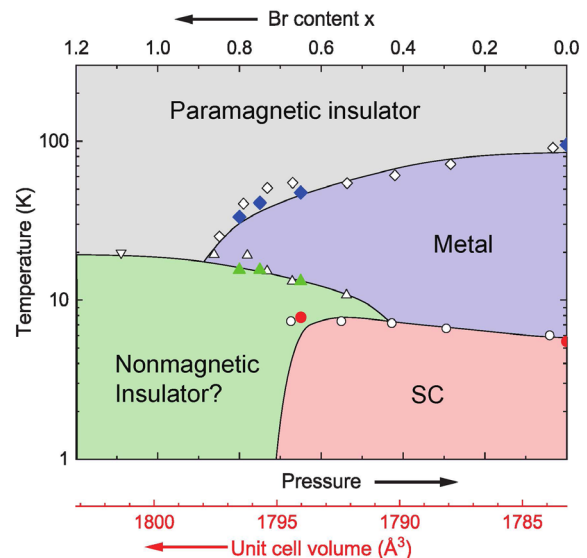


Fig. 1.  $p$ - $T$  phase diagram of  $\lambda$ -(BETS)<sub>2</sub>GaBr<sub>x</sub>Cl<sub>4-x</sub>. The red horizontal axis indicates the unit cell volume at room temperature [1]. The points marked with blue diamonds, green triangles, and red circles were determined in this study.

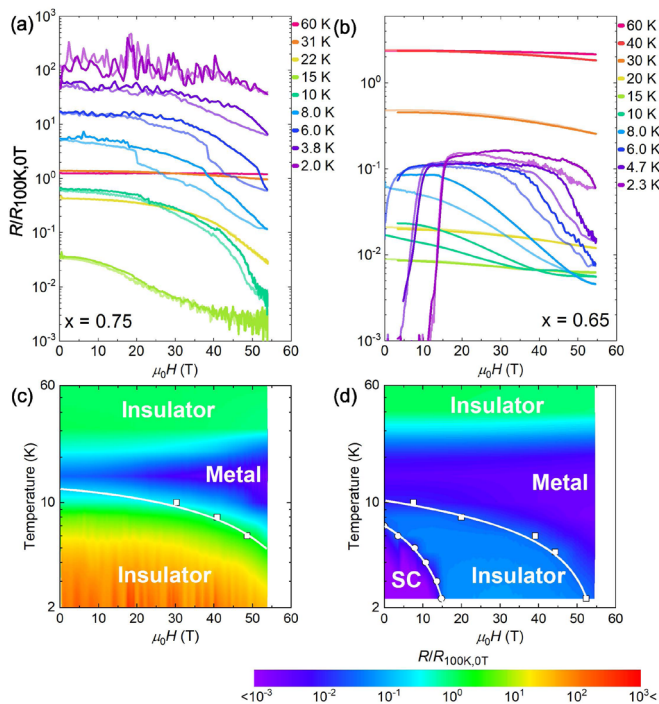


Fig. 2. (a), (b) Magnetic field dependence of the resistivity of the compound with  $x = 0.75$  and  $0.65$ . (c), (d)  $H - T$  phase diagram of the compound with  $x = 0.75$  and  $0.65$ .

ments using a 60 T pulse magnet at the International MegaGauss Science Laboratory. We synthesized  $\lambda$ -type organic conductors with  $x = 0.65$ ,  $0.75$ , and  $0.8$ , which are located near the Mott boundary. Figures 2 (a) and 2(b) show the temperature dependence of the magnetoresistance for compounds with  $x = 0.75$  and  $0.65$  [2]. We confirmed that in the compound with  $x = 0.75$ , a sharp drop with hysteresis in resistivity was observed at a certain magnetic field, suggesting that a first-order magnetic field induced insulator-to-metal Mott transition occurs. Interestingly, in the compound with  $x = 0.65$ , the suppression of the superconducting state at low magnetic fields and a Mott transition at high magnetic fields were observed, indicating a successive superconductor-to-insulator-to-metal transition. These results are summarized as a color plot of the field-temperature ( $H - T$ ) phase diagram shown in Figs. 2 (c) and 2(d). We note that the magnetic field induced Mott transition observed previously in  $\kappa$ -type organic conductors is a transition from the metallic to the insulating state by applying a magnetic field, whereas the Mott transition observed in  $\lambda$ -type salts in this study is a transition from the insulating to the metallic state, that is, the opposite magnetic field response was observed [3].

We proposed that the difference in magnetic susceptibility between the insulating and metallic phases across the Mott boundary is key to explaining the opposite magnetic field effects on the Mott transition. The previous studies reported that the magnetic susceptibility of  $\lambda$ -(BETS) $_2$ GaBr $_x$ Cl $_{4-x}$  decreases with increasing Br content at low temperatures [2]. This suggests that the magnetization of the metal phase is larger than that of the insulator phase. Since the spin state with larger magnetization is more stabilized under magnetic fields, the metallic state is stabilized in magnetic fields.

In this study, we have experimentally verified a magnetic-field-induced insulator-to-metal Mott transition and a successive superconductor-to-insulator-to-metal transition from magnetoresistance measurements for  $\lambda$ -type

organic Mott insulators. These experimental results not only provide new insight into the magnetic field effects on the Mott transition but also highlight that the Mott transition can be induced in experimentally feasible magnetic fields at ambient pressure conditions through the control of chemical pressure in  $\lambda$ -type organic conductors, thereby paving the way for future microscopic investigations of the field-induced Mott transition.

## References

- [1] H. Tanaka, A. Kobayashi, A. Sato, H. Akutsu, and H. Kobayashi, J. Am. Chem. Soc. **121**, 760(1999).
- [2] S. Fukuoka, T. Oka, Y. Ihara, A. Kawamoto, S. Imajo, and K. Kindo, Phys. Rev. B **109**, 195142 (2024).
- [3] F. Kagawa, T. Itou, K. Miyagawa, and K. Kanoda, Phys. Rev. Lett. **93**, 127001 (2004).

## Authors

S. Fukuoka<sup>a</sup>, T. Oka<sup>a</sup>, Y. Ihara<sup>a</sup>, A. Kawamoto<sup>a</sup>, S. Imajo, and K. Kindo<sup>a</sup>Hokkaido University

PI of Joint-use project: S. Fukuoka  
Host lab: Kindo Group

## Search for Valence and Structural Transition in Eu Alloy in Magnetic Field

The 122-type intermetallic compound  $\text{Eu}_x(\text{Co}_{1-x}\text{Ni}_x)_2\text{P}_2$  shows a correlation between multiple degrees of freedom in the solid resulting in various phenomena such as isostructural transition between the collapsed tetragonal (cT) and uncollapsed tetragonal (ucT) structures,  $3d$  magnetism, and the formation of P-P dimers. To gain insights on the correlated behavior and to search for magnetic-field-induced phase transitions, we investigate the effect of high magnetic fields on the samples of  $x = 0.4$  and  $0.5$ . As the samples are in the Eu valence fluctuating regime, the structural phase transition from cT to ucT may be induced by the Eu valence change under the strong magnetic fields. We have performed the magnetostriction and magnetization measurements up to 60 T in the pulsed high field generated at the IMGSL in ISSP.

Figure shows the magnetic field dependence of the magnetostriction and magnetization of the sample of  $x = 0.4$ . The magnetostriction smoothly increases with increasing magnetic fields. The behavior is in good agreement with the calculated results using the inter-configurational fluctuation model that describes the Eu valence change. This indicates that magnetostriction represents the change of the Eu valence state in the compound. The magnetization curve also shows relatively good agreement with the model at high magnetic fields. In contrast, in the low-magnetic-field region below 20 T, magnetization curves do not agree with the model. The anomalies in the magnetization at around 10 and 15 T are likely attributed to the spin-flop transitions of the  $3d$  electrons. These results indicate that the changes in the Eu valence manifest themselves in the magnetization curves at high magnetic fields, while the magnetism of the  $3d$  electrons manifests itself in the magnetization at low magnetic fields. We conclude that the valence change occurs within the Eu valence fluctuation regime coupled with the cT structure.

The absence of the abrupt changes in the magnetostriction should indicate that the transition to ucT structure, which is firmly coupled with the divalent Eu state, does not occur within the magnetic field range of the present study. Even higher magnetic fields or pulsed magnetic fields with

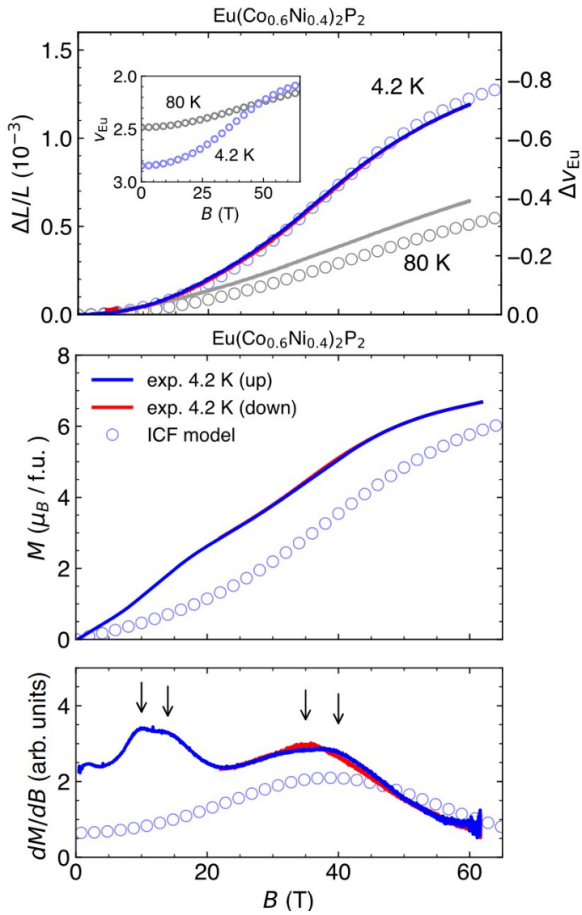


Fig. 1. Magnetic field dependence of the magnetostriction and magnetization of  $\text{Eu}_{0.4}(\text{Co}_{0.6}\text{Ni}_{0.4})_2\text{P}_2$

slower pulse durations may induce such large state changes in the present material, which is triggered by the Eu valence change under high magnetic fields. Searching for such phase transition in higher magnetic fields using the destructive magnetic field generation method in ISSP should be an interesting future work.

#### Reference

[1] R. Nakamura, A. Ishita, J. Nakamura, H. Ohta, Y. Haraguchi, H. Aruga Katori, H. Ishikawa, A. Matsuo, K. Kindo, M. Nohara, and A. Ikeda, *Phys. Rev. B* **107**, 235110 (2023).

#### Authors

R. Nakamura<sup>a</sup>, A. Ishita<sup>a</sup>, J. Nakamura<sup>a</sup>, H. Ohta<sup>b</sup>, Y. Haraguchi<sup>c</sup>, H. Aruga Katori<sup>c</sup>, H. Ishikawa, A. Matsuo, K. Kindo, M. Nohara<sup>d</sup>, and A. Ikeda<sup>a</sup>

<sup>a</sup>University of Electro-Communications

<sup>b</sup>Doshisha University

<sup>c</sup>Tokyo University of Agriculture and Technology

<sup>d</sup>Hiroshima University

PI of Joint-use project: A. Ikeda

Host lab: Kindo Group

## Nonvolatile Magnetothermal Switching Induced by Flux Trapping in Sn-Pb Solder

High-performance and high-density electronic devices require improvement of thermal management, especially thermal switch technology for controlling heat flow. Spintronic multilayer films [1] and superconductors [2] can control their thermal conductivity ( $\kappa$ ) using only a magnetic field ( $H$ ) without the mechanical motion. However, neither

spintronic nor superconducting materials achieved nonvolatile magnetothermal switching (MTS). This study shows nonvolatile MTS in commercial Sn-Pb solder and discuss the origin of its nonvolatility.

We used commercially available flux-core-free solder Sn45-Pb55 (mass ratio Sn : Pb = 45:55,  $\phi$ 1.6 mm, TAIYO ELECTRIC IND. CO., LTD.). The chemical composition and surface of Sn45-Pb55 solder was investigated by scanning-electron microscope and energy-dispersive X-ray spectroscopy, revealing that the Sn45-Pb55 solder is a completely phase-separated composite. Thermal conductivity ( $\kappa$ ) was measured using the Physical Property Measurement System (PPMS, Quantum Design) with the four-probe steady state method. Specific heat ( $C$ ) was measured using PPMS by a relaxation mode. Magnetization was measured using a superconducting quantum interference device magnetometer on the Magnetic Property Measurement System (MPMS3, Quantum Design) with a VSM mode. We performed magneto-optical (MO) imaging at Tokunaga laboratory to observe magnetic flux trapping of Sn45-Pb55 solder in superconducting state [3]. The  $H$  dependence of the MO images at 2.5 K was observed, and all the images were temperature difference images at 2.5 K (superconducting state) and 8 K (normal state), and then normalized to the 8 K images.

Figure 1(a) displays the  $H$  dependence of  $\kappa$  at 2.5 K. After zero field cooling (ZFC),  $\kappa$  shows a low value of  $10 \text{ WK}^{-1}\text{m}^{-1}$ . However, when the magnetic field is increased from 0 Oe to 1700 Oe,  $\kappa$  rises to  $35 \text{ WK}^{-1}\text{m}^{-1}$ . Notably,  $\kappa$  does not return to its initial value when the magnetic field is decreased from 1700 Oe to 0 Oe, and  $\kappa$  maintains a high value throughout any magnetic field process. The initial increase in  $\kappa$  by the magnetic field is conventionally understood to be due to the transition of Sn and Pb from the superconducting state to the normal state.

To discuss the nonvolatility of MTS in solder, we first examine the temperature dependence of  $C$ . Figure 1(b) shows the temperature dependence of specific heat in form of  $C/T$  at  $H=0$  after ZFC and field cooling (FC) under 1500 Oe. The  $C$  values of the ZFC and FC data is estimated as  $C(0 \text{ Oe}) - C(1500 \text{ Oe})$  to eliminate the specific heat of normal states. The ZFC data show a sharp peak due to the superconducting transition of Sn at 3.7 K and Pb at 7.2 K. However, in the FC data, while the sharp peak corresponding to the superconducting transition of Pb is observed, no peak appears near the superconducting transition temperature of Sn.

The upper panel of Fig. 2. shows the  $H$  dependence of the magnetic flux density ( $B$ ) at 2.5 K.  $B$  is the sum of  $H$  and the magnetization  $4\pi M$ :  $B = H + 4\pi M$ . Below  $H = 300 \text{ Oe}$ ,  $B = 0 \text{ G}$  because both Sn and Pb are in the Meissner state.

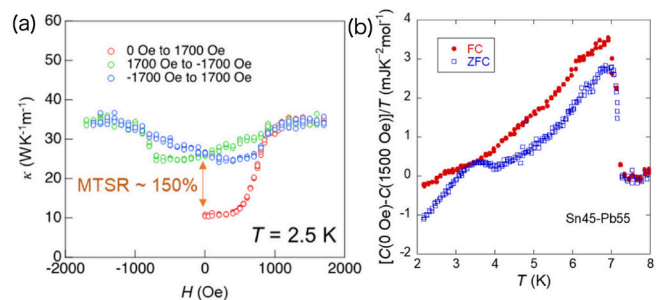


Fig. 1. (a) Magnetic field dependence of  $\kappa$  at 2.5 K. (b) Temperature dependence of residual specific heat estimated by  $C(0 \text{ Oe}) - C(1500 \text{ Oe})$  in the form of  $C/T$ . Both ZFC and FC data are taken at  $H = 0 \text{ Oe}$  ZFC and after FC under 1500 Oe, respectively.

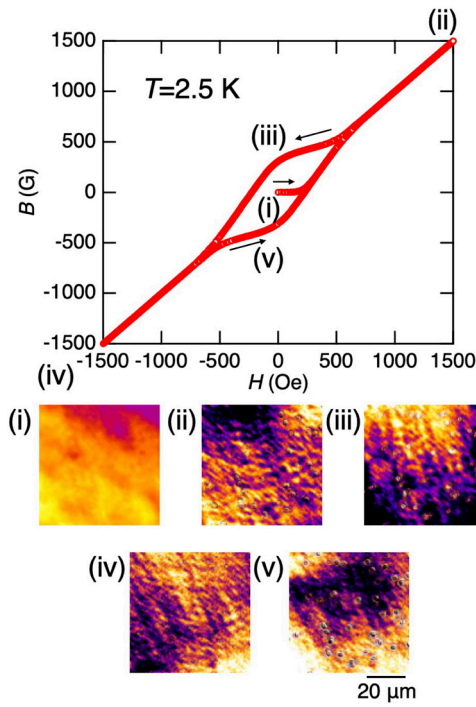


Fig. 2. The upper panel is the  $B$ - $H$  curve at 2.5 K. The lower panels are MO images at 2.5 K. An image (i) is taken after ZFC. Images (ii) and (iv) are taken at  $H = 1500$  Oe and  $H = -1500$  Oe, respectively. Images (iii) and (v) are taken at  $H = 0$  Oe after positive or negative magnetic field, respectively.

When  $H$  exceeds 300 Oe which is the critical field of Sn, magnetic flux penetrates and  $B$  shows a finite value. In the vicinity of the critical field of Pb at 700 Oe, the magnetic flux penetrates the entire Sn-Pb solder, and  $B = H$ . After  $H$  return to 0 Oe, a magnetic flux of about  $B = 400$  G is trapped. The specific heat results show that the superconducting state of Sn is suppressed by FC condition. This suggests that the superconducting bulkiness of Sn is suppressed due to trapping the magnetic flux in Sn region. The lower panels of Fig. 2 show a MO images of Sn-Pb solder. Bright areas indicate positive magnetic flux, and dark areas indicate negative magnetic flux. In the initial state (i), the MO image is uniform as there is no magnetic flux in the solder. In states (ii) and (iv), the magnetic flux penetrates the entire solder. In images (iii) and (v) at  $H = 0$ , after experiencing the magnetic field, bright or dark regions in certain clusters indicate that magnetic flux is trapped in specific region.

The findings of this study are summarized with the schematic images in Fig. 3. After ZFC, both Sn and Pb are in the superconducting state, resulting in low  $\kappa$  (Fig. 3(a)). When a magnetic field above the critical field of Sn and Pb is applied, both Sn and Pb transition to the normal state,

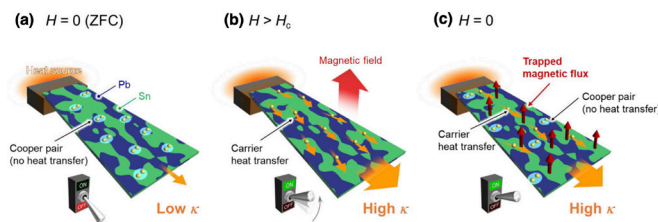


Fig. 3. Schematic images of nonvolatile magnetothermal switching in Sn-Pb solder. (a) The initial state of thermal conductivity ( $\kappa$ ) after ZFC. (b) A state in which a magnetic field exceeding the critical field ( $H_c$ ) of Sn and Pb is applied. (c) State of Sn-Pb solder in  $H = 0$  Oe after experiencing  $H_c$ .

causing  $\kappa$  to increase. Then, at  $H = 0$ , Pb returns to the superconducting state while Sn traps the magnetic flux, suppressing its superconductivity. Consequently, since the thermal conductivity in the Sn region remains high, the solder shows nonvolatile MTS. In this study, we focused on Sn-Pb solder as a phase-separated superconductor. Interestingly, the solder exhibited the nonvolatile MTS, and we clarified that the flux trapping played a crucial role in this nonvolatility.

## References

- [1] H. Nakayama *et al.*, Appl. Phys. Lett. **118**, 042409 (2021).
- [2] M. Yoshida *et al.*, J. Appl. Phys. **134**, 065102 (2023).
- [3] Y. Kinoshita *et al.*, Rev. Sci. Instrum. **93**, 073702 (2022).

## Authors

H. Arima<sup>a</sup>, Md. R. Kasem<sup>a</sup>, H. Sepehri-Amin<sup>b</sup>, F. Ando<sup>b</sup>, K. Uchida<sup>b</sup>, Y. Kinoshita, M. Tokunaga, and Y. Mizuguchi<sup>a</sup>  
<sup>a</sup>Tokyo Metropolitan University  
<sup>b</sup>NIMS

PI of Joint-use project: Y. Mizuguchi  
 Host lab: Tokunaga Group

## Magnetic Superstructure Phase Induced by Ultrahigh Magnetic Fields

Magnetic superstructures, where the magnetic unit cell is an integer multiple of the original crystallographic unit cell, have received considerable attention. For frustrated spin systems, a variety of quantum-entangled magnetic superstructures can appear in an external magnetic field. Of particular interest are a series of magnon crystals in the spin-1/2 kagome Heisenberg antiferromagnet [1] and successive transformations of singlet-triplet superstructures in the spin-1/2 orthogonal-dimer Heisenberg antiferromagnet [2]. Furthermore, the interplay between spin and lattice degrees of freedom can induce spin-lattice-coupled magnetic superstructures, as theoretically proposed for the Heisenberg antiferromagnet on the breathing pyrochlore lattice, where neighboring tetrahedra differ in size in an alternating pattern [3]. In this study, we verify this theoretical prediction in a model compound of the breathing pyrochlore antiferromagnet, LiGaCr<sub>4</sub>O<sub>8</sub>, by means of state-of-the-art magnetization and magnetostriction measurements under ultrahigh magnetic fields up to 600 T [4].

Figure 1(a) summarizes the magnetization data of LiGaCr<sub>4</sub>O<sub>8</sub> measured at  $\sim 5$  K. In the single-turn coil (STC) system, we observe a linear increase in the magnetization  $M$  with respect to the external magnetic field  $B$  up to a maximum field of 145 T, suggesting that spins are smoothly canting from the 2-up-2-down collinear ground state. Upon

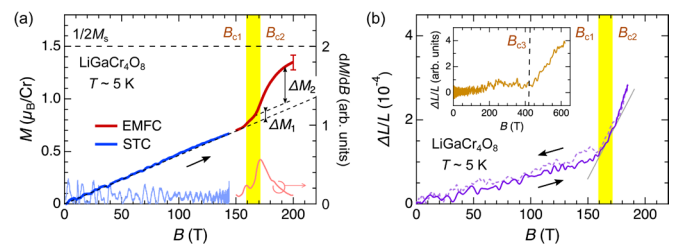


Fig. 1: (a) Magnetization curve of LiGaCr<sub>4</sub>O<sub>8</sub> at  $T \sim 5$  K. Field derivative of the magnetization,  $dM/dB$ , is displayed in the right axis. (b) Magnetostriction curve of LiGaCr<sub>4</sub>O<sub>8</sub> at  $T \sim 5$  K.

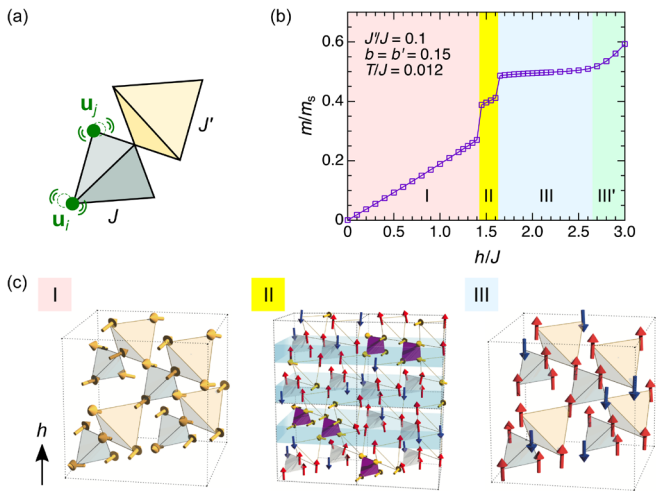


Fig. 2. (a) Site-phonon model taking account of the independent site displacement  $\mathbf{u}_i$ . (b) Calculated magnetization curve with the exchange parameter  $J'/J = 0.1$  and the spin–lattice coupling parameter  $b = 0.2$  (see details for Ref. [4]). (c) Schematics of the magnetic structures in Phases I ~ III.

the application of a higher magnetic field using the electromagnetic flux compression (EMFC) system, we observe a dramatic magnetization increase between 150 and 200 T, followed by a half plateau at  $M \sim 1.5 \mu_B/\text{Cr}$ , as reported in conventional chromium spinel oxides [5]. Notably, a double-hump structure can be seen in  $dM/dB$ , indicating a two-step metamagnetic transition at  $B_{c1} = 159$  T and  $B_{c2} = 171$  T. The existence of an intermediate-field phase is supported by the magnetostriction measurement. Figure 1(b) shows the magnetostriction data measured at  $\sim 5$  K using the STC system. The sample length starts to rapidly increase at  $B_{c1}$ , then the lattice expansion accelerates above  $B_{c2}$ . We also measured the magnetostriction up to 600 T using the EMFC system, as shown in the inset of Fig. 1(b). A plateau-like behavior is observed from 200 T up to  $B_{c3} \sim 420$  T, followed by an upturn behavior up to the saturation around 550 T. The observation of a wide plateau suggests the strong spin–lattice coupling inherent in  $\text{LiGaCr}_4\text{O}_8$ .

To understand these observations, we perform the classical Monte-Carlo simulations for a magnetoelastic Hamiltonian on the breathing pyrochlore lattice, incorporating the Einstein site-phonons [3,4]. Figure 2 shows the calculated magnetization curve obtained for a typical parameter set with relatively large breathing anisotropy and strong spin–lattice coupling. In addition to the low-field phase (Phase I) with an 8-sublattice canted 2-up-2-down state and the 1/2-plateau phase (Phase III) with a 16-sublattice 3-up-1-down state, an intermediate-field phase (Phase II) appears, associated with a two-step metamagnetic transition. The magnetic structure of phase II is characterized by a three-dimensional periodic array of canted 2-up-2-down and 3-up-1-down tetrahedral clusters in a 1:2 ratio, forming a magnetic superstructure with a  $6 \times 6 \times 6$  magnetic unit cell.

In summary, we experimentally demonstrate that the breathing pyrochlore antiferromagnet exhibits unconventional field-induced phase transitions, which could signal the emergence of a magnetic superstructure phase. The present work, combining the exotic experimental observations with the microscopic magnetoelastic theory in a complicated three-dimensional frustrated magnet, paves the way for further verifications of intriguing physical phenomena originating from the spin–lattice coupling and/or breathing anisotropy, both of which can be relevant in magnetic materials regardless of the geometry of the underlying crystalline lattice.

## References

- [1] J. Schulenburg *et al.*, Phys. Rev. Lett. **88**, 167207 (2002).
- [2] K. Kodama *et al.*, Science **298**, 395 (2002).
- [3] K. Aoyama *et al.*, Phys. Rev. B **104**, 184411 (2021).
- [4] M. Gen *et al.*, Proc. Natl. Acad. Sci. U.S.A. **120**, e2302756120 (2023).
- [5] A. Miyata *et al.*, J. Phys. Soc. Jpn. **81**, 114701 (2012)

## Authors

M. Gen<sup>a</sup> and Y. Kohama  
<sup>a</sup>RIKEN Center for Emergent Matter Science

PI of Joint-use project: M. Gen  
 Host lab: Kohama and Y. H. Matsuda Group



# Progress of Facilities

## Supercomputer Center

The Supercomputer Center (SCC) is a part of the Materials Design and Characterization Laboratory (MDCL) of ISSP. Its mission is to serve the whole community of computational condensed-matter physics of Japan, providing it with high performance computing environment. In particular, the SCC selectively promotes and supports large-scale computations. For this purpose, the SCC invites proposals for supercomputer-aided research projects and hosts the Steering Committee, as mentioned below, that evaluates the proposals.

The ISSP supercomputer system consists of two subsystems: System B, which was last replaced in Oct. 2020, is intended for larger total computational power and has more nodes with relatively loose connections whereas System C is intended for higher communication speed among nodes. System B (ohtaka) consists of 1680 CPU nodes of AMD EPYC 7702 (64 cores) and 8 FAT nodes of Intel Xeon Platinum 8280 (28 cores) with total theoretical performance of 6.881 PFlops. System C was replaced in June 2022 and the current system (kugui) consists of 128 nodes of AMD EPYC 7763 (128 cores) and 8 nodes of AMD EPYC 7763 (64 cores) with total theoretical performance of 0.973 PFLOPS.

In addition to the hardware administration, the SCC puts increasing effort on the software support. Since 2015, the SCC has been conducting “Project for advancement of software usability in materials science (PASUMS).” In this project, for enhancing the usability of the ISSP supercomputer system, we conduct several software-advancement activities: developing new application software that runs efficiently on the ISSP supercomputer system, adding new functions to existing codes, help releasing private codes for public use, creating/improving manuals for public codes, etc.

Two target programs were selected for fiscal year 2023: (1) Enhancement of TeNeS for finite-temperature calculation (proposed by T. Okubo (U. Tokyo)), and (2) First-principles high-throughput computation for database generation (proposed by K. Yoshimi (ISSP)). In addition, since 2021, we have been maintaining the data repository service for secure storage and enhanced usability of results of numerical calculation.

All staff members of university faculties or public research institutes in Japan are invited to propose research projects (called User Program). The proposals are evaluated by the Steering Committee of SCC. Pre-reviewing is done by the Supercomputer Project Advisory Committee. In fiscal year 2023, totally 345 projects were approved including the ones under the framework of Supercomputing Consortium for Computational Materials Science (SCCMS), which specially supports FUGAKU and other major projects in computational materials science. The total points applied and approved are listed on Table. 1 below.

The research projects are roughly classified into the following three (the number of projects approved, not including SCCMS):

First-Principles Calculation of Materials Properties (178)  
Strongly Correlated Quantum Systems (36)  
Cooperative Phenomena in Complex, Macroscopic Systems (119)

In all the three categories, most proposals involve both methodology and applications. The results of the projects are reported in 'Activity Report 2023' of the SCC. Every year 3-4 projects are selected for “invited papers” and published at the beginning of the Activity Report. In the SCC Activity Report 2023, the following four invited papers are included:

Class	Max Points		Application	Number of Projects	Total Points			
	System B	System C			Applied		Approved	
					System B	System C	System B	System C
A	100	50	any time	24	2.4k	1.2k	2.4k	1.2k
B	1k	100	twice a year	99	58.1k	7.3k	38.5k	6.5k
C	10k	1k	twice a year	185	996.9k	58.4k	513.6k	45.8k
D	10k	1k	any time	8	47.5k	2.3k	40.6k	1.9k
E	30k	3k	twice a year	17	317.0k	25.5k	185.0k	20.7k
S			twice a year	0	0k	0k	0k	0k
SCCMS				12	27.0k	2.6k	27.0k	2.6k
Total				345	1448.9k	97.3k	807.1k	78.7k

Table 1. Research projects approved in Academic Year 2023.

The maximum points allotted to the project of each class are the sum of the points for the two systems; Computation of one node for 24 hours corresponds to one point for the CPU nodes of System B and System C. The FAT nodes require four points for a 1-node 24-hours use.

1. “Density functional theory calculations of H<sub>2</sub>O adsorption monolayer on a Pt(111) surface”, Jun HARUYAMA, Osamu SUGINO (ISSP), and Toshiki SUGIMOTO (Institute for Molecular Science, JST)
2. “Theoretical studies on the spin-charge dynamics in Kondo-lattice models”, Masahito MOCHIZUKI, and Rintaro ETO (Waseda Univ.)
3. “Mixing Free Energy and Molecular Dynamics Simulations”, Naoko NAKAGAWA and Akira YOSHIDA (Ibaraki Univ.)
4. “Ab initio optical calculation by RESPACK”, Kazuma NAKAMURA (Kyutech)

## Neutron Science Laboratory

The Neutron Science Laboratory (NSL) has been playing a central role in neutron scattering activities in Japan since 1961 by performing its own research programs as well as providing a strong General User Program (GUP) for the university-owned various neutron scattering spectrometers installed at JRR-3 (20 MW) operated by Japan Atomic Energy Agency (JAEA) in Tokai, Ibaraki (Fig. 1). In 2003, the Neutron Scattering Laboratory was reorganized as the Neutron Science Laboratory to further promote the neutron science with use of the instruments in JRR-3. Under GUP supported by NSL, 12 university-group-owned spectrometers in the JRR-3 reactor are available for a wide scope of research on material science. The submitted proposals were about 300 and the visiting users reached over 6000 person-day in FY2010. In 2009, NSL and Neutron Science Division (KENS), High Energy Accelerator Research Organization (KEK) built a chopper spectrometer, High Resolution Chopper Spectrometer, HRC, at the beam line BL12 of MLF/J-PARC (Materials and Life Science Experimental Facility, J-PARC) (Fig. 2). HRC covers wide energy transfer ( $100 \mu\text{eV} < \hbar\omega < 0.5 \text{ eV}$ ) and momentum transfer ( $0.03 \text{ \AA}^{-1} < Q < 30 \text{ \AA}^{-1}$ ) ranges, and therefore becomes complementary to the existing inelastic spectrometers at JRR-3. HRC has accepted general users through the J-PARC proposal system since FY2011.

Triple axis spectrometers, HRC, a four-circle diffractometer, and a high resolution powder diffractometer are utilized mainly for a conventional solid state physics and a variety of research fields on hard-condensed matter, while in the field of soft-condensed matter science, researches are mostly carried out by using a small angle neutron scattering (SANS-U) and/or neutron spin echo (iNSE) instruments. The

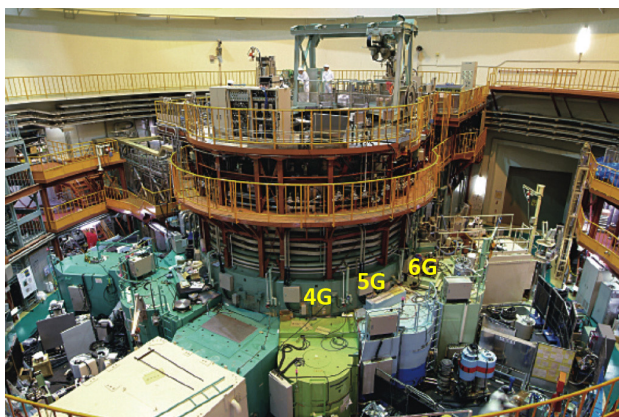


Fig. 1. Reactor hall of JRR-3. Three triple axis spectrometers are shown in the photo.

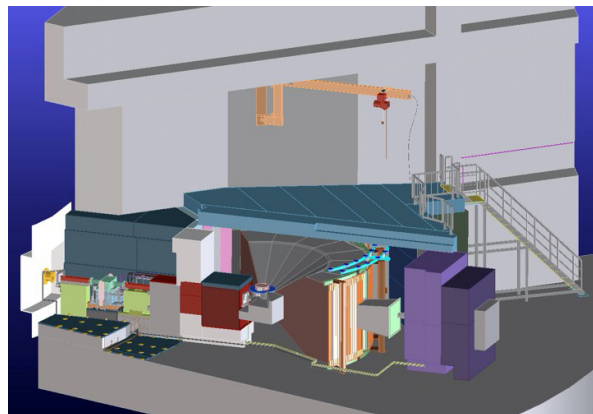


Fig. 2. Schematic view of HRC.

upgraded time-of-flight (TOF) inelastic scattering spectrometer, AGNES, is available both for hard- and soft-matter science. Our GUP has produced 2137 publications and 319 dissertations until April 23, 2024. Their lists for the last 10 years are given in Activity Report on Neutron Scattering Research which is available in ISSP and NSL web pages.

As for international cooperative programs, NSL operates the U.S.-Japan Cooperative Program on neutron scattering, providing further research opportunities to material scientists who utilize the neutron scattering technique for their research interests. In 2010, relocation of the U.S.-Japan triple-axis spectrometer, CTAX, was completed, and it is now open to Japanese users. In March 2024, we had an international review for the renewal of the cooperative program which is mandated by the MEXT every 10 years. The review and contract renewal were successfully completed and the cooperation program is now entering a new phase. Here, as proposed by the review committee, we plan to further revitalize soft matter science.

After the resumption of JRR-3 operation in 2021, many instrumental advances have been made. First, improvements to the instruments and guide tubes during the beam shutdown period (2011-2021) resulted in a 10-fold increase in the intensity of GPTAS (4G) and an 8-fold increase in AGNES (C3-1-1). Next, a new multiflex-type triple-axis spectrometer HODACA was constructed at C1-1. This spectrometer is 40 times more efficient than the conventional spectrometer (HER). The development and improvement of these instruments and the latest status of the other university spectrometers at JRR-3 are described in detail in a special topics of the Journal of the Physical Society of Japan (JPSJ) (Vol. 93(9)). Some improvements have also been made to the proposal adoption system: multibeam proposals (in cooperation with PF at KEK) were launched in 2022, student proposals (doctor-course students can apply as PIs) in 2023, international proposals (researchers from overseas institutions can apply as PIs) in 2024. Industrial proposals (in which researchers from industry can apply as PIs) are scheduled to begin in 2025.

We had conducted 84 experiments for 155 approved proposals in 2021 (reactor operation: 4 cycles, 92 days), 123 experiments for 166 approved proposals in 2022 (reactor operation: 7 cycles, 152 days), and 122 experiments for 154 approved proposals in 2023 (reactor operation: 6 cycles, 143 days). For these experiments, about 70 papers, including those under review, have been obtained as of May, 2024.

## International MegaGauss Science Laboratory

The objective of this laboratory (Fig. 1) is to study the physical properties of solid-state materials (such as metals, semiconductors, insulators, superconductors, and magnetic materials) in a high magnetic field of 100 T or even higher. Such a high magnetic field can control material phases and functions. Our pulsed magnets, at the moment, can generate up to 88.6 Tesla (T) in a non-destructive manner and up to 1200 T in a destructive manner. The world record for an indoor magnetic field of 1200 T was achieved in 2018. The laboratory is open for scientists both domestic and overseas. Lots of fruitful results have come out from the collaborative researches and our in-house activities.



Fig. 1. The building C of the IMGSL.

Our interests cover the studies on quantum phase transitions (QPT) induced by high magnetic fields. Field-induced QPT has been explored in various materials, such as quantum spin systems, strongly correlated electron systems, and other magnetic materials. One of our ultimate goals is to provide joint-research users with a 100 T millisecond-long pulse using a non-destructive magnet and to offer versatile high-precision physical measurements. Measurable physical quantities or properties are magneto-optical spectra, magnetization, magnetostriction, electrical transport, specific heat, nuclear magnetic resonance, and ultrasound propagation. They can be carried out with sufficiently high accuracy. Another ultimate goal is to extend the magnetic field region and discover novel phenomena happening only in extremely strong magnetic fields exceeding 100 T. Recent technical developments allow us to even measure magnetostriction and ultrasound propagation in destructive magnetic fields over 100 T, which can directly reach potential structural changes in the ultrahigh magnetic fields. The recent discovery of magnetic field-induced insulator-metal transitions of strongly correlated materials in 500 T would open a new direction of the megagauss field research, namely the exploration of field-induced novel phases in materials with strong interactions comparable to the thermal energy at room temperature.

A set of supercapacitor power supplies with a total accumulation energy of 150 MJ (Fig. 2) was installed in 2023 and used as an energy source for super-long pulse magnets. The magnet technologies are intensively devoted to the quasi-steady long pulse magnet (an order of 1-10 sec) energized by the giant DC power supply. The supercapacitor

	Alias	Type	$B_{max}$	Pulse width Bore	Power source	Applications	Others
Building C Room 101-113	ElectroMagnetic Flux Compression	Destructive	1200 T	3 $\mu$ s (100-1200T) 10 mm	5 MJ, 50 kV 2 MJ, 50 kV	Magneto-Optics Magnetization Magneto-Striction Magneto-Transport	5 K – room temperature
	Horizontal Single-turn Coil	Destructive	300 T 200 T	6 $\mu$ s 5 mm 10 mm	0.2 MJ, 50 kV	Magneto-Optics Magnetization Magneto-Striction Magneto-Transport Ultrasound	5 K – room temperature
	Vertical Single-turn Coil	Destructive	300 T 200 T	8 $\mu$ s 5 mm 10 mm	0.2 MJ, 40 kV	Magneto-Optics Magnetization Magneto-Striction Magneto-Transport Ultrasound	2 K – room temperature
Building C Room 114-120	Mid-pulse Magnet	Non-destructive	60 T  70 T	40 ms 18 mm  40 ms 10 mm	  0.9 MJ, 10 kV	Magneto-Optics Magnetization Magneto-Transport Electric-Polarization Magneto-Striction Magneto-Imaging Torque Magneto-Calorimetry Heat Capacity Ultrasound	Independent Experiment in 5 site  Lowest temperature 0.1 K
Building C Room 121	PPMS	Steady	14 T			Resistance Heat Capacity	Down to 0.3 K
	MPMS	Steady	7 T			Magnetization	Down to 2K
Building K	Short-Pulse Magnet	Non-destructive	86 T	2.5 ms 12 mm	0.5 MJ, 20 kV	Magnetization Magneto-Transport	1.4 K – room temperature
	Long-Pulse Magnet	Non-destructive	40 T	1 s 30 mm	150 MJ, 2.4 kV	Resistance Magneto-Calorimetry	0.5 K – room temperature

Table 1. Available Pulse Magnets, Specifications



Fig. 2. Upper: The K-building for the supercapacitor power supply (left-hand side) and a long pulse magnet station (right-hand side). Lower: The supercapacitors have a total accumulation energy of 150 MJ installed in 2023 and are planned to drive the long pulse 60 T magnet and the first stage of the dual-coil 100 T non-destructive magnet.

power source will also be used for the giant outer magnet coil to realize a 100 T nondestructive magnet by inserting a conventional pulse magnet coil in its center bore. Recently, the super-long pulsed magnet has been intensively used to investigate thermal properties such as specific heat and magnetocaloric effects.

Magnetic fields exceeding 100 T can only be obtained with the destruction of a magnet coil. The ultrahigh magnetic fields are obtained in a microsecond time scale. The project, financed by the Ministry of Education, Culture, Sports, Science and Technology aiming to generate 1000 T with the electromagnetic flux compression (EMFC) system (Fig. 3), has been completed. Our experimental techniques using the destructive magnetic fields have intensively been developed. The system, which is unique to ISSP on the world scale, is comprised of a power source of 5 MJ main condenser bank and 2 MJ condenser bank. Two magnet stations are constructed, and both are energized by each power source. Both systems are fed with another 2 MJ condenser bank used for a seed-field coil, the magnetic flux of which is to be compressed. The 2 MJ EMFC system can generate 450 T. The 5 MJ system is used for the generation of a 1000 T-class magnetic field. For the research in the magnetic field range



Fig. 3. View of the coil setup of the electromagnetic flux compression inside of an anti-explosive house. The world's strongest indoor magnetic field of 1200 T was achieved in 2018.

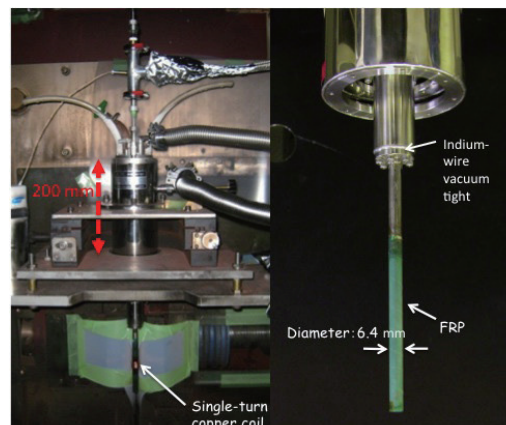


Fig. 4. Schematic picture of the V-type single-turn coil equipped with a 40 kV, 200 kJ fast capacitor bank system. The liquid-helium-bath cryostat with a plastic tail is also shown.

of 100-300 T, we have two single-turn coil (STC) systems that have a fast-capacitor bank system of 200 kJ for each. One is the horizontal type (H-type), and the other is a vertical type (V-type, Fig. 4). Various kinds of laser spectroscopy experiments, such as the cyclotron resonance and the Faraday rotation, are possible using the H-type STC, while a stable low-temperature condition of 2 K is available for the V-type STC.

## Center of Computational Materials Science

With the advancement of hardware and software technologies, large-scale numerical calculations have been making important contributions to materials science and will have even greater impact on the field in the near future. CCMS is a specialized research center established in 2011 for promoting computer-aided materials science with massively parallel computers, such as the Fugaku supercomputer, which has been developed in Kobe as the core of a billion-dollar national project. Activities of CCMS are divided into the following three categories: (1) highly efficient and large-scale use of the Fugaku supercomputer and its application to grand-challenge problems in computational materials science, (2) activities as the center for the community of computational condensed matter physics and materials science, and (3) computational physics research aiming to solve intriguing physics emerged from strongly correlated systems.

For the first category, each group in CCMS is carrying out various individual research projects in its own expertise to efficiently utilize large-scale parallel computers. For example, the Ozaki group has been developing efficient and accurate methods and software packages to extend the applicability of DFT to more realistic systems, and investigated the structural and electronic properties of various 2D materials in successful collaboration with experimental groups and industrial companies. There are other activities such as development of Tensor Network (TN) based numerical methods and Markov-chain Monte Carlo methods by the Kawashima group and the Todo group.

As for the activities in the second category, apart from major annual conferences and formal international meetings, the CCMS provided a series of lectures and training sessions at Kashiwa. For example, training sessions "Kashiwa Hands-

On" for getting accustomed to various application programs, such as OpenMX, Hphi, mVMC, AkaiKKR, and MateriApps LIVE!, as shown in Fig. 1, have been held monthly. Each session is designed for more than 10 trainees and takes 4-5 hours. We also coordinate the use of the computational resources available to our community, and support community members through various activities such as administering the website "MateriApps" for information on application software in computational science as shown in Fig. 2.

For the third category, the Misawa group addressed searching for topological insulators in solids which is one of the main issues of modern condensed-matter physics since robust gapless edge or surface states of the topological insulators can be used as building blocks of next-generation devices, and showed a way to realize a topological state characterized by the quantized Zak phase, termed the Zak insulator with spin-polarized edges in organic antiferromagnetic Mott insulators without relying on the spin-orbit coupling. The finding provides an unprecedented way to realize a topological state in strongly correlated electron systems. Prof. Misawa was also involved in the Data generation and utilisation materials Research and development projects (DxMT).

These activities are supported by funds for various governmental projects including the DxMT project and the Program for Promoting Researches on the Supercomputer Fugaku.

The following is the selected list of meetings organized by CCMS in recent years:

- 2023/3/29 DxMT workshop: recent progresses in



Fig. 1. Software in the CCMS community

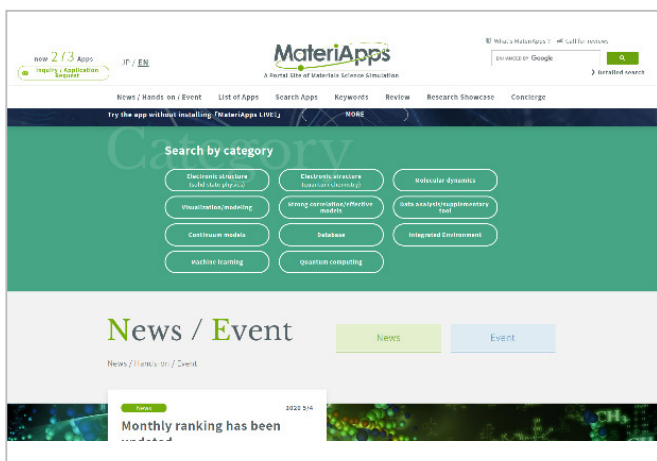


Fig. 2. MateriApps Website

machine-learning potentials.

- 2023/4/3-4 ISSP joint workshop for ISSP Supercomputer Co-use and CCMS.
- 2023/6/1 Matching Workshop for industries & graduate students/postdocs.
- 2023/6/26 Symposium of the Division of Data-Integrated Materials Science, Social Cooperation Research Department at ISSP.
- 2023/12/19-20 MP-CoMS lecture series for OpenMX Workshop: Fundamentals and Practice.
- 2024/2/12-14 MaterialAI2023: utilization of AI technologies in computational materials science
- 2024/2/19-20 ISSP workshop for Integration of Materials Science Simulations and Advanced Experimental Data.

In addition to the events listed above, we organize regular hands-on program for various application, such as RESPACK and SALMON.

## Laser and Synchrotron Research Center (LASOR Center)

Laser and synchrotron research center (LASOR Center) was established in October 2012 to push the frontiers of the photon and materials science. LASOR has 10 groups in 2023, which is the largest division in ISSP. Most of the research activities on the development of new high-power lasers and their application to materials science are conducted in specially designed buildings D and E with large clean rooms and vibration-isolated floors at the Kashiwa campus. We also have a clean room for a laser processing platform at the Kashiwa II campus. On the other hand, experiments using synchrotron radiation are conducted at SPring-8 and SACLA (Hyogo). Recently, a new beamline has been developed at Nano Terasu in Sendai.

The development of new laser light sources in the vacuum ultraviolet to soft x-ray range has revolutionized materials research, represented by high energy resolution photoelectron spectroscopy, ultrafast time domain spectroscopy, and ultrafast nonlinear spectroscopy. Materials science research with lasers has entered a new era. The ultrashort and high-power lasers are becoming an increasingly attractive light source for both basic research and industry. The state-of-the-art laser source and spectroscopy are being intensively explored.

Synchrotron-based research is another area of activity



Fig. 1. Optical frequency comb

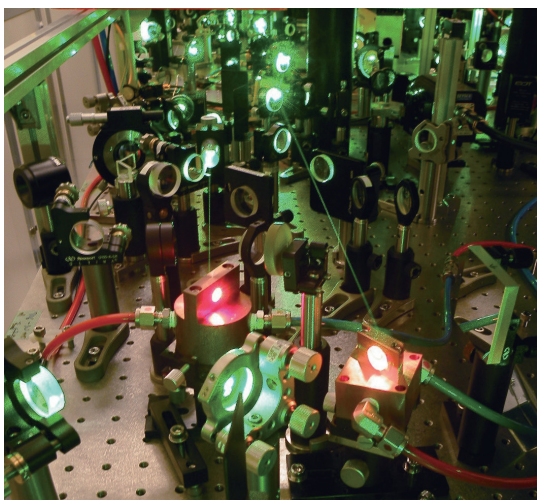


Fig. 2. Close look of a high-peak-power ultrashort-pulse laser

at the ISSP. The dramatic increase in the brilliance of synchrotron radiation has also opened up a new field of photon science. In 2018, the Japanese government has announced the construction of a new synchrotron facility in Tohoku (Nano Terasu). LASOR has decided to subjectively contribute to this facility from design to operation, and Nano Terasu is now under construction.

Lasers and synchrotrons have developed independently; today, both light sources cover a wide range of photon energies with an overlap in the vacuum-ultraviolet to soft X-ray regions. Recognizing their common interests in research areas and technologies, ISSP integrated the two streams, extreme lasers and synchrotron radiation, into a common platform. Through the mutual interactions between the frontiers of lasers and synchrotrons, LASOR will be the center of innovation in light and materials science through worldwide collaborative research and close cooperation with other divisions of ISSP such as New Materials Science, Nanoscale Science, and Condensed Matter Theory.

The mission of LASOR is to cultivate and advance the following three scientific fields:

1. Laser Science,
2. Synchrotron radiation science,
3. Extreme Spectroscopy,

• **Laser science group**

We have continued to develop various state-of-the-art laser systems, such as high-power solid-state or gas lasers,

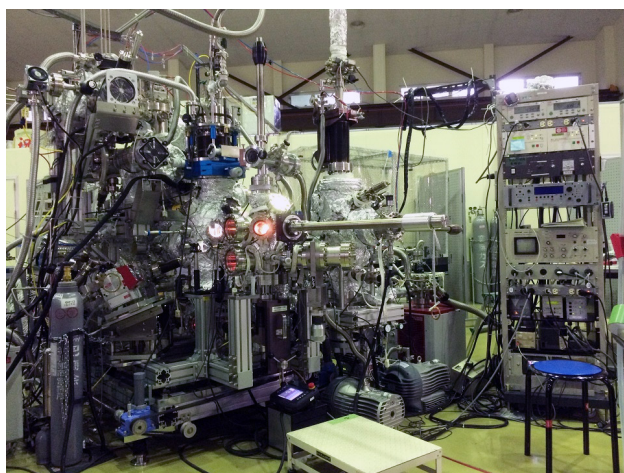


Fig. 3. Spin-resolved photo-emission spectroscopy.

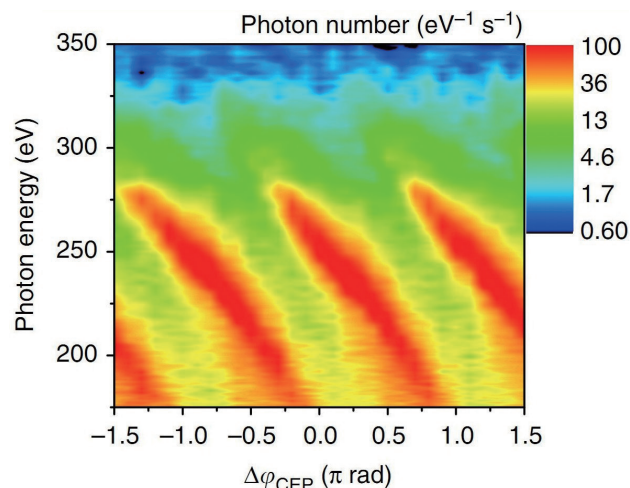


Fig. 4. Phase-dependence of high harmonic spectra in soft X rays.

high-intensity lasers, ultra-short pulse lasers down to the attosecond time scale (peta-Hz linewidth), ultra-stable 1-Hz linewidth lasers, optical frequency combs, mid-infrared lasers, THz light sources, and semiconductor lasers. The technology of high-power and ultrashort pulse lasers has progressed during these 10 years. It has opened two research directions. One is a coherent extreme ultraviolet light source realized by a high harmonic generation (HHG) scheme. The average power of HHG became high enough to be used for photoemission spectroscopy. Photon energies from 7 eV to 60 eV are now available. They can be either very narrow bandwidth or ultrashort pulse. The other is an industrial science such as laser processing. Variable pulse duration, 100 W average power, femtosecond laser is now available at LASOR for any collaborative research, including companies. We have a laser processing platform for both industrial and scientific applications.

We also aim to develop novel laser spectroscopy and coherent nonlinear optical physics enabled by emerging lasers and optical science/technology, and to comprehensively study fundamental light-matter physics, optical materials science, and applied photonics. Such research includes ultrafast spectroscopy for excited state dynamics, terahertz magnetic field spectroscopy for spin dynamics, quantitative microspectroscopy of semiconductor lasers, and nanostructured photonic devices such as quantum wire lasers, gain-switched semiconductor lasers, multi-junction solar cells, and bioluminescent systems.

• **Synchrotron radiation science group**

By inheriting and developing the synchrotron techniques cultivated for more than 20 years, we are continuously developing world-class spectroscopies such as time-resolved



Fig. 5. Generation of 7-eV, femtosecond light with (a) Xe and (b) Xe/Ar gases.

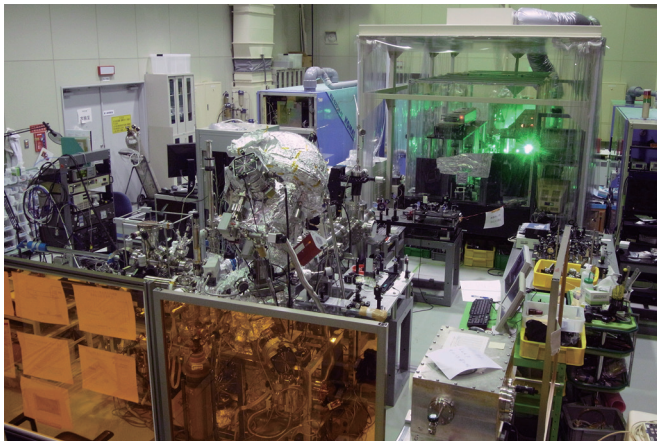


Fig. 6. Pump-probed photoemission system using 60-eV laser

photoemission/diffraction, ultra-high-resolution soft X-ray emission, 3D (depth + 2D microscopy) nano-ESCA, and X-ray magneto-optical effect, and providing these techniques for both basic materials science and applied science that contributes to the instrument applications in collaboration with outside researchers. In order to pioneer new spectroscopies for next-generation light sources, we are improving the fast polarization switching of the undulator light source in collaboration with SPring-8. In addition, we are promoting frontier work on the use of X-ray free-electron lasers, SACLA, with high spatial and temporal coherence comparable to optical lasers in collaboration with scientists of laser light sources and spectroscopy.

#### • Extreme spectroscopy group

The advent of laser-based light sources in the soft X-ray region opens a new stage in the field cultivated by synchrotron radiation. One of the milestones was the development of a laser-based light source of  $\sim 7$  eV for sub-meV resolution photoemission spectroscopy. In the last five years, the available photon energy has been increased to 11 eV using Yb fiber laser technology. It has high photon flux ( $10^{14}$  photons/sec) with sub-picosecond time resolution. Laser-based spin-resolved ARPES is realized in LASOR with 11 eV laser. This technology would open up a whole new field of spectroscopy. High-harmonic-generation based photoemission spectroscopy in the 20-60 eV region is another direction to be pursued. Femtosecond time domain spectroscopy has been achieved. Combined with picosecond time-domain spectroscopy using the pulsed light delivered by synchro-

trons, we are investigating the electronic structures and dynamics of matter in the bulk, on the surface, and down to the nanoscale. The ultimate goal is to extend soft x-ray operando methods to lasers. Diffractions, magneto-optical effects, and inelastic scattering now performed at synchrotrons will be performed by lasers to access the real-time dynamics of chemical reactions and phase transitions down to femtoseconds.

State-of-the-art laser-based organismal spectroscopy is a new direction in LASOR. The ISSP research field is shifting from simple materials and science to a complex one involving living bodies and functional materials with excited state physics.

## Synchrotron Radiation Laboratory

The Synchrotron Radiation Laboratory (SRL) was established in 1975 as a research division dedicated to solid state physics using synchrotron radiation. Currently, SRL is composed of three research sites, the Sendai office, the Harima office and the E-building of the Institute for Solid State Physics.

#### • Synchrotron soft X-ray experimental stations at Sendai office and Harima office

In 2009 SRL established the Harima branch laboratory in SPring-8 and operated a high brilliant and polarization-controlled 25-m long soft X-ray undulator beamline, BL07LSU until August 2022 in collaboration with Synchrotron Radiation Research Organization (SRRO) of the University of Tokyo. The management of the beamline was transferred to the RIKEN SPring-8 Center in September 2022. In November 2022, the Sendai office was formed on the Aobayama campus of Tohoku University under the auspices of a new SRRO launched in April 2022 and includes six departments of the University of Tokyo. At the end of FY2022, three endstations, ambient pressure X-ray photoemission (APXPS) (Fig. 1a), nanoESCA (Fig. 1c), and high resolution soft X-ray emission spectroscopy (HORNET) (Fig. 1d) stations were relocated to the new 3 GeV synchrotron facility NanoTerasu in Sendai, which started commissioning of the storage ring in early 2023. On March 25, 2022, the Sendai office relocated to the SRIS (International Center for Synchrotron Radiation Innovation Smart) building of Tohoku University which is one of the closest buildings to NanoTerasu. The three endstations, APXPS, nanoESCA and HORNET stations resumed commissioning in the summer of 2023 and were realigned to the beamlines BL07U (nanoESCA and HORNET) and BL08U (APXPS) by the end of FY 2023. During commissioning, the APXPS system achieved 10-100 Torr for XPS measurement; the 3DnanoESCA station obtained a spatial resolution of roughly 100-200 nm; and the HORNET station provided spectra with the energy resolution around 500 meV at 500 eV. All of achievements in NanoTerasu are still considerably below the standards established in SPring-8; however, they will recover and even exceed the criteria once the beamlines are aligned after official operation begins in April, 2024.

The Harima office at SPring-8 continues in 2023 and the soft X-ray imaging (ptychography) (Fig. 1b) station is being developed in collaboration with the RIKEN SPring-8 Center. The novel soft X-ray ptychography system, which uses a total-reflection Wolter mirror, has a resolution of approxi-

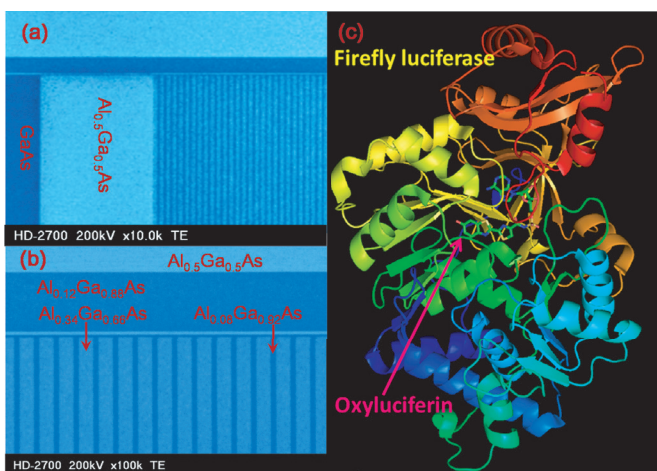


Fig. 7. Photonics devices under study: (left panel) semiconductor quantum wires and (right panel) firefly-bioluminescence system consisting of light emitter (oxyluciferin) and enzyme (luciferase)

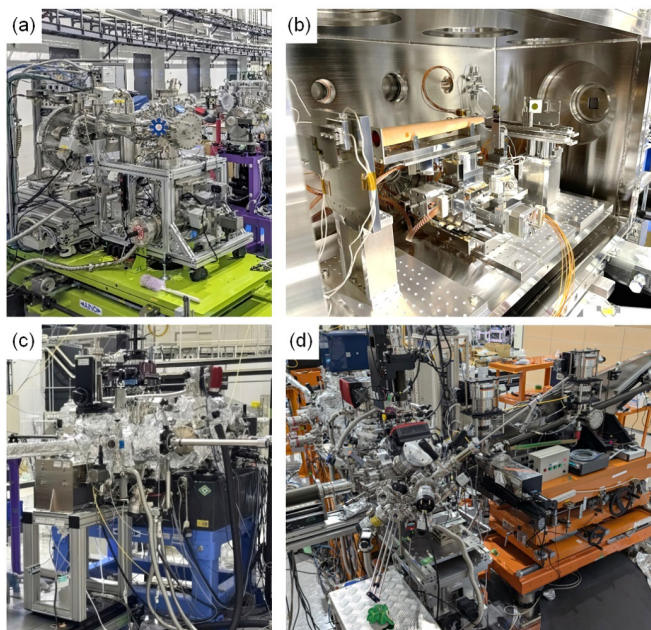


Fig. 1 Soft X-ray advanced experimental stations (a) Ambient pressure photoemission (APXPS) (b) Soft X-ray imaging (c) 3DnanoESCA (d) Soft X-ray emission (HORNET). APXPS, 3DnanoESCA and HORNET stations were transferred to the new 3 GeV synchrotron facility NanoTerasu at the end of FY2022 and installed in BL07U (3DnanoESCA, HORNET) and BL08U (APXPS) at the end of FY2023.

mately 50 nm and its long working distance allows for stereo imaging with a high rotation angle.

#### • High-resolution Laser SARPES and ARTOF systems at E-building

High-resolution Laser Spin- and Angle-Resolved Photoemission Spectroscopy (SARPES) is a powerful technique to investigate the spin-dependent electronic states in solids. In FY2014, LASOR and SRL staffs constructed a new SARPES apparatus (Fig. 2a), which was designed to provide high-energy and -angular resolutions and high efficiency of spin detection using a laser light at E-building. The achieved energy resolution of 1.7 meV in SARPES spectra is the highest in the world at present. From FY2015, the new SARPES system has been opened the joint-research program. The Laser-SARPES system consists of an analysis chamber, a carousel chamber connected to a load-lock chamber, and a molecular beam epitaxy chamber, which are kept ultra-high vacuum (UHV) environment and are connected to UHV gate valves. The electrons are excited with 6.994 eV photons, yielded by 6th harmonic of a Nd:YVO4 quasi-continuous wave laser with a repetition rate of 120 MHz, and 10.7 eV photons, driven by the third harmonic radiation at 347 nm of an Yb: fiber chirped pulse amplifier laser, which was developed by Kobayashi's lab in LASOR. The hemispherical electron analyzer is a custom-made Scienta Omicron DA30-L, modified for installing the spin detectors. The spectrometer is equipped with two

high-efficient spin detectors orthogonally placed each other, associating very low energy electron diffraction, which allows us to analyze the three-dimensional spin polarization of electrons. At the exit of the hemispherical analyzer, a multi-channel plate and a CCD camera are also installed, which enables us to perform the angle-resolved photoelectron spectroscopy with two-dimensional (energy-momentum) detection. The laser-SARPES with 7 eV laser can provide both high-resolution spin-integrated and spin-resolved photoemission spectra in various types of solids, such as spin-orbit coupled materials and ferromagnetic materials. In addition, using the 10.7 eV makes it possible to follow their ultrafast spin dynamics in the time domain by pump-probe scheme. A spectroscopy system using a dichroic mirror ( $\text{SiO}_2/\text{HfO}_2$  multilayer) was introduced for a stable switching of the 7 eV and 10.7 eV lasers. In 2023, an autocollimator and a laser evaluation system such as FROG have also been assembled to improve the instability of the light source (color dispersion and multi-pulse). In addition, the introduction of a new amplifier (rod fiber) has made it possible to use higher-power light. At present, the pulse laser and the optical system are being adjusted to stably use high-power, high-quality light by using the assembled laser evaluation system. This will enable stable operation of pump-probe time-resolved SARPES as well as wavelength conversion of pump light.

The time-resolved soft X-ray spectroscopy (TR-SX) station was moved from SPring-8 BL07LSU to the E-building in 2020. The measurement chamber is equipped with a unique electron spectrometer, the two-dimensional (2D) angle-resolved time-of-flight (ARTOF) analyzer (Fig. 2b). The system is currently operational for measurements of 2D angle-resolved photoemission spectroscopy with pulsed laser of 6 eV photon energy supplied by Itatani's lab in LASOR. Time-resolved measurements can also be conducted with temporal resolution of 600 fs. An ultra high-speed reading and visualization program is currently in development to enhance usability.

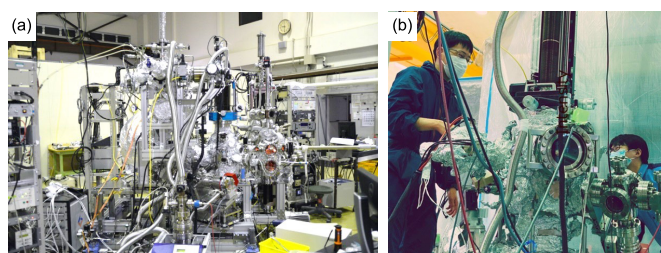


Fig. 2 (a) Laser-SARPES system and (b) ARTOF system at E-building.

# Conferences and Workshops

## 9th International Discussion Meeting on Relaxations in Complex Systems (9IDMRCS)

August 12-18, 2023

O. Yamamuro, K. Mayumi, H. Noguchi, H. Tanaka, and H. Shirota

9IDMRCS was co-sponsored by ISSP (as ISSP International Workshop) and held at the Makuhari Messe International Conference Center. The number of registered participants was almost the expected number of 621, but it was gratifying to see that more than half (347) were non-Japanese, despite the fact that COVID-19 was still in effect. The conference was a very successful and financially sound one, supported by 10 academic societies, 41 companies and research institutes (including financial support), and generous financial support from Chiba Prefecture, Chiba City, the Japan Tourism Agency. The first day of the conference opened with keynote lectures by five distinguished researchers on the main themes of the conference, i.e., the glass transition and the dynamics of polymers, proteins and granular materials. This was followed by a symposium (3 speakers) in honor of Professor Austen Angell, who passed away in 2021, and a memorial lecture for Professor Uri Buchenau, who passed away just before the conference. Both have contributed greatly to the conference over the years. Parallel sessions in seven rooms were held over the second through the seventh days. The number of presentations was 354 invited talks and 102 general presentations. Poster sessions (146 presentations in total) were held in the afternoons of days 4 and 6. The program consisted of 40 symposia which were organized by about 100 symposium leaders. In addition to the previous topics such as glass transition, water/hydrogen-bonded liquids, ionic liquids, polymers, gels, colloids, bio-related materials, surfaces, ion-conductive solids, intermediate phases (liquid crystals and plastic crystals), high-pressure measurements, and state-of-the-art measurements, this conference added new topics that have rarely (or never) covered inorganic glasses, metal glasses, spin glasses, electronic glasses, granular materials, active matter, pharmaceuticals, foods, MOFs, energy storage/conversion materials, etc., providing a forum for comprehensive discussion of relaxation phenomena in an increasingly diverse range of subjects. This conference also focused on booth exhibitions. 22 booths were set up in the same main hall as the poster area (and rest area), where companies, research facilities, and Grant-in-Aid groups introduced their products and activities. The social program was also well organized, with a Welcome Party on the first day, a tea ceremony and Ukiyo-e viewing tour for the accompanying guests on the third and fourth days, an excursion (3 courses: Tokyo, Nokogiri-Mt., Sawara) on the fifth day. The Banquet, which was held on the 6th day, was a groundbreaking event in which we rented out the Mihamaen Japanese garden to enjoy the beautiful garden and festival night stalls together, which was appreciated by many participants.



## Hierarchical Structure and Machine Learning 2023

October 2-13, 2023

O. Sugino, J. Haruyama, R. Akashi, T. Yokota, and R. Nagai

The physics of interacting particle systems is characterized by a hierarchical structure of many-body correlation functions. Density functional theory (DFT), one of the central themes of this workshop, has been developed independently for classical, electronic and nuclear systems, but they are all based on this hierarchical structure, and it is believed that common techniques hidden in these systems can be shared for their development. The aim of the workshop was to discuss and deepen understanding of this issue, and various techniques for overcoming hierarchy-based complexity were presented. The workshop featured 11 speakers working at the cutting edge of research, offering the audience two lectures a day on topics ranging from the fundamentals of the research field to recent findings. Among the topics covered were function renormalization group (FRG) methods that link different hierarchical levels and scales; applications of FRG methods to classical fluid and electronic systems were discussed, and the theory was compared with powerful DFT-based nonperturbative and time-dependent power functional approaches. Another important topic was dynamic mean-field theory (DMFT), which can handle many-body correlations beyond the typical two-particle level of conventional DFT. Applications to cuprate and nickelate superconductivity were discussed. For superconductivity, some of the refinements to the DFT approach were also presented: the diagrammatic approach as well as the path integral approach for phonon-mediated superconductivity were discussed. Particular attention was also paid to the hierarchical equations of motion developed for non-equilibrium systems. Numerically rigorous methods were developed to overcome the complexity inherent in the Feynman-Hibbs-type path integral approach due to its hierarchical nature. Finally, new theoretical schemes based on AI and machine learning were discussed. Breakthroughs in density functional development and materials design were presented. The symposium part of the workshop enabled young researchers to present their results in oral or poster form. Intensive discussions took place between young and established researchers. Researchers from different disciplines focused on the specific topics and learned the different computational schemes developed, stimulating speakers and audience alike to take new leaps forward.

## Hierarchical Equations and Machine Learning

October 6-10, 2023

O. Sugino, J. Haruyama, R. Akashi, T. Yokota, and R. Nagai

This workshop was organized as a satellite of the international workshop entitled Hierarchical Structure and Machine Learning (HISML2023). It enabled young researchers to present and discuss their results with the professors invited to HISML2023. The central theme of this year's workshop was the numerical study of many-body correlation problems. Active discussions took place on problems such as (a) superconductivity vs. hyperperiodicity, (b) finite-temperature geometry optimization, (c) structure determination based on data assimilation, (d) machine learning beyond neural networks and kernels, (e) inverse Hamiltonian design, (f) superconductivity in iron-based materials, (g) antiferromagnetism in high-throughput calculations, (h) DFT studies of excitonic insulators, (i) studies of vibrational properties using machine learning, (j) non-equilibrium energy flows using dynamic mean fields, and (k) DFT studies of solid oxygen. These studies include new research topics made possible for the first time by data science-based approaches and/or new developments in many-body theory. The activities of young researchers, who represent the promise of the future, received particular attention at the workshop.



## Annual Meeting of MDCL Supercomputer Center and CCMS —Condensed Matter Physics in the Era of Computation—

April 3-4, 2023

N. Kawashima, T. Ozaki, O. Sugino, H. Noguchi, T. Fukushima,  
K. Ido, H. Nakano, J. Haruyama, M. Fukuda, and K. Yoshimi

This is an annual meeting where the uses of ISSP joint-use supercomputers (currently, "ohtaka" and "kugui") meet each other where a member of the institute's computer-related staff takes turns serving as the representative organizer. The current total theoretical computing power of the ISSP joint-use supercomputer is about 8 PF. This year, it was the first time in three years that the meeting was held completely on-site, and there was some concern that the number of participants would be too high or low, as the rules on the maximum number of people allowed in the conference room still remained. It turned out that 60 people actually attended on April 3rd and 55 on the 4th. There was lively discussion following each presentation. There were 16 invited oral presentations, including two special talks by Arita (The University of Tokyo) and Furuya (NVIDIA), and 25 poster presentations. The poster session and a small social gathering that followed provided a good opportunity for the first time in a long time to promote in-person interaction among community members. For the posters, the three posters were selected by a vote of all participants as the winners of the Excellent Poster Award, and an awards ceremony was held at the end of the meeting. We would like to thank the external members of the program and organizing committees: T. Uneyama (Nagoya U.), Y. Hatsugai (U. Tsukuba), S. Watanabe (U. Tokyo), M. Kawamura (U. Tokyo) and S. Morita (Keio U.)



## Frontier of New Materials Research: Novel Electronic Properties and Functions Based on Characteristic Approaches

May 15-16, 2023

Y. Okamoto, T. Ideue, J. Yamaura, and H. Kageyama

This workshop was organized for participants to share the new methods, approaches, and directions that have recently been found in the research on materials science. The impact of the discovery of unprecedented new materials is significant for materials science. New materials can generate novel phenomena and functions, propelling materials science research and inspiring the next generation of researchers. However, it is not easy to get an overall picture of which studies in a wide range of research fields are generating innovations related to new materials. Research on new materials frequently divides and organizes itself based on functions, phenomena, and target material systems. Therefore, we organized a hybrid-style workshop focusing on recent materials research related to new materials spanning a wide range of fields on May 15th and 16th. As many as 145 people registered for the workshop and 45 attended on-site, where participants engaged in lively discussions. In addition to 18 invited talks and 3 comments, a special lecture was given by Prof. Takehiko Yagi.



# Recent Developments in Measurement Techniques with Pulsed Magnetic Fields for Condensed Matter Physics

June 22-23, 2023

K. Kindo, Y. H. Matsuda, M. Tokunaga, and Y. Kohama

This workshop was organized for the high magnetic field research community, especially for the users of the International MegaGauss Science Laboratory (IMGSL) in ISSP. We had some comments from the Advisory Committee for Joint Usage in ISSP that it would be necessary for users to have some tutorial lectures and some practice of the experiment. This workshop was planned to address the comments. The program consists of (1) the lecture part and (2) the experiment part. Basics of the experimental techniques required to use pulsed magnetic fields were first given. Subsequently, several specific measurement techniques for thermal, magnetic, electrical, and mechanical properties of matter. Several means using electric, optical, and acoustic signals were introduced. In the second part of the workshop, four kinds of pulsed-field experiments were demonstrated with attendees. Two of them were done with non-destructive magnets, and the other two utilized destructive magnets, namely the horizontal and vertical single-turn coils. The number of participants was limited to around 50 so that the experiments were conducted safely. According to the questionnaire, it seemed that attendees felt they had valuable time to experience real pulsed magnetic field experiments.



## Metastability from an Interdisciplinary Perspective

July 4, 2023

T. Oka, R. Takagi, and H. Oike

The recent workshop on metastability brought together researchers, including 7 invited speakers, from different disciplines to explore this complex phenomenon. Metastability, which manifests differently across various fields, is crucial in both solid state physics and chemistry. In solid state physics, it appears in photo-induced phase transitions and hysteresis during parameter sweeps (temperature, magnetic field, pressure). In chemistry and metallurgy, metastable phases are achieved through low-temperature synthesis, rapid cooling, and high-pressure synthesis. Understanding metastability across different time and spatial scales in various materials remains a significant challenge in non-equilibrium systems physics. The workshop aimed to bridge the gaps in understanding by fostering interdisciplinary discussions and collaborations.

The talks covered metastable states induced by light, heat, magnetic fields and strain, as well as general laws for metastable materials based on first-principles calculations and data science. There were 15 on-site participants and about 30 online participants, and active discussions continued after lunch and the talks, generating many ideas for collaborative research. A highlight of the workshop was a tour at the International MegaGauss Science Laboratory at ISSP. This tour introduced participants, especially those less familiar with condensed matter experiments, to cutting-edge facilities. The workshop underscored the growing synergy between materials science and physics, emphasizing that the field of metastability would benefit from greater involvement of condensed matter physicists for further advancements.



## ISSP Joint Research Results Presentation Meeting 2023

September 7, 2023  
Joint Research Program Office (Kyodo Riyou Gakari)

Joint Research Program is one of the most crucial functions of the Institute for Solid State Physics (ISSP). This symposium was organized to share the results achieved through the Joint Research Program at ISSP and to foster future collaborations. The program included four invited lectures: two by external and two by internal speakers. From outside ISSP, Prof. Kanazawa from the Institute of Industrial Science at The University of Tokyo presented his research on the properties of magnetic devices in collaboration with the Neutron Science Laboratory. Prof. Hashimoto from the Graduate School of Frontier Sciences at The University of Tokyo discussed his research on superconductivity under high pressure, conducted in collaboration with the Materials Design and Characterization Laboratory. From within ISSP, Dr. Imajo from the International MegaGauss Science Laboratory and Prof. Kondo from the Laser and Synchrotron Research Center showcased their work on ultra-high magnetic fields and angle-resolved photoemission spectroscopy, respectively.



## Spectroscopic Revolution by Cooperative and Constructive Relationships between High Harmonic Laser and Synchrotron Radiation

September 30, 2023  
Y. Harada, Y. Kobayashi, I. Matsuda, T. Kimura, T. Kondo, K. Okazaki, R. Matsunaga, K. Inoue, T. Taniuchi, T. Kisu, K. Ishizaka, Y. Tezuka, and T. Yokoya

In 2012, Laser and Synchrotron Research (LASOR) center was established to promote collaborative research among high-harmonic laser and synchrotron radiation communities. Prof. Shik Shin, who played a crucial role in LASOR's establishment and development, passed away in June 2022. This workshop was held to honor his contributions and discuss the future of materials research. The first part of the workshop focused on his achievements from the SOR-RING in the early days of Japanese synchrotron radiation to the birth of LASOR, and in particular discussed the development of synchrotron radiation soft X-ray spectroscopy and high-harmonic laser photoelectron spectroscopy. The second part explored the potential of combining laser and accelerator technologies for materials research. Special attention was given to Laser PEEM, a next-generation microscope combining high-order harmonic lasers and photoelectron microscopes, which was the final project of Prof. Shin. The workshop concluded with discussions and proposals on the future of LASOR at ISSP and the direction of Japanese photonics research, emphasizing the importance of continued innovation and collaboration in this field. Following the six invited lectures, a memorial event was held, attended by approximately 130 researchers who had been associated with Prof. Shin.

### 3rd Workshop on the Frontier and Future Trends in Nanoscale Science

October 6, 2023

M. Hashisaka, T. Ideue, Y. Otani, T. Osada, T. Kato, Y. Hasegawa, R. Matsunaga, and S. Miwa

Advances in nanoscale fabrication and measurement techniques have led to cutting-edge experiments that capture the essence of microscopic phenomena in condensed matter. We organized this workshop to provide an overview of this ever-growing research field, following the first and second workshops held in 2020 and 2021. This workshop consisted of three sessions, and ten young researchers were invited to give talks. The first session focused on quantum information technology, the second on the novel functionalities of new materials and devices for future technologies, and the third on signal processing using new device architectures. Although all the lectures were at the cutting edge of research in their respective fields, the speakers were considerate to the audience, which included individuals with a wide range of backgrounds, and provided clear explanations. Thanks to their efforts, the objective of this workshop, which aimed to facilitate cross-disciplinary information exchange with nanoscale science as the keyword, was fulfilled. A total of 138 people, including 42 on-site and 96 online, attended the workshop. Active discussions between the participants, particularly on-site, provided great opportunities to exchange information, which will stimulate and advance extensive studies in the future.



### ISSP Women's Week 2023

November 25-December 1, 2023

I. Matsuda, T. Ideue, Y. Otani, T. Oka, K. Okazaki, M. Oshikawa, M. Tokunaga, T. Nakajima, T. Fujino, M. Horio, J. Yamaura, and M. Lippmaa

In promoting diversity activities, ISSP organized "ISSP Women's Week 2023" from November 25 – December 1, 2023. The week focused on active participation of women in the workforce as well as work-life balance. It started with an event for female undergraduate and graduate students, followed by FD/SD training and division/facility seminars with female researchers as instructors. On the last two days, a workshop was held with invited lectures by researchers active in various fields, round-table discussions, and poster sessions. When the workshop concluded, a ISSP tour was held according to the participants' wishes. Through the week, the events were held with various styles, face-to-face, online, and hybrid. There were over 300 participants who discussed various topics, including interdisciplinary research, life event, and work efficiency. The week was supported by KIOXIA Holdings Corporation and by the MEXT Academic Transformative Research (A) project "Chemical Catastrophe in Ultra-Strong Magnetic Fields of 1000 Tesla: Science of Chemical Bonding in Non-Perturbative Magnetic Fields".



## How High Can We Raise Thermoelectric Performance?

December 5-6, 2023  
T. Mori

This Workshop dealt with recent experimental and theoretical advances in thermoelectric materials research based on the understanding of condensed matter properties. There was a Keynote Talk by Prof. Hidetoshi Fukuyama and 28 Invited Talks and 9 Poster Presentations. In addition to Peltier cooling, thermoelectric materials can directly convert thermal energy into electricity due to the Seebeck effect. They can be valuable for energy saving via waste heat power generation and as stand-alone power sources for innumerable sensors. There are paradoxical requirements between the physical parameters, namely between the Seebeck effect and electrical conductivity, and between the thermal and electrical conductivity. Therefore, it is generally not easy to improve performance. Various novel thermoelectric enhancement strategies leading to extremely high figure of merits and power factors were presented at the Workshop. Theoretical advances, for example, a quantum mechanical approach, the “thermoelectric linear response theory” (Kubo-Luttinger theory) were also presented, together with progress made in novel material systems such as topological materials, carbon nanotubes, and organic materials. At the Workshop there were intensive and exciting discussions, with around 100 participants in a full room, and new challenging perspectives in the field were opened up.



## Surface and Interface Spectroscopy 2023

December 20-21, 2023

R. Arafune, H. Okuyama, Y. Kim, T. Komeda, T. Kondo, T. Sugimoto, N. Takagi, A. Nakajima, T. Yokoyama, K. Watanabe, T. Ozaki, O. Sugino, Y. Hasegawa, I. Matsuda, and J. Yoshinobu

Surfaces and interfaces are becoming increasingly important not only from the viewpoint of basic science such as the surface states of topological materials but from the applications such as catalysts, solar cells, fuel cells, secondary batteries and various devices that can solve the issues in the global environment, energy, information technology, etc. This is because the surface and interface are the fields of energy exchange and reactions. Recent advances in experimental techniques and first-principles calculations have made it possible to investigate not only the ideal model surfaces but also the complex surfaces of real materials under the operating conditions in atomic scale. This ISSP workshop featured the recent experimental and theoretical studies on surface and interface spectroscopy, including surface vibrational spectroscopy, local probe microscopy/spectroscopy, surface nonlinear spectroscopy, photoelectron spectroscopy, and synchrotron radiation spectroscopy. The purpose of the workshop was to promote mutual understanding among researchers with diverse backgrounds through discussion and to generate new collaborative research.

We had 5 invited lectures, 8 contributed talks, 8 oral presentations for student award applications, and 47 poster presentations. 128 people registered in advance; the actual number of participants was 110 on December 20 and 81 on December 21.

The program and abstracts can be downloaded from [https://yoshinobu.issp.u-tokyo.ac.jp/ISSPWS\\_SIS2023.html](https://yoshinobu.issp.u-tokyo.ac.jp/ISSPWS_SIS2023.html)



## The 1st U-Tokyo ISSP • RIKEN CEMS Collaboration Workshop

January 24, 2024

Z. Hiroi, T. Arima, M. Tokunaga, T. Nakajima, M. Hahsisaka, and Y. Otani

The Institute for Solid State Physics (ISSP), established in 1957, has long been a central player in Japan's condensed matter science research. The RIKEN Center for Emergent Matter Science (CEMS), founded in 2013, brings together top researchers in physics, chemistry, and electronics to study emergent phenomena and their applications. Both institutes are dedicated to developing innovative materials and theories for the benefit of future society.

This workshop emphasized the importance of ISSP and CEMS collaborating to enhance Japan's research capabilities amidst growing international competition. Another goal was to identify potential research projects that could gain global recognition. Given the significant number of foreign researchers at CEMS, English was chosen as the workshop's common language, facilitating participation from Japanese and international researchers and students.

The event began with remarks from the ISSP director, followed by research presentations from both institutes highlighting their joint research achievements. Recent research results were shared, sparking extensive discussions. The afternoon session focused on recent findings in each institute's specialized fields, clarifying strengths and common research themes. Active exchanges of ideas on new research directions were held, aiming to foster new collaborative projects. Post-conference, exchanging opinions among organizers and speakers reinforced the decision to hold future workshops alternately at ISSP and CEMS.

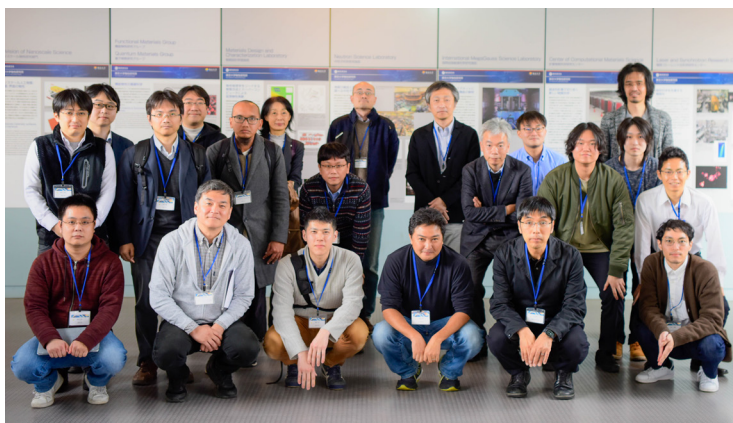


## Data Integration between Simulations and Advanced Experiments in Materials Science

February 19-20, 2024

T. Hoshi, I. Matsuda, T. Misawa, K. Yoshimi, T. Ozaki, and N. Kawashima

A current trend in material science is the data integration between simulations and advanced experiments. The aim of this workshop is an overview of the data integration in materials science and its future prospects. The workshop is composed of 11 invited talks, 2 contributed talks and 18 poster presentations. The number of applicants is 78, including 28 on-site participants. The number of participants in the reception was 20. The plenary talk was given by Masahiko Demura (NIM) with the title of 'Towards the realization of the Materials DX platform concept'. The other invited talks were focused on the systematic data collection and application studies using simulations by Yu Kumagai (Tohoku U.), Tetsuya Fukushima (AIST), Takashi Koretsune (Tohoku U.) and Masahiro Fukuda (U. Tokyo) and on two-dimensional materials by Tadashi Abukawa (Tohoku U.), Yuki Fukaya (JAEA), Shu-Jung Tang (National Tsinghua U.), Junji Yuhara (Nagoya U.), Takeshi Nakagawa (Kyushu U.) and Takeo Hoshi (NIFS). There were presentations from both experimental and computational research and lively discussions took place. The co-organizers of the workshop are National Institute for Fusion Science (<https://www.nifs.ac.jp/>) and DxMT CoLabo (<https://dxmt.mext.go.jp/>).



## Interdisciplinary Collaboration between Theoretical and Experimental Approach: Luciferin-Luciferase Reaction

March 8-9, 2024

M. Hiyama, T. Nakatsu, S. Maki, Y. Noguchi, O. Sugino, O. Yamamuro, and H. Akiyama

Bioluminescence, which is the luminescence reaction between a substrate (luciferin) and an enzyme (luciferase), is widely used for investigation of temporal changes in cell proliferation, observation of drug and cancer cell metastasis pathways, detecting microbial pollutions in food hygiene testing, and so on. Because of their usefulness, protein mutants and substrate analogues for different emission color have been developed as luminescence probes using bioluminescence. In this ISSP workshop, the experts in organic synthesis, theoretical calculations, and quantitative measurements introduced the latest research results on luciferin-luciferase reactions for not only extant fireflies but also ancient fireflies and other luminescent organisms. The methods to detect pesticide residues by firefly bioluminescence and the development of immunoassay elements using bioluminescent enzymes of marine organisms were also presented. In the last session, there were presentations for the studies on cell experiments and experiments using human models and the issues for new applications of bioluminescence were pointed out. There were 15 invited lectures and eleven poster presentations were given as general lectures. Total attendance of this workshop was 76.



## Future of Organic Conductors through Device Applications

March 26-27, 2024

T. Ideue, H. Oike, Y. Okamoto, R. Takagi, T. Fujino, and S. Miwa

Organic conductors have been extensively investigated because their low dimensionality and strong electron correlations give rise to emergent phenomena. In organic semiconductors and organic polymers, device fabrications have been developed to realize organic electronics. Recently, such device technology has been applied to organic conductors, enabling electrical control of emergent phenomena. Because organic conductors are difficult to synthesize, measure, and microfabricate, collaborations, and also because emergent phenomena are difficult to understand and predict, collaboration among the fields of chemistry, physics, and engineering is essential for the future development of the research of organic conductors.

This workshop invited 29 speakers, mainly young researchers from a wide range of research fields relating to "molecule", such as organic conductors and semiconductors, organic electronics and spintronics, inorganic van der Waals crystals, and graphite. Each lecture covered cutting-edge topics as well as the basic research concept in the respective fields. The workshop aimed to promote close discussion and interaction among researchers with diverse backgrounds in physics, chemistry, and engineering. On the day of the event, many questions were asked by participants from different research fields, and active discussions were held after the lectures and during the breaks. There were also some occasions when new perspectives and research directions emerged from simple questions posed by audience members outside of their fields of expertise. There were 35 on-site participants and about 50 online participants.





# Publications (2023.1 - 2024.4)

## Division of Condensed Matter Science

### Mori group

We have successfully developed and unveiled unprecedented functional properties for the molecular materials and systems. The major achievements in 2023 are to develop the metallic oligomer conductors that models doped PEDOT [poly(3,4-ethylenedioxythiophene)] family and (2) to discover the high conductive mixed-stack complexes via orbital hybridization of donor and acceptor.

1. †\*Ambipolar Nickel Dithiolene Complex Semiconductors: From One- to Two-Dimensional Electronic Structures Based upon Alkoxy Chain Lengths: M. Ito, T. Fujino, L. Zhang, S. Yokomori, T. Higashino, R. Makiura, K. J. Takeno, T. Ozaki and H. Mori, *J. Am. Chem. Soc.* **145**, 2127-2134 (2023).
2. †\*Metallic State of a Mixed-Sequence Oligomer Salt That Models Doped PEDOT Family: K. Onozuka, T. Fujino, R. Kameyama, S. Dekura, K. Yoshimi, T. Nakamura, T. Miyamoto, T. Yamakawa, H. Okamoto, H. Sato, T. Ozaki and H. Mori, *J. Am. Chem. Soc.* **145**, 15152-15161 (2023).
3. †Neutral Radical Molecular Conductors Based on a Gold Dimethoxybenzenedithiolene Complex with and without Crystal Solvent: S. Yokomori, S. Dekura, A. Ueda, T. Higashino and H. Mori, *Chem. Lett.* **52**, 25 (2023).
4. †\*Precise Control of the Molecular Arrangement of Organic Semiconductors for High Charge Carrier Mobility: R. Akai, K. Oka, S. Dekura, K. Yoshimi, H. Mori, R. Nishikubo, A. Saeki and N. Tohnai, *J. Phys. Chem. Lett.* **14**, 3461 (2023).
5. †\*Orbital hybridization of donor and acceptor to enhance the conductivity of mixed-stack complexes: T. Fujino, R. Kameyama, K. Onozuka, K. Matsuo, S. Dekura, T. Miyamoto, Z. Guo, H. Okamoto, T. Nakamura, K. Yoshimi, S. Kitou, T.-H. Arima, H. Sato, K. Yamamoto, A. Takahashi, H. Sawa, Y. Nakamura and H. Mori, *Nat Commun* **15**, 3028 (2024).
6. Single-crystalline oligomer-based conductors modeling the doped poly(3,4-ethylenedioxythiophene) family: T. Fujino, R. Kameyama, K. Onozuka, K. Matsuo, S. Dekura, K. Yoshimi and H. Mori, *Faraday Discuss.* **250**, 348 (2024).
7. 高性能かつ大気安定なアンバイポーラ型分子性半導体材料の開発：藤野 智子，伊藤 雅聡，森 初果，「有機半導体の開発と最新動向」，監修：安達千波矢，(シーエムシー出版，2024)，154-163.

### Osada group

The electronic state under magnetic fields in the  $\alpha$ -type organic Dirac fermion systems,  $\alpha$ -(ET)<sub>2</sub>I<sub>3</sub> and  $\alpha$ -(BETS)<sub>2</sub>I<sub>3</sub>, was studied to clarify the spatial order in the quantum Hall state. The four-band tight-binding model with Peierls phase factors was employed, and the generated Hofstadter butterfly and its Chern numbers confirmed the validity of the Dirac fermion picture in these materials. The four-component envelope function of the  $N = 0$  Landau level with valley degeneracy was investigated. It was found that the two degenerate valley states have different weights on A and A' molecules connected by inversion. This valley-site correspondence is also recognized for the  $N = 0$  spin-split Landau levels under the Zeeman effect and the spin-orbit interaction. The spontaneous valley symmetry breaking in the  $N = 0$  Landau levels due to the exchange interaction results in the  $\nu = \pm 1$  quantum Hall states accompanied by the spatial modulation of charge and spin densities at A and A' sites in a unit cell.

1. Magnetic-field periodic quantum Sondheimer oscillations in thin-film graphite: T. Taen, A. Kiswandhi and T. Osada, *Phys. Rev. B* **108**, 235411(1-9) (2023).
2. Quantized thermoelectric Hall plateau in the quantum limit of graphite as a nodal-line semimetal: A. Kiswandhi, T. Ochi, T. Taen, M. Sato, K. Uchida and T. Osada, *Phys. Rev. B* **107**, 195106(1-5) (2023).
3. Broken-Symmetry Quantum Hall State in an Organic Dirac Fermion System: T. Osada, *JPSJ News Comments* **20**, 06 (2023).
4. Hofstadter Butterfly and Broken-Symmetry Quantum Hall States in  $\alpha$ -Type Organic Dirac Fermion Systems: T. Osada,

\* Joint research among groups within ISSP.

## Yamashita group

We have been studying (1) quantum criticality in heavy-fermion materials by ultralow temperature cryostat, (2) thermal-Hall conductivity of exotic excitations in frustrated magnets and (3) a new technique for the study of strongly-correlated electron systems. In this year, we have performed (1) low-temperature thermal conductivity and magnetization measurements of a quantum spin ice candidate  $\text{Ce}_2\text{Hf}_2\text{O}_7$  (2) spontaneous thermal Hall measurements of candidate materials of chiral superconductivity, and (3) NMR measurements of  $\text{Cd}_2\text{Re}_2\text{O}_7$ .

1. <sup>†</sup>\*Modulation vector of the Fulde-Ferrell-Larkin-Ovchinnikov state in  $\text{CeCoIn}_5$  revealed by high-resolution magnetostriction measurements: S. Kittaka, Y. Kono, K. Tsunashima, D. Kimoto, M. Yokoyama, Y. Shimizu, T. Sakakibara, M. Yamashita and K. Machida, *Phys. Rev. B* **107**, L220505 (2023).
2. Magnon thermal Hall effect via emergent  $\text{SU}(3)$  flux on the antiferromagnetic skyrmion lattice: H. Takeda, M. Kawano, K. Tamura, M. Akazawa, J. Yan, T. Waki, H. Nakamura, K. Sato, Y. Narumi, M. Hagiwara, M. Yamashita and C. Hotta, *Nature Communications* **15**, 566 (2024).

## Ideue group

We have studied novel transport and optical properties of two-dimensional materials. We have successfully observed circular bulk photovoltaic effect at heterointerfaces of two-dimensional materials with different symmetries, which reflect the geometric nature of the electronic state. We have also shown that the anisotropy of transport and optical properties can be controlled in such symmetry-engineered van der Waals interfaces. Furthermore, we have reported a giant modulation of second harmonic generation in layered multiferroic  $\text{CuCrP}_2\text{S}_6$  and its unique thickness dependence.

1. Valley-dimensionality locking of superconductivity in cubic phosphides: L. Ao, J. Huang, F. Qin, Z. Li, T. Ideue, K. Akhtari, P. Chen, X. Bi, C. Qiu, D. Huang, L. Chen, R. V. Belosludov, H. Gou, W. Ren, T. Nojima, Y. Iwasa, M. S. Bahramy and H. Yuan, *Sci. Adv.* **9**, eadf6758 (2023).
2. An anisotropic van der Waals dielectric for symmetry engineering in functionalized heterointerfaces: Z. Li, J. Huang, L. Zhou, Z. Xu, F. Qin, P. Chen, X. Sun, G. Liu, C. Sui, C. Qiu, Y. Lu, H. Gou, X. Xi, T. Ideue, P. Tang, Y. Iwasa and H. Yuan, *Nat Commun* **14**, 5568 (2023).
3. Low-temperature phase transition in polar semimetal  $\text{Td-MoTe}_2$  probed by nonreciprocal transport: Y. M. Itahashi, Y. Nohara, T. Ideue, T. Akiba, H. Takahashi, S. Ishiwata and Y. Iwasa, *Phys. Rev. Research* **5**, L022022 (2023).
4. Berry curvature dipole generation and helicity-to-spin conversion at symmetry-mismatched heterointerfaces: S. Duan, F. Qin, P. Chen, X. Yang, C. Qiu, J. Huang, G. Liu, Z. Li, X. Bi, F. Meng, X. Xi, J. Yao, T. Ideue, B. Lian, Y. Iwasa and H. Yuan, *Nat. Nanotechnol.* **18**, 867 (2023).
5. Giant bulk piezophotovoltaic effect in  $3\text{R-MoS}_2$ : Y. Dong, M.-M. Yang, M. Yoshii, S. Matsuoka, S. Kitamura, T. Hasegawa, N. Ogawa, T. Morimoto, T. Ideue and Y. Iwasa, *Nat. Nanotechnol.* **18**, 36-41 (2023).
6. Continuous manipulation of magnetic anisotropy in a van der Waals ferromagnet via electrical gating: M. Tang, J. Huang, F. Qin, K. Zhai, T. Ideue, Z. Li, F. Meng, A. Nie, L. Wu, X. Bi, C. Zhang, L. Zhou, P. Chen, C. Qiu, P. Tang, H. Zhang, X. Wan, L. Wang, Z. Liu, Y. Tian, Y. Iwasa and H. Yuan, *Nat. Electron.* **6**, 28-36 (2023).
7. Giant Modulation of the Second Harmonic Generation by Magnetoelectricity in Two-Dimensional Multiferroic  $\text{CuCrP}_2\text{S}_6$ : S. Aoki, Y. Dong, Z. Wang, X. S. W. Huang, Y. M. Itahashi, N. Ogawa, T. Ideue and Y. Iwasa, *Advanced Materials* **36**, 2312781 (2024).

## Takagi group

We have been exploring new properties and functions related to topological magnetic structures, and novel electronic phases in strongly correlated electron systems. This year, we investigated the spontaneous topological Hall effect induced by non-coplanar antiferromagnetic order in intercalated van der Waals compounds. We also revealed the contribution of lattice degree of freedom to the rhombic and square lattice states of skyrmions in  $\text{EuAl}_4$ .

1. \*Nonreciprocal Phonon Propagation in a Metallic Chiral Magnet: T. Nomura, X. -X. Zhang, R. Takagi, K. Karube, A. Kikkawa, Y. Taguchi, Y. Tokura, S. Zherlitsyn, Y. Kohama and S. Seki, *Phys. Rev. Lett.* **130**, 176301(1-6) (2023).
2. \*Spontaneous topological Hall effect induced by non-coplanar antiferromagnetic order in intercalated van der Waals materials: H. Takagi, R. Takagi, S. Minami, T. Nomoto, K. Ohishi, M. -T. Suzuki, Y. Yanagi, M. Hirayama, N. D.

---

<sup>†</sup> Joint research with outside partners.

Khanh, K. Karube, H. Saito, D. Hashizume, R. Kiyonagi, Y. Tokura, R. Arita, T. Nakajima and S. Seki, *Nat. Phys.* **19**, 961-968 (2023).

3. SP-STM study of the multi-Q phases in GdRu<sub>2</sub>Si<sub>2</sub>: J. Spethmann, N. D. Khanh, H. Yoshimochi, R. Takagi, S. Hayami, Y. Motome, R. Wiesendanger, S. Seki and K. von Bergmann, *Phys. Rev. Materials* **8**, 064404 (2024).

## Division of Condensed Matter Theory

### Tsunetsugu group

We have studied various quadrupole orders on face center cubic lattice. This system has a few important points characteristic to quadrupole degrees of freedom. One is the presence of anisotropic interactions reflecting tensorial nature of the order parameter. Another is the third-order anisotropy, which exists only for degrees of freedom with even parity concerning time reversal symmetry. We have found various types of antiferro orders and discussed their stability based on phenomenological Landau theory. We have also studied a quadrupole impurity embedded in a host metal. Using the Wilson-type numerical renormalization technique, we have examined the related two-channel Kondo problem with taking account of the third-order local anisotropy taken into account. We have found two fixed points; one is the conventional local Fermi liquid and the other is the non-Fermi liquid, which is stable in a finite region of the parameter space. We have performed detailed analysis about the Kondo temperature in the local Fermi liquid phase. The Kondo temperature has a scaling behavior that differs from the conventional form, and the determined scaling function demonstrates the relevance of multiple coupling constants in the renormalization group equation.

1. †Theory of Energy Dispersion of Chiral Phonons: H. Tsunetsugu and H. Kusunose, *J. Phys. Soc. Jpn.* **92**, 023601 (2023).
2. Quadrupole partial orders and triple-q states on the face-centered cubic lattice: K. Hattori, T. Ishitobi and H. Tsunetsugu, *Phys. Rev. B* **107**, 205126 (2023).
3. All Local Conserved Quantities of the One-Dimensional Hubbard Model: K. Fukai, *Phys. Rev. Lett.* **131**, 256704 (2023).
4. Matrix product operator representations for the local conserved quantities of the Heisenberg chain: K. Yamada and K. Fukai, *SciPost Phys. Core* **6**, 069 (2023).
5. Numerical Renormalization Group Study of Quadrupole Kondo Effect with the Crystal-Field Excited State: Y. Kaneko and H. Tsunetsugu, *J. Phys. Soc. Jpn.* **93**, 033705 (2024).
6. On correlation functions in models related to the Temperley-Lieb algebra: K. Fukai, R. Kleinemühl, B. Pozsgay and E. Vernier, *SciPost Phys.* **16**, 003 (2024).

### Kato group

The main research subject of Kato Lab. is transport properties in mesoscopic and spintronic devices. We studied (1) spin pumping into two-dimensional electron gas and current induced by it, (2) ultrafast rotation of nanoparticles driven by ferromagnetic resonance and its quantum fluctuation, (3) spin pumping into twisted bilayer graphene and carbon nanotubes, (4) minimum ac injection into one-dimensional electron systems. We also published collaborated work with experimental group in ISSP about ac spin Hall effect.

1. Effect of vertex corrections on the enhancement of Gilbert damping in spin pumping into a two-dimensional electron gas: M. Yama, M. Matsuo and T. Kato, *Phys. Rev. B* **107**, 174414(1-15) (2023).
2. Gyromagnetic bifurcation in a levitated ferromagnetic particle: T. Sato, T. Kato, D. Oue and M. Matsuo, *Phys. Rev. B* **107**, L180406(1-6) (2023).
3. Minimal alternating current injection into carbon nanotubes: K. Fukuzawa, T. Kato, T. Jonckheere, J. Rech and T. Martin, *Phys. Rev. B* **108**, 125307(1-12) (2023).
4. Quantum fluctuation in rotation velocity of a levitated magnetic particle: T. Sato, D. Oue, M. Matsuo and T. Kato, *Phys. Rev. B* **108**, 094428(1-10) (2023).
5. \*Shear-strain controlled high-harmonic generation in graphene: T. Tamaya, H. Akiyama and T. Kato, *Phys. Rev. B* **107**, L081405 (2023).

---

\* Joint research among groups within ISSP.

6. Spin Hall magnetoresistance in quasi-two-dimensional antiferromagnetic-insulator/metal bilayer systems: T. Ishikawa, M. Matsuo and T. Kato, *Phys. Rev. B* **107**, 054426 (2023).
7. Spin Hall magnetoresistive detection of easy-plane magnetic order in the van der Waals antiferromagnet NiPS<sub>3</sub>: K. Sugi, T. Ishikawa, M. Kimata, Y. Shiota, T. Ono, T. Kato and T. Moriyama, *Phys. Rev. B* **108**, 064434 (2023).
8. Spin pumping into carbon nanotubes: K. Fukuzawa, T. Kato, M. Matsuo, T. Jonckheere, J. Rech and T. Martin, *Phys. Rev. B* **108**, 134429(1-9) (2023).
9. Theory of inverse Rashba-Edelstein effect induced by spin pumping into a two-dimensional electron gas: M. Yama, M. Matsuo and T. Kato, *Phys. Rev. B* **108**, 144430 (2023).
10. Twisted bilayer graphene reveals its flat bands under spin pumping: S. Haddad, T. Kato, J. Zhu and L. Mandhour, *Phys. Rev. B* **108**, L121101 (2023).
11. Nonequilibrium noise as a probe of pair-tunneling transport in the BCS-BEC crossover: H. Tajima, D. Oue, M. Matsuo, T. Kato and D. Abbott, *PNAS Nexus* **2**, pgad045 (2023).
12. \*Observation of Terahertz Spin Hall Conductivity Spectrum in GaAs with Optical Spin Injection: T. Fujimoto, T. Kurihara, Y. Murotani, T. Tamaya, N. Kanda, C. Kim, J. Yoshinobu, H. Akiyama, T. Kato and R. Matsunaga, *Phys. Rev. Lett.* **132**, 016301 (2024).
13. †\*Sub-photon accuracy noise reduction of a single shot coherent diffraction pattern with an atomic model trained autoencoder: T. Ishikawa, Y. Takeo, K. Sakurai, K. Yoshinaga, N. Furuya, Y. Inubushi, K. Tono, Y. Joti, M. Yabashi, T. Kimura and K. Yoshimi, *Opt. Express* **32**, 18301 (2024).
14. †\*H-wave – A Python package for the Hartree-Fock approximation and the random phase approximation: T. Aoyama, K. Yoshimi, K. Ido, Y. Motoyama, T. Kawamura, T. Misawa, T. Kato and A. Kobayashi, *Computer Physics Communications* **298**, 109087(1-10) (2024).
15. 磁氣的界面を通じて超伝導対称性を視る—強磁性共鳴変調を用いたスペクトロスコーピー—: 大湊 友也, 山影 相, 加藤 岳生, 松尾 衛, *固体物理* **58**, 433-440 (2023).

## Kawabata group

Recent years have seen remarkable progress in the physics of open quantum systems. In view of the recent rapid development of quantum information science and technology, it seems urgent to develop a general theory of open quantum systems. In our group, we are broadly interested in theoretical condensed matter physics, with a particular focus on nonequilibrium physics, to establish new foundations and principles in contemporary physics. Our recent research highlights topological phases of open quantum systems, as well as dissipative quantum chaos and lack thereof. On the basis of fundamental concepts such as symmetry and topology, we aim to uncover new physics intrinsic to far from equilibrium.

1. \*Dynamical quantum phase transitions in Sachdev-Ye-Kitaev Lindbladians: K. Kawabata, A. Kulkarni, J. Li, T. Numasawa and S. Ryu, *Phys. Rev. B* **108**, 075110 (2023).
2. Non-Hermitian boost deformation: T. Guo, K. Kawabata, R. Nakai and S. Ryu, *Phys. Rev. B* **108**, 075108 (2023).
3. Symmetry classification of typical quantum entanglement: Y. Liu, J. Kudler-Flam and K. Kawabata, *Phys. Rev. B* **108**, 085109 (2023).
4. Anisotropic Topological Anderson Transitions in Chiral Symmetry Classes: Z. Xiao, K. Kawabata, X. Luo, T. Ohtsuki and R. Shindou, *Phys. Rev. Lett.* **131**, 056301 (2023).
5. Hermitian Bulk – Non-Hermitian Boundary Correspondence: F. Schindler, K. Gu, B. Lian and K. Kawabata, *PRX Quantum* **4**, 030315 (2023).
6. Singular-Value Statistics of Non-Hermitian Random Matrices and Open Quantum Systems: K. Kawabata, Z. Xiao, T. Ohtsuki and R. Shindou, *PRX Quantum* **4**, 040312 (2023).
7. \*Symmetry of Open Quantum Systems: Classification of Dissipative Quantum Chaos: K. Kawabata, A. Kulkarni, J. Li, T. Numasawa and S. Ryu, *PRX Quantum* **4**, 030328 (2023).
8. Topological enhancement of nonnormality in non-Hermitian skin effects: Y. O. Nakai, N. Okuma, D. Nakamura, K. Shimomura and M. Sato, *Phys. Rev. B* **109**, 144203 (2024).
9. Lieb-Schultz-Mattis Theorem in Open Quantum Systems: K. Kawabata, R. Sohal and S. Ryu, *Phys. Rev. Lett.* **132**, 070402 (2024).

---

† Joint research with outside partners.

## Division of Nanoscale Science

### Otani group

Our research in 2023 spans diverse investigations on spin-mediated quasiparticles' interconversions and their intricate interactions. One study dissects the efficiency of orbital torque within ferromagnet/Cu/oxide heterostructures, emphasizing the pivotal role of oxide layers in this process. Another delves into the domain evolution and structure of Mn<sub>3</sub>Ge, an intriguing noncollinear Weyl antiferromagnet, spotlighting the presence and behavior of magnetic octupole domains. Acoustic waves are scrutinized for their impact on magnon dynamics in layered antiferromagnets, revealing acoustically induced magnon-phonon coupling phenomena. Furthermore, we explored the manipulation of magnon transport through valley-selective phonon-magnon scattering in magnetoelastic superlattices, offering a pathway for controlling magnetic information transfer. The investigation extends to nonlinear acoustic spin pumping driven by temperature-dependent surface acoustic wave frequency shifts, elucidating nuanced spin-phonon interactions. Additional studies employ innovative techniques like tip-induced temperature gradients in atomic force microscopy to map magneto-thermoelectric effects, providing insights into magnetic domain structure consisting of antiferromagnetic octupoles. These findings collectively advance our comprehension of noncollinear antiferromagnetic materials and their multifaceted behaviors, contributing to the evolution of spintronics and related fields.

1. Nonlinear Acoustic Spin Pumping Caused by Temperature-Dependent Frequency Shifts of Surface Acoustic Waves: Y. Hwang, J. Puebla, K. Kondou, C. S. Muñoz and Y. Otani, *J. Phys. Soc. Jpn.* **92**, 094702 (2023).
2. Acoustically Driven Magnon-Phonon Coupling in a Layered Antiferromagnet: T. P. Lyons, J. Puebla, K. Yamamoto, R. S. Deacon, Y. Hwang, K. Ishibashi, S. Maekawa and Y. Otani, *Phys. Rev. Lett.* **131**, 196701 (2023).
3. Valley-Selective Phonon-Magnon Scattering in Magnetoelastic Superlattices: L. Liao, J. Puebla, K. Yamamoto, J. Kim, S. Maekawa, Y. Hwang, Y. Ba and Y. Otani, *Phys. Rev. Lett.* **131**, 176701 (2023).
4. \*High-resolution magnetic imaging by mapping the locally induced anomalous Nernst effect using atomic force microscopy: N. Budai, H. Isshiki, R. Uesugi, Z. Zhu, T. Higo, S. Nakatsuji and Y. Otani, *Appl. Phys. Lett.* **122**, 102401 (2023).
5. Mid-infrared optical properties of non-magnetic-metal/CoFeB/MgO heterostructures: J. M. Flores-Camacho, B. Rana, R. E. Balderas-Navarro, A. Lastras-Martínez, Y. Otani and J. Puebla, *J. Phys. D: Appl. Phys.* **56**, 315301 (2023).
6. \*Temperature-induced anomalous magnetotransport in the Weyl semimetal Mn<sub>3</sub>Ge: M. Wu, K. Kondou, T. Chen, S. Nakatsuji and Y. Otani, *AIP Advances* **13**, 045102 (2023).
7. Emergence of spin-charge conversion functionalities due to spatial and time-reversal asymmetries and chiral symmetry: K. Kondou and Y. Otani, *Front. Phys.* **11**, 1140286 (2023).
8. †\*Oxide layer dependent orbital torque efficiency in ferromagnet/Cu/oxide heterostructures: J. Kim, J. Uzuhashi, M. Horio, T. Senoo, D. Go, D. Jo, T. Sumi, T. Wada, I. Matsuda, T. Ohkubo, S. Mitani, H.-W. Lee and Y. Otani, *Phys. Rev. Materials* **7**, L111401 (2023).
9. Magnetic octupole domain evolution and domain-wall structure in the noncollinear Weyl antiferromagnet Mn<sub>3</sub>Ge: M. Wu, K. Kondou, Y. Nakatani, T. Chen, H. Isshiki, T. Higo, S. Nakatsuji and Y. Otani, *AIP Publishing* **11**, 081115 (2023).

### Hasegawa group

We implemented the potentiometry function, which enabled us to observe the surface electrochemical potential profile and spatial distribution of resistance at sub-nanometer spatial resolution, using low-temperature scanning tunneling microscopy (STM). Using this setup, we can investigate potential profiles in a more stable manner under various temperatures and magnetic fields (up to 7 T). The temperature profile of the surface can also be investigated by detecting the Seebeck thermoelectric power. Using this system, we investigated the striped incommensurate (SIC) phase of a Pb monolayer formed on a non-doped Si(111) substrate. The structure is known to be metallic and exhibit superconductivity at low temperatures. Our previous study observing vortices pinned at steps demonstrated that the resistivity across a single height step is small. The small resistivity was proved directly through the observation of potential differences across single-height steps. We also performed magnetic-field-dependent potential profile measurements and successfully probed the Hall voltage locally in the nanoscale area, providing information on the charge carrier and density of the two-dimensional monolayer metallic states. We plan to investigate quantum nonlocal potential phenomena, as well as classical local phenomena in real space.

1. Squeezed Abrikosov-Josephson Vortex in Atomic-Layer Pb Superconductors Formed on Vicinal Si(111) Substrates: Y. Sato, M. Haze, R. Nemoto, W. Qian, S. Yoshizawa, T. Uchihashi and Y. Hasegawa, *Phys. Rev. Lett.* **130**, 106002(1-6) (2023).
2. †\*Quasi-Periodic Growth of One-Dimensional Copper Boride on Cu(110): Y. Tsujikawa, X. Zhang, K. Yamaguchi, M. Haze, T. Nakashima, A. Varadwaj, Y. Sato, M. Horio, Y. Hasegawa, F. Komori, M. Oshikawa, M. Kotsugi, Y. Ando, T.

---

\* Joint research among groups within ISSP.

## Lippmaa group

We are developing a new autonomous synthesis method for thin films. Structural information on a thin film is obtained during growth by monitoring RHEED patterns. The diffraction images are semantically segmented using a neural network to locate various diffraction features, such as surface streaks, surface diffraction spots, bulk diffraction spots, the direct electron beam location, the Kikuchi lines, etc. The extracted data is used for periodicity analysis and lattice parameter data clustering, which produces a phase composition estimate of a growing crystal. This information is used in a Gaussian process optimization to predict the best process parameters for the film growth to obtain the desired crystalline phase.

1. \*Semiconducting Electronic Structure of the Ferromagnetic Spinel  $\text{HgCr}_2\text{Se}_4$  Revealed by Soft-X-Ray Angle-Resolved Photoemission Spectroscopy: H. Tanaka, A. V. Telegin, Y. P. Sukhorukov, V. A. Golyashov, O. E. Tereshchenko, A. N. Lavrov, T. Matsuda, R. Matsunaga, R. Akashi, M. Lippmaa, Y. Arai, S. Ideta, K. Tanaka, T. Kondo and K. Kuroda, Phys. Rev. Lett. **130**, 186402(1-6) (2023).
2. \*Fabrication of single-crystalline  $\text{YFeO}_3$  films with large antiferromagnetic domains: C. Wang, M. Lippmaa and S. Nakatsuji, J. Appl. Phys. **135**, 113901(1-8) (2024).
3. †The use of He buffer gas for moderating the plume kinetic energy during Nd:YAG-PLD growth of  $\text{Eu}_x\text{Y}_{2-x}\text{O}_3$  phosphor films: S. Suzuki, T. Dazai, T. Tokunaga, T. Yamamoto, R. Katoh, M. Lippmaa and R. Takahashi, J. Appl. Phys. **135**, 195302 (2024).
4. \*Broken Screw Rotational Symmetry in the Near-Surface Electronic Structure of *AB*-Stacked Crystals: H. Tanaka, S. Okazaki, M. Kobayashi, Y. Fukushima, Y. Arai, T. Iimori, M. Lippmaa, K. Yamagami, Y. Kotani, F. Komori, K. Kuroda, T. Sasagawa and T. Kondo, Phys. Rev. Lett. **132**, 136402(1-6) (2024).
5. 機械学習による意思決定とデータ解釈：物質合成パラメータの最適化と in situ 測定結果の自動解析：大久保 勇男 and M. Lippmaa, 「ケモインフォマティクスにおけるデータ収集の最適化と解析手法」, 5, (株式会社技術情報協会, Tokyo, 2023), 359-366.

## Hashisaka group

Our group was newly inaugurated at ISSP in April 2023. We are working on setting up equipment for electrical transport measurements at cryogenic temperatures, and the experimental environment is being prepared. While working on these startups, we also worked on the edge transport mechanism at a fractional-integer quantum Hall junction and the evaluation of superconducting nonreciprocal transport phenomena in few-layer Td-MoTe<sub>2</sub>. We also studied the single-electron coherence in interacting copropagating integer quantum Hall edge channels, where an electron experiences fractionalization due to the Tomonaga-Luttinger liquid nature.

1. Coherent-Incoherent Crossover of Charge and Neutral Mode Transport as Evidence for the Disorder-Dominated Fractional Edge Phase: M. Hashisaka, T. Ito, T. Akiho, S. Sasaki, N. Kumada, N. Shibata and K. Muraki, Phys. Rev. X **13**, 031024 (2023).
2. Gate-tunable giant superconducting nonreciprocal transport in few-layer Td-MoTe<sub>2</sub>: T. Wakamura, M. Hashisaka, S. Hoshino, M. Bard, S. Okazaki, T. Sasagawa, T. Taniguchi, K. Watanabe, K. Muraki and N. Kumada, Phys. Rev. Research **6**, 013132 (2024).

## Yoshinobu group

We conducted several research projects in the fiscal year 2023: (1) The hydrogenation of formate species on the H-Cu(997) surface was studied by HREELS and TPD. Desorption of formaldehyde was observed by TPD, and a possible intermediate species was investigated. (2) The adsorption and decomposition of methanol on the Cu(977) and Pd-Cu(977) surfaces were studied by TPD, IRAS and SR-XPS. (3) The reactive desorption of  $\text{CO} + \text{O} \rightarrow \text{CO}_2$  on Pt(111) was studied using ab-initio molecular dynamics (AIMD) with van der Waals DFT functionals. The desorption dynamics of  $\text{CO}_2$  including kinetic energy, angular distribution and vibrational excitation were analyzed. (4) The chemical states and reactions on the basal plane and the edge plane of  $\text{MoS}_2$  were studied in vacuum and under the exposure to water or  $\text{CO}_2$  by SR-XPS. (5) Gapless detection of broadband terahertz pulses using a metal surface was newly developed. (6) SFG spectroscopy was developed using broadband terahertz and visible ultra-short pulse laser.

1. \*Disentangling the Competing Mechanisms of Light-Induced Anomalous Hall Conductivity in Three-Dimensional Dirac Semimetal: Y. Murotani, N. Kanda, T. Fujimoto, T. Matsuda, M. Goyal, J. Yoshinobu, Y. Kobayashi, T. Oka, S. Stemmer and R. Matsunaga, Phys. Rev. Lett. **131**, 096901 (2023).

---

† Joint research with outside partners.

2. †Termination of graphene edges created by hydrogen and deuterium plasmas: T. Ochi, M. Kamada, T. Yokosawa, K. Mukai, J. Yoshinobu and T. Matsui, *Carbon* **203**, 727-731 (2023).
3. †Carbon Nitride Loaded with an Ultrafine, Monodisperse, Metallic Platinum - Cluster Cocatalyst for the Photocatalytic Hydrogen - Evolution Reaction: D. Yazaki, T. Kawawaki, D. Hirayama, M. Kawachi, K. Kato, S. Oguchi, Y. Yamaguchi, S. Kikkawa, Y. Ueki, S. Hossain, D. J. Osborn, F. Ozaki, S. Tanaka, J. Yoshinobu, G. F. Metha, S. Yamazoe, A. Kudo, A. Yamakata and Y. Negishi, *Small* **19**, 2208287 (12 pages) (2023).
4. The quantitative study of methane adsorption on the Pt(997) step surface as the initial process for reforming reactions: Y. H. Choi, S. E. M. Putra, Y. Shiozawa, S. Tanaka, K. Mukai, I. Hamada, Y. Morikawa and J. Yoshinobu, *Surface Science* **732**, 122284 (2023).
5. \*Gapless detection of broadband terahertz pulses using a metal surface in air based on field-induced second-harmonic generation: S. Tanaka, Y. Murotani, S. A. Sato, T. Fujimoto, T. Matsuda, N. Kanda, R. Matsunaga and J. Yoshinobu, *Applied Physics Letters* **122**, 251101 (6 pages) (2023).
6. \*Hydrogen - induced Sulfur Vacancies on the MoS<sub>2</sub> Basal Plane Studied by Ambient Pressure XPS and DFT Calculations: F. Ozaki, S. Tanaka, Y. Choi, W. Osada, K. Mukai, M. Kawamura, M. Fukuda, M. Horio, T. Koitaya, S. Yamamoto, I. Matsuda, T. Ozaki and J. Yoshinobu, *ChemPhysChem* **24**, e202300477 (2023).
7. †\*In Situ Electrical Detection of Methane Oxidation on Atomically Thin IrO<sub>2</sub> Nanosheet Films Down to Room Temperature: Y. Ishihara, T. Koitaya, Y. Hamahiga, W. Sugimoto, S. Yamamoto, I. Matsuda, J. Yoshinobu and R. Nouchi, *Adv. Materials Inter.* **10**, 2300258 (2023).
8. \*Observation of Terahertz Spin Hall Conductivity Spectrum in GaAs with Optical Spin Injection: T. Fujimoto, T. Kurihara, Y. Murotani, T. Tamaya, N. Kanda, C. Kim, J. Yoshinobu, H. Akiyama, T. Kato and R. Matsunaga, *Phys. Rev. Lett.* **132**, 016301 (2024).
9. \*Anomalous Hall Transport by Optically Injected Isospin Degree of Freedom in Dirac Semimetal Thin Film: Y. Murotani, N. Kanda, T. Fujimoto, T. Matsuda, M. Goyal, J. Yoshinobu, Y. Kobayashi, T. Oka, S. Stemmer and R. Matsunaga, *Nano Lett.* **24**, 222 (2024).
10. Low-temperature dissociation of CO<sub>2</sub> molecules on vicinal Cu surfaces: T. Koitaya, Y. Shiozawa, Y. Yoshikura, K. Mukai, S. Yoshimoto and J. Yoshinobu, *Phys. Chem. Chem. Phys.* **26**, 9226-9233 (2024).
11. 「空気分子と金属表面を利用した広帯域 THz パルスのギャップレス検出法」: 田中 駿介, 松永 隆佑, 吉信 淳, *分光研究* **72**, 199-202 (2023).
12. パラジウム蒸着により機能化したモデル触媒表面における 水素の活性化とスピルオーバー: 長田 渉, 尾崎 文彦, 田中 駿介, 吉信 淳, *Acc. Mater. Surf. Res.* **8**, 147-158 (2023).
13. 巻頭言「悪魔の作品を観ようではないか!」: 吉信 淳, *表面と真空* **67**, 99 (2024).
14. 準大気圧光電子分光法による二酸化炭素水素化のオペランド観測: 小坂谷 貴典, 山本 達, 松田 巖, 吉信 淳, 横山 利彦, *表面と真空* **67**, 117-122 (2024).

## Functional Materials Group

### Akiyama group

In 2023, we accomplished ultra-fast gain-switching experiment in 30GHz-modulation-bandwidth 1270nm DFB-type single-mode laser diodes (LDs) with and without chirp compensation, and analyzed generated 5.3 ps short pulses near the Fourier transform limit via rate equations and other laser theory framework. We developed our original 10 ps LD-seed-pulse prototype modules with improvements in packaging and software. We extended our high-efficiency-solar-cell study to efficient power conversion of laser light, and achieved high conversion efficiency of about 50%. Collaboration work and papers with Hiyama-team in Gunma University were accomplished on quantitative spectroscopy on bioluminescence quantum yield of new luciferin analogs.

1. \*Shear-strain controlled high-harmonic generation in graphene: T. Tamaya, H. Akiyama and T. Kato, *Phys. Rev. B* **107**, L081405 (2023).
2. \*Twisting and Protonation of Retinal Chromophore Regulate Channel Gating of Channelrhodopsin C1C2: K. Shibata, K. Oda, T. Nishizawa, Y. Hazama, R. Ono, S. Takaramoto, R. Bagherzadeh, H. Yawo, O. Nureki, K. Inoue and H. Akiyama, *J. Am. Chem. Soc.* **145**, 10779-10789 (2023).

---

\* Joint research among groups within ISSP.

3. Gain-switched pulse generation of 5.3 ps from 30 GHz-modulation-bandwidth 1270 nm DFB laser diode: M. Kobayashi, T. Nakamura, H. Nakamae, C. Kim and H. Akiyama, *Opt. Lett.* **48**, 6344-6347 (2023).
4. Output-power equivalence of two- and four-terminal photovoltaic-thermoelectric hybrid tandems: J. Sakuma, K. Kamide, T. Mochizuki, H. Takato and H. Akiyama, *Appl. Phys. Express* **16**, 014003 (2023).
5. Optimisation of Sb<sub>2</sub>S<sub>3</sub> thin-film solar cells via Sb<sub>2</sub>Se<sub>3</sub> post-treatment: R. Wang, D. Qin, X. Ding, Q. Zhang, Y. Wang, Y. Pan, G. Weng, X. Hu, J. Tao, J. Chu, H. Akiyama and S. Chen, *Journal of Power Sources* **556**, 232451 (2023).
6. Impacts of SiO<sub>2</sub>-Buried Structure on Performances of GaN-Based Vertical-Cavity Surface-Emitting Lasers: R. Xu, H. Akiyama and B. Zhang, *IEEE Trans. Electron Devices* **70**, 5701 (2023).
7. Crystallization mechanism and lasing properties of CsPbBr<sub>3</sub> perovskites by chemical vapor deposition: Z. Su, Z. Cao, F. Cao, Y. He, J. Zhang, G. Weng, X. Hu, J. Chu, H. Akiyama and S. Chen, *Chemical Engineering Journal* **472**, 144906 (2023).
8. Influence of S-content ratios on the defect properties of Sb<sub>2</sub>(S, Se)<sub>3</sub> thin-film solar cells: R. Wang, D. Qin, S. Zheng, G. Weng, X. Hu, J. Tao, J. Chu, H. Akiyama and S. Chen, *Solar Energy Materials and Solar Cells* **260**, 112501 (2023).
9. Temperature sensitivity of adjustable band gaps of Sb<sub>2</sub>(S, Se)<sub>3</sub> solar cells via vapor transport deposition: D. Qin, X. Pan, R. Wang, Y. Pan, Y. Wang, J. Zhang, X. Ding, Y. Chen, S. Zheng, S. Ye, Y. Pan, G. Weng, X. Hu, J. Tao, Z. Zhu, J. Chu, H. Akiyama and S. Chen, *Solar Energy Materials and Solar Cells* **263**, 112582 (2023).
10. †Photo-cleaving and photo-bleaching quantum yields of coumarin-caged luciferin: R. Kumagai, R. Ono, S. Sakimoto, C. Suzuki, K.-I. Kanno, H. Aoyama, J. Usukura, M. Kobayashi, H. Akiyama, H. Itabashi and M. Hiyama, *Journal of Photochemistry and Photobiology A: Chemistry* **434**, 114230 (2023).
11. †Quantum yield of near-infrared bioluminescence with firefly luciferin analog: AkaLumine: R. Ono, K. Osawa, Y. Takahashi, Y. Noguchi, N. Kitada, R. Saito-Moriya, T. Hirano, S. A. Maki, K. Shibata, H. Akiyama, K.-I. Kanno, H. Itabashi and M. Hiyama, *Journal of Photochemistry and Photobiology A: Chemistry* **434**, 114270 (2023).
12. Lasing properties and carrier dynamics of CsPbBr<sub>3</sub> perovskite nanocrystal vertical-cavity surface-emitting laser: Y. He, Z. Su, F. Cao, Z. Cao, Y. Liu, C. Zhao, G. Weng, X. Hu, J. Tao, J. Chu, H. Akiyama and S. Chen, *Nanophotonics* **12**, 2133 (2023).
13. \*Observation of Terahertz Spin Hall Conductivity Spectrum in GaAs with Optical Spin Injection: T. Fujimoto, T. Kurihara, Y. Murotani, T. Tamaya, N. Kanda, C. Kim, J. Yoshinobu, H. Akiyama, T. Kato and R. Matsunaga, *Phys. Rev. Lett.* **132**, 016301 (2024).
14. Regulating the crystal orientation of vapor-transport-deposited GeSe thin films by a post-annealing treatment: S. Zheng, D. Qin, R. Wang, Y. Pan, G. Weng, X. Hu, J. Chu, H. Akiyama and S. Chen, *Appl. Opt.* **63**, 2752 (2024).
15. Subnanosecond Marx Generators for Picosecond Gain-Switched Laser Diodes: F. Cao, D. Jiang, Y. Liu, Y. Tian, X. Ran, Y. Long, T. Ito, X. Hu, G. Weng, H. Akiyama and S. Chen, *IEEE Photonics J.* **16**, 1 (2024).
16. Carrier tunneling and transport in coupled quantum wells: Modeling and experimental verification: F. Cao, Z. Su, C. Wang, Y. Chen, G. Weng, C. Wang, X. Hu, H. Akiyama, J. Chu and S. Chen, *Appl. Phys. Lett.* **124**, 161106 (2024).

## Sugino group

This year, this group performed first-principles calculations of the structure of water-Pt(111) interface, oxygen reduction reaction on a defective ZrO<sub>2</sub> surface, quantum mechanical hydrogen diffusion on noble metal surfaces, magnetic structure of a superconducting cuprate material Sr<sub>1-x</sub>La<sub>x</sub>CuO<sub>2</sub>. In addition, a model Hamiltonian was used to study the nonadiabatic quantum dynamics of an electrochemical reaction on a metal surface.

1. Theoretical calculation and comparison of H diffusion on Cu(111), Ni(111), Pd(111), and Au(111): Y. Kataoka, J. Haruyama and O. Sugino, *Phys. Rev. B* **107**, 205414 (2023).
2. †\*Suppression of atomic displacive excitation in photo-induced A<sub>1g</sub> phonon mode of bismuth unveiled by low-temperature time-resolved x-ray diffraction: Y. Kubota, Y. Tanaka, T. Togashi, T. Ebisu, K. Tamasaku, H. Osawa, T. Wada, O. Sugino, I. Matsuda and M. Yabashi, *Appl. Phys. Lett.* **122**, 092201 (2023).
3. †First-principles study of water adsorption monolayer on Pt(111): Adsorption energy and second-order nonlinear susceptibility: J. Haruyama, T. Sugimoto and O. Sugino, *Phys. Rev. Materials* **7**, 115803 (2023).
4. †Elucidation of Spin-Correlations, Fermi Surface and Pseudogap in a Copper Oxide Superconductor: H. Kamimura, M. Araidai, K. Ishida, S. Matsuno, H. Sakata, K. Sasaoka, K. Shiraishi, O. Sugino, J.-S. Tsai and K. Yamada, *Condensed*

---

† Joint research with outside partners.

Matter **8**, 33 (2023).

5. Magnetic phases of electron-doped infinite-layer  $\text{Sr}_{1-x}\text{La}_x\text{CuO}_2$  from first-principles density functional calculations: A. N. Tatan, J. Haruyama and O. Sugino, *Phys. Rev. B* **109**, 165134 (2024).
6. Time-dependent electron transfer and energy dissipation in condensed media: E. F. Arguelles and O. Sugino, *J. Chem. Phys.* **160**, 144102 (2024).

## Oka group

Oka group has worked on Nonequilibrium quantum materials including Floquet engineering of Dirac semimetals, spin systems, and many-body systems.

1. \*Dynamical quantum phase transitions in Sachdev-Ye-Kitaev Lindbladians: K. Kawabata, A. Kulkarni, J. Li, T. Numasawa and S. Ryu, *Phys. Rev. B* **108**, 075110 (2023).
2. Mott memristors based on field-induced carrier avalanche multiplication: F. Peronaci, S. Ameli, S. Takayoshi, A. S. Landsman and T. Oka, *Phys. Rev. B* **107**, 075154 (2023).
3. Phase transition and evidence of fast-scrambling phase in measurement-only quantum circuits: Y. Kuno, T. Orito and I. Ichinose, *Phys. Rev. B* **108**, 094104 (2023).
4. \*Disentangling the Competing Mechanisms of Light-Induced Anomalous Hall Conductivity in Three-Dimensional Dirac Semimetal: Y. Murotani, N. Kanda, T. Fujimoto, T. Matsuda, M. Goyal, J. Yoshinobu, Y. Kobayashi, T. Oka, S. Stemmer and R. Matsunaga, *Phys. Rev. Lett.* **131**, 096901 (2023).
5. Demonstration of geometric diabatic control of quantum states: K. Sasaki, Y. Nakamura, T. Teraji, T. Oka and K. Kobayashi, *Phys. Rev. A* **107**, 053113 (2023).
6. \*Symmetry of Open Quantum Systems: Classification of Dissipative Quantum Chaos: K. Kawabata, A. Kulkarni, J. Li, T. Numasawa and S. Ryu, *PRX Quantum* **4**, 030328 (2023).
7. \*Anomalous Hall Transport by Optically Injected Isospin Degree of Freedom in Dirac Semimetal Thin Film: Y. Murotani, N. Kanda, T. Fujimoto, T. Matsuda, M. Goyal, J. Yoshinobu, Y. Kobayashi, T. Oka, S. Stemmer and R. Matsunaga, *Nano Lett.* **24**, 222 (2024).

## Inoue group

In 2023, we studied the ion-transporting mechanism of channelrhodopsin C1C2 using time-resolved Raman spectroscopy in collaboration with Prof. Akiyama's laboratory. We clarified that the highly twisted retinal chromophore drives the channel opening. We also successfully converted the function of the outward proton-pumping rhodopsin, PspR, into an inward proton-pumping one by mutating three residues in PspR to mimic those in the natural inward proton-pumping rhodopsin, SzR. This study revealed that the directionality of proton transport in rhodopsins is determined by just a few residues. Furthermore, we identified new rhodopsins homologous to TAT rhodopsin in several marine bacteria and classified them into a new family, TwR. Additionally, we investigated the photoreaction cycle of a new class of outward proton-pumping rhodopsin that binds to antennae 3-OH type carotenoids, previously considered incapable of binding to rhodopsins. Moreover, we reported on the photochemical properties of the Retinal G protein-coupled receptor, a new rhodopsin family with a DSE motif, and the structural dynamics of heliorhodopsin.

1. Converting a Natural-Light-Driven Outward Proton Pump Rhodopsin into an Artificial Inward Proton Pump: M. D. C. Marín, M. Konno, H. Yawo and K. Inoue, *J. Am. Chem. Soc.* **145**, 10938-10942 (2023).
2. \*Twisting and Protonation of Retinal Chromophore Regulate Channel Gating of Channelrhodopsin C1C2: K. Shibata, K. Oda, T. Nishizawa, Y. Hazama, R. Ono, S. Takaramoto, R. Bagherzadeh, H. Yawo, O. Nureki, K. Inoue and H. Akiyama, *J. Am. Chem. Soc.* **145**, 10779-10789 (2023).
3. Phototrophy by antenna-containing rhodopsin pumps in aquatic environments: A. Chazan, I. Das, T. Fujiwara, S. Murakoshi, A. Rozenberg, A. Molina-Márquez, F. K. Sano, T. Tanaka, P. Gómez-Villegas, S. Larom, A. Pushkarev, P. Malakar, M. Hasegawa, Y. Tsukamoto, T. Ishizuka, M. Konno, T. Nagata, Y. Mizuno, K. Katayama, R. Abe-Yoshizumi, S. Ruhman, K. Inoue, H. Kandori, R. León, W. Shihoya, S. Yoshizawa, M. Sheves, O. Nureki and O. Bèjà, *Nature* **615**, 535-540 (2023).
4. Difference FTIR Spectroscopy of Jumping Spider Rhodopsin-1 at 77K: S. Hanai, T. Nagata, K. Katayama, S. Inukai, M. Koyanagi, K. Inoue, A. Terakita and H. Kandori, *Biochemistry* **62**, 1347-1359 (2023).

---

\* Joint research among groups within ISSP.

5. Reversible Photoreaction of a Retinal Photoisomerase, Retinal G-Protein-Coupled Receptor RGR: N. Morimoto, T. Nagata and K. Inoue, *Biochemistry* **62**, 1429-1432 (2023).
6. Time-resolved detection of light-induced conformational changes of heliorhodopsin: Y. Nakasone, Y. Kawasaki, M. Konno, K. Inoue and M. Terazima, *Phys. Chem. Chem. Phys.* **25**, 12833-12840 (2023).
7. Effects of the Unique Chromophore-Protein Interactions on the Primary Photoreaction of Schizorhodopsin: C.-F. Chang, M. Konno, K. Inoue and T. Tahara, *J. Phys. Chem. Lett.* **14**, 7083 (2023).
8. Biophysical characterization of microbial rhodopsins with DSE motif: M. D. C. Marín, A. L. Jaffé, P. T. West, M. Konno, J. F. Banfield and K. Inoue, *Biophys. Physicobiol.* **20**, e201023 (2023).
9. Structural basis for ion selectivity in potassium-selective channelrhodopsins: S. Tajima, Y. S. Kim, M. Fukuda, Y. Jo, P. Y. Wang, J. M. Paggi, M. Inoue, E. F. X. Byrne, K. E. Kishi, S. Nakamura, C. Ramakrishnan, S. Takaramoto, T. Nagata, M. Konno, M. Sugiura, K. Katayama, T. E. Matsui, K. Yamashita, S. Kim, H. Ikeda, J. Kim, H. Kandori, R. O. Dror, K. Inoue, K. Deisseroth and H. E. Kato, *Cell* **186**, 4325.e26 (2023).
10. Protein dynamics of a light-driven Na<sup>+</sup> pump rhodopsin probed using a tryptophan residue near the retinal chromophore: A. Otomo, M. Mizuno, K. Inoue, H. Kandori and Y. Mizutani, *Biophys. Physicobiol.* **20**, e201016 (2023).
11. Characterization of retinal chromophore and protonated Schiff base in Thermoplasmatales archaeon heliorhodopsin using solid-state NMR spectroscopy: S. Suzuki, S. Kumagai, T. Nagashima, T. Yamazaki, T. Okitsu, A. Wada, A. Naito, K. Katayama, K. Inoue, H. Kandori and I. Kawamura, *Biophysical Chemistry* **296**, 106991 (2023).
12. Functional characterization of four opsins and two G alpha subtypes co-expressed in the molluscan rhabdomeric photoreceptor: R. Matsuo, M. Koyanagi, T. Sugihara, T. Shirata, T. Nagata, K. Inoue, Y. Matsuo and A. Terakita, *BMC Biol* **21**, 291 (2023).
13. Multiple roles of a conserved glutamate residue for unique biophysical properties in a new group of microbial rhodopsins homologous to TAT rhodopsin: K. Mannen, T. Nagata, A. Rozenberg, M. Konno, M. D. C. Marín, R. Bagherzadeh, O. Béjà, T. Uchihashi and K. Inoue, *Journal of Molecular Biology* **436**, 168331 (2023).
14. Chromophore-Protein Interactions Affecting the Polyene Twist and  $\pi$ - $\pi^*$  Energy Gap of the Retinal Chromophore in Schizorhodopsins: T. Urui, T. Shionoya, M. Mizuno, K. Inoue, H. Kandori and Y. Mizutani, *J. Phys. Chem. B* **128**, 2389-2397 (2024).
15. *Cis* - *Trans* Reisomerization Preceding Reprotonation of the Retinal Chromophore Is Common to the Schizorhodopsin Family: A Simple and Rational Mechanism for Inward Proton Pumping: T. Urui, K. Hayashi, M. Mizuno, K. Inoue, H. Kandori and Y. Mizutani, *J. Phys. Chem. B* **128**, 744-754 (2024).
16. Molecular Mechanisms behind Circular Dichroism Spectral Variations between Channelrhodopsin and Heliorhodopsin Dimers: K. J. Fujimoto, Y. A. Tsuzuki, K. Inoue and T. Yanai, *J. Phys. Chem. Lett.* **15**, 5788-5794 (2024).
17. Photochemistry of the Retinal Chromophore in Microbial Rhodopsins: K. Inoue, *J. Phys. Chem. B* **127**, 9212-9222 (2023).
18. アスガルドアーキアの持つ内向きプロトンポンプ型ロドプシン:シゾロドプシン: 井上 圭一, 今野 雅恵, 川崎 佑真, M. D. C. Marín, *生物物理* **63**, 257-260 (2023).
19. Iron-limitation light switch: O. Béjà and K. Inoue, *Nature Microbiology* **295**, 1942-1943 (2023).
20. ゲノム時代に変わりゆくロドプシン観: 井上 圭一, *酵素工学ニュース* **90**, 6-12 (2023).
21. ロドプシンを用いた光受容と新奇シゾロドプシンファミリー: 井上 圭一, 「未培養微生物研究の最新動向」, 青柳 秀紀, (シーエムシー出版, 2023), 74-81.

## Hayashi group

After transferring from Tohoku University to the Institute for Solid State Physics in 2023, we spent this year summarizing experiments performed at Tohoku University. Transport phenomena such as heat conduction, electric current, and diffusion are the subjects of non-equilibrium statistical mechanics. There are also transport phenomena in the body, and we specifically focus on axonal transport by motor proteins (kinesin and dynein) in neurons as subjects of mathematics and physics research. Last year, we performed fluorescence imaging of axonal transport in neurons of *C. elegans* worms at Tohoku University. We measured the transport velocity data from the recorded movies of the fluorescence imaging. This year, we analyzed the transport velocity of axonal transport obtained last year using extreme value statistics [1]. Applying extreme value statistics to nanoscale biological systems is novel, and we presented the results at a research meeting at the Institute of Statistical Mathematics on

---

† Joint research with outside partners.

"Applications of Extreme Value Theory in Engineering," discussing the validity of its application. Mutations in motor proteins can lead to axonal transport disorders, leading to the death of neurons and associated with neurological diseases [3]. We presented the results of our lab's physical measurements at the annual meeting of the Japan Neuroscience Society, aiming to elucidate the mechanisms of neurological diseases. Because it's important for doctors, patients, and researchers to consider these issues together, the discussions with doctors at the annual meeting were fruitful. Motor protein research is actively conducted in the United States, so to deepen academic exchange with the US, we organized a joint Japan-US symposium at the Japan Society for Biophysics [2]. Additionally, we gave an oral presentation at the Biophysical Society (USA) annual meeting.

1. The third Japan-U.S. symposium on motor proteins and associated single-molecule biophysics: T. Shima and K. Hayashi, *Biophysics and Physicobiology* **20**, e200037 (2023).
2. Extreme Value Analysis of Intracellular Cargo Transport by Motor Proteins: T. Naoi, Y. Kagawai, K. Nagino, S. Niwa and K. Hayashi, *Communications Physics* **7**, Article number: 50 (2024).
3. Number of kinesins engaged in axonal cargo transport: A novel biomarker for neurological disorders: K. Hayashi and K. Sasaki, *Neuroscience Research* **197**, 25-30 (2023).

## Quantum Materials Group

### Oshikawa group

We have reformulated the Kennedy-Tasaki duality mapping, which was originally proposed in 1992, based on the modern understanding of the Symmetry-Protected Topological (SPT) phases. The duality maps between a SPT phase and a Spontaneous Symmetry Breaking (SSB) phase; a non-local "string" order parameter is mapped to a conventional correlation function of a local order parameter. Although it was originally defined only on open chains, we have generalized it to closed chains as a non-invertible transformation. Applying our reformulated version of the duality to various simple systems, we have constructed numerous SPT phases systematically, including new types of "gapless SPT" phases.

1. Drude weights in one-dimensional systems with a single defect: K. Takasan, M. Oshikawa and H. Watanabe, *Phys. Rev. B* **107**, 075141 (2023).
2. Duality, criticality, anomaly, and topology in quantum spin-1 chains: H. Yang, L. Li, K. Okunishi and H. Katsura, *Phys. Rev. B* **107**, 125158 (2023).
3. Finite-size and finite bond dimension effects of tensor network renormalization: A. Ueda and M. Oshikawa, *Phys. Rev. B* **108**, 024413(1-13) (2023).
4. <sup>†</sup>Many-body multipole index and bulk-boundary correspondence: Y. Tada and M. Oshikawa, *Phys. Rev. B* **108**, 235150(1-12) (2023).
5. Noninvertible duality transformation between symmetry-protected topological and spontaneous symmetry breaking phases: L. Li, M. Oshikawa and Y. Zheng, *Phys. Rev. B* **108**, 214429(1-19) (2023).
6. Subsystem non-invertible symmetry operators and defects: W. Cao, L. Li, M. Yamazaki and Y. Zheng, *SciPost Phys.* **15**, 155 (2023).
7. Fermionization of fusion category symmetries in 1+1 dimensions: K. Inamura, *JHEP* **2023**, 101(1-63) (2023).
8. Symmetry TFTs and anomalies of non-invertible symmetries: J. Kaidi, E. Nardoni, G. Zafrir and Y. Zheng, *JHEP* **2023**, 53 (2023).
9. Symmetry TFTs for Non-invertible Defects: J. Kaidi, K. Ohmori and Y. Zheng, *Commun. Math. Phys.* **404**, 1021 (2023).
10. <sup>†\*</sup>Quasi-Periodic Growth of One-Dimensional Copper Boride on Cu(110): Y. Tsujikawa, X. Zhang, K. Yamaguchi, M. Haze, T. Nakashima, A. Varadwaj, Y. Sato, M. Horio, Y. Hasegawa, F. Komori, M. Oshikawa, M. Kotsugi, Y. Ando, T. Kondo and I. Matsuda, *Nano Lett.* **24**, 1160 (2024).

### Nakatsuji group

The myths of quantum mechanics render electronic, magnetic, and optical properties in materials that defy common sense while inspiring future technologies. Through decades of effort, researchers studying quantum materials have uncovered a wealth of fascinating properties, ranging from superconductivity that allows electric current to flow without any resistance to topolog-

---

\* Joint research among groups within ISSP.

ical insulators whose surface states serve as superhighways for electrons to flow freely. Discoveries in the field of quantum materials offer a central thread linking the previously disparate fields, like condensed matter physics, high-energy physics, quantum computing, and cosmology. Moreover, the functionalities of quantum materials provide the basis for emerging transformational technologies, such as antiferromagnetic memory. Our vision is to lead the quest for functional quantum materials to bear a groundbreaking impact on fundamental science and benefit humanity in the future. The main research topics in our group are (1) Quantum transport in topological materials; (2) Coherent quantum transport in antiferromagnetic spintronics; (3) Strange metal and exotic superconductivity in strongly correlated electron systems; (4) Long-range quantum entanglement in topologically ordered states.

1. \*Ultrafast Dynamics of Intrinsic Anomalous Hall Effect in the Topological Antiferromagnet  $\text{Mn}_3\text{Sn}$ : T. Matsuda, T. Higo, T. Koretsune, N. Kanda, Y. Hirai, H. Peng, T. Matsuo, N. Yoshikawa, R. Shimano, S. Nakatsuji and R. Matsunaga, *Phys. Rev. Lett.* **130**, 126302 (2023).
2. \*High-resolution magnetic imaging by mapping the locally induced anomalous Nernst effect using atomic force microscopy: N. Budai, H. Isshiki, R. Uesugi, Z. Zhu, T. Higo, S. Nakatsuji and Y. Otani, *Appl. Phys. Lett.* **122**, 102401 (2023).
3. \*Octupole-driven magnetoresistance in an antiferromagnetic tunnel junction: X. Chen, T. Higo, K. Tanaka, T. Nomoto, H. Tsai, H. Idzuchi, M. Shiga, S. Sakamoto, R. Ando, H. Kosaki, T. Matsuo, D. Nishio-Hamane, R. Arita, S. Miwa and S. Nakatsuji, *Nature* **613**, 490-495 (2023).
4. \*Temperature-induced anomalous magnetotransport in the Weyl semimetal  $\text{Mn}_3\text{Ge}$ : M. Wu, K. Kondou, T. Chen, S. Nakatsuji and Y. Otani, *AIP Advances* **13**, 045102 (2023).
5. \*Fabrication of single-crystalline  $\text{YFeO}_3$  films with large antiferromagnetic domains: C. Wang, M. Lippmaa and S. Nakatsuji, *J. Appl. Phys.* **135**, 113901 (1-8) (2024).

## Miwa group

This year we have worked on the following topics: (1) chirality-induced spin selectivity in the absence of bias current, (2) tunneling magnetoresistance using the chiral antiferromagnet  $\text{Mn}_3\text{Sn}$ , and (3) interfacial magnetic anisotropy of the Fe/MgO system. In topic (1), we have summarized our recent work and published a review paper (*J. Magn. Magn. Mater.* **585**, 171157). In topic (2) we find a novel tunneling magnetoresistance effect in an all antiferromagnetic  $\text{Mn}_3\text{Sn}/\text{MgO}/\text{Mn}_3\text{Sn}$  junction. This is a collaboration work with the groups of Nakatsuji and Otani (*Nature* **613**, 490). In topic (3), we find that among various alkali halides, fluoride insertion is effective in enhancing the perpendicular magnetic anisotropy of the Fe/MgO system (*Phys. Rev. B* **107**, 094420).

1. Magnetic anisotropy of Fe/MgO interfaces inserted with alkali halide layers: J. Chen, S. Sakamoto, H. Kosaki and S. Miwa, *Phys. Rev. B* **107**, 094420 (2023).
2. \*Octupole-driven magnetoresistance in an antiferromagnetic tunnel junction: X. Chen, T. Higo, K. Tanaka, T. Nomoto, H. Tsai, H. Idzuchi, M. Shiga, S. Sakamoto, R. Ando, H. Kosaki, T. Matsuo, D. Nishio-Hamane, R. Arita, S. Miwa and S. Nakatsuji, *Nature* **613**, 490-495 (2023).
3. Observation of large spin conversion anisotropy in bismuth: N. Fukumoto, R. Ohshima, M. Aoki, Y. Fuseya, M. Matsushima, E. Shigematsu, T. Shinjo, Y. Ando, S. Sakamoto, M. Shiga, S. Miwa and M. Shiraishi, *Proceedings of the National Academy of Sciences* **102**, e2215030120 (2023).
4. Influence of alkali-fluoride insertion layers on the perpendicular magnetic anisotropy at the Fe/MgO interface: J. Chen, S. Sakamoto and S. Miwa, *Phys. Rev. B* **109**, 064413 (2024).
5. Spontaneous spin selectivity in chiral molecules at the interface: K. Kondou, S. Miwa and D. Miyajima, *Journal of Magnetism and Magnetic Materials* **585**, 171157 (2023).

## Materials Design and Characterization Laboratory

### Hiroi group

The nodal-line semimetals  $\text{NaAlSi}$  and  $\text{NaAlGe}$  have significantly different ground states despite having similar electronic structures:  $\text{NaAlSi}$  exhibits superconductivity below 7 K, while  $\text{NaAlGe}$  exhibits semiconductive electrical conductivity at low temperatures, indicating the formation of a pseudogap at approximately 100 K. The origin of the pseudogap in  $\text{NaAlGe}$  is unknown but may be associated with excitonic instability. We investigated hole-doping effects on the ground state in the solid solution  $\text{Na}(\text{Al}_{1-x}\text{Zn}_x)\text{Ge}$  and discovered that the pseudogap is suppressed continuously with increasing Zn content, followed

---

† Joint research with outside partners.

by the appearance of a superconducting dome with the highest transition temperature of 2.8 K. This superconductivity most likely results from excitonic fluctuations.

1. †\*Fermi surface and light quasi particles in hourglass nodal chain metal  $\beta$ -ReO<sub>2</sub>: D. Hirai, T. Anbai, T. Konoike, S. Uji, Y. Hattori, T. Terashima, H. Ishikawa, K. Kindo, N. Katayama, T. Oguchi and Z. Hiroi, *J. Phys.: Condens. Matter* **35**, 405503 (2023).
2. Anomalous Diamagnetic Torque Signals in Topological Nodal-Line Semimetal NaAlSi: S. Uji, T. Konoike, Y. Hattori, T. Terashima, T. Oguchi, T. Yamada, D. Hirai, T. Ikenobe and Z. Hiroi, *J. Phys. Soc. Jpn.* **92**, 074703 (2023).
3. \*Large magnetic-field-induced strains in sintered chromium tellurides: Y. Kubota, Y. Okamoto, T. Kanematsu, T. Yajima, D. Hirai and K. Takenaka, *Appl. Phys. Lett.* **122**, 042404 (2023).
4. Superconductivity induced by doping holes in the nodal-line semimetal NaAlGe: T. Ikenobe, T. Yamada, D. Hirai, H. Yamane and Z. Hiroi, *Phys. Rev. Materials* **7**, 104801 (2023).
5. Nonmagnetic Ground State in RuO<sub>2</sub> Revealed by Muon Spin Rotation: M. Hiraishi, H. Okabe, A. Koda, R. Kadono, T. Muroi, D. Hirai and Z. Hiroi, *Phys. Rev. Lett.* **132**, 166702 (2024).

## Kawashima group

We developed efficient methods, algorithms, parallelized programs, and sometimes new concepts, based on novel numerical techniques such as the tensor network (TN) method and quantum Monte Carlo (QMC). We then applied them to relevant physical problems. To list subjects of our research in 2023: (1) Classical spin systems with novel phase transitions and excitations [Okubo and Kawashima, *JPSJ*92; Tu, et al, *PRB*107; Watanabe, et al, *PTP*2023, *PRR*5], (2) Data-scientific approach to material design [Kavacs, et al, *Front.Mater.*9], (3) Development of open-source software for condensed matter calculations [Kurita, *CPC*292], (4) Down-folding method for strongly correlated electron systems such as superconductors [Ido, et al, *JPSJ*92]

1. \*Data Analysis of Ab initio Effective Hamiltonians in Iron-Based Superconductors — Construction of Predictors for Superconducting Critical Temperature: K. Ido, Y. Motoyama, K. Yoshimi and T. Misawa, *J. Phys. Soc. Jpn.* **92**, 064702(1-13) (2023).
2. Possibility of a Topological Phase Transition in Two-dimensional RP3 Model: T. Okubo and N. Kawashima, *J. Phys. Soc. Jpn.* **92**, 114701 (2023).
3. Cubic ferromagnet and emergent U(1) symmetry on its phase boundary: W.-L. Tu, X. Lyu, S. R. Ghazanfari, H.-K. Wu, H.-Y. Lee and N. Kawashima, *Phys. Rev. B* **107**(1-14) (2023).
4. \*Interface tool from Wannier90 to RESPACK: wan2respack: K. Kurita, T. Misawa, K. Yoshimi, K. Ido and T. Koretsune, *Comput. Phys. Commun.* **292**, 108854(1-7) (2023).
5. Non-monotonic behavior of the Binder parameter in discrete spin systems: H. Watanabe, Y. Motoyama, S. Morita and N. Kawashima, *Prog. Theor. Exp. Phys.* **2023**, 033A02 (2023).
6. Ashkin-Teller phase transition and multicritical behavior in a classical monomer-dimer model: S. Morita, H.-Y. Lee, K. Damle and N. Kawashima, *Physical Review Research* **5**, 043061(1-12) (2023).
7. Physics-informed machine learning combining experiment and simulation for the design of neodymium-iron-boron permanent magnets with reduced critical-elements content: A. Kovacs, J. Fischbacher, H. Oezelt, A. Kornell, Q. Ali, M. Gusenbauer, M. Yano, N. Sakuma, A. Kinoshita, T. Shoji, A. Kato, Y. Hong, S. Grenier, T. Devillers, N. M. Dempsey, T. Fukushima, H. Akai, N. Kawashima, T. Miyake and T. Schrefl, *Front. Mater.* **9**, 1094055 (2023).
8. †\*H-wave – A Python package for the Hartree-Fock approximation and the random phase approximation: T. Aoyama, K. Yoshimi, K. Ido, Y. Motoyama, T. Kawamura, T. Misawa, T. Kato and A. Kobayashi, *Computer Physics Communications* **298**, 109087(1-10) (2024).
9. †\*Update of HΦ : Newly added functions and methods in versions 2 and 3: K. Ido, M. Kawamura, Y. Motoyama, K. Yoshimi, Y. Yamaji, S. Todo, N. Kawashima and T. Misawa, *Comp. Phys. Commun.* **298**, 109093(1-15) (2024).

## Uwatoko group

MnP is found to be superconducting below ~ 1 K around 8 GPa. To elucidate the magnetic ground state adjacent to the superconducting phase first discovered in Mn-based materials, high-pressure neutron diffraction measurements have been performed at hydrostatic pressures up to 7.5 GPa. Combining the experimental and theoretical results, the details of exchange interactions

---

\* Joint research among groups within ISSP.

in the vicinity of the superconducting phase are described, which is critical to understanding the pairing mechanism of the unconventional superconductivity in MnP. The study of the iron-based superconductor, FeSe, has resulted in various interesting topics. We present the observation of spin fluctuations originating from Bogoliubov Fermi surfaces in the superconducting state via  $^{77}\text{Se}$ -nuclear magnetic resonance measurements to 100 mK. In S-substituted FeSe, an abnormal enhancement of low-energy spin fluctuations deep in the SC state is established, which cannot be explained by an impurity effect. The recently discovered  $\text{CsV}_3\text{Sb}_5$  is a new family of kagome superconductors with the superconducting transition temperature  $T_c$  of 2.5 K. Our results support that material is a non-chiral, anisotropic s-wave superconductor with no sign change both at ambient and under pressure.  $\text{CeNiC}_2$  features unique properties such as heavy fermionic behavior and multiple magnetic ordering. With applying pressure, a superconducting dome with a maximum  $T_c \sim 3.5$  K emerges in a narrow pressure range of around 11 GPa. We investigate its crystal structure from ambient pressure to 18.6 GPa via single crystal x-ray diffraction. The pressure dependence of unit-cell parameters reveals anisotropic linear compressibility  $\kappa$ , following  $|\kappa_a|$  ( $3.70 \times 10^{-3} \text{ GPa}^{-1}$ )  $>$   $|\kappa_c|$  ( $1.97 \times 10^{-3} \text{ GPa}^{-1}$ )  $>$   $|\kappa_b|$  ( $1.39 \times 10^{-3} \text{ GPa}^{-1}$ ), and a bulk modulus,  $B_0 \sim 134 \pm 3$  GPa. The directions of the first nearest and the second nearest neighbors between both the Ce-Ce and Ni-Ni atoms switch at  $\sim 7$  GPa. The 12442-type hybrid structure compound  $\text{BaTh}_2\text{Fe}_4\text{As}_4(\text{Na}_{0.7}\text{O}_{0.3})_2$  shows the superconducting transition at  $T_c^{\text{onset}} \sim 30$  K and  $T_c^{\text{zero}} \sim 20$  K. We found that  $T_c(P)$  exhibits a nonmonotonic variation with pressure, forming a dome-shaped superconducting temperature at optimal values of  $\sim 46$  K at 2.6 GPa. We have measured the high-pressure experiments of  $\text{La}_3\text{Ni}_2\text{O}_7$  polycrystalline samples. The constructed T-P phase diagram shares similar features with that of  $\text{La}_3\text{Ni}_2\text{O}_7$  crystals and reveals the close relationship between superconductivity, density wave order, and strange-metal-like behavior in this system.

1. Pressure-induced linear enhancement of the superconducting transition in  $\text{Nd}_{0.8}\text{Sr}_{0.2}\text{NiO}_2$  thin films: N. N. Wang, G. Wang, Q. Gao, K. Y. Chen, J. Hou, X. L. Ren, Y. Uwatoko, B. S. Wang, Z. H. Zhu, J. P. Sun and J.-G. Cheng, *J. Phys.: Condens. Matter* **36**, 125601(1-6) (2023).
2. Destabilization of Excitonic Phase by Elemental Substitution in  $(\text{Ta}_{1-x}\text{M}_x)_2\text{NiSe}_5$  ( $\text{M}=\text{V}, \text{Nb}$ ) and  $\text{Ta}_2(\text{Ni}_{1-y}\text{T}_y)\text{Se}_5$  ( $\text{T}=\text{Fe}, \text{Co}$ ): Y. Hirose, S. Sano, T. Hirahara, Y. Uwatoko, J. Gouchi, T. Takeuchi and R. Settai, *J. Phys. Soc. Jpn.* **92**, 084705(1-7) (2023).
3. Pressure-induced Structural Phase Transition and New Superconducting Phase in  $\text{UTe}_2$ : F. Honda, S. Kobayashi, N. Kawamura, S. I. Kawaguchi, T. Koizumi, Y. J. Sato, Y. Homma, N. Ishimatsu, J. Gouchi, Y. Uwatoko, H. Harima, J. Flouquet and D. Aoki, *J. Phys. Soc. Jpn.* **92**, 044702(1-10) (2023).
4. Pressure-Induced Structural Phase Transition in  $\text{Eu}_3\text{Bi}_2\text{S}_4\text{F}_4$ : K. Ishigaki, H. Ma, H.-F. Zhai, Y. Jing, H. Kobayashi and Y. Uwatoko, *J. Phys. Soc. Jpn.* **92**, 075001 (2023).
5. Atomic coordinates of  $\text{CeNiC}_2$  under pressure: Switching of the Ce-Ce first nearest neighbor direction: H. Ma, D. Bhoi, J. Gouchi, H. Sato, T. Shigeoka, J. -G. Cheng and Y. Uwatoko, *Phys. Rev. B* **108**, 064435(1-6) (2023).
6. Complex evolution of the magnetic transitions and unexpected absence of bulk superconductivity in chemically precompressed  $\text{NaMn}_6\text{Bi}_5$ : P. F. Shan, Q. X. Dong, P. T. Yang, L. Xu, Z. Y. Liu, L. F. Shi, N. N. Wang, J. P. Sun, Y. Uwatoko, G. F. Chen, B. S. Wang and J. -G. Cheng, *Phys. Rev. B* **107**, 094519(1-7) (2023).
7. Effect of hydrostatic pressure on the unconventional charge density wave and superconducting properties in two distinct phases of doped kagome superconductors  $\text{CsV}_{3-x}\text{Ti}_x\text{Sb}_5$ : J. Hou, K. Y. Chen, J. P. Sun, Z. Zhao, Y. H. Zhang, P. F. Shan, N. N. Wang, H. Zhang, K. Zhu, Y. Uwatoko, H. Chen, H. T. Yang, X. L. Dong, H. -J. Gao and J. -G. Cheng, *Phys. Rev. B* **107**, 144502(1-8) (2023).
8. Pressure-driven evolution of upper critical field and Fermi surface reconstruction in the strong-coupling superconductor  $\text{Ti}_4\text{Ir}_2\text{O}$ : L. Shi, B. Ruan, P. Yang, N. Wang, P. Shan, Z. Liu, J. Sun, Y. Uwatoko, G. Chen, Z. Ren, B. Wang and J. Cheng, *Phys. Rev. B* **107**, 174525(1-7) (2023).
9. \*Piston-cylinder cell made of Ni-Cr-Al alloy for magnetic susceptibility measurements under high pressures in pulsed high magnetic fields: K. Nihongi, T. Kida, Y. Narumi, N. Kurita, H. Tanaka, Y. Uwatoko, K. Kindo and M. Hagiwara, *Rev. Sci. Instrum.* **94**, 113903(1-7) (2023).
10. Magnetic ground state of  $\text{YbCo}_2\text{Zn}_{20}$  probed by muon spin relaxation: W. Higemoto, K. Satoh, T. U. Ito, K. Ohishi, Y. Saiga, M. Kosaka, K. Matsubayashi and Y. Uwatoko, *J. Phys.: Conf. Ser.* **2462**, 012039(1-5) (2023).
11. Pressure-enhanced superconducting transition in the inter-block-layer electron-transfer superconductor  $\text{BaTh}_2\text{Fe}_4\text{As}_4(\text{N}_{0.7}\text{O}_{0.3})_2$ : P. Shan, P. Yang, Y. Shao, Z. Liu, J. Hou, B. Wang, Y. Uwatoko, G. Cao, J. Sun and J. Cheng, *Phys. Rev. Materials* **7**, 124801(1-8) (2023).
12. Bulk evidence of anisotropic s-wave pairing with no sign change in the kagome superconductor  $\text{CsV}_3\text{Sb}_5$ : M. Roppongi, K. Ishihara, Y. Tanaka, K. Ogawa, K. Okada, S. Liu, K. Mukasa, Y. Mizukami, Y. Uwatoko, R. Grasset, M. Konczykowski, B. R. Ortiz, S. D. Wilson, K. Hashimoto and T. Shibauchi, *Nat Commun* **14**, 667(1-8) (2023).
13. \*Helical magnetic state in the vicinity of the pressure-induced superconducting phase in MnP: S. E. Dissanayake, M.

† Joint research with outside partners.

- Matsuda, K. Yoshimi, S. Kasamatsu, F. Ye, S. Chi, W. Steinhardt, G. Fabbri, S. Haravifard, J. Cheng, J. Yan, J. Gouchi and Y. Uwatoko, *Phys. Rev. Research* **5**, 043026(1-13) (2023).
- Spin fluctuations from Bogoliubov Fermi surfaces in the superconducting state of S-substituted FeSe: Z. Yu, K. Nakamura, K. Inomata, X. Shen, T. Mikuri, K. Matsuura, Y. Mizukami, S. Kasahara, Y. Matsuda, T. Shibauchi, Y. Uwatoko and N. Fujiwara, *Commun Phys* **6**, 175(1-6) (2023).
  - Emergence of High-Temperature Superconducting Phase in Pressurized  $\text{La}_3\text{Ni}_2\text{O}_7$  Crystals: J. Hou, P.-T. Yang, Z.-Y. Liu, J.-Y. Li, P.-F. Shan, L. Ma, G. Wang, N.-N. Wang, H.-Z. Guo, J.-P. Sun, Y. Uwatoko, M. Wang, G.-M. Zhang, B.-S. Wang and J.-G. Cheng, *Chinese Phys. Lett.* **40**, 117302(1-6) (2023).
  - Pressure-induced Superconductivity in  $\text{BiS}_2$ -based Superconductors  $\text{Eu}_2\text{SrBi}_2\text{S}_{2.5}\text{Se}_{1.5}\text{F}_4$ : K. Ishigaki, J. Gouchi, K. Torizuka, S. Arumugam, A. K. Ganguli, Z. Haque, K. Ganesan, G. S. Thakur and Y. Uwatoko, *J. Phys. Soc. Jpn.* **93**, 024706(1-4) (2024).
  - From semiconductor to Fermi metal and emergent density-wave-like transition in the quasi-one-dimensional  $n$ -type  $\text{Bi}_{19}\text{S}_{27}\text{I}_3$  under hydrostatic pressure: S. Xu, Z. Liu, P. Yang, B. Ruan, Z. Ren, J. Sun, Y. Uwatoko, B. Wang and J. Cheng, *Phys. Rev. B* **109**, 144107(1-10) (2024).
  - Quantum criticality in  $\text{YbCu}_4\text{Ni}$ : K. Osato, T. Taniguchi, H. Okabe, T. Kitazawa, M. Kawamata, Z. Hongfei, Y. Ikeda, Y. Nambu, D. P. Sari, I. Watanabe, J. G. Nakamura, A. Koda, J. Gouchi, Y. Uwatoko and M. Fujita, *Phys. Rev. B* **109**, 024435(1-6) (2024).
  - Pressure-Induced Superconductivity In Polycrystalline  $\text{La}_3\text{Ni}_2\text{O}_{7-\delta}$ : G. Wang, N. N. Wang, X. L. Shen, J. Hou, L. Ma, L. F. Shi, Z. A. Ren, Y. D. Gu, H. M. Ma, P. T. Yang, Z. Y. Liu, H. Z. Guo, J. P. Sun, G. M. Zhang, S. Calder, J. Q. Yan, B. S. Wang, Y. Uwatoko and J. -G. Cheng, *Phys. Rev. X* **14**, 011040(1-8) (2024).
  - Pressure Effect on the Magnetic Properties of the Heusler Alloy  $\text{Co}_2\text{NbGa}$ : Y. Adachi, Y. Ogi, T. Osaki, T. Eto, T. Kihara, H. Nishihara, T. Sakon, J. Gouchi, Y. Uwatoko and T. Kanomata, *J Supercond Nov Magn* **37**, 249-254 (2024).

## Ozaki group

For more than last 5 years, we have been collaborating with the Sugimoto laboratory in the graduate school of frontier sciences, the University of Tokyo to unveil surface structures and their electronic structures of silicene and diamond surface, which have been investigated by scanning tunneling microscopy (STM) and atomic force microscopy (AFM). Our role in the collaboration is to theoretically understand their experimental observation by making use of first-principles calculations. We have established computational schemes to calculate the force spectroscopy, in which perpendicular forces acting on model tips consisting of silicon atoms and the surfaces are directly calculated, and compared calculated force spectroscopy data with the experimental data. The comparison leads to excellent agreement with the experimentally data not only qualitatively and but also quantitatively. In the fiscal year, our special focus was to investigate detailed structures of Si adatoms on silicene on  $\text{Ag}(111)$  surface and the surface structures of diamond(001). These studies provided clear pictures for the thermodynamic energetics of the surface structures, and an evidence that the high resolution of AFM image in the experiments should be attributed to bond formation between the tip and surface atoms which is far from the non-contact regime.

- <sup>†\*</sup>Ambipolar Nickel Dithiolene Complex Semiconductors: From One- to Two-Dimensional Electronic Structures Based upon Alkoxy Chain Lengths: M. Ito, T. Fujino, L. Zhang, S. Yokomori, T. Higashino, R. Makiura, K. J. Takeno, T. Ozaki and H. Mori, *J. Am. Chem. Soc.* **145**, 2127-2134 (2023).
- <sup>†\*</sup>Metallic State of a Mixed-Sequence Oligomer Salt That Models Doped PEDOT Family: K. Onozuka, T. Fujino, R. Kameyama, S. Dekura, K. Yoshimi, T. Nakamura, T. Miyamoto, T. Yamakawa, H. Okamoto, H. Sato, T. Ozaki and H. Mori, *J. Am. Chem. Soc.* **145**, 15152-15161 (2023).
- Atomically thin metallic Si and Ge allotropes with high Fermi velocities: C. -E. Hsu, Y. -T. Lee, C. -C. Wang, C. -Y. Lin, Y. Yamada-Takamura, T. Ozaki and C. -C. Lee, *Physical Review B* **107**, 115410 (2023).
- Atomic arrangement of Si adatom on the Silicene/ $\text{Ag}(111)$  surface: Y. Adachi, R. Zhang, X. Wang, M. Fukuda, T. Ozaki and Y. Sugimoto, *Applied Surface Science* **630**, 157336 (2023).
- <sup>\*</sup>Hydrogen - induced Sulfur Vacancies on the  $\text{MoS}_2$  Basal Plane Studied by Ambient Pressure XPS and DFT Calculations: F. Ozaki, S. Tanaka, Y. Choi, W. Osada, K. Mukai, M. Kawamura, M. Fukuda, M. Horio, T. Koitaya, S. Yamamoto, I. Matsuda, T. Ozaki and J. Yoshinobu, *ChemPhysChem* **24**, e202300477 (2023).

## Noguchi group

We have studied (1) microphase separation with checkerboard and kagome lattice patterns induced by the binding of curvature-

---

\* Joint research among groups within ISSP.

inducing proteins onto both sides of a membrane, (2) excitable waves on a deformable membrane tube, (3) estimation of anisotropic bending coefficients of crescent proteins from experimental data, and (4) the effects of interfacial tension of phase boundary on membrane rupture.

1. Phase-Separated Giant Liposomes for Stable Elevation of  $\alpha$ -Hemolysin Concentration in Lipid Membranes: M. Kobayashi, H. Noguchi, G. Sato, C. Watanabe, K. Fujiwara and M. Yanagisawa, *Langmuir* **39**, 11481-11489 (2023).
2. Estimation of anisotropic bending rigidities and spontaneous curvatures of crescent curvature-inducing proteins from tethered-vesicle experimental data: H. Noguchi, N. Walani and M. Arroyo, *Soft Matter* **19**, 5300-5310 (2023).
3. Membrane domain formation induced by binding/unbinding of curvature-inducing molecules on both membrane surfaces: H. Noguchi, *Soft Matter* **19**, 679-688 (2023).
4. Disappearance, division, and route change of excitable reaction-diffusion waves in deformable membranes: H. Noguchi, *Sci Rep* **13**, 6207(1-8) (2023).
5. Curvature sensing of curvature-inducing proteins with internal structure: H. Noguchi, *Phys. Rev. E* **109**, 024403/1-10 (2024).

## Yoshimi group

We have developed and enhanced the usability of programs adopted in the project for advancement of software usability in materials science (PASUMS). Our group's activity of 2023 include functional and usability enhancement of (1) TeNeS and making new tools (2) cif2x and Moller. We published five papers about the developed software packages (abICS, H-wave, and H $\phi$ ) in PASUMS. In addition, using the software packages developed by PASUMS, we have studied electronic properties of organic conductors such as  $\alpha$ -(BEDT-TTF)<sub>2</sub>I<sub>3</sub>,  $\alpha$ -(BEDT-TSeF)<sub>2</sub>I<sub>3</sub>, and TM salts.

1. \*Data Analysis of Ab initio Effective Hamiltonians in Iron-Based Superconductors — Construction of Predictors for Superconducting Critical Temperature: K. Ido, Y. Motoyama, K. Yoshimi and T. Misawa, *J. Phys. Soc. Jpn.* **92**, 064702(1-13) (2023).
2. †\*Gap opening mechanism for correlated Dirac electrons in organic compounds  $\alpha$ -(BEDT-TTF)<sub>2</sub>I<sub>3</sub> and  $\alpha$ -(BEDT-TSeF)<sub>2</sub>I<sub>3</sub>: D. Ohki, K. Yoshimi, A. Kobayashi and T. Misawa, *Phys. Rev. B* **107**, L041108(1-6) (2023).
3. †\*Comprehensive Ab Initio Investigation of the Phase Diagram of Quasi-One-Dimensional Molecular Solids: K. Yoshimi, T. Misawa, T. Tsumuraya and H. Seo, *Phys. Rev. Lett.* **131**, 036401(1-7) (2023).
4. †\*Metallic State of a Mixed-Sequence Oligomer Salt That Models Doped PEDOT Family: K. Onozuka, T. Fujino, R. Kameyama, S. Dekura, K. Yoshimi, T. Nakamura, T. Miyamoto, T. Yamakawa, H. Okamoto, H. Sato, T. Ozaki and H. Mori, *J. Am. Chem. Soc.* **145**, 15152-15161 (2023).
5. †\*Precise Control of the Molecular Arrangement of Organic Semiconductors for High Charge Carrier Mobility: R. Akai, K. Oka, S. Dekura, K. Yoshimi, H. Mori, R. Nishikubo, A. Saeki and N. Tohrai, *J. Phys. Chem. Lett.* **14**, 3461 (2023).
6. \*Interface tool from Wannier90 to RESPACK: wan2respack: K. Kurita, T. Misawa, K. Yoshimi, K. Ido and T. Koretsune, *Comput. Phys. Commun.* **292**, 108854(1-7) (2023).
7. \*Helical magnetic state in the vicinity of the pressure-induced superconducting phase in MnP: S. E. Dissanayake, M. Matsuda, K. Yoshimi, S. Kasamatsu, F. Ye, S. Chi, W. Steinhardt, G. Fabbris, S. Haravifard, J. Cheng, J. Yan, J. Gouchi and Y. Uwatoko, *Phys. Rev. Research* **5**, 043026(1-13) (2023).
8. sparse-ir: Optimal compression and sparse sampling of many-body propagators: M. Wallerberger, S. Badr, S. Hoshino, S. Huber, F. Kakizawa, T. Koretsune, Y. Nagai, K. Nogaki, T. Nomoto, H. Mori, J. Otsuki, S. Ozaki, T. Plaikner, R. Sakurai, C. Vogel, N. Witt, K. Yoshimi and H. Shinaoka, *SoftwareX* **21**, 101266 (2023).
9. †Configuration sampling in multi-component multi-sublattice systems enabled by ab Initio Configuration Sampling Toolkit (abICS): S. Kasamatsu, Y. Motoyama, K. Yoshimi and T. Aoyama, *Science and Technology of Advanced Materials: Methods* **3**, 2284128 (2023).
10. †\*Compensated Ferrimagnets with Colossal Spin Splitting in Organic Compounds: T. Kawamura, K. Yoshimi, K. Hashimoto, A. Kobayashi and T. Misawa, *Phys. Rev. Lett.* **132**, 156502(1-6) (2024).
11. †\*Sub-photon accuracy noise reduction of a single shot coherent diffraction pattern with an atomic model trained autoencoder: T. Ishikawa, Y. Takeo, K. Sakurai, K. Yoshinaga, N. Furuya, Y. Inubushi, K. Tono, Y. Joti, M. Yabashi, T. Kimura and K. Yoshimi, *Opt. Express* **32**, 18301 (2024).
12. †\*H-wave – A Python package for the Hartree-Fock approximation and the random phase approximation: T. Aoyama, K.

---

† Joint research with outside partners.

Yoshimi, K. Ido, Y. Motoyama, T. Kawamura, T. Misawa, T. Kato and A. Kobayashi, *Computer Physics Communications* **298**, 109087(1-10) (2024).

13. †\*Orbital hybridization of donor and acceptor to enhance the conductivity of mixed-stack complexes: T. Fujino, R. Kameyama, K. Onozuka, K. Matsuo, S. Dekura, T. Miyamoto, Z. Guo, H. Okamoto, T. Nakamura, K. Yoshimi, S. Kitou, T.-H. Arima, H. Sato, K. Yamamoto, A. Takahashi, H. Sawa, Y. Nakamura and H. Mori, *Nat Commun* **15**, 3028 (2024).
14. †\*Update of HΦ : Newly added functions and methods in versions 2 and 3: K. Ido, M. Kawamura, Y. Motoyama, K. Yoshimi, Y. Yamaji, S. Todo, N. Kawashima and T. Misawa, *Comp. Phys. Commun.* **298**, 109093(1-15) (2024).

## Okamoto group

The discovery of a new material has a potential to trigger the evolution of condensed matter physics. We aim at discovering new materials of crystalline solids that exhibit novel quantum phenomena and innovative electronic functions. In this year, we reported the results of our research on new superconductors  $\text{Sc}_6\text{MTe}_2$ ,  $\text{Zr}_6\text{MTe}_2$ ,  $\text{ScPdGe}$ , and  $\text{ScPdSi}$ , where M is transition metal elements, and a frustrated spin system  $\text{NaLnTe}_2$ . In these materials,  $\text{Sc}_6\text{MTe}_2$  is a unique  $d$ -electron superconducting family incorporating  $3d$ ,  $4d$ , and  $5d$  electrons systems. The critical temperatures  $T_c$  for  $M = 3d$  elements are higher than those for  $4d$  and  $5d$  elements and increase in the order of  $M = \text{Ni}$ ,  $\text{Co}$ , and  $\text{Fe}$  with the highest  $T_c$  of 4.7 K in  $\text{Sc}_6\text{FeTe}_2$ , suggesting that the Fe  $3d$  electrons play important roles in realizing the highest  $T_c$ . On the other hand,  $\text{Sc}_6\text{OsTe}_2$  and  $\text{Sc}_6\text{IrTe}_2$  show a superconductivity with a high upper critical field  $H_{c2}$  violating the Pauli limit, caused by the strong spin-orbit coupling of Os and Ir  $5d$  electrons. It is rare that such  $3d$  and  $5d$  electron features play major roles in an isostructural  $d$ -electron superconductor family.

1. †\*Structural and Electronic Properties of a Triangular Lattice Magnet  $\text{NaPrTe}_2$  Compared with  $\text{NaNdTe}_2$  and  $\text{NaTbTe}_2$ : K. Eto, Y. Okamoto, N. Katayama, H. Ishikawa, K. Kindo and K. Takenaka, *J. Phys. Soc. Jpn.* **92**, 094707(1-6) (2023).
2. Superconductivity in Ternary Scandium Telluride  $\text{Sc}_6\text{MTe}_2$  with  $3d$ ,  $4d$ , and  $5d$  Transition Metals: Y. Shinoda, Y. Okamoto, Y. Yamakawa, H. Matsumoto, D. Hirai and K. Takenaka, *J. Phys. Soc. Jpn.* **92**, 103701(1-5) (2023).
3. クロム化合物磁性体における磁場誘起歪: 岡本 佳比古, 竹中 康司, *固体物理* **58**, 273-282 (2023).
4. \*Large magnetic-field-induced strains in sintered chromium tellurides: Y. Kubota, Y. Okamoto, T. Kanematsu, T. Yajima, D. Hirai and K. Takenaka, *Appl. Phys. Lett.* **122**, 042404 (2023).
5. †\*Signatures of a magnetic superstructure phase induced by ultrahigh magnetic fields in a breathing pyrochlore antiferromagnet: M. Gen, A. Ikeda, K. Aoyama, H. O. Jeschke, Y. Ishii, H. Ishikawa, T. Yajima, Y. Okamoto, X. Zhou, D. Nakamura, S. Takeyama, K. Kindo, Y. H. Matsuda and Y. Kohama, *Proc. Natl. Acad. Sci. U.S.A.* **120**, e2302756120(1-7) (2023).
6. Superconductivity in Ternary Germanide  $\text{ScPdGe}$  and Silicide  $\text{ScPdSi}$ : Y. Shinoda, Y. Okamoto, Y. Yamakawa, H. Takatsu, H. Kageyama, D. Hirai and K. Takenaka, *J. Phys. Soc. Jpn.* **93**, 023701(1-4) (2024).
7. Superconductivity in Ternary Zirconium Telluride  $\text{Zr}_6\text{MTe}_2$  with  $3d$  Transition Metals: H. Matsumoto, Y. Yamakawa, R. Okuma, D. Nishio-Hamane and Y. Okamoto, *J. Phys. Soc. Jpn.* **93**, 023705(1-5) (2024).
8. †Anisotropic Optical Conductivity Accompanied by a Small Energy Gap in One-Dimensional Thermoelectric Telluride  $\text{Ta}_4\text{SiTe}_4$ : F. Matsunaga, Y. Okamoto, Y. Yokoyama, K. Takehana, Y. Imanaka, Y. Nakamura, H. Kishida, S. Kawano, K. Matsuhira and K. Takenaka, *Phys. Rev. B* **109**, L161105(1-6) (2024).
9. 1次元ファンデルワールス結晶  $\text{Ta}_4\text{SiTe}_4$  における熱電効果: 岡本 佳比古, 山川 洋一, 竹中 康司, *固体物理* **59**, 95-105 (2024).
10. クロムテルル化物焼結体に現れる巨大な磁場誘起体積変化: 岡本 佳比古, 竹中 康司, *FC Report* **42**, 7-12 (2024).

## Yamaura group

Our laboratory started in 2023, and this year we used quantum beams to determine the structures of various materials from basic to applied sciences, including magnetic nanowires, novel ferroelectrics, novel high dielectrics, novel thermoelectric materials, magnetic thin films, nodal line semimetals, and more. Moreover, the joint use operation of the X-Ray Diffraction Section at the Materials Design and Characterization Laboratory (MDCL) is progressing smoothly, providing not only user support to various users inside and outside the institute, but also analytical advice, new research proposals, and even paths to quantum beam applications. In addition, the radiation safety laboratory was operated to educate and control radiation workers at the facility, control nuclear fuel materials, and conduct periodic inspections of X-ray generators.

1. \*Distinctive doping dependence of upper critical field in iron-based superconductor  $\text{LaFeAsO}_{1-x}\text{H}_x$ : S. Kawachi, J.-I.

---

\* Joint research among groups within ISSP.

- Yamaura, Y. Kuramoto, S. Iimura, T. Nomura, Y. Kohama, T. Sasaki, M. Tokunaga, Y. Murakami and H. Hosono, *Phys. Rev. B* **108**, L100503(1-5) (2023).
- \*Local spin dynamics in the geometrically frustrated Mo pyrochlore antiferromagnet  $\text{Lu}_2\text{Mo}_2\text{O}_5\text{-yN}_2$ : S. K. Dey, K. Ishida, H. Okabe, M. Hiraishi, A. Koda, T. Honda, J. Yamaura, H. Kageyama and R. Kadono, *Phys. Rev. B* **107**, 024407 (2023).
  - \* $J_{\text{eff}}=1/2$  Hyperoctagon Lattice in Cobalt Oxalate Metal-Organic Framework: H. Ishikawa, S. Imajo, H. Takeda, M. Kakegawa, M. Yamashita, J.-I. Yamaura and K. Kindo, *Phys. Rev. Lett.* **132**, 156702 (2024).
  - Phonon drag thermopower persisting over 200 K in  $\text{FeSb}_2$  thin film on  $\text{SrTiO}_3$  single crystal: C. Yamamoto, X. He, K. Hanzawa, T. Katase, M. Sasase, J.-I. Yamaura, H. Hiramatsu, H. Hosono and T. Kamiya, *Appl. Phys. Lett.* **124**, 193902 (2024).
  - †\*Crystal structure and properties of perovskite-type rubidium niobate, a high-pressure phase of  $\text{RbNbO}_3$ : A. Yamamoto, K. Murase, T. Sato, K. Sugiyama, T. Kawamata, Y. Inaguma, J.-I. Yamaura, K. Shitara, R. Yokoi and H. Moriwake, *Dalton Trans.* **53**, 7044 (2024).

## Neutron Science Laboratory

### Yamamuro group

Our laboratory is studying chemical physics of complex condensed matters by using neutron scattering, X-ray diffraction, calorimetric, dielectric, and viscoelastic techniques. Our target materials are glasses, liquids, and various disordered systems. In 2023, we have measured the heat capacities of vapor-deposited  $\text{H}_2\text{O}$  and  $\text{CS}_2$  by using a custom-made adiabatic calorimeter. Their heat capacities were consistent with the inelastic neutron scattering data obtained before. We have also measured the X-ray (BL04B2@SPRING-8) and neutron (BL21@J-PARC) diffractions and quasielastic neutron scattering (AGNES@JRR-3) data of vapor-deposited amorphous methane hydrate. These data revealed that methane molecules are accommodated in cage-like spaces in an amorphous structure, and they exhibit a classical rotation at higher temperatures and a quantum (tunneling) rotation at lower temperatures. The quasielastic neutron scattering using AGNES@JRR-3 and BL02@J-PARC were conducted also for a typical metal-organic framework MOF-101 including acetonitrile molecules and  $\text{Mg}(\text{TFSI})_2$  in the pores. This material is a good candidate of future solid batteries because of its higher volumetric capacity than lithium-ion batteries and the abundance of Mg. The motion of acetonitrile molecules was quite high, being associated with the high mobility of Mg ions.

- Nanoscale structure of a hybrid aqueous–nonaqueous electrolyte: M. -L. Saboungi, O. Borodin, D. Price, B. Farago, M. A. González, S. Kohara, L. Mangin-Thro, A. Wildes and O. Yamamuro, *J. Chem. Phys.* **158**, 124502 (2023).
- Quasielastic Neutron Scattering Study on Thermal Gelation in Aqueous Solution of Agarose: N. Onoda-Yamamuro, Y. Inamura and O. Yamamuro, *Gels* **9(11)**, 879 (2023).
- Reversible Transition between Discrete and 1D Infinite Architectures: A Temperature-Responsive Cu(I) Complex with a Flexible Disilane-Bridged Bis(pyridine) Ligand: Y. Zhao, T. Nakae, S. Takeya, M. Hattori, D. Saito, M. Kato, Y. Ohmasa, S. Sato, O. Yamamuro, T. Galica, E. Nishibori, S. Kobayashi, T. Seki, T. Yamada and Y. Yamanoi, *Chemistry-A European Journal* **29**, e202204002 (8 pages) (2023).
- The phase diagram of the API benzocaine and its highly persistent, metastable crystalline polymorphs: I. B. Rietveld, H. Akiba, O. Yamamuro, M. D. Barrio, R. Céolin and J. L. Tamarit, *Pharmaceutics* **15**, 1549 (17 pages) (2023).
- Ice-Like Dynamics of Water Clusters: K. Oka, H. Akiba, N. Tohnai, T. Shibue and O. Yamamuro, *J. Phys. Chem. Lett.* **15**, 267-271 (2024).
- Non-Newtonian Dynamics in Water-in-Salt Electrolytes: T. Yamaguchi, A. Dukhin, Y. -J. Ryu, D. Zhang, O. Borodin, M. A. González, O. Yamamuro, D. L. Price and M. -L. Saboungi, *J. Phys. Chem. Lett.* **15**, 76-80 (2024).
- 熱測定と中性子散乱による複雑凝縮系の物性研究：山室 修，熱測定 **50(3)**, 89-95 (2023).

### Masuda group

The goal of our research is to discover a new quantum phenomenon and to reveal the mechanism of it. In this fiscal year we studied the following topics; Inelastic neutron scattering in the weakly coupled triangular spin tube candidate  $\text{CsCrF}_4$ , Magnetic structure of the magnetoelectric material  $\text{Ba}_2\text{MnGe}_2\text{O}_7$ , Spin excitation in the coupled honeycomb lattice compound  $\text{Ni}_2\text{InSbO}_6$ , Magnetic Resonance in the Quasi-2D Square Lattice Easy-Plane Antiferromagnet  $\text{Ba}_2\text{MnGe}_2\text{O}_7$ , and so on.

---

† Joint research with outside partners.

1. Inelastic neutron scattering in the weakly coupled triangular spin tube candidate CsCrF<sub>4</sub>: H. Kikuchi, S. Asai, H. Manaka, M. Hagihala, S. Itoh and T. Masuda, *Phys. Rev. B* **107**, 184405(1-8) (2023).
2. Magnetic structure of the magnetoelectric material Ba<sub>2</sub>MnGe<sub>2</sub>O<sub>7</sub>: A. Sazonov, H. Thoma, R. Dutta, M. Meven, A. Gukasov, R. Fittipaldi, V. Granata, T. Masuda, B. Nafradi and V. Hutnanu, *Phys. Rev. B* **108**, 094412(1-8) (2023).
3. Spin excitation in the coupled honeycomb lattice compound Ni<sub>2</sub>InSbO<sub>6</sub>: Z. Liu, Y. Araki, T.-H. Arima, S. Itoh, S. Asai and T. Masuda, *Phys. Rev. B* **107**, 064428(1-8) (2023).
4. Magnetic Resonance in the Quasi-2D Square Lattice Easy-Plane Antiferromagnet Ba<sub>2</sub>MnGe<sub>2</sub>O<sub>7</sub>: V. N. Glazkov, Yu. V. Krasnikova, I. K. Rodygina, M. Hemmida, M. Hirrle, H. -A. Krug von Nidda and T. Masuda, *J. Exp. Theor. Phys.* **137**, 542-554 (2023).
5. Magnetic Excitations of the Spin-Chain Compound Tb<sub>3</sub>RuO<sub>7</sub>: M. Hase, A. Donni, V. Yu. Pomjakushin, K. Nawa, D. Okuyama, T. J. Sato, S. Asai and T. Masuda, *JPS Conf. Proc.* **38**, 011129(1-5) (2023).
6. Q-dependent electron-phonon coupling induced phonon softening and non-conventional critical behavior in the CDW superconductor LaPt<sub>2</sub>Si<sub>2</sub>: E. Nocerino, U. Stuhr, I. San Lorenzo, F. Mazza, D. G. Mazzone, J. Hellsvik, S. Hasegawa, S. Asai, T. Masuda, S. Itoh, A. Minelli, Z. Hossain, A. Thamizhavel, K. Lefmann, Y. Sassa and M. Månsson, *Journal of Science: Advanced Materials and Devices* **8**, 100621(1-10) (2023).
7. A New Inelastic Neutron Spectrometer HODACA: H. Kikuchi, S. Asai, T. J. Sato, T. Nakajima, L. Harriger, I. Zaliznyak and T. Masuda, *J. Phys. Soc. Jpn.* **93**, 091004(1-11) (2024).
8. Inelastic neutron scattering studies on the eight-spin zigzag-chain compound KCu<sub>4</sub>P<sub>3</sub>O<sub>12</sub> : Confirmation of the validity of a data-driven technique based on machine learning: M. Hase, R. Tamura, K. Hukushima, S. Asai, T. Masuda, S. Itoh and A. Dönni, *Phys. Rev. B* **109**, 094434(1-8) (2024).
9. Neutron scattering study on dimerized 4f1 intermetallic compound Ce<sub>5</sub>Si<sub>3</sub>: D. Ueta, Y. Iwata, R. Kobayashi, K. Kuwahara, T. Masuda and S. Itoh, *Phys. Rev. B* **109**, 205127(1-8) (2024).
10. \*Sample Environment of the HRC Spectrometer at J-PARC: D. Ueta, S. Itoh, T. Masuda, T. Yokoo, T. Nakajima, S. Asai, H. Saito, D. Kawana, R. Sugiura, T. Asami, S. Yamauchi, S. Torii, Y. Ihata and H. Tanino, *JPS Conf. Proc.* **41**, 011008(1-5) (2024).
11. Field control of quasiparticle decay in a quantum antiferromagnet: S. Hasegawa, H. Kikuchi, S. Asai, Z. Wei, B. Winn, G. Sala, S. Itoh and T. Masuda, *Nat Commun* **15**, 125(1-7) (2024).
12. Spin Dynamics in Equilateral Triangular Spin Tube Material CsCrF<sub>4</sub>: H. Kikuchi, S. Asai, H. Manaka, M. Hagihala, S. Itoh and T. Masuda, *Neutron News* **35**, 13-14 (2024).

## Nakajima group

Nakajima group is studying magnetic materials with cross-correlated phenomena associated with the symmetry of the magnetic structures by means of neutron and X-ray scattering techniques. We are also responsible for a polarized-neutron triple-axis neutron spectrometer PONTA in the research reactor JRR-3 in Tokai, which restarted in 2021 after the long shutdown since the east Japan great earthquake in 2011. As the instrument team of PONTA, we have been supporting the users of the joint-use program, and have collaborated in their researches. One of the successful experiments at PONTA in the fiscal year of 2023 is the observation of the incommensurate magnetic modulation associated the charge density wave in UPt<sub>2</sub>Si<sub>2</sub>. Prof. Amitsuka's group in the Hokkaido university grew single crystal of this compound, which was known to exhibit a commensurate antiferromagnetic (AF) order and incommensurate charge density wave (CDW). They found that the commensurate AF order was affected by the CDW, and that the incommensurate magnetic modulations appear below the transition temperature. By utilizing the polarized neutron scattering technique, they successfully observed incommensurate magnetic reflections appearing at the same position as nuclear superlattice reflection associated with the CDW. Nakajima group is also working on developing new neutron scattering techniques in extreme conditions. Since 2019, we have been collaborating with Prof. Kohama's group in IMGSL of ISSP to realize stroboscopic neutron diffraction in long pulsed magnetic fields. We recently employed this technique to explore field induced magnetic phases in a triangular lattice antiferromagnet CuFe<sub>1-x</sub>Ga<sub>x</sub>O<sub>2</sub>. We are planning to apply this technique to various magnetic materials in the future.

1. †Direct observations of spin fluctuations in hedgehog–anti-hedgehog spin lattice states in MnSi<sub>1-x</sub>Ge<sub>x</sub> (x = 0.6 and 0.8) at zero magnetic field: S. Aji, T. Oda, Y. Fujishiro, N. Kanazawa, H. Saito, H. Endo, M. Hino, S. Itoh, T.-H. Arima, Y. Tokura and T. Nakajima, *Phys. Rev. B* **108**, 054445 (2023).
2. †In-plane anisotropy of single-q and multiple-q ordered phases in the antiferromagnetic metal CeRh<sub>2</sub>Si<sub>2</sub>: H. Saito, F. Kon, H. Hidaka, H. Amitsuka, C. Kwanghee, M. Hagihala, T. Kamiyama, S. Itoh and T. Nakajima, *Phys. Rev. B* **108**, 094440 (2023).

---

\* Joint research among groups within ISSP.

3. †Polarized neutron scattering study of the centrosymmetric skyrmion host material Gd<sub>2</sub>PdSi<sub>3</sub>: J. Ju, H. Saito, T. Kurumaji, M. Hirschberger, A. Kikkawa, Y. Taguchi, T.-H. Arima, Y. Tokura and T. Nakajima, *Phys. Rev. B* **107**, 024405 (2023).
4. †Colossal negative magnetoresistance in field-induced Weyl semimetal of magnetic half-Heusler compound: K. Ueda, T. Yu, M. Hirayama, R. Kurokawa, T. Nakajima, H. Saito, M. Kriener, M. Hoshino, D. Hashizume, T.-H. Arima, R. Arita and Y. Tokura, *Nat Commun* **14**, 6339 (2023).
5. \*Spontaneous topological Hall effect induced by non-coplanar antiferromagnetic order in intercalated van der Waals materials: H. Takagi, R. Takagi, S. Minami, T. Nomoto, K. Ohishi, M. -T. Suzuki, Y. Yanagi, M. Hirayama, N. D. Khanh, K. Karube, H. Saito, D. Hashizume, R. Kiyonagi, Y. Tokura, R. Arita, T. Nakajima and S. Seki, *Nat. Phys.* **19**, 961-968 (2023).
6. †Crystal electric field level scheme leading to giant magnetocaloric effect for hydrogen liquefaction.: N. Terada, H. Mamiya, H. Saito, T. Nakajima, T. D. Yamamoto, K. Terashima, H. Takeya, O. Sakai, S. Itoh, Y. Takano, M. Hase and H. Kitazawa, *Commun. Mater.* **4**, 13 (2023).
7. †Polarized and Unpolarized Neutron Scattering for Magnetic Materials at the Triple-axis Spectrometer PONTA in JRR-3: T. Nakajima, H. Saito, N. Kobayashi, T. Kawasaki, T. Nakamura, H. Kawano-Furukawa, S. Asai and T. Masuda, *J. Phys. Soc. Jpn.* **93**, 091002 (2024).
8. †Polarized Neutron Diffraction Study on UPt<sub>2</sub>Si<sub>2</sub>: F. Kon, C. Tabata, H. Saito, T. Nakajima, H. Hidaka, T. Yanagisawa and H. Amitsuka, *J. Phys. Soc. Jpn.* **93**, 044701 (2024).
9. Development of Polarization Analysis at TAIKAN under Magnetic Field at Low Temperature: T. Morikawa, K. Ohishi, K. Hiroi, Y. Kawamura, S.-I. Takata, J.-I. Suzuki and T. Nakajima, *JPS Conf. Proc.* **41**, 011012 (2024).
10. \*Sample Environment of the HRC Spectrometer at J-PARC: D. Ueta, S. Itoh, T. Masuda, T. Yokoo, T. Nakajima, S. Asai, H. Saito, D. Kawana, R. Sugiura, T. Asami, S. Yamauchi, S. Torii, Y. Ihata and H. Tanino, *JPS Conf. Proc.* **41**, 011008(1-5) (2024).
11. †Non-coplanar helimagnetism in the layered van-der-Waals metal DyTe<sub>3</sub>: S. Akatsuka, S. Esser, S. Okumura, R. Yambe, R. Yamada, M. M. Hirschmann, S. Aji, J. S. White, S. Gao, Y. Onuki, T.-H. Arima, T. Nakajima and M. Hirschberger, *Nat Commun* **15**, 4291 (2024).
12. Stroboscopic time-of-flight neutron diffraction in long pulsed magnetic fields: T. Nakajima, M. Watanabe, Y. Inamura, K. Matsui, T. Kanda, T. Nomoto, K. Ohishi, Y. Kawamura, H. Saito, H. Tamatsukuri, N. Terada and Y. Kohama, *Phys. Rev. Research* **6**, 023109 (2024).
13. †Multistep topological transitions among meron and skyrmion crystals in a centrosymmetric magnet: H. Yoshimochi, R. Takagi, J. Ju, N. D. Khanh, H. Saito, H. Sagayama, H. Nakao, S. Itoh, Y. Tokura, T. Arima, S. Hayami, T. Nakajima and S. Seki, *Nat. Phys.* **20**, 1001-1008 (2024).

## Mayumi group

For separator membranes of flexible batteries, mechanical stiffness (high Young's modulus) and toughness (high fracture energy) are required. Mayumi group has successfully developed tough and stiff ion gels using phase separation and strain-induced crystallization. In addition, we have investigated network structure of polysaccharide hydrogels for food applications by using SANS. The rigidity and size of chain aggregates dominate their macroscopic rheological properties.

1. Epoxy resins containing epoxy-modified polyrotaxanes: A. Hanafusa, S. Ando, T. Yuge, S. Ozawa, M. Ito, R. Hasegawa, H. Yokoyama, K. Mayumi and K. Ito, *Polymer* **278**, 126007 (2023).
2. †Elaborating Spatiotemporal Hierarchical Structure of Carrageenan Gels and Their Mixtures during Sol–Gel Transition: L. C. Geonzon, K. Hashimoto, T. Oda, S. Matsukawa and K. Mayumi, *Macromolecules* **56**, 8676 (2023).
3. Fabrication of Polyelectrolyte Sheets of Unimolecular Thickness via MOF-Templated Polymerization: A. Nishijima, Y. Hayashi, K. Mayumi, N. Hosono and T. Uemura, *Macromolecules* **56**, 3141–3148 (2023).
4. †Heterogeneities at the Onset of Reaction Acceleration during Bulk Polymerization of Methyl Methacrylate Investigated by Small-Angle Neutron Scattering: Y. Suzuki, Y. Doi, R. Mishima, K. Mayumi and A. Matsumoto, *Macromolecules* **56**, 3731 (2023).
5. Phantom-Chain Simulations for the Effect of Node Functionality on the Fracture of Star-Polymer Networks: Y. Masubuchi, Y. Doi, T. Ishida, N. Sakumichi, T. Sakai, K. Mayumi, K. Satoh and T. Uneyama, *Macromolecules* **56**, 9359 (2023).

---

† Joint research with outside partners.

6. Phantom Chain Simulations for the Fracture of Energy-Minimized Tetra- and Tri-Branched Networks: Y. Masubuchi, Y. Doi, T. Ishida, N. Sakumichi, T. Sakai, K. Mayumi and T. Uneyama, *Macromolecules* **56**, 2217-2223 (2023).
7. Strain-induced crystallization and phase separation used for fabricating a tough and stiff slide-ring solid polymer electrolyte: K. Hashimoto, T. Shiwaku, H. Aoki, H. Yokoyama, K. Mayumi and K. Ito, *Sci. Adv.* **9**, eadi8505 (2023).
8. Mechanochromic luminescence of phase-separated hydrogels that contain cyclophane mechanophores: S. Shimizu, H. Yoshida, K. Mayumi, H. Ajiro and Y. Sagara, *Mater. Chem. Front.* **7**, 4073 (2023).
9. Strain-Induced Crystallization in Tetra-Branched Poly(ethylene glycol) Hydrogels with a Common Network Structure: K. Hashimoto, T. Enoki, C. Liu, X. Li, T. Sakai and K. Mayumi, *Macromolecules* **57**, 1461 (2024).
10. †Ionic Conductive Organogels Based on Cellulose and Lignin-Derived Metabolic Intermediates: H. Jia, K. Jimbo, K. Mayumi, T. Oda, T. Sawada, T. Serizawa, T. Araki, N. Kamimura, E. Masai, E. Togawa, M. Nakamura and T. Michinobu, *ACS Sustainable Chem. Eng.* **12**, 501 (2024).
11. Understanding the rheological properties from linear to nonlinear regimes and spatiotemporal structure of mixed kappa and reduced molecular weight lambda carrageenan gels: L. C. Geonzon, T. Enoki, S. Humayun, R. Tuvikene, S. Matsukawa and K. Mayumi, *Food Hydrocolloids* **150**, 109752 (2024).
12. Mechanical properties of polymer networks with polyrotaxane crosslinkers with different molecular structures based on polyethylene glycol and  $\alpha$ -cyclodextrin: S. Liu, K. Watanabe, E. Miwa, M. Hara, T. Seki, K. Mayumi, K. Ito and Y. Takeoka, *Giant* **17**, 100224 (2024).
13. Composites with aligned and plasma-surface-modified graphene nanoplatelets and high dielectric constants: K. Nagayama, T. Goto, K. Mayumi, R. Maeda, T. Ito, Y. Shimizu, K. Ito, Y. Hakuta and K. Terashima, *Materials Letters: X* **22**, 100233 (2024).

## International MegaGauss Science Laboratory

### Kindo group

A better Cu-Ag magnet wire was developed. Our mono-coil renewed the world record of the non-destructive pulsed field. 88.6 T was generated by using the new Cu-Ag wire.

1. †\*Fermi surface and light quasi particles in hourglass nodal chain metal  $\beta$ -ReO<sub>2</sub>: D. Hirai, T. Anbai, T. Konoike, S. Uji, Y. Hattori, T. Terashima, H. Ishikawa, K. Kindo, N. Katayama, T. Oguchi and Z. Hiroi, *J. Phys.: Condens. Matter* **35**, 405503 (2023).
2. Erratum: “Electrical and Magnetic Properties of New Yb-based Compound YbPd<sub>5</sub>Al<sub>2</sub>” [*J. Phys. Soc. Jpn.* **81**, SB057 (2012)]: Y. Hirose, N. Nishimura, K. Enoki, F. Honda, T. Takeuchi, K. Sugiyama, M. Hagiwara, K. Kindo, R. Settai and Y. Onuki, *J. Phys. Soc. Jpn.* **92**, 018001 (2023).
3. †\*Gradual Charge Order Melting in Bi<sub>0.5</sub>Ca<sub>0.5</sub>MnO<sub>3</sub> Induced by Ultrahigh Magnetic Fields: Y. Ishii, A. Ikeda, M. Tokunaga, K. Kindo, A. Matsuo and Y. H. Matsuda, *J. Phys. Soc. Jpn.* **92**, 074702(1-6) (2023).
4. Magnetic Excitation in the S = 1/2 Ising-like Antiferromagnetic Chain CsCoCl<sub>3</sub> in Longitudinal Magnetic Fields Studied by High-field ESR Measurements: S. Kimura, H. Onishi, K. Okunishi, M. Akaki, Y. Narumi, M. Hagiwara, K. Kindo and H. Kikuchi, *J. Phys. Soc. Jpn.* **92**, 094701 (2023).
5. Magnetic Properties of Single Crystalline Tb<sub>5</sub>Sb<sub>3</sub>: A. Kitaori, N. Kanazawa, T. Kida, Y. Narumi, M. Hagiwara, K. Kindo, T. Takeuchi, A. Nakamura, D. Aoki, Y. Haga, Y. Kaneko, Y. Tokura and Y. Onuki, *J. Phys. Soc. Jpn.* **92**, 024702 (2023).
6. †Single Crystal Growth, Magnetic Anisotropy, Specific Heat, and High-Field Magnetization in RInCu<sub>4</sub>, R = Gd, Tb: T. Waki, F. Kihara, Y. Tabata, T. Takeuchi, Y. Narumi, M. Hagiwara, K. Kindo and H. Nakamura, *J. Phys. Soc. Jpn.* **92**, 104706(1-7) (2023).
7. †\*Structural and Electronic Properties of a Triangular Lattice Magnet NaPrTe<sub>2</sub> Compared with NaNdTe<sub>2</sub> and NaTbTe<sub>2</sub>: K. Eto, Y. Okamoto, N. Katayama, H. Ishikawa, K. Kindo and K. Takenaka, *J. Phys. Soc. Jpn.* **92**, 094707(1-6) (2023).
8. †\*High-field magnetization and magnetic phase diagrams for three symmetry axes in single-crystal CeAl<sub>2</sub>: T. Ebihara, J. Jatmika, A. Miyake, M. Tokunaga and K. Kindo, *Phys. Rev. B* **108**, 205148(1-8) (2023).

---

\* Joint research among groups within ISSP.

9. †Ladder-based two-dimensional spin model in a radical-Co complex: H. Yamaguchi, Y. Tominaga, A. Matsuo, S. Morota, Y. Hosokoshi, M. Hagiwara and K. Kindo, *Phys. Rev. B* **107**, 174422 (2023).
10. †Magnetic-field-induced valence change in  $\text{Eu}(\text{Co}_{1-x}\text{Ni}_x)_2\text{P}_2$  up to 60 T: R. Nakamura, A. Ishita, J. Nakamura, H. Ohta, Y. Haraguchi, H. A. Katori, H. Ishikawa, A. Matsuo, K. Kindo, M. Nohara and A. Ikeda, *Phys. Rev. B* **107**, 235110 (2023).
11. †Mixed-spin two-dimensional lattice composed of spins 1/2 and 1 in a radical-Ni complex: Y. Tominaga, A. Matsuo, K. Kindo, S. Shimono, K. Araki, Y. Iwasaki, Y. Hosokoshi, S. Noguchi and H. Yamaguchi, *Phys. Rev. B* **108**, 024424 (2023).
12. †\*Quantum oscillations in the centrosymmetric skyrmion-hosting magnet  $\text{GdRu}_2\text{Si}_2$ : N. Matsuyama, T. Nomura, S. Imajo, T. Nomoto, R. Arita, K. Sudo, M. Kimata, N. D. Khanh, R. Takagi, Y. Tokura, S. Seki, K. Kindo and Y. Kohama, *Phys. Rev. B* **107**, 104421 (2023).
13. Thermodynamic properties of the Mott insulator-metal transition in a triangular lattice system without magnetic order: E. Yesil, S. Imajo, S. Yamashita, H. Akutsu, Y. Saito, A. Pustogow, A. Kawamoto and Y. Nakazawa, *Phys. Rev. B* **107**, 045133 (2023).
14. \*Liquid helium-cooled high-purity copper coil for generation of long pulsed magnetic fields: Y. Kohama, Y. Ihara, Z. Yang, K. Matsui and K. Kindo, *Rev. Sci. Instrum.* **94**, 074701 (2023).
15. \*Piston-cylinder cell made of Ni–Cr–Al alloy for magnetic susceptibility measurements under high pressures in pulsed high magnetic fields: K. Nihongi, T. Kida, Y. Narumi, N. Kurita, H. Tanaka, Y. Uwatoko, K. Kindo and M. Hagiwara, *Rev. Sci. Instrum.* **94**, 113903(1-7) (2023).
16. \*Simultaneous measurement of specific heat and thermal conductivity in pulsed magnetic fields: T. Nomoto, C. Zhong, H. Kageyama, Y. Suzuki, M. Jaime, Y. Hashimoto, S. Katsumoto, N. Matsuyama, C. Dong, A. Matsuo, K. Kindo, K. Izawa and Y. Kohama, *Rev. Sci. Instrum.* **94**, 054901 (2023).
17. †\*Signatures of a magnetic superstructure phase induced by ultrahigh magnetic fields in a breathing pyrochlore antiferromagnet: M. Gen, A. Ikeda, K. Aoyama, H. O. Jeschke, Y. Ishii, H. Ishikawa, T. Yajima, Y. Okamoto, X. Zhou, D. Nakamura, S. Takeyama, K. Kindo, Y. H. Matsuda and Y. Kohama, *Proc. Natl. Acad. Sci. U.S.A.* **120**, e2302756120(1-7) (2023).
18. †Enhanced Superconducting Pairing Strength near a Pure Nematic Quantum Critical Point: K. Mukasa, K. Ishida, S. Imajo, M. Qiu, M. Saito, K. Matsuura, Y. Sugimura, S. Liu, Y. Uezono, T. Otsuka, M. Culo, S. Kasahara, Y. Matsuda, N. E. Hussey, T. Watanabe, K. Kindo and T. Shibauchi, *Phys. Rev. X* **13**, 011032 (2023).
19. †\*Breathing pyrochlore magnet  $\text{CuGaCr}_4\text{S}_8$ : Magnetic, thermodynamic, and dielectric properties: M. Gen, H. Ishikawa, A. Miyake, T. Yajima, H. O. Jeschke, H. Sagayama, A. Ikeda, Y. H. Matsuda, K. Kindo, M. Tokunaga, Y. Kohama, T. Kurumaji, Y. Tokunaga and T.-H. Arima, *Phys. Rev. Materials* **7**, 104404(1-12) (2023).
20. †Field-induced quantum phase in a frustrated zigzag-square lattice: H. Yamaguchi, K. Shimamura, Y. Yoshida, A. Matsuo, K. Kindo, K. Nakano, S. Morota, Y. Hosokoshi, T. Kida, Y. Iwasaki, S. Shimono, K. Araki and M. Hagiwara, *Phys. Rev. Materials* **7**, L091401(1-5) (2023).
21. Pseudogap formation in organic superconductors: S. Imajo, T. Kobayashi, Y. Matsumura, T. Maeda, Y. Nakazawa, H. Taniguchi and K. Kindo, *Phys. Rev. Materials* **7**, 124803 (2023).
22. Superconductivity at 12 K in  $\text{La}_2\text{IOs}_2$ : A 5d metal with osmium honeycomb layer: H. Ishikawa, T. Yajima, D. Nishio-Hamane, S. Imajo, K. Kindo and M. Kawamura, *Phys. Rev. Materials* **7**, 054804 (2023).
23. †Expanded quantum vortex liquid regimes in the electron nematic superconductors  $\text{FeSe}_{1-x}\text{S}_x$  and  $\text{FeSe}_{1-x}\text{Te}_x$ : M. Culo, S. Licciardello, K. Ishida, K. Mukasa, J. Ayres, J. Buhot, Y. -T. Hsu, S. Imajo, M. W. Qiu, M. Saito, Y. Uezono, T. Otsuka, T. Watanabe, K. Kindo, T. Shibauchi, S. Kasahara, Y. Matsuda and N. E. Hussey, *Nat Commun* **14**, 4150 (2023).
24. †\*Possible intermediate quantum spin liquid phase in  $\alpha\text{-RuCl}_3$  under high magnetic fields up to 100 T: X.-G. Zhou, H. Li, Y. H. Matsuda, A. Matsuo, W. Li, N. Kurita, G. Su, K. Kindo and H. Tanaka, *Nat Commun* **14**, 5613 (7 pages) (2023).
25. \*Dimerization-enhanced exotic magnetization plateau and magnetoelectric phase diagrams in skew-chain  $\text{Co}_2\text{V}_2\text{O}_7$ : Z. H. Li, X. T. Han, C. Dong, H. W. Wang, Z. Z. He, R. Chen, W. X. Liu, C. L. Lu, Y. Kohama, M. Tokunaga, K. Kindo, Z. W. Ouyang, J. F. Wang and M. Yang, *Phys. Rev. B* **109**, 094432 (2024).
26. \*Quantum Liquid States of Spin Solitons in a Ferroelectric Spin-Peierls State: S. Imajo, A. Miyake, R. Kurihara, M. Tokunaga, K. Kindo, S. Horiuchi and F. Kagawa, *Phys. Rev. Lett.* **132**, 096601(1-6) (2024).

---

† Joint research with outside partners.

## Tokunaga group

In the quantum limit state realized in high field limit, we can increase the effect of electron correlation by applied magnetic fields. In our study on BiSb alloys, we induced transitions from topological insulator to topologically non-trivial semimetal by magnetic fields applied along the trigonal axis. In addition, we found the system changes into insulator again by further increasing applied field in the quantum limit state of the field-induced semimetallic state. We discussed possibility of the excitonic insulator state that has been anticipated over half a century.

1. †\*Gradual Charge Order Melting in  $\text{Bi}_{0.5}\text{Ca}_{0.5}\text{MnO}_3$  Induced by Ultrahigh Magnetic Fields: Y. Ishii, A. Ikeda, M. Tokunaga, K. Kindo, A. Matsuo and Y. H. Matsuda, *J. Phys. Soc. Jpn.* **92**, 074702(1-6) (2023).
2. †Coherent description of the magnetic properties of  $\text{SeCuO}_3$  versus temperature and magnetic field: X. Rocquefelte, M. Herak, A. Miyake, W. Lafargue-Dit-Hauret, H. Berger, M. Tokunaga and A. Saúl, *Phys. Rev. B* **107**, 054407(1-8) (2023).
3. Field-induced reentrant insulator state of a gap-closed topological insulator ( $\text{Bi}_{1-x}\text{Sb}_x$ ) in quantum-limit states: Y. Kinoshita, T. Fujita, R. Kurihara, A. Miyake, Y. Izaki, Y. Fuseya and M. Tokunaga, *Phys. Rev. B* **107**, 125140(1-9) (2023).
4. †Field-tunable Weyl points and large anomalous Hall effect in the degenerate magnetic semiconductor  $\text{EuMg}_2\text{Bi}_2$ : M. Kondo, M. Ochi, R. Kurihara, A. Miyake, Y. Yamasaki, M. Tokunaga, H. Nakao, K. Kuroki, T. Kida, M. Hagiwara, H. Murakawa, N. Hanasaki and H. Sakai, *Phys. Rev. B* **107**, L121112(1-7) (2023).
5. †\*High-field magnetization and magnetic phase diagrams for three symmetry axes in single-crystal  $\text{CeAl}_2$ : T. Ebihara, J. Jatmika, A. Miyake, M. Tokunaga and K. Kindo, *Phys. Rev. B* **108**, 205148(1-8) (2023).
6. \*High-field phase diagram of the chiral-lattice antiferromagnet  $\text{Sr}(\text{TiO})\text{Cu}_4(\text{PO}_4)_4$ : T. Nomura, Y. Kato, Y. Motome, A. Miyake, M. Tokunaga, Y. Kohama, S. Zherlitsyn, J. Wosnitzer, S. Kimura, T. Katsuyoshi, T. Kimura and K. Kimura, *Phys. Rev. B* **108**, 054434 (2023).
7. †Ising-type quasi-one-dimensional ferromagnetism with anisotropic hybridization in  $\text{UNi}_4\text{P}_2$ : A. Maurya, A. Miyake, H. Kotegawa, Y. Shimizu, Y. J. Sato, A. Nakamura, D. Li, Y. Homma, F. Honda, M. Tokunaga and D. Aoki, *Phys. Rev. B* **107**, 085142(1-6) (2023).
8. †Variation of Landau level splitting in the Fermi level controlled Dirac metals  $(\text{Eu,Gd})\text{MnBi}_2$ : H. Sakai, K. Nakagawa, K. Tsuruda, J. Shiozaki, K. Akiba, M. Tokunaga, S. Kimura, S. Awaji, A. Tsukazaki, H. Murakawa and N. Hanasaki, *Phys. Rev. B* **108**, 115142(1-7) (2023).
9. †Magnetic field-induced phase transition in ilmenite-type  $\text{CoVO}_3$ : H. Yamamoto, H.-C. Wu, A. Miyake, M. Tokunaga, A. Suzuki, T. Honda and H. Kimura, *Appl. Phys. Lett.* **123**, 132404(1-4) (2023).
10. †Magnetoelectricity Enhanced by Electron Redistribution in a Spin Crossover  $[\text{FeCo}]$  Complex: X. Zhang, W.-H. Xu, W. Zheng, S.-Q. Su, Y.-B. Huang, Q. Shui, T. Ji, M. Uematsu, Q. Chen, M. Tokunaga, K. Gao, A. Okazawa, S. Kanegawa, S.-Q. Wu and O. Sato, *J. Am. Chem. Soc.* **145**, 15647-15651 (2023).
11. †\*Breathing pyrochlore magnet  $\text{CuGaCr}_4\text{S}_8$ : Magnetic, thermodynamic, and dielectric properties: M. Gen, H. Ishikawa, A. Miyake, T. Yajima, H. O. Jeschke, H. Sagayama, A. Ikeda, Y. H. Matsuda, K. Kindo, M. Tokunaga, Y. Kohama, T. Kurumaji, Y. Tokunaga and T.-H. Arima, *Phys. Rev. Materials* **7**, 104404(1-12) (2023).
12. †\*One-dimensional magnetism in synthetic Pauflerite,  $\beta\text{-VOSO}_4$ : D. L. Quintero-Castro, G. J. Nilsen, K. Meier-Kirchner, A. Benitez-Castro, G. Guenther, T. Sakakibara, M. Tokunaga, C. Agu, I. Mandal and A. A. Tsirlin, *Phys. Rev. Materials* **7**, 045003(1-7) (2023).
13. †Ordered and disordered variants of the triangular lattice antiferromagnet  $\text{Ca}_3\text{NiNb}_2\text{O}_9$ : Crystal growth and magnetic properties: D. Rout, R. Tang, M. Skoulatos, B. Ouladdiaf, Y. Kinoshita, A. Miyake, M. Tokunaga, S. Mahapatra and S. Singh, *Phys. Rev. Materials* **7**, 024419(1-14) (2023).
14. †Double dome structure of the Bose–Einstein condensation in diluted  $S=3/2$  quantum magnets: Y. Watanabe, A. Miyake, M. Gen, Y. Mizukami, K. Hashimoto, T. Shibauchi, A. Ikeda, M. Tokunaga, T. Kurumaji, Y. Tokunaga and T.-H. Arima, *Nat Commun* **14**, 1260(1-9) (2023).
15. Low-temperature hysteresis broadening emerging from domain-wall creep dynamics in a two-phase competing system: K. Matsuura, Y. Nishizawa, Y. Kinoshita, T. Kurumaji, A. Miyake, H. Oike, M. Tokunaga, Y. Tokura and F. Kagawa, *Commun Mater* **4**, 71(1-8) (2023).
16. † $\text{Pd}_2\text{MnGa}$  Metamagnetic Shape Memory Alloy with Small Energy Loss: T. Ito, X. Xu, A. Miyake, Y. Kinoshita, M. Nagasako, K. Takahashi, T. Omori, M. Tokunaga and R. Kainuma, *Advanced Science* **10**, 2207779(1-12) (2023).

---

\* Joint research among groups within ISSP.

17. †Physical Properties of a New Ternary Compound  $R\text{Pt}_3\text{Al}_5$  ( $R$  = rare earth): H. Fukuda, T. Koizumi, Y. J. Sato, Y. Shimizu, A. Nakamura, D. Li, Y. Homma, A. Miyake, D. Aoki, M. Tokunaga, R. Kato, M. Shiga, T. Kawae and F. Honda, *New Physics: Sae Mulli* **73**, 1135-1139 (2023).
18. †Edge and Bulk States in Weyl-Orbit Quantum Hall Effect as Studied by Corbino Measurements: Y. Nakazawa, R. Kurihara, M. Miyazawa, S. Nishihaya, M. Kriener, M. Tokunaga, M. Kawasaki and M. Uchida, *J. Phys. Soc. Jpn.* **93**, 023706(1-5) (2024).
19. \*Dimerization-enhanced exotic magnetization plateau and magnetoelectric phase diagrams in skew-chain  $\text{Co}_2\text{V}_2\text{O}_7$ : Z. H. Li, X. T. Han, C. Dong, H. W. Wang, Z. Z. He, R. Chen, W. X. Liu, C. L. Lu, Y. Kohama, M. Tokunaga, K. Kindo, Z. W. Ouyang, J. F. Wang and M. Yang, *Phys. Rev. B* **109**, 094432 (2024).
20. Field-induced electric polarization and elastic softening caused by parity-mixed d-p hybridized states with electric multipoles in  $\text{Ba}_2\text{CuGe}_2\text{O}_7$ : R. Kurihara, Y. Sato, A. Miyake, M. Akaki, K. Mitsumoto, M. Hagiwara, H. Kuwahara and M. Tokunaga, *Phys. Rev. B* **109**, 125129(1-26) (2024).
21. Multiple magnetoelectric plateaus in the polar magnet  $\text{Fe}_2\text{Mo}_3\text{O}_8$ : Q. Chen, A. Miyake, T. Kurumaji, K. Matsuura, F. Kagawa, S. Miyahara, Y. Tokura and M. Tokunaga, *Phys. Rev. B* **109**, 094419(1-7) (2024).
22. \*Quantum Liquid States of Spin Solitons in a Ferroelectric Spin-Peierls State: S. Imajo, A. Miyake, R. Kurihara, M. Tokunaga, K. Kindo, S. Horiuchi and F. Kagawa, *Phys. Rev. Lett.* **132**, 096601(1-6) (2024).
23. †Magnetic properties and magnetocaloric effect of  $\text{DyCo}_9\text{Si}_4$ : N. Tsujii, A. Miyake, M. Tokunaga, J. Valenta and H. Sakurai, *Journal of Alloys and Compounds* **980**, 173653(1-7) (2024).
24. Novel anisotropy of upper critical fields in  $\text{Fe}_{1+y}\text{Te}_{0.6}\text{Se}_{0.4}$ : Y. Pan, Y. Sun, N. Zhou, X. Yi, Q. Hou, J. Wang, Z. Zhu, H. Mitamura, M. Tokunaga and Z. Shi, *Journal of Alloys and Compounds* **976**, 173262(1-6) (2024).
25. †High-field immiscibility of electrons belonging to adjacent twinned bismuth crystals: Y. Ye, A. Yamada, Y. Kinoshita, J. Wang, P. Nie, L. Xu, H. Zuo, M. Tokunaga, N. Harrison, R. D. McDonald, A. V. Suslov, A. Ardavan, M.-S. Nam, D. LeBoeuf, C. Proust, B. Fauqué, Y. Fuseya, Z. Zhu and K. Behnia, *npj Quantum Mater.* **9**, 12(1-9) (2024).
26. †Observation of nonvolatile magneto-thermal switching in superconductors: H. Arima, Md. Riad Kasem, H. Sepehri-Amin, F. Ando, K.-I. Uchida, Y. Kinoshita, M. Tokunaga and Y. Mizuguchi, *Commun Mater* **5**, 34(1-8) (2024).
27. †Peculiar magnetotransport properties in epitaxially stabilized orthorhombic  $\text{Ru}^{3+}$  perovskite  $\text{LaRuO}_3$  and  $\text{NdRuO}_3$ : L. Zhang, T. C. Fujita, Y. Masutake, M. Kawamura, T.-H. Arima, H. Kumigashira, M. Tokunaga and M. Kawasaki, *Commun Mater* **5**, 35(1-8) (2024).

## Y. Matsuda group

We have investigated magnetic states in several frustrated spin systems such as breathing pyrochlore, Kitaev, and Shastry-Sutherland systems with ultrahigh-magnetic fields exceeding 100 T. In the breathing pyrochlore systems, the strong spin-lattice coupling was found to be important. The magnetic field-induced quantum spin liquid state appeared in a Kitaev system  $\text{RuCl}_3$  when the field was perpendicular to the honeycomb plane, which was in good agreement with a theoretical calculation. An unusual decrease in the sound velocity was observed at the 1/2 plateau in the Shastry-Sutherland system  $\text{SrCu}_2(\text{BO}_3)_2$  in addition to the success of having a saturation at around 140 T. The electronic structure in a functional semiconductor  $\text{In}_{1-x}\text{As}_x\text{P}$  has been revealed by using cyclotron resonance in magnetic fields of up to 140 T. The strongly correlated transition metal perovskite oxides,  $\text{Bi}_{0.5}\text{Ca}_{0.5}\text{MnO}_3$  and  $\text{LaCoO}_3$  were also studied. The charge order in  $\text{Bi}_{0.5}\text{Ca}_{0.5}\text{MnO}_3$  gradually melts with the increasing magnetic field, while the re-order occurs rather sharply, which indicates an interesting metastable state that appears in magnetic fields fastly varying with time. As for  $\text{LaCoO}_3$ , the quantum condensed exciton state is indicated at ultrahigh magnetic fields up to 600 T. The spin-state transition with a strong quantum entanglement occurs in the ultrahigh magnetic fields.

1. †\*Gradual Charge Order Melting in  $\text{Bi}_{0.5}\text{Ca}_{0.5}\text{MnO}_3$  Induced by Ultrahigh Magnetic Fields: Y. Ishii, A. Ikeda, M. Tokunaga, K. Kindo, A. Matsuo and Y. H. Matsuda, *J. Phys. Soc. Jpn.* **92**, 074702(1-6) (2023).
2. †\*Band structure, g-factor, and spin relaxation in n-type  $\text{InAsP}$  alloys: S. K. Thapa, R. R. H. H. Mudiyansele, T. Paleologu, S. Choi, Z. Yang, Y. Kohama, Y. H. Matsuda, J. Spencer, B. A. Magill, C. J. Palmstrøm, C. J. Stanton and G. A. Khodaparast, *Phys. Rev. B* **108**, 115202(1-12) (2023).
3. †\*Signatures of a magnetic superstructure phase induced by ultrahigh magnetic fields in a breathing pyrochlore antiferromagnet: M. Gen, A. Ikeda, K. Aoyama, H. O. Jeschke, Y. Ishii, H. Ishikawa, T. Yajima, Y. Okamoto, X. Zhou, D. Nakamura, S. Takeyama, K. Kindo, Y. H. Matsuda and Y. Kohama, *Proc. Natl. Acad. Sci. U.S.A.* **120**, e2302756120(1-7) (2023).

---

† Joint research with outside partners.

4. †\*Breathing pyrochlore magnet CuGaCr<sub>4</sub>S<sub>8</sub>: Magnetic, thermodynamic, and dielectric properties: M. Gen, H. Ishikawa, A. Miyake, T. Yajima, H. O. Jeschke, H. Sagayama, A. Ikeda, Y. H. Matsuda, K. Kindo, M. Tokunaga, Y. Kohama, T. Kurumaji, Y. Tokunaga and T.-H. Arima, *Phys. Rev. Materials* **7**, 104404(1-12) (2023).
5. †\*Possible intermediate quantum spin liquid phase in  $\alpha$ -RuCl<sub>3</sub> under high magnetic fields up to 100 T: X.-G. Zhou, H. Li, Y. H. Matsuda, A. Matsuo, W. Li, N. Kurita, G. Su, K. Kindo and H. Tanaka, *Nat Commun* **14**, 5613 (7 pages) (2023).
6. †\*Signature of spin-triplet exciton condensations in LaCoO<sub>3</sub> at ultrahigh magnetic fields up to 600 T: A. Ikeda, Y. H. Matsuda, K. Sato, Y. Ishii, H. Sawabe, D. Nakamura, S. Takeyama and J. Nasu, *Nat Commun* **14**, 1744(1-6) (2023).
7. †\*Unveiling new quantum phases in the Shastry-Sutherland compound SrCu<sub>2</sub>(BO<sub>3</sub>)<sub>2</sub> up to the saturation magnetic field: T. Nomura, P. Corboz, A. Miyata, S. Zherlitsyn, Y. Ishii, Y. Kohama, Y. H. Matsuda, A. Ikeda, C. Zhong, H. Kageyama and F. Mila, *Nat Commun* **14**, 3769(1-7) (2023).

## Kohama group

We have investigated high-field properties on various compounds. In magnetic materials, such as CuGaCr<sub>4</sub>S<sub>8</sub>, Sr(TiO)Cu<sub>4</sub>(PO<sub>4</sub>)<sub>4</sub>, LiGaCr<sub>4</sub>O<sub>8</sub>, and SrCu<sub>2</sub>(BO<sub>3</sub>)<sub>2</sub>, the field-induced phase transitions have been investigated by magnetization and thermodynamic experiments using non-destructive and destructive magnetic fields. In two dimensional conductors, graphite, high-Tc cuprates, and Iron based superconductors, we have investigated the quantum transport properties. Here, the TDO, torque magnetometry, and specific heat measurements have revealed rich quantum phenomena. We have also successfully develop rf transport measurement technique and field generatoin technique for further detailed investigations in high magnetic fields.

1. †\*Band structure, g-factor, and spin relaxation in n-type InAsP alloys: S. K. Thapa, R. R. H. H. Mudiyansele, T. Paleologu, S. Choi, Z. Yang, Y. Kohama, Y. H. Matsuda, J. Spencer, B. A. Magill, C. J. Palmstrøm, C. J. Stanton and G. A. Khodaparast, *Phys. Rev. B* **108**, 115202(1-12) (2023).
2. \*High-field phase diagram of the chiral-lattice antiferromagnet Sr(TiO)Cu<sub>4</sub>(PO<sub>4</sub>)<sub>4</sub>: T. Nomura, Y. Kato, Y. Motome, A. Miyake, M. Tokunaga, Y. Kohama, S. Zherlitsyn, J. Wosnitza, S. Kimura, T. Katsuyoshi, T. Kimura and K. Kimura, *Phys. Rev. B* **108**, 054434 (2023).
3. †\*Quantum oscillations in the centrosymmetric skyrmion-hosting magnet GdRu<sub>2</sub>Si<sub>2</sub>: N. Matsuyama, T. Nomura, S. Imajo, T. Nomoto, R. Arita, K. Sudo, M. Kimata, N. D. Khanh, R. Takagi, Y. Tokura, S. Seki, K. Kindo and Y. Kohama, *Phys. Rev. B* **107**, 104421 (2023).
4. \*Random singlets in the  $s = 5/2$  coupled frustrated cubic lattice Lu<sub>3</sub>Sb<sub>3</sub>Mn<sub>2</sub>O<sub>14</sub>: C. Lee, S. Lee, H.-S. Kim, S. Kittaka, Y. Kohama, T. Sakakibara, K. H. Lee, J. van Tol, D. I. Gorbunov, S.-H. Do, S. Yoon, A. Berlie and K.-Y. Choi, *Phys. Rev. B* **107**, 214404 (2023).
5. Rhombic skyrmion lattice coupled with orthorhombic structural distortion in EuAl<sub>4</sub>: M. Gen, R. Takagi, Y. Watanabe, S. Kitou, H. Sagayama, N. Matsuyama, Y. Kohama, A. Ikeda, Y. Onuki, T. Kurumaji, T.-H. Arima and S. Seki, *Phys. Rev. B* **107**, L020410 (2023).
6. \*Liquid helium-cooled high-purity copper coil for generation of long pulsed magnetic fields: Y. Kohama, Y. Ihara, Z. Yang, K. Matsui and K. Kindo, *Rev. Sci. Instrum.* **94**, 074701 (2023).
7. Radio frequency electrical resistance measurement under destructive pulsed magnetic fields: T. Shitaokoshi, S. Kawachi, T. Nomura, F. F. Balakirev and Y. Kohama, *Rev. Sci. Instrum.* **94**, 094706 (2023).
8. \*Simultaneous measurement of specific heat and thermal conductivity in pulsed magnetic fields: T. Nomoto, C. Zhong, H. Kageyama, Y. Suzuki, M. Jaime, Y. Hashimoto, S. Katsumoto, N. Matsuyama, C. Dong, A. Matsuo, K. Kindo, K. Izawa and Y. Kohama, *Rev. Sci. Instrum.* **94**, 054901 (2023).
9. \*Nonreciprocal Phonon Propagation in a Metallic Chiral Magnet: T. Nomura, X. -X. Zhang, R. Takagi, K. Karube, A. Kikkawa, Y. Taguchi, Y. Tokura, S. Zherlitsyn, Y. Kohama and S. Seki, *Phys. Rev. Lett.* **130**, 176301 (1-6) (2023).
10. パルス強磁場での熱測定：小濱 芳允，野本 哲也，*固体物理* **58(8)**, 411-417 (2023).
11. フラットトップ磁場を用いたパルス磁場中 NMR 測定：井原 慶彦，小濱 芳允，*固体物理* **58**, 89-98 (2023).
12. 新しいカイラル有機超伝導体：野村 肇宏，*固体物理* **58**, 41-45 (2023).
13. 強磁場下の物性研究における+アルファの研究技術：Y. Kohama, *応用物理* **92(9)**, 556-559 (2023).
14. †\*Signatures of a magnetic superstructure phase induced by ultrahigh magnetic fields in a breathing pyrochlore

---

\* Joint research among groups within ISSP.

antiferromagnet: M. Gen, A. Ikeda, K. Aoyama, H. O. Jeschke, Y. Ishii, H. Ishikawa, T. Yajima, Y. Okamoto, X. Zhou, D. Nakamura, S. Takeyama, K. Kindo, Y. H. Matsuda and Y. Kohama, Proc. Natl. Acad. Sci. U.S.A. **120**, e2302756120(1-7) (2023).

15. Critical Current Measurements of HTS Tapes Using Pulsed Current in High Fields at Low Temperatures: Y. Tsuchiya, I. Sakai, K. Mizuno, Y. Kohama, Y. Yoshida and S. Awaji, IEEE Trans. Appl. Supercond. **33**, 1 (2023).
16. †\*Breathing pyrochlore magnet CuGaCr4S8: Magnetic, thermodynamic, and dielectric properties: M. Gen, H. Ishikawa, A. Miyake, T. Yajima, H. O. Jeschke, H. Sagayama, A. Ikeda, Y. H. Matsuda, K. Kindo, M. Tokunaga, Y. Kohama, T. Kurumaji, Y. Tokunaga and T.-H. Arima, Phys. Rev. Materials **7**, 104404(1-12) (2023).
17. Correlation-driven organic 3D topological insulator with relativistic fermions: T. Nomoto, S. Imajo, H. Akutsu, Y. Nakazawa and Y. Kohama, Nat Commun **14**, 2130 (2023).
18. †\*Unveiling new quantum phases in the Shastry-Sutherland compound SrCu<sub>2</sub>(BO<sub>3</sub>)<sub>2</sub> up to the saturation magnetic field: T. Nomura, P. Corboz, A. Miyata, S. Zherlitsyn, Y. Ishii, Y. Kohama, Y. H. Matsuda, A. Ikeda, C. Zhong, H. Kageyama and F. Mila, Nat Commun **14**, 3769(1-7) (2023).
19. †\*Unveiling phase diagram of the lightly doped high-T<sub>c</sub> cuprate superconductors with disorder removed: K. Kurokawa, S. Isono, Y. Kohama, S. Kunisada, S. Sakai, R. Sekine, M. Okubo, M. D. Watson, T. K. Kim, C. Cacho, S. Shin, T. Tohyama, K. Tokiwa and T. Kondo, Nat Commun **14**, 4064 (2023).
20. Unveiling the double-peak structure of quantum oscillations in the specific heat: Z. Yang, B. Fauque, T. Nomura, T. Shitaokoshi, S. Kim, D. Chowdhury, Z. Pribulova, J. Kacmarcik, A. Pourret, G. Knebel, D. Aoki, T. Klein, D. K. Maude, C. Marcenat and Y. Kohama, Nat Commun **14**, 7006 (2023).
21. Analytical model for a hydrogen atom in a magnetic field: Implications for the diamagnetic shift: D. K. Maude, P. Plochocka and Z. Yang, Phys. Rev. B **109**, 155201 (2024).
22. \*Dimerization-enhanced exotic magnetization plateau and magnetoelectric phase diagrams in skew-chain Co<sub>2</sub>V<sub>2</sub>O<sub>7</sub>: Z. H. Li, X. T. Han, C. Dong, H. W. Wang, Z. Z. He, R. Chen, W. X. Liu, C. L. Lu, Y. Kohama, M. Tokunaga, K. Kindo, Z. W. Ouyang, J. F. Wang and M. Yang, Phys. Rev. B **109**, 094432 (2024).
23. Magnetic anisotropy of CeCoSi under high magnetic field: T. Kanda, H. Ishikawa, S. Imajo, K. Kindo, H. Tanida and Y. Kohama, Phys. Rev. B **109**, 174402 (2024).
24. Characterization of In-Field Critical Currents in REBCO Tapes Over Wide Temperature Range by Pulsed Current Source With Supercapacitor: Y. Tsuchiya, K. Mizuno, Y. Kohama, A. Zampa, T. Okada and S. Awaji, IEEE Trans. Appl. Supercond. **34**, 1 (2024).

## Miyata group

We have worked on magneto-optical experiments under pulsed magnetic fields to search for exotic magneto-optical phenomena in van der Waals magnets. The vdW magnet FePS<sub>3</sub>, which has a zigzag magnetic order below TN ~ 120 K, exhibits giant linear dichroism, i.e., linearly polarized lights parallel and perpendicular to the zigzag chain direction show different responses. Magnetic fields can quench the giant linear dichroism in a wide energy range from 1.6 to 2.0 eV by collapsing the robust zigzag magnetic order.

## Center of Computational Materials Science

### Misawa group

We have developed numerical methods and software packages for strongly correlated electron systems. We have updated HΦ (software for exact diagonalization), released H-wave (software for Hartree-Fock calculations and random phase approximations), and wan2respack (an interface tool from Wannier90 to RESPACK). Using these software packages, we have performed ab initio calculations for molecular solids, such as TMTTF/TMTSF salts.

1. \*Data Analysis of Ab initio Effective Hamiltonians in Iron-Based Superconductors — Construction of Predictors for Superconducting Critical Temperature: K. Ido, Y. Motoyama, K. Yoshimi and T. Misawa, J. Phys. Soc. Jpn. **92**, 064702(1-13) (2023).
2. †Correlated Zak insulator in organic antiferromagnets: T. Misawa and M. Naka, Phys. Rev. B **108**, L081120(1-7) (2023).

---

† Joint research with outside partners.

- †\*Gap opening mechanism for correlated Dirac electrons in organic compounds  $\alpha$ -(BEDT-TTF)<sub>2</sub>I<sub>3</sub> and  $\alpha$ -(BEDT-TSeF)<sub>2</sub>I<sub>3</sub>: D. Ohki, K. Yoshimi, A. Kobayashi and T. Misawa, Phys. Rev. B **107**, L041108(1-6) (2023).
- †Interedge spin resonance in the Kitaev quantum spin liquid: T. Misawa, J. Nasu and Y. Motome, Phys. Rev. B **108**, 115117(1-11) (2023).
- †\*Comprehensive Ab Initio Investigation of the Phase Diagram of Quasi-One-Dimensional Molecular Solids: K. Yoshimi, T. Misawa, T. Tsumuraya and H. Seo, Phys. Rev. Lett. **131**, 036401(1-7) (2023).
- \*Interface tool from Wannier90 to RESPACK: wan2respack: K. Kurita, T. Misawa, K. Yoshimi, K. Ido and T. Koretsune, Comput. Phys. Commun. **292**, 108854(1-7) (2023).
- †Monte Carlo study on low-temperature phase diagrams of the J1-J2 classical XY kagome antiferromagnet: F. Kakizawa, T. Misawa and H. Shinaoka, Phys. Rev. B **109**, 014439(1-15) (2024).
- †\*Compensated Ferrimagnets with Colossal Spin Splitting in Organic Compounds: T. Kawamura, K. Yoshimi, K. Hashimoto, A. Kobayashi and T. Misawa, Phys. Rev. Lett. **132**, 156502(1-6) (2024).
- †\*H-wave – A Python package for the Hartree-Fock approximation and the random phase approximation: T. Aoyama, K. Yoshimi, K. Ido, Y. Motoyama, T. Kawamura, T. Misawa, T. Kato and A. Kobayashi, Computer Physics Communications **298**, 109087(1-10) (2024).
- †\*Update of HΦ : Newly added functions and methods in versions 2 and 3: K. Ido, M. Kawamura, Y. Motoyama, K. Yoshimi, Y. Yamaji, S. Todo, N. Kawashima and T. Misawa, Comp. Phys. Commun. **298**, 109093(1-15) (2024).

## Laser and Synchrotron Research Center

### Kobayashi group

#### Laser processing and artificial intelligence

- †\*Observation of infrared interband luminescence in magnesium by femtosecond spectroscopy: T. Suemoto, S. Ono, A. Asahara, T. Okuno, T. Suzuki, K. Okazaki, S. Tani and Y. Kobayashi, J. Appl. Phys. **134**, 163105 (2023).
- \*Disentangling the Competing Mechanisms of Light-Induced Anomalous Hall Conductivity in Three-Dimensional Dirac Semimetal: Y. Murotani, N. Kanda, T. Fujimoto, T. Matsuda, M. Goyal, J. Yoshinobu, Y. Kobayashi, T. Oka, S. Stemmer and R. Matsunaga, Phys. Rev. Lett. **131**, 096901 (2023).
- \*Jitter correction for asynchronous optical sampling terahertz spectroscopy using free-running pulsed lasers: M. Nakagawa, N. Kanda, T. Otsu, I. Ito, Y. Kobayashi and R. Matsunaga, Opt. Express **31**, 19371 (2023).
- \*Anomalous Hall Transport by Optically Injected Isospin Degree of Freedom in Dirac Semimetal Thin Film: Y. Murotani, N. Kanda, T. Fujimoto, T. Matsuda, M. Goyal, J. Yoshinobu, Y. Kobayashi, T. Oka, S. Stemmer and R. Matsunaga, Nano Lett. **24**, 222 (2024).

### Harada group

In 2023, we made significant progress in the analysis of single crystalline LiFe<sub>0.6</sub>Mn<sub>0.4</sub>PO<sub>4</sub> (LFMP) nanowires with carbon sheath using scanning transmission X-ray microscopy (STXM) with a spatial resolution of around 130 nm. The pinpoint Fe *L*-edge and O *K*-edge X-ray absorption spectroscopy (XAS) spectra revealed the natural oxidation of Fe<sup>2+</sup> to Fe<sup>3+</sup> near the tip of the nanowire by air exposure, while the Mn *L*-edge XAS spectra showed a stable Mn<sup>2+</sup> state throughout the nanowires. We also investigated the spatial distributions of the chemical states in prototypical layered LiCoO<sub>2</sub> cathode particles at different charging conditions using STXM. The Co *LL*<sub>3</sub>- and O *K*-edge XAS spectra demonstrated the spatial distribution of the chemical state changes depending on individual particles, and the element maps derived from the STXM stack images revealed the inhomogeneous reactions and the existence of non-active particles. Furthermore, we applied microscopic resonant photoelectron spectroscopy with a spatial resolution of 100 nm (3DnanoESCA system) to study the electronic structure of different facets of LiCoO<sub>2</sub> cathode particles, detecting differences in the binding energies of the dominant Co 3d bands at the valence band of the (001), (104), and (012) facets. Lastly, we prepared for the operation of the next generation synchrotron radiation facility NanoTerasu starting from April 2024 by setting up the RIXS and 3D nanoESCA stations.

- †放射光軟 X 線オペランド顕微光電子分光測定のためのプラスαの研究技術：細野 英司，原田 慈久，応用物理 **92**, 438-442 (2023).

---

\* Joint research among groups within ISSP.

2. †\* ウォルターミラーを利用した軟 X 線タイコグラフィ装置の開発：木村 隆志，竹尾 陽子，櫻井 快，古谷 登，江川 悟，山口 豪太，松澤 雄介，久米 健大，三村 秀和，志村 まり，大橋 治彦，松田 巖，原田 慈久，放射光 **36**, 10 (2023).
3. †Facet-dependent electrochemical performance and electronic structure of LiCoO<sub>2</sub> polyhedral particles revealed by microscopic resonant X-ray photoelectron spectroscopy: W. Zhang, E. Hosono, D. Asakura, S. Tanaka, M. Kobayashi, N. Nagamura, M. Oshima, J. Miyawaki, H. Kiuchi and Y. Harada, *CrystEngComm* **25**, 183-188 (2023).
4. †Visualization of air-induced oxidation in single crystalline LiFe<sub>0.6</sub>Mn<sub>0.4</sub>PO<sub>4</sub> nanowires with carbon sheath using soft X-ray spectromicroscopy: W. Zhang, E. Hosono, D. Asakura, H. Yuzawa, T. Ohigashi, M. Kobayashi, H. Kiuchi and Y. Harada, *Journal of Electron Spectroscopy and Related Phenomena* **266**, 147338(1-6) (2023).
5. †Chemical-state distributions in charged LiCoO<sub>2</sub> cathode particles visualized by soft X-ray spectromicroscopy: W. Zhang, E. Hosono, D. Asakura, H. Yuzawa, T. Ohigashi, M. Kobayashi, H. Kiuchi and Y. Harada, *Sci Rep* **13**, 4639(1-8) (2023).

## I. Matsuda group

We have conducted instrumentations at the new synchrotron radiation (SR) facility, NanoTerasu, at Sendai in Miyagi-prefecture. We have updated our experimental station of ambient-pressure X-ray spectroscopy and developed a system of process-informatics robot units. We have also devoted ourselves in supporting the beamline construction. On December 7, 2023, the first beam was successfully achieved in NanoTerasu. Tuning of the SR beam has been carried out at the beamline and at the end-station. At the X-ray free electron laser (XFEL) beamline, SACLA BL-1, we have succeeded in observing the magnetization-induced second harmonic generation. Based on results of the SR and XFEL experiments, we discovered new 2D boron materials and examined the properties.

1. †Resonant photoemission spectroscopy of atomic layer Fe<sub>2</sub>N on Cu(111) with continuous angular rotation of linearly polarized light: M. Horio, Y. Kudo, T. Wada, T. Sumi, Y. Hirata, M. Niibe, F. Komori and I. Matsuda, *J. Phys.: Condens. Matter* **35**, 425001 (2023).
2. Influence of oxygen coordination number on the electronic structure of single-layer La-based cuprates: M. Horio, X. Peiao, M. Miyamoto, T. Wada, K. Isomura, J. Osiecki, B. Thiagarajan, C. M. Polley, K. Tanaka, M. Kitamura, K. Horiba, K. Ozawa, T. Taniguchi, M. Fujita and I. Matsuda, *Phys. Rev. B* **108**, 035105 (2023).
3. \*Ultrafast control of the crystal structure in a topological charge-density-wave material: T. Suzuki, Y. Kubota, N. Mitsuishi, S. Akatsuka, J. Koga, M. Sakano, S. Masubuchi, Y. Tanaka, T. Togashi, H. Ohsumi, K. Tamasaku, M. Yabashi, H. Takahashi, S. Ishiwata, T. Machida, I. Matsuda, K. Ishizaka and K. Okazaki, *Phys. Rev. B* **108**, 184305 (2023).
4. Element-selective magnetization states in a Gd<sub>23</sub>Fe<sub>67</sub>Co<sub>10</sub> alloy, probed by soft X-ray resonant magneto-optical Kerr effect: T. Sumi, T. Senoo, M. Horio, S. E. Moussaoui, E. Nakamura, K. Tanaka, A. Tsukamoto and I. Matsuda, *Jpn. J. Appl. Phys.* **62**, SB8001 (2023).
5. Detecting driving potentials at the buried SiO<sub>2</sub> nanolayers in solar cells by chemical-selective nonlinear x-ray spectroscopy: M. Horio, T. Sumi, J. Bullock, Y. Hirata, M. Miyamoto, B. R. Nebgen, T. Wada, T. Senoo, Y. Tsujikawa, Y. Kubota, S. Owada, K. Tono, M. Yabashi, T. Iimori, Y. Miyauchi, M. W. Zuerch, I. Matsuda, C. P. Schwartz and W. S. Drisdell, *Appl. Phys. Lett.* **123**, 031602 (2023).
6. Observing soft x-ray magnetization-induced second harmonic generation at a heterojunction interface: T. Sumi, M. Horio, T. Senoo, Y. Kubota, G. Yamaguchi, T. Wada, M. Miyamoto, K. Yamaguchi, Y. Tsujikawa, Y. Sato, M. Niibe, Y. Hirata, Y. Miyauchi, D. Oshima, T. Kato, S. Owada, K. Tono, M. Yabashi and I. Matsuda, *Appl. Phys. Lett.* **122**, 171601 (1-5) (2023).
7. †\*Suppression of atomic displacive excitation in photo-induced A<sub>1g</sub> phonon mode of bismuth unveiled by low-temperature time-resolved x-ray diffraction: Y. Kubota, Y. Tanaka, T. Togashi, T. Ebisu, K. Tamasaku, H. Osawa, T. Wada, O. Sugino, I. Matsuda and M. Yabashi, *Appl. Phys. Lett.* **122**, 092201 (2023).
8. †\* ウォルターミラーを利用した軟 X 線タイコグラフィ装置の開発：木村 隆志，竹尾 陽子，櫻井 快，古谷 登，江川 悟，山口 豪太，松澤 雄介，久米 健大，三村 秀和，志村 まり，大橋 治彦，松田 巖，原田 慈久，放射光 **36**, 10 (2023).
9. Effective treatment of hydrogen boride sheets for long-term stabilization: S.-I. Ito, M. Hikichi, N. Noguchi, M. Yuan, Z. Kang, K. Fukuda, M. Miyauchi, I. Matsuda and T. Kondo, *Phys. Chem. Chem. Phys.* **25**, 15531 (2023).
10. †\*Oxide layer dependent orbital torque efficiency in ferromagnet/Cu/oxide heterostructures: J. Kim, J. Uzuhashi, M. Horio, T. Senoo, D. Go, D. Jo, T. Sumi, T. Wada, I. Matsuda, T. Ohkubo, S. Mitani, H.-W. Lee and Y. Otani, *Phys. Rev. Materials* **7**, L111401 (2023).
11. †\*Developing a Simple Scanning Probe System for Soft X-ray Spectroscopy with a Nano-focusing Mirror: H. Ando, M.

---

† Joint research with outside partners.

- Horio, Y. Takeo, M. Niibe, T. Wada, Y. Ando, T. Kondo, T. Kimura and I. Matsuda, *e-J. Surf. Sci. Nanotechnol.* **21**, 200 (2023).
12. Orbital-selective metal skin induced by alkali-metal-dosing Mott-insulating  $\text{Ca}_2\text{RuO}_4$ : M. Horio, F. Forte, D. Sutter, M. Kim, C. G. Fatuzzo, C. E. Matt, S. Moser, T. Wada, V. Granata, R. Fittipaldi, Y. Sassa, G. Gatti, H. M. Rønnow, M. Hoesch, T. K. Kim, C. Jozwiak, A. Bostwick, E. Rotenberg, I. Matsuda, A. Georges, G. Sangiovanni, A. Vecchione, M. Cuoco and J. Chang, *Commun Phys* **6**, 323 (2023).
  13. †\*Observing an ordered surface phase by B deposition on Cu(110): Y. Tsujikawa, X. Zhang, M. Horio, T. Wada, M. Miyamoto, T. Sumi, F. Komori, T. Kondo and I. Matsuda, *Surface Science* **732**, 122282 (2023).
  14. Probing lithium mobility at a solid electrolyte surface: C. Woodahl, S. Jamnuch, A. Amado, C. B. Uzundal, E. Berger, P. Manset, Y. Zhu, Y. Li, D. D. Fong, J. G. Connell, Y. Hirata, Y. Kubota, S. Owada, K. Tono, M. Yabashi, S. G. E. T. Velthuis, S. Tepavcevic, I. Matsuda, W. S. Drisdell, C. P. Schwartz, J. W. Freeland, T. A. Pascal, A. Zong and M. Zuercher, *Nat. Mater.* **22**, 848 (2023).
  15. Enhanced Superconductivity and Rashba Effect in a Buckled Plumbene - Au Kagome Superstructure: W. Chen, C. Chen, G. Chen, W. Chen, F. R. Chen, P. Chen, C. Ku, C. Lee, N. Kawakami, J. Li, I. Matsuda, W. Chang, J. Lin, C. Wu, C. Mou, H. Jeng, S. Tang and C. Lin, *Advanced Science* **10**, 2300845 (2023).
  16. †\*Accelerated Synthesis of Borophane (HB) Sheets through HCl-Assisted Ion-Exchange Reaction with YCrB<sub>4</sub>: X. Zhang, M. Hikichi, T. Iimori, Y. Tsujikawa, M. Yuan, M. Horio, K. Yubuta, F. Komori, M. Miyauchi, T. Kondo and I. Matsuda, *Molecules* **28**, 2985(1-15) (2023).
  17. Prediction of a Cyclic Hydrogenated Boron Molecule as a Promising Building Block for Borophane: Y. Ando, T. Nakashima, H. Yin, I. Tateishi, X. Zhang, Y. Tsujikawa, M. Horio, N. T. Cuong, S. Okada, T. Kondo and I. Matsuda, *Molecules* **28**, 1225(1-13) (2023).
  18. Controlling Photoinduced H<sub>2</sub> Release from Freestanding Borophane Sheets Under UV Irradiation by Tuning B–H Bonds (*Adv. Mater. Interfaces* 25/2023): M. Hikichi, J. Takeshita, N. Noguchi, S. Ito, Y. Yasuda, L. T. Ta, K. I. M. Rojas, I. Matsuda, S. Tominaka, Y. Morikawa, I. Hamada, M. Miyauchi and T. Kondo, *Adv Materials Inter* **10**, 2370074 (2023).
  19. Ultrafast Subpicosecond Magnetization of a 2D Ferromagnet: L. D. Anh, M. Kobayashi, T. Takeda, K. Araki, R. Okano, T. Sumi, M. Horio, K. Yamamoto, Y. Kubota, S. Owada, M. Yabashi, I. Matsuda and M. Tanaka, *Advanced Materials* **35**, 2301347 (2023).
  20. \*Hydrogen - induced Sulfur Vacancies on the MoS<sub>2</sub> Basal Plane Studied by Ambient Pressure XPS and DFT Calculations: F. Ozaki, S. Tanaka, Y. Choi, W. Osada, K. Mukai, M. Kawamura, M. Fukuda, M. Horio, T. Koitaya, S. Yamamoto, I. Matsuda, T. Ozaki and J. Yoshinobu, *ChemPhysChem* **24**, e202300477 (2023).
  21. †\*In Situ Electrical Detection of Methane Oxidation on Atomically Thin IrO<sub>2</sub> Nanosheet Films Down to Room Temperature: Y. Ishihara, T. Koitaya, Y. Hamahiga, W. Sugimoto, S. Yamamoto, I. Matsuda, J. Yoshinobu and R. Nouchi, *Adv. Materials Inter.* **10**, 2300258 (2023).
  22. Phase stability and band degeneracy of quasi-one-dimensional boron chain polymorphs embedded in LiB crystals: T. Nakashima, I. Tateishi, Y. Tsujikawa, M. Horio, T. Kondo, I. Matsuda and Y. Ando, *Phys. Rev. B* **109**, 165104 (2024).
  23. Pioneering preparation and analysis of a clean surface on a microcrystal, mined by a focused ion beam: Y. Guan, F. Komori, M. Horio, A. Fukuda, Y. Tsujikawa, K. Ozawa, M. Kamiko, D. Nishio-Hamane, T. Kawauchi, K. Fukutani, Y. Tokumoto, K. Edagawa, R. Tamura and I. Matsuda, *Jpn. J. Appl. Phys.* **63**, 030906 (2024).
  24. †\*Quasi-Periodic Growth of One-Dimensional Copper Boride on Cu(110): Y. Tsujikawa, X. Zhang, K. Yamaguchi, M. Haze, T. Nakashima, A. Varadwaj, Y. Sato, M. Horio, Y. Hasegawa, F. Komori, M. Oshikawa, M. Kotsugi, Y. Ando, T. Kondo and I. Matsuda, *Nano Lett.* **24**, 1160 (2024).
  25. †Structure and Electronic State of Boron Atomic Chains on a Noble Metal (111) Surface: Y. Tsujikawa, X. Zhang, M. Horio, F. Komori, T. Nakashima, Y. Ando, T. Kondo and I. Matsuda, *e-J. Surf. Sci. Nanotechnol.* **22**, 1 (2024).
  26. *New Science of Boron Allotropes, Compounds, and Nanomaterials*: I. Matsuda, T. Kondo and J. M. Oliva-Enrich ed., (MDPI AG, Basel, Switzerland, 2023).
  27. *Nonlinear X-ray Spectroscopy for Materials Science*: I. Matsuda and R. Arafune ed., (Springer, Berlin, 2023).

## Itatani group

---

\* Joint research among groups within ISSP.

We have promoted soft X-ray attosecond spectroscopy by using a thin flat water jet introduced into a newly developed attosecond beamline in collaboration with RIKEN. An optical parametric amplifier was also installed in the beamline for various pump-probe experiments. We have also developed a new optical parametric amplifier in the infrared (wavelength around 2 micrometers) pumped by a compact Yb:KGW laser system at 1030 nm with a repetition rate of 100 kHz. The output pulse duration is 16 fs with an extremely stable carrier-envelope phase. This system is designed as a front-end for future high-power ultrafast light sources for high-throughput attosecond soft-X-ray spectroscopy. We have also pursued the ultrafast strong field phenomena in liquids using a thin flat jet setup with an improved intense MIR source. With the sub-cycle spectroscopy experiment, unusual superluminal propagation of MIR pulses was observed due to strong resonance absorption. High harmonic generation with resonant MIR pulses in water was studied and a novel thermal enhancement was observed for the first time, opening a new direction in strong-field attosecond science in condensed matter.

1. †\*Quasi One-Dimensional Band Structure of Photoinduced Semimetal Phase of  $\text{Ta}_2\text{Ni}_{1-x}\text{Co}_x\text{Se}_5$  ( $x = 0.0$  and  $0.1$ ): T. Mitsuoka, Y. Takahashi, T. Suzuki, M. Okawa, H. Takagi, N. Katayama, H. Sawa, M. Nohara, M. Watanabe, J. Xu, Q. Ren, M. Fujisawa, T. Kanai, J. Itatani, K. Okazaki, S. Shin and T. Mizokawa, *J. Phys. Soc. Jpn.* **92**, 023703 (2023).
2. †\*Temporal Evolution and Fluence Dependence of Band Structure in Photoexcited  $\text{Ta}_2\text{Ni}_{0.9}\text{Co}_{0.1}\text{Se}_5$  Probed by Time- and Angle-Resolved Photoemission Spectroscopy: Y. Takahashi, T. Suzuki, M. Hattori, M. Okawa, H. Takagi, N. Katayama, H. Sawa, M. Nohara, Y. Zhong, K. Liu, T. Kanai, J. Itatani, S. Shin, K. Okazaki and T. Mizokawa, *J. Phys. Soc. Jpn.* **92**, 064706 (2023).
3. \*Phase-resolved frequency-domain analysis of the photoemission spectra for photoexcited  $1T\text{-TaS}_2$  in the Mott insulating charge density wave state: Q. Ren, T. Suzuki, T. Kanai, J. Itatani, S. Shin and K. Okazaki, *Appl. Phys. Lett.* **122**, 221902 (2023).
4. Comparative study of photoelectron momentum distributions from Kr and  $\text{CO}_2$  near a backward rescattering caustic by carrier-envelope-phase mapping: T. Mizuno, T. Yang, T. Kurihara, N. Ishii, T. Kanai, O. I. Tolstikhin, T. Morishita and J. Itatani, *Phys. Rev. A* **107**, 033101 (2023).
5. Highly CEP-stable optical parametric amplifier at 2  $\mu\text{m}$  with a few-cycle duration and 100 kHz repetition rate: T. Kurihara, T. Yang, T. Mizuno, T. Kanai and J. Itatani, *Opt. Express* **31**, 11649 (2023).
6. ‡100-mJ class, sub-two-cycle, carrier-envelope phase-stable dual-chirped optical parametric amplification: L. Xu, B. Xue, N. Ishii, J. Itatani, K. Midorikawa and E. J. Takahashi, *arXiv* **2202**, 03658 (2023).
7. †‡Three-wave mixing of anharmonically coupled magnons: Z. Zhang, F. Y. Gao, J. B. Curtis, Z.-J. Liu, Y.-C. Chien, A. von Hoegen, T. Kurihara, T. Suemoto, P. Narang, E. Baldini and K. A. Nelson, *arXiv* **2301**, 12555 (2023).
8. ‡Ultrafast spontaneous spin switching in an antiferromagnet: M. A. Weiss, A. Herbst, J. Schlegel, T. Dannegger, M. Evers, A. Donges, M. Nakajima, A. Leitenstorfer, S. T. B. Goennenwein, U. Nowak and T. Kurihara, *arXiv* **2301**, 02006 (2023).
9. †Real-time observation of the Woodward–Hoffmann rule for 1,3-cyclohexadiene by femtosecond soft X-ray transient absorption: T. Sekikawa, N. Saito, Y. Kurimoto, N. Ishii, T. Mizuno, T. Kanai, J. Itatani, K. Saita and T. Taketsugu, *Phys. Chem. Chem. Phys.* **25**, 8497 (2023).
10. †\*Direct observation of multiple conduction-band minima in high-performance thermoelectric SnSe: M. Okawa, Y. Akabane, M. Maeda, G. Tan, L.-D. Zhao, M. G. Kanatzidis, T. Suzuki, M. Watanabe, J. Xu, Q. Ren, M. Fujisawa, T. Kanai, J. Itatani, S. Shin, K. Okazaki, N. L. Saini and T. Mizokawa, *Scripta Materialia* **223**, 115081 (2023).
11. Discovery of ultrafast spontaneous spin switching in an antiferromagnet by femtosecond noise correlation spectroscopy: M. A. Weiss, A. Herbst, J. Schlegel, T. Dannegger, M. Evers, A. Donges, M. Nakajima, A. Leitenstorfer, S. T. B. Goennenwein, U. Nowak and T. Kurihara, *Nature Commun.* **14**, 7651(1-9) (2023).
12. †‡Observation of terahertz-induced dynamical spin canting in orthoferrite magnon by magnetorefractive probing: T. Kurihara, M. Bamba, H. Watanabe, M. Nakajima and T. Suemoto, *Commun Phys* **6**, 51 (2023).
13. \*Observation of Terahertz Spin Hall Conductivity Spectrum in GaAs with Optical Spin Injection: T. Fujimoto, T. Kurihara, Y. Murotani, T. Tamaya, N. Kanda, C. Kim, J. Yoshinobu, H. Akiyama, T. Kato and R. Matsunaga, *Phys. Rev. Lett.* **132**, 016301 (2024).
14. 超高速光パルスによる強誘電体の光制御(「光と物質の量子相互作用ハンドブック」第3編 第9章): 沖本 洋一, 板谷 治郎, 堀内左 智雄, (エヌ・ティー・エス, 東京都千代田区, 2023).
15. 高強度レーザーとアト秒科学 (解説): 板谷 治郎, 「UTokyo Focus」, 東京大学, (東京大学, 東京都文京区, 2023).
16. 高強度レーザーとアト秒科学 (解説): 板谷 治郎, 「現代化学」, 株式会社東京化学同人, (株式会社東京化学同人, 東京都文京区, 2023), 28-30.

† Joint research with outside partners.

- 2023年ノーベル物理学賞：Pierre Agostini氏, Ferenc Krausz氏, Anne L'Huillier氏 - 物質中の電子ダイナミクスを研究するためのアト秒パルス光の生成に関する実験的手法の業績 (学界ニュース)：板谷 治郎, 「日本物理学会誌」, 日本物理学会, (日本物理学会, 東京都文京区, 2024), 36.
- 高繰り返しアト秒光源の開発とその応用 (解説・「高次高調波とアト秒光科学の将来」特集)：板谷 治郎, 「月刊オプトロニクス」, 株式会社オプトロニクス社, (株式会社オプトロニクス社, 2024), 153-158.

## Kondo group

We revealed the semiconducting electronic structure of the ferromagnetic spinel  $\text{HgCr}_2\text{Se}_4$  and determined the phase diagram of the lightly doped high-Tc cuprate superconductors with disorder removed via observing six-layered cuprates.

- \*Semiconducting Electronic Structure of the Ferromagnetic Spinel  $\text{HgCr}_2\text{Se}_4$  Revealed by Soft-X-Ray Angle-Resolved Photoemission Spectroscopy: H. Tanaka, A. V. Telegin, Y. P. Sukhorukov, V. A. Golyashov, O. E. Tereshchenko, A. N. Lavrov, T. Matsuda, R. Matsunaga, R. Akashi, M. Lippmaa, Y. Arai, S. Ideta, K. Tanaka, T. Kondo and K. Kuroda, *Phys. Rev. Lett.* **130**, 186402 (1-6) (2023).
- \*Nodeless electron pairing in  $\text{CsV}_3\text{Sb}_5$ -derived kagome superconductors: Y. Zhong, J. Liu, X. Wu, Z. Guguchia, J. -X. Yin, A. Mine, Y. Li, S. Najafzadeh, D. Das, C. Mielke, R. Khasanov, H. Luetkens, T. Suzuki, K. Liu, X. Han, T. Kondo, J. Hu, S. Shin, Z. Wang, X. Shi, Y. Yao and K. Okazaki, *Nature* **617**, 488 (2023).
- \*Testing electron-phonon coupling for the superconductivity in kagome metal  $\text{CsV}_3\text{Sb}_5$ : Y. Zhong, S. Li, H. Liu, Y. Dong, K. Aido, Y. Arai, H. Li, W. Zhang, Y. Shi, Z. Wang, S. Shin, H. N. Lee, H. Miao, T. Kondo and K. Okazaki, *Nat. Commun.* **14**, 1945 (2023).
- †\*Unveiling phase diagram of the lightly doped high-Tc cuprate superconductors with disorder removed: K. Kurokawa, S. Isono, Y. Kohama, S. Kunisada, S. Sakai, R. Sekine, M. Okubo, M. D. Watson, T. K. Kim, C. Cacho, S. Shin, T. Tohyama, K. Tokiwa and T. Kondo, *Nat Commun* **14**, 4064 (2023).
- \*Broken Screw Rotational Symmetry in the Near-Surface Electronic Structure of *AB*-Stacked Crystals: H. Tanaka, S. Okazaki, M. Kobayashi, Y. Fukushima, Y. Arai, T. Iimori, M. Lippmaa, K. Yamagami, Y. Kotani, F. Komori, K. Kuroda, T. Sasagawa and T. Kondo, *Phys. Rev. Lett.* **132**, 136402 (1-6) (2024).

## Matsunaga group

We have studied light-matter interactions and light-induced nonequilibrium phenomena in solids by utilizing terahertz (THz) pulse. By using polarization-resolved THz spectroscopy, we have reported ultrafast dynamics of the anomalous Hall effect in a magnet with sub-100 fs time resolution for the first time. We also observed the light-induced anomalous Hall effect in a Dirac semimetal and succeeded in providing classification of the competing mechanisms. Our THz polarimetry technique offers a unique pathway to disentangle the microscopic mechanisms of anomalous transport in solids.

- \*Disentangling the Competing Mechanisms of Light-Induced Anomalous Hall Conductivity in Three-Dimensional Dirac Semimetal: Y. Murotani, N. Kanda, T. Fujimoto, T. Matsuda, M. Goyal, J. Yoshinobu, Y. Kobayashi, T. Oka, S. Stemmer and R. Matsunaga, *Phys. Rev. Lett.* **131**, 096901 (2023).
- \*Semiconducting Electronic Structure of the Ferromagnetic Spinel  $\text{HgCr}_2\text{Se}_4$  Revealed by Soft-X-Ray Angle-Resolved Photoemission Spectroscopy: H. Tanaka, A. V. Telegin, Y. P. Sukhorukov, V. A. Golyashov, O. E. Tereshchenko, A. N. Lavrov, T. Matsuda, R. Matsunaga, R. Akashi, M. Lippmaa, Y. Arai, S. Ideta, K. Tanaka, T. Kondo and K. Kuroda, *Phys. Rev. Lett.* **130**, 186402 (1-6) (2023).
- \*Ultrafast Dynamics of Intrinsic Anomalous Hall Effect in the Topological Antiferromagnet  $\text{Mn}_3\text{Sn}$ : T. Matsuda, T. Higo, T. Koretsune, N. Kanda, Y. Hirai, H. Peng, T. Matsuo, N. Yoshikawa, R. Shimano, S. Nakatsuji and R. Matsunaga, *Phys. Rev. Lett.* **130**, 126302 (2023).
- ディラック半金属  $\text{Cd}_3\text{As}_2$  における赤外広帯域超高速応答とスローライト生成：室谷 悠太, 神田 夏輝, 松永 隆佑, *固体物理* **58**, 457 (2023).
- \*Jitter correction for asynchronous optical sampling terahertz spectroscopy using free-running pulsed lasers: M. Nakagawa, N. Kanda, T. Otsu, I. Ito, Y. Kobayashi and R. Matsunaga, *Opt. Express* **31**, 19371 (2023).
- \*Gapless detection of broadband terahertz pulses using a metal surface in air based on field-induced second-harmonic generation: S. Tanaka, Y. Murotani, S. A. Sato, T. Fujimoto, T. Matsuda, N. Kanda, R. Matsunaga and J. Yoshinobu, *Applied Physics Letters* **122**, 251101 (6 pages) (2023).
- \*Pump-probe spectroscopy for non-equilibrium condensed matter: R. Matsunaga and K. Okazaki, *Encyclopedia of*

---

\* Joint research among groups within ISSP.

8. \*Observation of Terahertz Spin Hall Conductivity Spectrum in GaAs with Optical Spin Injection: T. Fujimoto, T. Kurihara, Y. Murotani, T. Tamaya, N. Kanda, C. Kim, J. Yoshinobu, H. Akiyama, T. Kato and R. Matsunaga, *Phys. Rev. Lett.* **132**, 016301 (2024).
9. 3次元ディラック半金属によるテラヘルツ高次高調波発生：松永 隆佑，神田 夏輝，池田 達彦，日本物理学会誌 **79**, 12 (2024).
10. 光誘起異常ホール効果を解き明かすテラヘルツ偏光計測：室谷 悠太，神田 夏輝，松永 隆佑，光アライアンス **35**, 44 (2024).
11. \*Anomalous Hall Transport by Optically Injected Isospin Degree of Freedom in Dirac Semimetal Thin Film: Y. Murotani, N. Kanda, T. Fujimoto, T. Matsuda, M. Goyal, J. Yoshinobu, Y. Kobayashi, T. Oka, S. Stemmer and R. Matsunaga, *Nano Lett.* **24**, 222 (2024).
12. Time-domain characterization of electric field vector in multi-terahertz pulses using polarization-modulated electro-optic sampling: N. Kanda, M. Nakagawa, Y. Murotani and R. Matsunaga, *Opt. Express* **32**, 1576 (2024).
13. 「半金属」、光と物質の量子相互作用ハンドブック (監修 荒川泰彦) 第3篇 第11章：松永 隆佑，森本 高裕，(NTS, 2023).

## Okazaki group

We have investigated the superconducting-gap structures of unconventional superconductors by a low-temperature and high-resolution laser ARPES apparatus and transient electronic structures in photo-excited non-equilibrium states by a time-resolved ARPES apparatus using EUV and SX lasers. In the academic year 2023, we have successfully observed the superconducting gap in a pristine sample of the Kagome superconductor CsV<sub>3</sub>Sb<sub>5</sub> by high-resolution laser ARPES. In addition, we have successfully observed the pump-wavelength-dependent photoexcited electron dynamics in a rare-earth trichalcogenide material exhibiting a CDW by HHG laser time-resolved ARPES.

1. †\*Quasi One-Dimensional Band Structure of Photoinduced Semimetal Phase of Ta<sub>2</sub>Ni<sub>1-x</sub>Co<sub>x</sub>Se<sub>5</sub> (x = 0.0 and 0.1): T. Mitsuoka, Y. Takahashi, T. Suzuki, M. Okawa, H. Takagi, N. Katayama, H. Sawa, M. Nohara, M. Watanabe, J. Xu, Q. Ren, M. Fujisawa, T. Kanai, J. Itatani, K. Okazaki, S. Shin and T. Mizokawa, *J. Phys. Soc. Jpn.* **92**, 023703 (2023).
2. †\*Temporal Evolution and Fluence Dependence of Band Structure in Photoexcited Ta<sub>2</sub>Ni<sub>0.9</sub>Co<sub>0.1</sub>Se<sub>5</sub> Probed by Time- and Angle-Resolved Photoemission Spectroscopy: Y. Takahashi, T. Suzuki, M. Hattori, M. Okawa, H. Takagi, N. Katayama, H. Sawa, M. Nohara, Y. Zhong, K. Liu, T. Kanai, J. Itatani, S. Shin, K. Okazaki and T. Mizokawa, *J. Phys. Soc. Jpn.* **92**, 064706 (2023).
3. †\*Observation of infrared interband luminescence in magnesium by femtosecond spectroscopy: T. Suemoto, S. Ono, A. Asahara, T. Okuno, T. Suzuki, K. Okazaki, S. Tani and Y. Kobayashi, *J. Appl. Phys.* **134**, 163105 (2023).
4. Pure nematic state in the iron-based superconductor FeSe: Y. Kubota, F. Nabeshima, K. Nakayama, H. Ohsumi, Y. Tanaka, K. Tamasaku, T. Suzuki, K. Okazaki, T. Sato, A. Maeda and M. Yabashi, *Phys. Rev. B* **108**, L100501 (2023).
5. \*Ultrafast control of the crystal structure in a topological charge-density-wave material: T. Suzuki, Y. Kubota, N. Mitsuishi, S. Akatsuka, J. Koga, M. Sakano, S. Masubuchi, Y. Tanaka, T. Togashi, H. Ohsumi, K. Tamasaku, M. Yabashi, H. Takahashi, S. Ishiwata, T. Machida, I. Matsuda, K. Ishizaka and K. Okazaki, *Phys. Rev. B* **108**, 184305 (2023).
6. \*Coexistence of Bulk-Nodal and Surface-Nodeless Cooper Pairings in a Superconducting Dirac Semimetal: X. P. Yang, Y. Zhong, S. Mardanya, T. A. Cochran, R. Chapai, A. Mine, J. Zhang, J. S'anchez-Barriga, Z. -J. Cheng, O. J. Clark, J. -X. Yin, J. Blawat, G. Cheng, I. Belopolski, T. Nagashima, S. Najafzadeh, S. Gao, N. Yao, A. Bansil, R. Jin, T. -R. Chang, S. Shin, K. Okazaki and M. Z. Hasan, *Phys. Rev. Lett.* **130**, 046402 (2023).
7. \*Phase-resolved frequency-domain analysis of the photoemission spectra for photoexcited 1T-TaS<sub>2</sub> in the Mott insulating charge density wave state: Q. Ren, T. Suzuki, T. Kanai, J. Itatani, S. Shin and K. Okazaki, *Appl. Phys. Lett.* **122**, 221902 (2023).
8. \*Nodeless electron pairing in CsV<sub>3</sub>Sb<sub>5</sub>-derived kagome superconductors: Y. Zhong, J. Liu, X. Wu, Z. Guguchia, J. -X. Yin, A. Mine, Y. Li, S. Najafzadeh, D. Das, C. Mielke, R. Khasanov, H. Luetkens, T. Suzuki, K. Liu, X. Han, T. Kondo, J. Hu, S. Shin, Z. Wang, X. Shi, Y. Yao and K. Okazaki, *Nature* **617**, 488 (2023).
9. \*Testing electron-phonon coupling for the superconductivity in kagome metal CsV<sub>3</sub>Sb<sub>5</sub>: Y. Zhong, S. Li, H. Liu, Y. Dong, K. Aido, Y. Arai, H. Li, W. Zhang, Y. Shi, Z. Wang, S. Shin, H. N. Lee, H. Miao, T. Kondo and K. Okazaki, *Nat. Commun.* **14**, 1945 (2023).

† Joint research with outside partners.

10. †\*Direct observation of multiple conduction-band minima in high-performance thermoelectric SnSe: M. Okawa, Y. Akabane, M. Maeda, G. Tan, L.-D. Zhao, M. G. Kanatzidis, T. Suzuki, M. Watanabe, J. Xu, Q. Ren, M. Fujisawa, T. Kanai, J. Itatani, S. Shin, K. Okazaki, N. L. Saini and T. Mizokawa, *Scripta Materialia* **223**, 115081 (2023).
11. \*Pump-probe spectroscopy for non-equilibrium condensed matter: R. Matsunaga and K. Okazaki, *Encyclopedia of Condensed Matter Physics, Second Edition* **1**, 981 (2023).

## Kimura group

In FY2023, we developed soft X-ray optics techniques using BL07LSU, which is now owned by RIKEN. In particular, we worked on the construction of a soft X-ray microscope using a total reflection mirror, the development of a lensless imaging technique, the ptychography method, and an ultrafast imaging technique using magnification imaging optics. Using such soft X-ray microscopes, we were engaged in the observation of mouse neurons and pancreatic cells and the development of operando measurement techniques for device evaluation.

1. †\* ウォルターミラーを利用した軟 X 線タイコグラフィ装置の開発：木村 隆志，竹尾 陽子，櫻井 快，古谷 登，江川 悟，山口 豪太，松澤 雄介，久米 健大，三村 秀和，志村 まり，大橋 治彦，松田 巖，原田 慈久，*放射光* **36**, 10 (2023).
2. Development of soft X-ray ptychography and fluorescence microscopy system using total-reflection wolter mirror and application to measurement of drug-treated mammalian cells: Y. Takeo, K. Sakurai, N. Furuya, K. Yoshinaga, T. Shimamura, S. Egawa, H. Kiuchi, H. Mimura, H. Ohashi, Y. Harada, M. Shimura and T. Kimura, *Journal of Electron Spectroscopy and Related Phenomena* **267**, 147380 (2023).
3. Fabrication of ultrashort sub-meter-radius x-ray mirrors using dynamic stencil deposition with figure correction: T. Shimamura, Y. Takeo, T. Kimura, F. Perrin, A. Vivo, Y. Senba, H. Kishimoto, H. Ohashi and H. Mimura, *Review of Scientific Instruments* **94**, 043102 (2023).
4. †\*Developing a Simple Scanning Probe System for Soft X-ray Spectroscopy with a Nano-focusing Mirror: H. Ando, M. Horio, Y. Takeo, M. Niibe, T. Wada, Y. Ando, T. Kondo, T. Kimura and I. Matsuda, *e-J. Surf. Sci. Nanotechnol.* **21**, 200 (2023).
5. Propagation-based phase-contrast imaging method for full-field X-ray microscopy using advanced Kirkpatrick–Baez mirrors: Y. Tanaka, J. Yamada, T. Inoue, T. Kimura, M. Shimura, Y. Kohmura, M. Yabashi, T. Ishikawa, K. Yamauchi and S. Matsuyama, *Optics Express* **31(16)**, 26135-26135 (2023).
6. Design of soft x-ray fluorescence microscopy beyond 100-nm spatial resolution with ultrashort Kirkpatrick-Baez mirror: T. Shimamura, Y. Takeo, F. Moriya, T. Kimura, M. Shimura, Y. Senba, H. Kishimoto, H. Ohashi, K. Shimba, Y. Jimbo, H. Mimura, H. Mimura, C. Morawe and A. M. Khounsary, *Advances in X-Ray/EUV Optics and Components XVII* **12240**, 20-33 (2023).
7. Soft-X-ray nanobeams formed by aberration-reduced elliptical mirrors with large numerical aperture.: T. Shimamura, Y. Takeo, T. Kimura, Y. Senba, H. Kishimoto, H. Ohashi and H. Mimura, *Optics express* **31(23)**, 38132-38145 (2023).
8. †\*Sub-photon accuracy noise reduction of a single shot coherent diffraction pattern with an atomic model trained autoencoder: T. Ishikawa, Y. Takeo, K. Sakurai, K. Yoshinaga, N. Furuya, Y. Inubushi, K. Tono, Y. Joti, M. Yabashi, T. Kimura and K. Yoshimi, *Opt. Express* **32**, 18301 (2024).
9. Ultracompact mirror device for forming 20-nm achromatic soft-X-ray focus toward multimodal and multicolor nanoanalyses: T. Shimamura, Y. Takeo, F. Moriya, T. Kimura, M. Shimura, Y. Senba, H. Kishimoto, H. Ohashi, K. Shimba, Y. Jimbo and H. Mimura, *Nat Commun* **15**, 665 (2024).

---

\* Joint research among groups within ISSP.

# Subject of Joint Research

2023年度 共同利用課題一覧（前期） / Joint Research List 2023 (First Term)

2023年度 共同利用課題一覧（後期） / Joint Research List 2023 (Latter Term)

2023年度 中性子科学研究施設 共同利用課題一覧 / Joint Research List of Neutron Scattering Research Project 2023

2023年度 軌道放射物性研究施設 共同利用課題一覧 / Joint Research List of Synchrotron Radiation Research Project 2023

2023年度 スーパーコンピュータ共同利用課題一覧 / Joint Research List of Supercomputer System 2023

2023年度 CCMSスパコン共用事業枠課題一覧 / Supercomputing Consortium for Computational Materials Science Project List of Supercomputer System 2023

## 2023年度 共同利用課題一覧（前期） / Joint Research List (First Term)

※実施課題一覧、所属は申請時のデータ

## 嘱託課題 / Comission Research Project

No.	課題番号	課題名	氏名	所属	分担者	Title	Name	Organization	Member of research project	担当所属
1	202304-CMBXX-0029	極低温における高感度磁化測定	清水 悠晴	東北大学金属材料研究所		High-sensitive magnetization measurements at ultra-low temperatures	Yusei Shimizu	Tohoku University, Institute for Materials Research		山下 穰
2	202304-CMBXX-0030	テンソルネットワークに基づく量子格子系ソルバ TeNeSの有温度度対応	森田 悟史	慶應義塾大学		Finite temperature support in tensor network solver TeNeS for quantum lattice models	Satoshi Morita	Keio University		川島 直輝
3	202211-CMBXX-0017	高圧下单結晶X線回折測定法の研究	江藤 徹二郎	久留米工業大学		Study of High Pressure X-ray diffraction measurements on single crystal	Tetsujiro Eto	Kurume Institute of Technology		上床 美也
4	202211-CMBXX-0018	無冷媒式マルチアンビル圧力装置の開発	高橋 博樹	日本大学		Development of refrigerant type Multi-anvil high pressure apparatus	Hiroki Takahashi	Nihon University		上床 美也
5	202211-CMBXX-0019	低次元有機導体における圧力効果の研究	糸井 充穂	東京都市大学		Study of pressure effect on the &nbsp;low dimension organic materials	Miho Itoi	Tokyo City University		上床 美也
6	202211-CMBXX-0020	3d遷移化合物に関する圧力効果の研究	鹿又 武	東北学院大学工学総合研究所		Pressure Effect on the 3d magnetic metals	Takeshi Kanomata	Research Institute for Engineering and Technology, Tohoku Gakuin University		上床 美也
7	202211-CMBXX-0021	希釈冷凍機温度における高圧下物性測定法の開発	松林 和幸	電気通信大学		Development of high pressure measurement technique under low temperature	Kazuyuki Matsubayashi	The University of Electro-Communications		上床 美也
8	202211-CMBXX-0023	高圧下で良質静水圧性維持する圧力媒体の開発	村田 恵三	大阪公立大学		Development of pressure medium for good hydrostatic under high pressure	Keizo Murata	Osaka Metropolitan University		上床 美也
9	202211-CMBXX-0024	極低温下での磁化測定法開発	鳥塚 潔	千葉工業大学		Development of magnetic measurement method	Kiyoshi Torizuka	Chiba Institute of Technology		上床 美也
10	202211-CMBXX-0025	圧力下極低温でのNMR測定法の研究	藤原 直樹	京都大学		Study of NMR measurement under high pressure	Naoki Fujiwara	Kyoto University		上床 美也
11	202211-CMBXX-0026	軽希土類化合物の良質単結晶試料の作製	繁岡 透	山口大学		High-quality single crystal samples growing of light rare earth compounds	Toru Shigeoka	Yamaguchi University		上床 美也
12	202211-CMBXX-0001	超強磁場におけるスピン格子強結合系の研究	池田 暁彦	電気通信大学		Study of the strongly spin-lattice-coupled systems in ultrahigh magnetic fields	Akihiko Ikeda	University of Electro-Communications		松田 康弘
13	202211-CMBXX-0003	トポロジカル絶縁体の探索	坂野 昌人	東京大学		Search for topological insulators	masato sakano	The University of Tokyo		近藤 猛
14	202211-CMBXX-0004	光電子分光法を用いた各種分子性結晶の電子状態の研究及び装置の低温化	木須 孝幸	大阪大学		Research on electron state of molecular crystals using photoemission spectroscopy	Kisu Takayuki	Osaka University, Graduate School of Engineering Science		近藤 猛
15	202211-CMBXX-0005	トポロジカル絶縁体の電子状態の解明	木村 昭夫	広島大学		Electronic-structure study of topological insulators	akio kimura	Hiroshima University, Graduate School of Advanced Science and Engineering		近藤 猛
16	202211-CMBXX-0006	レーザースピン角度分解光電子分光による表面電子状態の研究	矢治 光一郎	物質・材料研究機構		SARPES studies of atomic layer materials at surfaces	Koichiro Yaji	National Institute for Materials Science		近藤 猛
17	202211-CMBXX-0008	反強磁性を示す近似結晶の精密光電子分光測定	津田 俊輔	物質・材料研究機構		Laser-Photoemission Study on antiferromagnetic approximant crystals	Shunsuke Tsuda	National Institute for Materials Science		近藤 猛

18	202211-CMBXX-0009	光スピントロニクスに向けたスピン軌道ダイナミクスの研究	黒田 健太	広島大学		Studying spin-orbit dynamics for opt-spintronics	Kenta Kuroda	Hiroshim University		近藤 猛
19	202211-CMBXX-0015	高次高調波レーザー時間分解光電子分光を用いた強相関物質の研究	石坂 香子	東京大学		HHG laser time-resolve ARPES Study on strongly correlated materials	kyoko Ishizaka	The University of Tokyo		岡崎 浩三

一般課題 / General Research Project

No.	課題番号	課題名	氏名	所属	分担者	Title	Name	Organization	Member of research project	担当所員
1	202212-GNBXX-0047	傾角反強磁性を有する単一成分分子性導体における置換基修飾・元素置換効果の研究	横森 創	立教大学		Study of effects of substituent modulation and element substitution in single-component molecular conductors with canted antiferromagnetism	So Yokomori	Rikkyo University		森 初果
2	202212-GNBXX-0042	希釈冷凍機を用いたウラン系スピン三重項多重超伝導体に関する高感度磁化測定	清水 悠晴	東北大学金属材料研究所	福田 大翔	High-resolution magnetization measurements for uranium-based multiple spin-triplet superconductors using dilution refrigerators	Yusei Shimizu	Tohoku University, Institute for Materials Research	Hiroto Fukuda	山下 穰
3	202212-GNBXX-0043	極低温高感度磁化測定による局所対称性の破れたCe系多重超伝導の磁気特性と隠れた自由度の探索	清水 悠晴	東北大学金属材料研究所		Superconducting properties and search for hidden symmetry in Ce-based multiple-phase superconductor using high-resolution magnetization measurements	Yusei Shimizu	Tohoku University, Institute for Materials Research		山下 穰
4	202306-GNBXX-0137	有機導体を対象とした核磁気共鳴測定	宮川 和也	宮川 和也		Nuclear magnetic resonance measurements on organic conductors	Kazuya Miyagawa	The University of Tokyo		高木 里奈
5	202210-GNBXX-0001	Si(111) $\sqrt{3}\times\sqrt{3}$ 超構造基板上に成長したBi(110)超薄膜の電子状態	中辻 寛	東京工業大学	小森 文夫 河添 理央 織田 孝幸 吉田 陸馬	Electronic structure of Bi(110) ultra-thin films grown on Si(111) $\sqrt{3}\times\sqrt{3}$ superstructures	Kan Nakatsuji	Tokyo Institute of Technology	Fumio Komori Rio Kawazoe Orita Takayuki Yoshida Rikuma	吉信 淳
6	202210-GNBXX-0002	SiC基板上に成長したグラフェンへの金属原子インターカレーション	中辻 寛	東京工業大学	小森 文夫 片野 達貴 河添 理央	Intercalation of metal atoms into graphene grown on a SiC substrate	Kan Nakatsuji	Tokyo Institute of Technology	Fumio Komori KATANO TATSUKI Rio Kawazoe	吉信 淳
7	202210-GNBXX-0005	低速電子線回折による自己組織化カゴメ格子Mn3C6O6の構造の観測	金井 要	東京理科大学	馬上 怜奈 山崎 弘人	Observation of structure of self-assembled Kagome lattice Mn3C6O6 using low energy electron diffraction	Kaname Kanai	Tokyo University of Science	Rena Moue Hiroto Yamazaki	吉信 淳
8	202304-GNBXX-0065	透過 FTIR によるかんらん石単結晶表面での水素吸着状態解析	橘 省吾	東京大学	稲田 栞里	Transmission FTIR spectroscopy of hydrogen adsorbed on olivine single crystals	Shogo Tachibana	The University of Tokyo	Inada Shiori	吉信 淳

9	202211-GNBXX-0014	希土類金属間化合物および金属超伝導体の結晶育成と低温電子物性	海老原 孝雄	静岡大学	小林 和 荒川 尚也	Crystal Growth and Physical Properties at low temperatures in rare earth intermetallic compounds and metallic superconductors	Takao Ebihara	Shizuoka University	Kazu Kobayashi Naoya Arakawa	大谷 義近
10	202211-GNBXX-0053	金属表面上のプランベンの電子状態の精密測定	柚原 淳司	名古屋大学	大野 誠貴 前田 匠太	Electronic structure of plumbene on metal surfaces	Junji Yuhara	Nagoya University	ono masaki Shota Maeda	長谷川 幸雄
11	202211-GNBXX-0024	ホタル生物発光基質類似体seMpaiの蛍光測定	樋山 みやび	群馬大学	原田 昌拓	Fluorescence spectra of seMpai in aqueous solution	Miyabi Hiyama	Gunma University	masahiro harada	秋山 英文
12	202211-GNBXX-0037	窒素原子対による等電子トラップの共鳴励起	矢口 裕之	埼玉大学	高宮 健吾 我妻 利樹	Resonant excitation of isoelectronic traps formed by nitrogen pairs	Hiroyuki Yaguchi	Saitama University	Kengo Takamiya Wagatsuma Riki	秋山 英文
13	202212-GNBXX-0056	分子線エビタキシー法を用いて作製したGaN/AlN半導体超格子の フォトルミネッセンスによる光学特性評価	小柴 俊	香川大学	西山 心喬 前山 綾汰	Optical properties of GaN/AlN superlattices grown by MBE	Shyun Koshiba	Kagawa University	Mitaka Nishiyama Maeyama Ryota	秋山 英文
14	202210-GNBXX-0003	水素吸蔵させたPd薄膜の超伝導特性に関する研究	志賀 雅亘	九州大学	加藤 遼馬	Study of the superconducting properties on hydrogen absorbed Pd thin film	Masanobu Shiga	Kyushu University	Ryoma Kato	三輪 真嗣
15	202211-GNBXX-0035	インターカレート系Co <sub>2</sub> +ハニカム格子磁性体の物性解明	原口 祐哉	東京農工大学	伊藤 正明	Physical Properties of Intercalated Co <sub>2</sub> + Honeycomb Lattice Magnets	Yuya Haraguchi	Tokyo University of Agriculture and Technology	Masaaki Ito	広井 善二
16	202211-GNBXX-0008	電荷秩序型ダイマーモット絶縁体β <sup>-</sup> -(ET)2SF5CF2SO3の超高静水圧印加による超伝導相の探索	小林 拓矢	埼玉大学	谷口 弘三 佐藤 慧一 山田 英寿	Search for pressure-induced superconductivity by applying quasi-hydrostatic ultra-high pressures to charge-ordered dimer-Mott insulator β <sup>-</sup> -(ET)2SF5CF2SO3	Takuya Kobayashi	Saitama University	Hiromi Taniguchi Keichi Sato Yamada Hidetoshi	上床 美也
17	202211-GNBXX-0009	CeNiC <sub>2</sub> の結晶育成と物質評価 3	繁岡 透	山口大学	内間 清晴 (沖縄キリスト教学院・沖縄キリスト教短期大学)	Crystal growth and characterization of CeNiC <sub>2</sub> 3	Toru Shigeoka	Yamaguchi University	Kiyoharu Uchima (Okinawa Christian Institute Okinawa christian junior College)	上床 美也
18	202211-GNBXX-0010	擬三元化合物Ce <sub>1-x</sub> La <sub>x</sub> NiC <sub>2</sub> の結晶育成と物質評価 4	繁岡 透	山口大学	内間 清晴 (沖縄キリスト教学院・沖縄キリスト教短期大学)	Crystal growth and characterization of pseudo-ternary compounds Ce <sub>1-x</sub> La <sub>x</sub> NiC <sub>2</sub> 4	Toru Shigeoka	Yamaguchi University	Kiyoharu Uchima (Okinawa Christian Institute Okinawa christian junior College)	上床 美也
19	202211-GNBXX-0016	Eu <sub>2</sub> Ge <sub>2</sub> の圧力誘起価数揺動	大貫 惇睦	東京都立大学	本多 史憲 (九州大学アイソトープ統合安全管理センター) 松田 達磨 仲地 立	Pressure-induced Valence Fluctuation in Eu <sub>2</sub> Ge <sub>2</sub>	Yoshichika Onuki	Tokyo Metropolitan University	Fuminori Honda (Central Institute of Radioisotope Science and Safety Management, Kyushu University) Tatsuma D. Matsuda nakachi ryu	上床 美也
20	202211-GNBXX-0018	Eu <sup>2+</sup> 状態を持つEu-T-X化合物の高圧下における電子状態の研究	本多 史憲	九州大学アイソトープ統合安全管理センター	福田 大翔 (東北大学)	Electronic properties of Eu-T-X compounds with Eu <sup>2+</sup> state under high pressures	Fuminori Honda	Central Institute of Radioisotope Science and Safety Management, Kyushu University	Hiroto Fukuda (Tohoku University)	上床 美也

21	202211-GNBXX-0019	ウラン化合物の磁性の圧力効果	本多 史憲	九州大学アイソトープ統合安全管理センター	福田 大翔 (東北大学)	Effect of Pressure on the magnetism of uranium compounds	Fuminori Honda	Central Institute of Radioisotope Science and Safety Management, Kyushu University	Hiroto Fukuda (Tohoku University)	上床 美也
22	202211-GNBXX-0023	圧力媒体の固化点の再現性	村田 恵三	大阪公立大学		Reproducibility of the Solidification Pressure of Pressure Medium	Keizo Murata	Osaka Metropolitan University		上床 美也
23	202211-GNBXX-0026	Ni2In型強磁性体の自発磁化の圧力効果	安達 義也	山形大学		Pressure effects on the spontaneous magnetization for Ni2In-type ferromagnets	Yoshiya Adachi	Yamagata University		上床 美也
24	202211-GNBXX-0049	10GPa超の高圧発生可能なブリッジマンアンビル型クランプセルのための部品製作	大橋 政司	金沢大学	小笠原 悠太	Parts production for Bridgman-type high pressure clamp cell which can apply above 10 GPa	Masashi Ohashi	Kanazawa University	Yuta Ogasawara	上床 美也
25	202211-GNBXX-0050	単結晶CeMnSiの高圧下精密構造解析	川村 幸裕	室蘭工業大学	西山 紗恵	Structural Refinement of Single Crystal CeMnSi under pressure	Yukihiro Kawamura	Muroran Institute of Technology	Sae Nishiyama	上床 美也
26	202211-GNBXX-0052	多型化合物 RIr2Si2 (R=希土類)の磁気特性 8	内間 清晴	学校法人沖繩キリスト教学院・沖繩キリスト教短期大学	繁岡 透 (山口大学)	Magnetic characteristics of polymorphic compounds RIr2Si2 (R=Rare earth) 8	Kiyoharu Uchima	Okinawa Christian Institute Okinawa christian junior College	Toru Shigeoka (Yamaguchi University)	上床 美也
27	202212-GNBXX-0029	ホイスラー化合物Fe3-xMnxSiの圧力下磁気相転移	廣井 政彦	鹿児島大学	高本 翼	Magnetic phase transitions under pressure in Heuser compounds Fe3-xMnxSi	Masahiko HIROI	Kagoshima University	Tsubasa Takamoto	上床 美也
28	202212-GNBXX-0030	単結晶X線構造解析による金属有機構造体 Cu3(btc)2へのイオン液体充填効果の解明	木下 健太郎	東京理科大学	大平 一路	Elucidating confinement effect of ionic liquids in metal-organic framework Cu3(btc)2 using single crystal X-ray diffraction analysis	Kentaro Kinoshita	Tokyo University of Science	Ichiro Ohira	上床 美也
29	202212-GNBXX-0031	不定比化合物ErCr <sub>x</sub> Ge <sub>2</sub> の単結晶育成	藤原 哲也	山口大学	新谷 令和	Single Crystal growth of non stoichiometric compounds ErCr <sub>x</sub> Ge <sub>2</sub>	Tetsuya Fujiwara	Yamaguchi University	reo niya	上床 美也
30	202212-GNBXX-0032	不定比化合物HoCr <sub>x</sub> Ge <sub>2</sub> 単結晶の磁化測定	藤原 哲也	山口大学	新谷 令和	Magnetization measurements of non stoichiometric HoCr <sub>x</sub> Ge <sub>2</sub> single crystals	Tetsuya Fujiwara	Yamaguchi University	reo niya	上床 美也
31	202212-GNBXX-0048	極低温磁化測定用圧力セルの開発と非従来型超伝導体への応用	清水 悠晴	東北大学金属材料研究所	福田 大翔	Development of high-pressure cell for low-temperature dc magnetization measurements and application to unconventional superconductors	Yusei Shimizu	Tohoku University, Institute for Materials Research	Hiroto Fukuda	上床 美也
32	202212-GNBXX-0054	高スピン分極ホイスラー合金における圧力誘起量子臨界現象の探索	重田 出	鹿児島大学	青島 英樹	Search for the pressure-induced quantum critical phenomenon in highly spin-polarized Heusler alloys	Iduru Shigeta	Kagoshima University	Aoshima Hideki	上床 美也
33	202303-GNBXX-0058	S置換したFeSeの高圧低温NMR測定	藤原 直樹	京都大学	Yu Zhongyu	NMR studies on S-substituted FeSe at high pressures and low temperatures	Naoki Fujiwara	Kyoto University	Zhongyu Yu	上床 美也
34	202304-GNBXX-0063	超高压下量子振動効果測定装置の開発	菅原 仁	神戸大学	松林 和幸 (電気通信大学) 藤田 拓也	Development of the quantum oscillation measuring system under the ultra high pressure	Hitoshi Sugawara	Kobe university	Kazuyuki Matsubayashi (The University of Electro-Communications) Takuya Komoda	上床 美也
35	202306-GNBXX-0138	電荷秩序型ダイマート絶縁体β'-(ET)2SF5CF2SO3の超静水圧印加による超伝導相の探索 (II)	小林 拓矢	埼玉大学	谷口 弘三 佐藤 慧一 山田 英寿	Search for pressure-induced superconductivity by applying quasi-hydrostatic ultra-high pressures to charge-ordered dimer-Mott insulator β'-(ET)2SF5CF2SO3 (II)	Takuya Kobayashi	Saitama University	Hiromi Taniguchi Keiichi Sato Yamada Hidetoshi	上床 美也

36	202306-GNBXX-0140	単結晶Eu3Bi2S4F4の高圧下物性測定	石垣 賢卯	東京理科大学		Measurement of single crystal Eu3Bi2S4F4 under high pressure	Kento Ishigaki	Tokyo University of Science		上床 美也
37	202211-GNBXX-0006	新規トポロジカル磁性半金属の合成と磁気構造の解明	車地 崇	東京大学	有馬 孝尚 徳永 祐介 上野 正人	Magnetic structure analysis of novel magnetic topological semimetals	Takashi Kurumaji	The University of Tokyo	Taka-hisa Arima Yusuke Tokunaga Masato Ueno	益田 隆嗣
38	202211-GNBXX-0013	3元系におけるレーザー誘起合金化のバルス時間幅依存性	富田 卓朗	徳島大学	関 宏都	Pulse duration dependence of laser induced 3-elemental alloy	Takuro Tomita	Tokushima University	Hiroto Seki	小林 洋平
39	202211-GNBXX-0015	ダイヤモンド上に蒸着した鉄薄膜におけるレーザー誘起相変態	岡田 達也	徳島大学	岸田 崇秀	Laser-induced phase transformation of iron thin film deposited on diamond	Tatsuya OKADA	Tokushima University	Kishida Takahide	小林 洋平
40	202211-GNBXX-0020	次世代レーザーとレーザー加工の基礎技術研究	吉富 大	産業技術総合研究所	高田 英行 奈良崎 愛子 小川 博嗣 澁谷 達則 佐藤 大輔 黒田 隆之助 田中 真人 丸 征那	Basic research on next generation laser systems and laser machining technology	Dai Yoshitomi	National Institute of Advanced Industrial Science and Technology	Takada Hideyuki Aiko Narazaki Hiroshi Ogawa Tatsunori Shibuya Daisuke Satoh Ryunosuke Kuroda Masahito Tanaka Sena Maru	小林 洋平
41	202211-GNBXX-0021	熱可塑性高分子におけるレーザー照射による微視的結晶化度の制御	山口 誠	秋田大学		Control of Microscopic Crystallinity in Thermoplastic Polymers by Laser Irradiation	Yamaguchi Makoto	Akita University		小林 洋平
42	202212-GNBXX-0044	イメージングのためのファイバーレーザーの作製	大間知 潤子	関西学院大学		Development of fiber laser for optical imaging	Junko Omachi	Kwansei Gakuin University		小林 洋平
43	202212-GNBXX-0045	紫外光レーザー光源を用いた加工応用研究	藤本 靖	千葉工業大学		Research on laser processing application by ultraviolet laser light source	Yasushi Fujimoto	Chiba Institute of Technology		小林 洋平
44	202211-GNBXX-0011	高分解能レーザー励起光電子顕微鏡を用いた鉄系超伝導体の電子ネマティック状態の実空間観察VII	影山 通一	東京大学	大西 朝登	Real-space observation of electronic nematicity in iron-based superconductors by using a high-resolution laser photoemission electron microscope VII	Yoichi Kageyama	The University of Tokyo	Asato Onishi	岡崎 浩三
45	202211-GNBXX-0036	HfO2系強誘電体キャパシタの信頼性向上に向けた破壊現象の解析	糸矢 祐喜	東京大学		Analysis of Break-down Phenomena for Improving the Reliability of Ferroelectric HfO2&nbsp;Capacitors	Yuki Itoya	The University of Tokyo		岡崎 浩三
46	202304-GNBXX-0061	カロリメトリによる金属ナノ構造の赤外吸収率測定	末元 徹	電気通信大学	森野 春樹	Measurement of infrared absorptivity on metal nanostructures by calorimetry	Suemoto Tohru	The University of Electro-Communications	Haruki Morino	岡崎 浩三
47	202304-GNBXX-0062	カルシウム挿入グラフェンの電子格子相互作用の研究	一ノ倉 聖	東京工業大学	中村 達哉 秋山 亮介	Study of electron-phonon interaction in Ca-intercalated graphene	Satoru Ichinokura	Tokyo Institute of Technology	Tatsuya Nakamura Ryosuke Akiyama	岡崎 浩三
48	202304-GNBXX-0060	酸素アニール処理によって過剰ホールドープしたBi(Pb)2223 相超伝導体のホール係数測定	神戸 士郎	山形大学	内藤 聖羅 加藤 貴大 萩野 拓哉	Hall coefficient measurement of Bi(Pb)2223 superconductors over-doped by oxygen annealing	Shiro Kambe	Graduate School of Science and Engineering, Yamagata University	Seira Naito Takahiro Kato OGINO TAKUYA	量子物質ナノ構造ラボ運営委員会 (橋坂昌幸)
49	202304-GNBXX-0064	宙吊りグラフェン素子の作製と伝導測定	原 正大	熊本大学	堤 康二郎	Fabrication and transport measurement of suspended graphene devices	Masahiro Hara	Kumamoto University	Tsutsumi Kojiro	量子物質ナノ構造ラボ運営委員会 (橋坂昌幸)

No.	課題番号	課題名	氏名	所属	分担者	Title	Name	Organization	Member of research project	担当実験室
1	202211-MCBXG-0017	超臨界水熱法によるBaTiO <sub>3</sub> 微粒子合成における粒径と欠陥の制御	秋月 信	東京大学	徐 思キ	Synthesis and growth control of BaTiO <sub>3</sub> by supercritical hydrothermal method	Makoto Akizuki	The University of Tokyo	SIQI XU	化学分析室
2	202211-MCBXG-0013	超臨界メタノールと固体塩基触媒を用いたバイオディーゼル燃料合成	秋月 信	東京大学	東郷 宣弘	Synthesis of biodiesel fuels in supercritical methanol using solid base catalysts	Makoto Akizuki	The University of Tokyo	Nobuhiro TOGO	X線測定室
3	202212-MCBXG-0007	層状化合物における新規トポロジカル量子相の探索	水上 雄太	東北大学	大野 綾太郎	Investigation for novel topological quantum phases in layered compounds	Yuta Mizukami	Tohoku University	ryotaro ono	X線測定室
4	202212-MCBXG-0030	Mn <sub>3</sub> WO <sub>6</sub> の磁気強誘電性の起源	有馬 孝尚	東京大学	徳永 祐介 虎頭 大輔 西田 祥太 YAN ZHICHEN	Spin-driven Ferroelectricity in Mn <sub>3</sub> WO <sub>6</sub>	Taka-hisa Arima	The University of Tokyo	Yusuke Tokunaga Koto Daisuke Shota Nishida ZHICHEN YAN	X線測定室
5	202212-MCBXG-0033	キタエフ量子スピン液体候補物質の大型単結晶合成と物性評価	橋本 顕一郎	東京大学	今村 薫平 ファン センジェ 劉 蘇鵬 吉田 悠生 難波 隆一	Single crystal growth and characterization of Kitaev quantum spin liquid materials	Kenichiro Hashimoto	The University of Tokyo	Kumpei Imamura Shengjie Fang SUPENG LIU Yusei Yoshida Ryuichi Namba	X線測定室
6	202212-MCBXG-0037	高エントロピーカルコゲナイドの物性と結晶構造の関係の解明	山本 文子	芝浦工業大学		Relationship between physical properties and crystal structure in high-entropy chalcogenides	Ayako Yamamoto	Shibaura Institute of Technology		X線測定室
7	202212-MCBXG-0038	Co基ホイスラー合金におけるマルテンサイト変態材料の探索	重田 出	鹿児島大学	青島 英樹	Search for materials with the Martensitic transformation in Co-based Heusler alloys	Iduru Shigeta	Kagoshima University	Aoshima Hideki	X線測定室
8	202212-MCBXG-0040	トポロジカル磁性体を用いた機能性薄膜の開発	肥後 友也	東京大学	上杉 良太 朝倉 海寛 黒沢 駿一郎	Fabrication of thin films of topological magnets	Tomoya Higo	The University of Tokyo	Ryota Uesugi Mihiro Asakura Shunichiro Kurosawa	電子顕微鏡室
9	202212-MCBXG-0042	トポロジカルな電子構造に基づく機能性材料の探索	酒井 明人	東京大学	王 陽明 Feng Zili 梶原 悠人 黒沢 駿一郎 小池 祐樹 段 之直	Search for the functional material based on the topological electronic structure	Akito Sakai	The University of Tokyo	Yangming Wang Zili Feng yuto kajiwara Shunichiro Kurosawa Yuki Koike Zhiyi Duan	電子顕微鏡室
10	202210-MCBXG-0001	Nd <sub>1-x</sub> (Ba <sub>0.10</sub> Sr <sub>0.65</sub> Ca <sub>0.25</sub> ) <sub>x</sub> FeO <sub>3-δ</sub> ; (0.1 ≤ x ≤ 0.9) の高温における磁性と熱電特性に関する研究	中津川 博	横浜国立大学		Magnetism and thermoelectric properties at high temperature in Nd <sub>1-x</sub> (Ba <sub>0.10</sub> Sr <sub>0.65</sub> Ca <sub>0.25</sub> ) <sub>x</sub> FeO <sub>3-δ</sub> ; (0.1 ≤ x ≤ 0.9)	Hiroshi Nakatsugawa	Yokohama National University		電磁気測定室
11	202211-MCBXG-0005	二次元酸化物の磁化率測定 IV	神戸 士郎	山形大学	荻野 拓哉	Magnetic susceptibility measurement of 2D oxides IV	Shiro Kambe	Graduate School of Science and Engineering, Yamagata University	OGINO TAKUYA	電磁気測定室
12	202212-MCBXG-0009	ホイスラー化合物での反強磁性の研究	廣井 政彦	鹿児島大学	高本 翼	Study on antiferromagnetism in Heusler compounds	Masahiko HIROI	Kagoshima University	Tsubasa Takamoto	電磁気測定室

13	202212-MCBXG-0010	ハニカム型磁性体の磁気熱輸送現象	有馬 孝尚	東京大学	車地 崇 上野 正人	Magneto-Thermal Transport in Honeycomb Magnets	Taka-hisa Arima	The University of Tokyo	Takashi Kurumaji Masato Ueno	電磁気測定室
14	202212-MCBXG-0011	低温で合成されたフラストレート磁性体の磁性	香取 浩子	東京農工大学	原口 祐哉 北村 昌大 伊藤 正明	Magnetism of frustrated magnetic materials synthesized at low temperatures	Hiroko Katori	Tokyo University of Agriculture and Technology	Yuya Haraguchi masahiro kitamura Masaaki Ito	電磁気測定室
15	202212-MCBXG-0012	鉄系超伝導体に対するアニール効果の検証	栗原 綾佑	東京理科大学	矢口 宏 小暮 琉介 太田 知孝	Annealing effect on iron-based superconductors	Ryosuke Kurihara	Tokyo University of Science	Hiroshi Yaguchi Ryusuke Kogure Ota Tomotaka	電磁気測定室
16	202212-MCBXG-0039	高スピン分極ホイスラー合金の磁気特性のスピンゆらぎ理論による解析に関する研究	重田 出	鹿児島大学	青島 英樹	Study on analysis of magnetic properties for highly spin-polarized Heusler alloys by the spin fluctuation theory	Iduru Shigeta	Kagoshima University	Aoshima Hideki	電磁気測定室
17	202211-MCBXG-0006	重希土類を含む充填スクテルダイト化合物の高圧合成と多極子物性	関根 ちひろ	室蘭工業大学	寺坂 聡志 長瀬 竜也 曾野 大翔 尾崎 蒼空	High-pressure synthesis and multipole properties of filled skutterudite compounds containing heavy rare earths	Chihiro Sekine	Muroran Institute of Technology	Satoshi Terasaka Tatsuya Nagase Hiroyuki Sono Sora Ozaki	高圧合成室
18	202212-MCBXG-0026	高温高圧下におけるFe-S-H三元系における水素原子の占有サイトと水素誘起体積膨張係数の解明	鍵 裕之	東京大学	高野 将大	Masahiro Takano	Hiroyuki Kagi	The University of Tokyo	Masahiro Takano	高圧合成室
19	202211-MCBXG-0015	亜臨界水と固体塩基触媒の組み合わせによる新規有機合成プロセスの開発	秋月 信	東京大学	王一琦	Development of novel organic synthesis process with a combination of subcritical water and solid base catalyst	Makoto Akizuki	The University of Tokyo	Yiqi Wang	X線測定室 化学分析室
20	202212-MCBXG-0008	高圧合成法を用いたハニカム化合物Ru(Br <sub>1-x</sub> I <sub>x</sub> ) <sub>3</sub> 粉末試料の作製	今井 良宗	東北大学	佐藤 楓貴	High pressure synthesis of powder samples of honeycomb compounds Ru(Br <sub>1-x</sub> I <sub>x</sub> ) <sub>3</sub>	Yoshinori Imai	Tohoku university	Fuki Sato	X線測定室 高圧合成室
21	202212-MCBXG-0025	水素化反応に用いるメソポーラスシリカ上に担持したイオン液体含有バイメタル触媒の合成と構造的特徴	クスマワティ エツティヌル リア	岩手大学		Synthesis and structural characterization of bimetallic catalysts containing ionic liquids on mesoporous silica for hydrogenation reaction	Etty Nurlia Kusumawati	Iwate University		X線測定室
22	202212-MCBXG-0046	合金ナノ粒子のキャラクタリゼーション	佐々木 岳彦	東京大学	張 凱朝 徐 浩然 胡 寧睿	Characterization of alloy nanoparticles	Takehiko Sasaki	The University of Tokyo	KAICHAO ZHANG Haoran Xu Hu Ningrui	X線測定室 電子顕微鏡室 光学測定室
23	202211-MCBXG-0044	圧力誘起超伝導-絶縁体転移を示す9族スピネル化合物の構造物性研究	片山 尚幸	名古屋大学	小島 慶太 江見 方敏 久保 泰星	Structural properties of group 9 spinel compounds showing pressure-induced superconductor-insulator transition	Naoyuki Katayama	Nagoya University	Keita Kojima Masatoshi Emi taisei kubo	X線測定室 電磁気測定室
24	202211-MCBXG-0045	低温で直線型三量体をもつRuX (X = P,As,Sb)の高圧相局所構造解析	片山 尚幸	名古屋大学	小島 慶太	Local structure analysis of RuX (X = P,As,Sb) with linear trimer at low temperature in high pressure phase	Naoyuki Katayama	Nagoya University	Keita Kojima	X線測定室 電磁気測定室

25	202211-MCBXG-0031	フェロアキシアル物質の合成と試料評価	木村 剛	東京大学	林田 健志 山岸 茂直 諸見里 真人 吉岡 知輝 永井 隆 木村 健太 (大阪公立大 学) 梶田 通一	Synthesis and characterization of ferroaxial materials	Tsuyoshi Kimura	The University of Tokyo	Takeshi Hayashida Shigetada Yamagishi Masato Moromizato Tomoki Yoshioka Takayuki Nagai Kenta Kimura (Osaka Metropolitan University) Yoichi Kajita	X線測定室 物質合成室
26	202211-MCBXG-0016	連続式超臨界水熱合成法による銀ナノ粒子の調製	秋月 信	東京大学	李 琰琛	Preparation Of Silver Nanoparticles Via Continuous Supercritical Hydrothermal Synthesis Method	Makoto Akizuki	The University of Tokyo	LI Yanchen	化学分析室 電子顕微鏡室 X線測定室
27	202212-MCBXG-0023	亜臨界水及び超臨界水中におけるPLA樹脂のガス化に関する研究	布浦 鉄兵	東京大学環境安全研究センター	WU Fan	Gasification of PLA in subcritical and supercritical water	Teppei Nunoura	Environmental Science Center, The University of Tokyo	WU FAN	電子顕微鏡室 X線測定室
28	202212-MCBXG-0024	高炉スラグ系改質材によるメッキ廃液からの重金属イオンの除去	布浦 鉄兵	東京大学環境安全研究センター	WANG Jiaqi	Removal of heavy metal ions from electroplating wastewater by blast furnace slag based modified materials	Teppei Nunoura	Environmental Science Center, The University of Tokyo	WANG Jiaqi	電子顕微鏡室 X線測定室
29	202212-MCBXG-0020	リグニンの有用化合物への変換を可能にする固体触媒及び反応条件の検討	布浦 鉄兵	東京大学環境安全研究センター	堂脇 大志	Study on solid catalysts and reaction conditions for lignin conversion into valuable chemicals	Teppei Nunoura	Environmental Science Center, The University of Tokyo	Taishi Dowaki	電子顕微鏡室 X線測定室 化学分析室
30	202210-MCBXG-0002	遷移金属化合物の量体化近傍における電子状態の研究	平井 大悟郎	名古屋大学		Electronic states of transition metal compounds in the vicinity of molecular orbital crystallization	Daigorou Hirai	Nagoya University		電磁気測定室 高圧合成室
31	202211-MCBXG-0003	新規トポロジカル磁性半金属の合成と物性開拓	車地 崇	東京大学	有馬 孝尚 徳永 祐介 上野 正人	Synthesis of novel magnetic topological semimetals	Takashi Kurumaji	The University of Tokyo	Taka-hisa Arima Yusuke Tokunaga Masato Ueno	電磁気測定室 物質合成室
32	202212-MCBXG-0021	超臨界二酸化炭素合成二硫化モリブデンによる有機色素の光触媒分解に関する検討	布浦 鉄兵	東京大学環境安全研究センター	カン ジシン	Photocatalytic degradation of organic dyes by supercritical carbon dioxide processed molybdenum disulfide	Teppei Nunoura	Environmental Science Center, The University of Tokyo	HAN Zixin	物質合成室 化学分析室 光学測定室

物質合成・評価設備Uクラス / Materials Synthesis and Characterization U Class Research Project

No.	課題番号	課題名	氏名	所属	分担者	Title	Name	Organization	Member of research project	担当実験室
1	202308-MCBXU-0106	スマートソックスの歩行イベント検出	ファスティア ウーラー ジャ レッド	大学院工学系研究科 精密工学 専攻		Smart sock gait event detection	Jarred Fastier- Wooler	Department of Precision Engineering, Graduate School of Engineering		X線測定室
2	202303-MCBXU-0047	セラミックスナノ粒子の連続製造技術開発	陶 究	産業技術総合研究所		Development of continuous process for ceramics nanoparticles production	Kiwamu Sue	AIST		電子顕微鏡室
3	202303-MCBXU-0048	月資源現地利用を目指したレーザーによるアルミナ還元	高崎 大吾	東京大学	室原 昌弥 西村 将太郎 渡邊 真隆 峯松 涼 土屋 祐人	Laser alumina reduction toward utilization of lunar resources	Daigo Takasaki	The University of Tokyo	Murohara Masaya Shotaro Nishimura watanabe masataka Ryo Minematsu Tsuchiya Yuto	電子顕微鏡室

4	202303-MCBXU-0049	開殻・閉殻分子種を組み合わせた単一成分分子性導体・磁性体の合成とその単結晶中の元素組成比の解析	横森 創	立教大学		Synthesis and characterization of Single Component Molecular Conductors and Magnets from Open-Shell and Closed-Shell Molecular Species, and Elucidation of Elemental Composition Ratios in their Single Crystals	So Yokomori	Rikkyo University		電子顕微鏡室
5	202305-MCBXU-0051	カリウムに富むアルミニウム含有鉱物への高圧下での希ガス取り込み機構の解明	飯塚 理子	早稲田大学		Incorporation of noble gases into K-rich aluminous phase under lower mantle condition	Riko Iizuka-Oku	Waseda University		高圧合成室

国際超強磁場科学施設 / International MegaGauss Science Laboratory

No.	課題番号	課題名	氏名	所属	分担者	Title	Name	Organization	Member of reseach project	担当所員
1	202211-HMBXX-0012	重い電子系化合物が示す非従来型超伝導と量子臨界的挙動の相関	横山 淳	茨城大学	高橋 哲平	Relationship between unconventional superconductivity and quantum critical behavior in heavy-fermion compounds	Makoto Yokoyama	Ibaraki University	Teppeï Takahashi	金道 浩一
2	202211-HMBXX-0015	幾何学的フラストレート磁性体の強磁場磁化測定	菊池 彦光	福井大学		Magnetization measurements of the frustrated magnets	Hikomitsu Kikuchi	University of Fukui		金道 浩一
3	202211-HMBXX-0022	新しい硫化物フラストレート磁性体における強磁場物性	原口 祐哉	東京農工大学	北村 昌大	High Magnetic Field Properties in Sulfide Frustrate Magnets	Yuya Haraguchi	Tokyo University of Agriculture and Technology	masahiro kitamura	金道 浩一
4	202212-HMBXX-0020	トポロジカル近藤絶縁体YbB12と高圧合成希土類ホウ化物RBn (n=12, 25, 50, 66) の強磁場磁化と輸送特性	伊賀 文俊	茨城大学	上條 力	Magnetic and transport properties in high fields of topological Kondo insulator YbB12 and novel rare earth borides RBn (n=12, 25, 50, 66) produced by high pressure synthesis	Fumitoshi Iga	Ibaraki University	Kamijo Riki	金道 浩一
5	202212-HMBXX-0027	強磁場磁化測定によるNi2MnAl結晶の磁場促進規則化現象の解明	小林 領太	鹿児島大学		Study of field-enhanced atomic ordering phenomena in Ni2MnAl crystal by High field magnetization measurement	Ryota Kobayashi	Kagoshima university		金道 浩一
6	202303-HMBXX-0039	有機量子スピン液体物質の強磁場磁化測定	杉浦 菜理	東北大学 金属材料研究所	高橋 大典	High field magnetometry in organic quantum spin liquid system	Shiori Sugiura	Institute for Materials Research, Tohoku University	Daisuke Takahashi	金道 浩一
7	202305-HMBXX-0046	量子臨界ゆらぎがもたらす異常超伝導物性	横山 淳	茨城大学	并能 楓 高橋 哲平	Anomalous superconducting properties originating from quantum critical fluctuations	Makoto Yokoyama	Ibaraki University	Kaede Inoh Teppeï Takahashi	金道 浩一
8	202212-HMBXX-0021	トポロジカル近藤絶縁体YbB12と新規高圧合成RBn (n=12, 25, 50, 66) の100Tまでの強磁場磁化過程	伊賀 文俊	茨城大学		Magnetic properties in high fields of topological Kondo insulator YbB12 and novel rare earth borides RBn (n=12, 25, 50, 66) produced by high pressure synthesis	Fumitoshi Iga	Ibaraki University		松田 康弘
9	202303-HMBXX-0036	パルス強磁場と急冷を利用した準安定物質の探索	大池 広志	東京大学		Exploration of metastable materials with pulsed high magnetic field and rapid cooling	Hiroshi Oike	The University of Tokyo		松田 康弘
10	202211-HMBXX-0005	六方晶QS型鉄酸化物 Ba2Me1+xSn2+xFe10-2xO22 の強磁場磁気特性	神島 謙二	埼玉大学	原澤 秀明	Magnetic properties of hexagonal QS-type iron oxide Ba2Me1+xSn2+xFe10-2xO22 under high magnetic fields	Kenji Kamishima	Saitama University	Harasawa Hideaki	徳永 将史
11	202211-HMBXX-0007	鉄系超伝導体の磁気光学イメージングによる磁場分布の観測	矢口 宏	東京理科大学	小暮 琉介 栗原 綾佑 太田 知孝	Observations of magnetic-field distributions in iron-based superconductors using an MO imaging technique	Hiroshi Yaguchi	Tokyo University of Science	Ryusuke Kogure Ryosuke Kurihara Ota Tomotaka	徳永 将史

12	202211-HMBXX-0013	第一超伝導体における中間状態のダイナミクスの観察	井澤 公一	大阪大学	伏屋 雄紀 (電気通信大学)	Observation&nbsp;of the dynamics of intermediate states in type I superconductors	Koichi Izawa	Osaka university	Yuki Fuseya (University of Electro-Communications)	徳永 将史
13	202211-HMBXX-0025	超音波を軸とした複合物性測定による強相関電子系の強磁場中量子状態の探索	栗原 綾佑	東京理科大学	矢口 宏 小峰 智弥	Quantum states in strongly-correlated electron systems under high-magnetic fields by multiprobe measurements	Ryosuke Kurihara	Tokyo University of Science	Hiroshi Yaguchi Tomoya Komine	徳永 将史
14	202212-HMBXX-0017	低温で合成されたフラストレート磁性体の強磁場下での物性	香取 浩子	東京農工大学	原口 祐哉 久米田 理桜 若杉 和弘	Physical properties of frustrated magnetic materials synthesized at low temperatures under high magnetic fields	Hiroko Katori	Tokyo University of Agriculture and Technology	Yuya Haraguchir Rio Kumeda wakasugi kazuhiko	徳永 将史
15	202212-HMBXX-0030	キャリア濃度を制御したワイル電子系磁性体の量子振動	酒井 英明	大阪大学	近藤 雅哉 宮本 雄哉	Quantum transport for a carrier-density-controlled Weyl magnet	Hideaki Sakai	Osaka University	Masaki Kondo Yuya Miyamoto	徳永 将史
16	202212-HMBXX-0031	電子ダイナミクスを用いた分子結晶における磁場誘起極スイッチング	呉 樹旗	九州大学先端物質化学研究所	ZHANG XIAOPENG	Magnetic Field-Induced Polarization Switching in Molecular Crystals with Electron Dynamics	Shu-Qi Wu	Institute for Materials Chemistry and Engineering, Kyushu University	ZHANG XIAOPENG	徳永 将史
17	202303-HMBXX-0037	Magnetic structure and spin dynamics of distorted honeycomb BaNa <sub>2</sub> Co <sub>7</sub> Te <sub>3</sub> O <sub>18</sub>	Techathitinan Satayu	Mahidol University		Magnetic structure and spin dynamics of distorted honeycomb BaNa <sub>2</sub> Co <sub>7</sub> Te <sub>3</sub> O <sub>18</sub>	Satayu Techathitinan	Mahidol University		徳永 将史
18	202305-HMBXX-0089	カゴメ量子スピン液体における磁化プラトー状態の探索	末次 祥大	京都大学	浅場 智也	Magnetization plateau in a kagome quantum spin liquid	Shota Suetsugu	Kyoto University	Tomoya Asaba	徳永 将史
19	202306-HMBXX-0090	ハンダの超伝導状態における磁束トラップの観察	水口 佳一	東京都立大学	有馬 寛人	Observation of trapped magnetic flux in superconducting solder	Yoshikazu Mizuguchi	Tokyo Metropolitan University	Arima Hiroto	徳永 将史
20	202307-HMBXX-0091	光磁気ドメイン発達過程のKerr効果顕微鏡観察	所 裕子	筑波大学	長島 俊太郎	Observation of development of magnetic domain in photo-induced magnetization using Kerr effect microscopy	Hiroko Tokoro	University of Tsukuba	Shuntaro Nagashima	徳永 将史
21	202211-HMBXX-0003	金属超伝導体および強相関電子系の結晶育成と強磁場物性研究	海老原 孝雄	静岡大学	エスティアク アフメド 大窪 悠太 小林 和	Crystal growth and physical Properties at high magnetic fields in metallic superconductors and strongly correlated electron system	Takao Ebihara	Shizuoka University	Esteaque Ahmed Yuta Okubo Kazu Kobayashi	小濱 芳允
22	202303-HMBXX-0040	Quantum oscillation on CaAs <sub>3</sub> and YMn <sub>6</sub> Sn <sub>6</sub>	Jun Sung-Kim	POSTECH		Quantum oscillation on CaAs <sub>3</sub> and YMn <sub>6</sub> Sn <sub>6</sub>	Sung-Kim Jun	POSTECH		小濱 芳允
23	202303-HMBXX-0041	Magnetization Plateaus in a Pyrochlore Heisenberg Antiferromagnet	Marcelo Jaime	Los Alamos National Laboratory		Magnetization Plateaus in a Pyrochlore Heisenberg Antiferromagnet	Jaime Marcelo	Los Alamos National Laboratory		小濱 芳允

大阪大学大学院理学研究科附属先端強磁場科学研究センター / Center for Advanced High Magnetic Field Science, Graduate School of Science, Osaka University

No.	課題番号	課題名	氏名	所属	分担者	Title	Name	Organization	Member of research project	担当所属
1	202210-HMOXX-0011	RInCu <sub>4</sub> のパルス強磁場を利用した磁場温度相図の構築	和氣 剛	京都大学		Construction of magnetic field-temperature phase diagram using pulsed high magnetic field in RInCu <sub>4</sub>	Takeshi Waki	Kyoto University		萩原 政幸 (大阪大学)
2	202211-HMOXX-0002	Eu化合物の磁気異方性の研究	竹内 徹也	大阪大学	大貫 惇睦	Magnetic Anisotropy in Eu Compounds	Tetsuya Takeuchi	Osaka University	Yoshichika Onuki	萩原 政幸 (大阪大学)
3	202211-HMOXX-0004	強磁性ホイスラー合金Ni <sub>2</sub> (MnCr)Ga系合金の磁気的機能性の研究	左近 拓男	龍谷大学		Research on magnetic functionalities of Ni <sub>2</sub> (MnCr)Ga type Heusler alloys	Takuo Sakon	Ryukoku University		萩原 政幸 (大阪大学)

4	202211-HMOXX-0006	ナノ界面制御による異常ネルンスト係数増大	中村 芳明	大阪大学	石部 貴史 北浦 怜旺奈 小松原 祐樹	Enhancement of anomalous Nernst coefficient using the controlled nanoscale interfaces	Yoshiaki Nakamura	Osaka University	Takafumi Ishibe reona kitaura Komatsubara Yuki	萩原 政幸 (大阪大学)
5	202211-HMOXX-0008	偏光依存・強磁場ESR測定によるSr2CoSi2O7のелеクトロマグノン研究	赤木 暢	東北大学		Study of the electromagnon in Sr2CoSi2O7 by using the light-polarization dependence ESR measurement	Mitsuru Akaki	Tohoku University		萩原 政幸 (大阪大学)
6	202211-HMOXX-0028	パルス強磁場用極低温実験装置の開発	野口 悟	大阪公立大学		Development of the cryostat for pulsed high magnetic field	Satoru Noguchi	Osaka Metropolitan University		萩原 政幸 (大阪大学)
7	202211-HMOXX-0033	非従来型超伝導体微細構造のパルス強磁場下輸送特性	掛谷 一弘	京都大学		Transport measurements on micro-structured unconventional superconductors under pulsed high magnetic fields	Itsuhiro Kakeya	Kyoto University		萩原 政幸 (大阪大学)
8	202212-HMOXX-0016	S = 1/2 一次元Ising型反強磁性体CsCoCl3におけるストリング励起の光学選択則	木村 尚次郎	東北大学		Optical selection rule of the string excitation in the S = 1/2 one-dimensional Ising-like antiferromagnet CsCoCl3	Shojiro Kimura	Tohoku University		萩原 政幸 (大阪大学)
9	202212-HMOXX-0018	BaPt(As1-xSbx)における超伝導転移温度の非単調なx依存性の起源についての研究	工藤 一貴	大阪大学		Study on the origin of the non-monotonic x dependence of the superconducting transition temperature in BaPt(As1&dash;xSbx)	Kazutaka Kudo	Osaka University		萩原 政幸 (大阪大学)
10	202212-HMOXX-0019	PtBi2における化学ドーブによる超伝導増強の起源についての研究	工藤 一貴	大阪大学		Study on the origin of the enhanced superconductivity by chemical doping in PtBi2	Kazutaka Kudo	Osaka University		萩原 政幸 (大阪大学)
11	202212-HMOXX-0026	強いスピン軌道相互作用を活かした酸化物スピントロニクス	松野 丈夫	大阪大学	塩貝 純一 上田 浩平	Oxide spintronics utilizing strong spin-orbit coupling	Jobu Matsuno	Osaka University	Junichi Shiogai Kohei Ueda	萩原 政幸 (大阪大学)
12	202212-HMOXX-0029	ThCr2Si2型構造を有するEu系新物質の磁気相図の解明	酒井 英明	大阪大学		Study of magnetic phase diagram for ThCr2Si2-type Eu-based new compounds	Hideaki Sakai	Osaka University		萩原 政幸 (大阪大学)
13	202212-HMOXX-0032	2本鎖梯子銅錯体Cu(naphac)(OH)の磁性	本多 善太郎	埼玉大学		Magnetic properties of two-leg ladder copper complex Cu(naphac)(OH)	Zentaro Honda	Saitama University		萩原 政幸 (大阪大学)
14	202306-HMOXX-0055	一次元反強磁性体Henmiliteの強磁場ESR	石川 裕也	福井大学	藤井 裕 林 哉汰	High-Field ESR measurements of one-dimensional antiferromagnet Henmilite	Yuya Ishikawa	University of Fukui	Yutaka Fujii Kanata Hayashi	萩原 政幸 (大阪大学)

強磁場コラボラトリー / The High Magnetic Field Collaboratory

No.	課題番号	課題名	氏名	所属	分担者	Title	Name	Organization	Member of research project	担当所属
1	202212-HMCXX-0023	カゴメ磁性体において実現する新奇磁気状態の磁場制御とNMR測定による微視的機構解明	井原 慶彦	北海道大学大学院		High-field control and NMR study of exotic magnetic states in kagome magnets	Yoshihiko Ihara	Hokkaido University		小濱 芳允
2	202303-HMCXX-0034	Magnetic field phase diagram of the exotic superconductor UTe2	Marcenat Christophe	Interdisciplinary Research Institute of Grenoble (IRIG), Alternative Energies and Atomic Energy Commission (CEA)		Magnetic field phase diagram of the exotic superconductor UTe2	Christophe Marcenat	Interdisciplinary Research Institute of Grenoble (IRIG), Alternative Energies and Atomic Energy Commission (CEA)		小濱 芳允
3	202303-HMCXX-0035	パルス電流通電を用いた強磁場中超伝導特性測定手法の開発	土屋 雄司	東北大学		Development of the measurement for superconductor characterization under high field by using pulsed current	Tsuchiya Yuji	Tohoku University		小濱 芳允

4	202211-HMBXX-0001	ラジカル系錯体における多様な量子スピンモデルの強磁場物性	山口 博則	大阪公立大学		High-field magnetic properties of various quantum spin models in radical-based complexes	Hironori Yamaguchi	Osaka Metropolitan University		萩原 政幸
---	-------------------	------------------------------	-------	--------	--	------------------------------------------------------------------------------------------	--------------------	-------------------------------	--	-------

留学研究課題 / External Research Project Long / Short-term

No.	課題番号	課題名	氏名	所属	分担者	Title	Name	Organization	Member of research project	担当所属
1	202211-VSBXL-0001	新規ケージドルシフェリンの光開裂定量計測	中野 智哉	群馬大学		Study for photocleavage of new caged luciferin	Nakano Tomoya	Gunma University		秋山 英文
2	202211-VSBXL-0002	青色波長領域における発光量絶対値測定系の校正	倉田 洋佑	群馬大学		Calibration of bio/chemiluminescence spectrometer with cooled&nbsp;charge-coupled device (CCD) detector at blue wavelengths	KURATA YOSUKE	GUNMA UNIVERSITY		秋山 英文
3	202211-VSBXL-0005	酵素環境下における AkaLumine-oxy 体の分光学的研究	大澤 敬太	群馬大学院理工学府		Spectroscopic Study of AkaLumine-oxy form in an Enzymatic Environment	Osawa Keita	Gunma University		秋山 英文
4	202211-VSBXL-0006	UVレーザー及びLED光源によるD-Luciferin光破壊条件の探索	松永 大輝	群馬大学		Study for photo-breaching condition of D-luciferin using UV laser and LED light	Hiroki Matsunaga	Gunma University		秋山 英文
5	202212-VSBXL-0003	レーザー光によるクマリンケージドルシフェリンの光開裂実験	今西 勇輔	群馬大学		Photocleavage of coumarin caged luciferin by laser irradiation	Yusuke Imanishi	Gunma University		秋山 英文
6	202212-VSBXL-0004	超短パルスレーザー照射により誘起される微細構造変化の評価	高林 圭佑	秋田大学		Evaluation of structural changes induced by ultrashort pulsed laser	Keisuke Takabayashi	Akita University		小林 洋平

## 2023年度 共同利用課題一覧（後期） / Joint Research List (Latter Term)

※実施課題一覧、所属は申請時のデータ

## 嘱託課題 / Comission Research Project

No.	課題番号	課題名	氏名	所属	分担者	Title	Name	Organization	Member of reseach project	担当所属
1	202305-CMBXX-0073	マルチアンビル圧力発生装置の改良	高橋 博樹	日本大学		Improvement of multi-anvil pressure apparatus	Hiroki Takahashi	Nihon University		上床 美也
2	202305-CMBXX-0074	良質な静水圧力環境での物性測定法の開発	村田 恵三	大阪公立大学		Development of physical property measurement method in high-quality hydrostatic pressure environment	Keizo Murata	Osaka Metropolitan University		上床 美也
3	202305-CMBXX-0075	高圧下物性測定方法の開発	辺土 正人	琉球大学		Development of measurement system for physical properties under high pressure	Masato Hedo	University of the Ryukyus		上床 美也
4	202305-CMBXX-0076	単結晶試料の純良化方法の研究	繁岡 透	山口大学		Research on purification methods for single crystal&nbsp;	Toru Shigeoka	Yamaguchi University		上床 美也
5	202305-CMBXX-0077	圧力下NMR測定方法の開発	藤原 直樹	京都大学		Development of NMR measurement method under high pressure	Naoki Fujiwara	Kyoto University		上床 美也
6	202305-CMBXX-0078	高圧下量子振動観測システムの開発II	摂待 力生	新潟大学		Development of High Pressure Quantum Oscillation Observation System II	Rikio Settai	Niigata University		上床 美也
7	202305-CMBXX-0079	希釈冷凍機環境下での物性測定装置の開発	松林 和幸	電気通信大学		Development of high pressure apparatus for low temperature	Kazuyuki Matsubayashi	The University of Electro-Communications		上床 美也
8	202305-CMBXX-0080	3d遷移化合物に関する圧力効果	鹿又 武	東北学院大学工学総合研究所		Effect of pressure on the 3d transition compounds	Takeshi Kanomata	Research Institute for Engineering and Technology, Tohoku Gakuin University		上床 美也
9	202305-CMBXX-0081	低次元有機物質の圧力下構造物性の研究	糸井 充穂	東京都市大学		Structural properties of low-dimensional organic materials under pressure	Miho Itoi	Tokyo City University		上床 美也
10	202305-CMBXX-0082	高圧下構造解析法の開発	江藤 徹二郎	久留米工業大学		Development of High Pressure X-ray diffraction measurements	Tetsujiro Eto	Kurume Institute of Technology		上床 美也
11	202305-CMBXX-0083	複合環境下（横磁場）での物性測定法の開発	鳥塚 潔	千葉工業大学		Development of physical property measurement method under complex environment (horizontal magnetic field)	Kiyoshi Torizuka	Chiba Institute of Technology		上床 美也
12	202305-CMBXX-0049	4G、T2-2における共同利用推進（A）	佐藤 卓	東北大学		Research and Support of General-Use at 4G and T2-2（A）	Taku J Sato	Tohoku University		眞弓 皓一
13	202305-CMBXX-0050	4G、T2-2における共同利用推進（B）	那波 和宏	東北大学		Research and Support of General-Use at 4G and T2-2（B）	Kazuhiro Nawa	Tohoku University		眞弓 皓一
14	202305-CMBXX-0051	6G、T1-2、T1-3における共同利用推進（A）	藤田 全基	東北大学		Research and Support of General-Use at 6G, T1-2 and T1-3（A）	Masaki Fujita	Tohoku University		眞弓 皓一
15	202305-CMBXX-0053	6G、T1-2、T1-3における共同利用推進（C）	池田 陽一	東北大学金属材料研究所		Research and Support of General-Use at 6G, T1-2 and T1-3（C）	Yoichi Ikeda	Institute for materials research, Tohoku university		眞弓 皓一
16	202305-CMBXX-0054	6G、T1-2、T1-3における共同利用推進（D）	谷口 貴紀	東北大学		Research and Support of General-Use at 6G, T1-2 and T1-3（D）	Takanori Taniguchi	Tohoku University		眞弓 皓一

17	202305-CMBXX-0055	6G、T1-1における共同利用推進	岩佐 和晃	茨城大学		Research and Support of General-Use at 6G and T1-1	Kazuaki Iwasa	Ibaraki University		眞弓 皓一
18	202305-CMBXX-0058	T1-1における共同利用推進 (C)	横山 淳	茨城大学		Research and Support of General-Use at T1-1 (C)	Makoto Yokoyama	Ibaraki University		眞弓 皓一
19	202305-CMBXX-0061	T1-2における共同利用推進	山本 孟	東北大学		Research and Support of General-Use at T1-2	Hajime Yamamoto	多元物質科学研究所		眞弓 皓一
20	202305-CMBXX-0062	C1-2における共同利用推進 (A)	杉山 正明	京都大学		Research and Support of General-Use at C1-2 (A)	Masaaki Sugiyama	Kyoto University		眞弓 皓一
21	202305-CMBXX-0063	C1-2、C2-3-1における共同利用推進	井上 倫太郎	京都大学		Research and Support of General-Use at C1-2 and C2-3-1	Rintaro Inoue	Kyoto University		眞弓 皓一
22	202305-CMBXX-0064	C1-2における共同利用推進 (B)	守島 健	京都大学		Research and Support of General-Use at C1-2 (B)	Ken Morishima	Kyoto University		眞弓 皓一
23	202305-CMBXX-0065	C1-2における共同利用推進 (C)	Li Xiang	北海道大学		Research and Support of General-Use at C1-2 (C)	Li Xiang	Hokkaido University		眞弓 皓一
24	202305-CMBXX-0066	C3-1-2における共同利用推進 (A)	日野 正裕	京都大学		Research and Support of General-Use at C3-1-2 (A)	Masahiro Hino	Kyoto University		眞弓 皓一
25	202305-CMBXX-0068	C3-1-2における共同利用推進 (C)	田崎 誠司	京都大学		Research and Support of General-Use at C3-1-2 (C)	Seiji Tasaki	Kyoto University		眞弓 皓一
26	202305-CMBXX-0069	C3-1-2における共同利用推進 (D)	關 義親	東北大学		Research and Support of General-Use at C3-1-2 (D)	Yoshichika Seki	Tohoku University		眞弓 皓一
27	202305-CMBXX-0070	4Gにおける共同利用推進	金城 克樹	東北大学		Research and Support of General-Use at 4G	Katsuki Kinjo	Tohoku University		眞弓 皓一
28	202305-CMBXX-0071	T2-2における共同利用推進 (A)	高橋 美和子	筑波大学		Research and Support of General-Use at T2-2 (A)	Miwako Takahashi	University of Tsukuba		眞弓 皓一
29	202305-CMBXX-0072	T2-2における共同利用推進 (B)	小林 悟	岩手大学		Research and Support of General-Use at T2-2 (B)	Satoru Kobayashi	Iwate University		眞弓 皓一
30	202305-CMBXX-0038	高分解能スピン分解光電子分光による強相関物質の研究	横谷 尚睦	岡山大学		High resolution spin-resolved photoemission study on strongly correlated materials	Takayoshi Yokoya	Okayama University		近藤 猛
31	202305-CMBXX-0043	レーザースピン角度分解光電子分光による表面電子状態の研究	矢治 光一郎	物質・材料研究機構		SARPES studies of atomic layer materials at surfaces	Koichiro Yaji	National Institute for Materials Science		近藤 猛
32	202305-CMBXX-0044	有機化合物の光電子分光	金井 要	東京理科大学		Photoemission study on organic compounds	Kaname Kanai	Tokyo University of Science		近藤 猛
33	202305-CMBXX-0046	光スピントロニクスに向けたスピン軌道ダイナミクスの研究	黒田 健太	広島大学		Studying spin-orbit dynamics for opt-spintronics	Kenta Kuroda	Hiroshima University		近藤 猛
34	202305-CMBXX-0033	時間分解光電子分光を用いた強相関物質の研究	溝川 貴司	早稲田大学		Time-resolved photoemission study on strongly-correlated materials	Takashi Mizokawa	Waseda University		岡崎 浩三

一般課題 / General Research Project

No.	課題番号	課題名	氏名	所属	分担者	Title	Name	Organization	Member of research project	担当所属
1	202309-CNXX-0141	傾角反強磁性を有する単一成分分子性導体における置換基修飾・元素置換効果の研究 (2)	横森 創	立教大学		Study of effects of substituent modulation and element substitution in single-component molecular conductors with canted antiferromagnetism (2)	So Yokomori	Rikkyo University		森 初果

2	202309-GNBXX-0142	高い分子設計自由度を活かしたオリゴマー型有機伝導体の開発	小野塚 洸太	長岡工業高等専門学校		Development of oligomeric organic conductors with high molecular design freedom	Kota Onozuka	National Institute of Technology, Nagaoka College		森 初果
3	202304-GNBXX-0116	新規高移動度2次元系における分数量子ホール効果の極低温計測	小塚 裕介	物質・材料研究機構	岩崎 拓哉	Fractional quantum Hall effects in unconventional 2DEG at ultra-low temperature	Yusuke Kozuka	National Institute for Materials Science	Takuya Iwasaki	山下 穰
4	202305-GNBXX-0131	非自明超伝導体の理論的研究	町田 一成	立命館大学		Theoretical studies on unconventional superconductors	Kazushige Machida	Ritsumeikan University		山下 穰
5	202306-GNBXX-0121	有機スピン液体候補物質の核磁気共鳴測定による研究	宮川 和也	工学系研究科・物理工学専攻		NMR Studies on organic spin liquid candidate materials	Kazuya Miyagawa	Department of Applied Physics, School of Engineering		高木 里奈
6	202305-GNBXX-0079	SiC基板上に成長したグラフェンへの金属原子インターカレーション	中辻 寛	東京工業大学	小森 文夫 片野 達貴	Intercalation of metal atoms into graphene grown on a SiC substrate	Kan Nakatsuji	Tokyo Institute of Technology	Fumio Komori KATANO TATSUKI	吉信 淳
7	202305-GNBXX-0080	Si(111) $\sqrt{3}\times\sqrt{3}$ 超構造基板上に成長したBi(110)超薄膜の電子状態	中辻 寛	東京工業大学	小森 文夫 河添 理央 織田 孝幸 吉田 陸馬	Electronic structure of Bi(110) ultra-thin films grown on Si(111) $\sqrt{3}\times\sqrt{3}$ superstructures	Kan Nakatsuji	Tokyo Institute of Technology	Fumio Komori Rio Kawazoe Orita Takayuki Yoshida Rikuma	吉信 淳
8	202305-GNBXX-0113	赤外反射吸収分光による金表面に吸着した一酸化窒素の光脱離の評価	越田 裕之	生産技術研究所	奥山 弘 (京都大学)	Evaluation of photodesorption of nitric oxide from a Au surface by infrared reflection adsorption spectroscopy	Hiroyuki Koshida	Institute of Industrial Science	Hiroshi Okuyama	吉信 淳
9	202306-GNBXX-0095	透過FTIRによるかんらん石単結晶表面での水素・水吸着状態解析	橘 省吾	東京大学	稲田 菜里	Transmission FTIR spectroscopy of hydrogen and water adsorbed on olivine single crystals	Shogo Tachibana	The University of Tokyo	Inada Shiori	吉信 淳
10	202305-GNBXX-0122	希土類金属間化合物および金属超伝導体の結晶育成と低温電子物性	海老原 孝雄	静岡大学	小林 和 荒川 尚也 大窪 悠太	Crystal Growth and Physical Properties at low temperatures in rare earth intermetallic compounds and metallic superconductors	Takao Ebihara	Shizuoka University	Kazu Kobayashi Naoya Arakawa Yuta Okubo	大谷 義近
11	202306-GNBXX-0088	金属表面上のプランベンの電子状態の精密測定	柚原 淳司	名古屋大学	大野 誠貴 前田 匠太 ルレイ ギー	Electronic structure of plumbene on metal surfaces	Junji Yuhara	Nagoya University	ono masaki Shota Maeda Guy Le Lay	長谷川 幸雄
12	202305-GNBXX-0072	窒素原子対による等電子トラップの共鳴励起	矢口 裕之	埼玉大学	高宮 健吾 我妻 利樹	Resonant excitation of isoelectronic traps formed by nitrogen pairs	Hiroyuki Yaguchi	Saitama University	Kengo Takamiya Wagatsuma Riki	秋山 英文
13	202309-GNBXX-0143	分子線エピタキシー法を用いて作製したGaN/AlN半導体超格子の フォトルミネッセンスによる光学特性評価	小柴 俊	香川大学	西山 心喬 前山 綾汰	Optical properties of GaN/AlN superlattices grown by MBE	Shyun Koshiba	Kagawa University	Mitaka Nishiyama Maeyama Ryota	秋山 英文
14	202310-GNBXX-0145	点接合法を用いたPd水素化物の超伝導状態に関する研究	志賀 雅亘	九州大学	加藤 遼馬	Study of the superconducting properties on hydrogen absorbed Pd thin film using point-contact spectroscopy	Masanobu Shiga	Kyushu University	Ryoma Kato	三輪 真嗣
15	202304-GNBXX-0067	CeMnSiの高圧下における電気抵抗 II	川村 幸裕	室蘭工業大学	西山 紗恵	Electrical Resistivity of CeMnSi under high pressure II	Yukihiro Kawamura	Muroran Institute of Technology	Sae Nishiyama	上床 美也
16	202304-GNBXX-0069	超高圧下での強相関電子系の量子振動効果測定	菅原 仁	神戸大学	松林 和幸 (電気通信大学) 藤田 拓也	Quantum oscillation measurements on strongly correlated electron systems under the ultra-high pressure	Hitoshi Sugawara	Kobe university	Kazuyuki Matsubayashi Takuya Komoda	上床 美也

17	202304-GNBXX-0114	電荷秩序型ダイマーモット絶縁体 $\beta$ -'(BEDT-TTF)2CF3CF2SO3の超高静水圧印加による超伝導相の探索	小林 拓矢	埼玉大学	谷口 弘三 佐藤 慧一 山田 英寿	Search for pressure-induced superconductivity by applying quasi-hydrostatic ultra-high pressures to charge-ordered dimer-Mott insulator $\beta$ -'(BEDT-TTF)2CF3CF2SO3	Takuya Kobayashi	Saitama University	Hiromi Taniguchi Keichi Sato Yamada Hidetoshi	上床 美也
18	202305-GNBXX-0071	S置換したFeSeの高压低温下NMR測定	藤原 直樹	京都大学	Yu Zhongyu	NMR studies on S-substituted FeSe at high pressures and low temperatures	Naoki Fujiwara	Kyoto University	Zhongyu Yu	上床 美也
19	202305-GNBXX-0074	Fe1-xRuxSiの高压物性に関する研究 (3)	江藤 徹二郎	久留米工業大学		Study of physical properties on Fe1-xRuxSi under high pressure (3)	Tetsujiro Eto	Kurume Institute of Technology		上床 美也
20	202305-GNBXX-0075	新ガスケット方式の高压装置開発と鉄系超伝導研究への適用	久田 旭彦	徳島大学	高木 拓海	Development of high-pressure apparatus with new gasket system and application to iron-based superconductors	Akihiko Hisada	Tokushima University	Takumi Takagi	上床 美也
21	202305-GNBXX-0082	$\beta$ -EuP3の圧力下絶縁体-金属転移と価数揺動	大貫 惇睦	東京都立大学	本多 史憲 (九州大学アイソトープ統合安全管理センター) 松田 達磨 仲地 立	Pressure-induced Insulator-Metal Transition and Valence Fluctuation in $\beta$ -EuP3	Yoshichika Onuki	Tokyo Metropolitan University	Fuminori Honda (Central Institute of Radioisotope Science and Safety Management, Kyushu University) Tatsuma D. Matsuda nakachi ryu	上床 美也
22	202305-GNBXX-0084	ホイスラー化合物Fe3-xMnxSiの圧力下磁気相転移	廣井 政彦	鹿児島大学	高本 翼	Magnetic phase transitions under pressure in Heuser compounds Fe3-xMnxSi	Masahiko HIROI	Kagoshima University	Tsubasa Takamoto	上床 美也
23	202305-GNBXX-0086	電気伝導性酸化物材料の低温磁場中輸送特性の研究	藪田 久人	九州大学		Study on transport property of electro-conductive oxide materials under magnetic field at low temperature	Hisato Yabuta	Kyushu University		上床 美也
24	202305-GNBXX-0108	多型化合物 R1r2Si2(R=希土類)の磁気特性 8	内間 清晴	学校法人沖縄キリスト教学院・沖縄キリスト教短期大学	繁岡 透 (山口大学)	Magnetic characteristics of polymorphic compounds R1r2Si2(R=Rare earth) 8	Kiyoharu Uchima	Okinawa Christian Institute Okinawa christian junior College	Toru Shigeoka	上床 美也
25	202305-GNBXX-0109	擬三元化合物Ce1-xLaxNiC2の結晶育成と物質評価 4	繁岡 透	山口大学	内間 清晴 (沖縄キリスト教学院・沖縄キリスト教短期大学)	Crystal growth and characterization of pseudo-ternary compounds Ce1-xLaxNiC2 4	Toru Shigeoka	Yamaguchi University	Kiyoharu Uchima (Okinawa Christian Institute Okinawa christian junior College)	上床 美也
26	202305-GNBXX-0110	CeNiC2の結晶育成と物質評価 3	繁岡 透	山口大学	内間 清晴 (沖縄キリスト教学院・沖縄キリスト教短期大学)	Crystal growth and characterization of CeNiC2 3	Toru Shigeoka	Yamaguchi University	Kiyoharu Uchima (Okinawa Christian Institute Okinawa christian junior College)	上床 美也
27	202305-GNBXX-0120	極低温磁化測定のための非磁性高压セル・トランスデューサーの開発と強相関物質への応用	清水 悠晴	東北大学金属材料研究所	三宅 厚志	Development of non-magnetic high-pressure cell and capacitive transducer for low-temperature dc magnetization measurements and application to correlated electron systems	Yusei Shimizu	Tohoku University, Institute for Materials Research	Atsushi Miyake	上床 美也
28	202305-GNBXX-0127	圧力媒体の固化点の再現性と安定性	村田 恵三	大阪公立大学		Reproducibility of the Solidification Pressure of Pressure Medium and its Stability	Keizo Murata	Osaka Metropolitan University		上床 美也

29	202306-GNBXX-0087	マルチサイト化合物の単結晶育成と物性	中野 智仁	新潟大学	武藤 颯人	Single crystal growth of Multi-site Ce compounds and its properties.	Tomohito NAKANO	Faculty of Engineering, Niigata University	Hayato Muto	上床 美也
30	202306-GNBXX-0091	高スピン分極ホイスラー合金における圧力誘起量子臨界現象の探索	重田 出	鹿児島大学	青島 英樹	Search for the pressure-induced quantum critical phenomenon in highly spin-polarized Heusler alloys	Iduru Shigeta	Kagoshima University	Aoshima Hideki	上床 美也
31	202306-GNBXX-0094	10GPa超の高圧発生可能なブリッジマンアンビル型クランプセルのための部品製作	大橋 政司	金沢大学	小笠原 悠太	Parts production for Bridgman-type high pressure clamp cell which can apply above 10 GPa	Masashi Ohashi	Kanazawa University	Yuta Ogasawara	上床 美也
32	202306-GNBXX-0096	局所的に空間反転対称性の破れた希土類化合物の圧力効果	三宅 厚志	東北大学	本多 史憲 (九州大学アイソトープ統合安全管理センター) 清水 悠晴	Pressure effects on rare-earth compounds without local spatial inversion symmetry	Atsushi Miyake	Tohoku University	Fuminori Honda (Central Institute of Radioisotope Science and Safety Management, Kyushu University) Yusei Shimizu	上床 美也
33	202306-GNBXX-0102	不定比化合物DyCr <sub>x</sub> Ge <sub>2</sub> 単結晶の磁場中比熱測定	藤原 哲也	山口大学	新谷 令和	Specific measurements under magnetic field of non-stoichiometric DyCr <sub>x</sub> Ge <sub>2</sub> single crystals	Tetsuya Fujiwara	Yamaguchi University	reo niya	上床 美也
34	202306-GNBXX-0103	不定比化合物ErCr <sub>x</sub> Ge <sub>2</sub> 単結晶の磁化測定	藤原 哲也	山口大学	新谷 令和	Magnetization measurements of non-stoichiometric ErCr <sub>x</sub> Ge <sub>2</sub> single crystals	Tetsuya Fujiwara	Yamaguchi University	reo niya	上床 美也
35	202306-GNBXX-0104	不定比化合物HoCr <sub>x</sub> Ge <sub>2</sub> 単結晶の磁場中比熱測定	藤原 哲也	山口大学	新谷 令和	Specific measurements under magnetic field of non-stoichiometric HoCr <sub>x</sub> Ge <sub>2</sub> single crystals	Tetsuya Fujiwara	Yamaguchi University	reo niya	上床 美也
36	202306-GNBXX-0105	不定比化合物TbCr <sub>x</sub> Ge <sub>2</sub> 単結晶の磁場中比熱測定	藤原 哲也	山口大学	新谷 令和	Specific measurements under magnetic field of non-stoichiometric TbCr <sub>x</sub> Ge <sub>2</sub> single crystals	Tetsuya Fujiwara	Yamaguchi University	reo niya	上床 美也
37	202306-GNBXX-0106	Eu <sup>2+</sup> 状態を持つEu化合物の高圧下における電子状態の研究	本多 史憲	九州大学アイソトープ統合安全管理センター	大貫 惇睦 (東京都立大学) 福田 大翔 (東北大学大学院) 仲地 立 (東京都立大学)	Electronic properties of Eu compounds with Eu <sup>2+</sup> state under high pressures	Fuminori Honda	Central Institute of Radioisotope Science and Safety Management, Kyushu University	Yoshichika Onuki (Tokyo Metropolitan University) Hiroto Fukuda (Tohoku University) nakachi ryu (tokyo metropolitan university)	上床 美也
38	202306-GNBXX-0107	ウラン化合物の磁性的圧力効果と圧力誘起超伝導の探索	本多 史憲	九州大学アイソトープ統合安全管理センター	福田 大翔 (東北大学) 三宅 厚志 (東北大学)	Effect of pressure on the magnetism and search for pressure-induced superconductivity of uranium compounds	Fuminori Honda	Central Institute of Radioisotope Science and Safety Management, Kyushu University	Hiroto Fukuda (Tohoku University) Atsushi Miyake (Tohoku University)	上床 美也
39	202306-GNBXX-0134	特異な構造相転移を示す低次元伝導体の高圧力下電気抵抗測定	広瀬 雄介	新潟大学	諸橋 達也	Electrical resistivity measurement under pressure of a low dimensional conductor with a characteristic structural transition	Yusuke Hirose	Niigata University	Tatsuya Morohashi	上床 美也
40	202306-GNBXX-0135	金属化されたTa <sub>2</sub> NiSe <sub>5</sub> および関連物質の極低温の電子状態の研究	摂待 力生	新潟大学	土田 駿	Study of the electronic state of metallized Ta <sub>2</sub> NiSe <sub>5</sub> and related materials at low temperatures	Rikio Settai	Niigata University	Shun Tsuchida	上床 美也
41	202311-GNBXX-0148	反強磁性化合物 CeSi の電気抵抗の圧力効果	加賀山 朋子	大阪大学	大石 健翔	Pressure effect on the electrical resistance of antiferromagnetic compound CeSi	Tomoko KAGAYAMA	Osaka University	健翔 大石	上床 美也

42	202306-GNBXX-0128	インターカレート系Co <sub>2</sub> +ハニカム格子磁性体の物性解明	原口 祐哉	東京農工大学	伊藤 正明	Physical Properties of Intercalated Co <sub>2</sub> + Honeycomb Lattice Magnets	Yuya Haraguchi	Tokyo University of Agriculture and Technology	Masaaki Ito	岡本 佳比古
43	202401-GNBXX-0149	高エネルギーX線ラウエ装置を利用した中性子散乱実験用単結晶試料のアSEMBル	小林 理気	琉球大学	植田 大地 (高エネルギー加速器研究機構) 富井 大海	Assembly of Single Crystal Samples for Neutron Scattering Experiments Using High Energy X-ray Laue System	Riki Kobayashi	University of the Ryukyus	Daichi Ueta Tomii Hiromi	益田 隆嗣
44	202304-GNBXX-0068	紫外光レーザー光源を用いた加工応用研究	藤本 靖	千葉工業大学		Research on laser processing application by ultraviolet laser light source	Yasushi Fujimoto	Chiba Institute of Technology		小林 洋平
45	202304-GNBXX-0070	3元系におけるレーザー誘起合金化のバルス時間幅依存性	富田 卓朗	徳島大学	須藤 直也	Pulse duration dependence of laser induced 3-elemental alloy	Takuro Tomita	Tokushima University	Naoya Suto	小林 洋平
46	202304-GNBXX-0115	ダイヤモンド上に蒸着した鉄薄膜におけるレーザー誘起相変態	岡田 達也	徳島大学	岸田 崇秀	Laser-induced phase transformation of iron thin film deposited on diamond	Tatsuya OKADA	Tokushima University	Kishida Takahide	小林 洋平
47	202304-GNBXX-0130	超短パルスYbファイバーレーザー光源を用いた生体組織の分子振動イメージング	長島 優	浜松医科大学		Molecular vibrational imaging of biological tissues using Yb fiber-based ultrashort pulse laser source	Yu Nagashima	Hamamatsu University School of Medicine		小林 洋平
48	202305-GNBXX-0085	超高速発光分光による金属の研究	末元 徹	電気通信大学		Studies on metals using ultrafast luminescence spectroscopy	Suemoto Tohru	The University of Electro-Communications		小林 洋平
49	202305-GNBXX-0111	次世代レーザーとレーザー加工の基礎技術研究	吉富 大	産業技術総合研究所	高田 英行 奈良崎 愛子 小川 博嗣 寺澤 英知 澁谷 達則 佐藤 大輔 黒田 隆之助 丸 征那	Basic research on next generation laser systems and laser machining technology	Dai Yoshitomi	National Institute of Advanced Industrial Science and Technology	Takada Hideyuki Aiko Narazaki Hiroshi Ogawa Eichi Terasawa Tatsunori Shibuya Daisuke Satoh Ryunosuke Kuroda Sena Maru	小林 洋平
50	202305-GNBXX-0073	自己組織化カゴメ格子Mn <sub>3</sub> C <sub>6</sub> O <sub>6</sub> の電子構造の観測	金井 要	東京理科大学	馬上 怜奈 山崎 弘人	Observation of electronic structure of self-assembled Kagome lattice Mn <sub>3</sub> C <sub>6</sub> O <sub>6</sub>	Kaname Kanai	Tokyo University of Science	Rena Moue Hiroto Yamazaki	近藤 猛
51	202306-GNBXX-0097	炭化タングステン薄膜上グラフェンのスピン分解角度分解光電子分光	伊藤 孝寛	名古屋大学	乗松 航 (早稲田大学) 三田 愛也 強 博文 河野 健人 柳原 涼太郎 NI YUANZHI	Spin- and angle-resolved photoemission spectroscopy of Graphene on WC thin film	Takahiro Ito	Nagoya University	Wataru Norimatsu (Waseda University) Mita Manaya Bowen Qiang Kento Kawano Ryotaro Sakakibara YUANZHI NI	近藤 猛
52	202306-GNBXX-0124	ハーフメタル強磁性体の時間分解スピン分解高分解能光電子分光	横谷 尚睦	岡山大学	東川 知樹 大岸 勇太 齋藤 竜聖	Time and spin-resolved high-resolution photoemission spectroscopy of half metallic ferromagnet	Takayoshi Yokoya	Okayama University	higashikawa tomoki Okishi Yuta Ryusei Saito	近藤 猛
53	202306-GNBXX-0133	ニッケル基板上的多層グラフェンの電子状態の研究	矢治 光一郎	物質・材料研究機構	竹澤 伸吾 (東京理科大学) 津田 俊輔 ファンディン タン	Electronic structure of multilayer graphene on a Ni substrate	Koichiro Yaji	National Institute for Materials Science	Shingo Takezawa (Tokyo University of Science) Shunsuke Tsuda THANG DINH PHAN	近藤 猛

54	202310-GNBXX-0146	強磁性金属酸化物SrRuO3薄膜における量子輸送特性の解明	小林 正起	東京大学		Unveiling quantum transport property of ferromagnetic metallic oxide SrRuO3	Masaki Kobayashi	The University of Tokyo		近藤 猛
55	202311-GNBXX-0147	光電子スピン干渉を用いたアト秒光電子ダイナミクスへの研究	黒田 健太	広島大学	岩田 拓万 高佐 永遠	Study of attosecond photoemission dynamics through photoelectron spin interference	Kenta Kuroda	Hiroshim University	Takuma Iwata Towa Kousa	近藤 猛
56	202305-GNBXX-0077	カロリメトリによる金属ナノ構造の赤外吸収率測定	末元 徹	電気通信大学	森野 春樹 須田 順子	Measurement of infrared absorptivity on metal nanostructures by calorimetry	Suemoto Tohru	The University of Electro-Communications	Haruki Morino Yoriko Suda	岡崎 浩三
57	202305-GNBXX-0100	励起子絶縁体及び鉄系超伝導体における光誘起相転移の研究	久保田 雄也	理化学研究所		Investigation of the photo-induced phase transitions in excitonic insulators and Fe-based superconductors	Yuya Kubota	RIKEN		岡崎 浩三
58	202305-GNBXX-0117	HfO2系強誘電体キャパシタの信頼性向上に向けた破壊現象の解析	糸矢 祐喜	東京大学		Analysis of Break-down Phenomena for Improving the Reliability of Ferroelectric HfO2&nbsp;Capacitors	Yuki Itoya	The University of Tokyo		岡崎 浩三
59	202306-GNBXX-0092	高分解能レーザー励起光電子顕微鏡を用いた鉄系超伝導体の電子ネマティック状態の実空間観察VII	影山 通一	東京大学	大西 朝登	Real-space observation of electronic nematicity in iron-based superconductors by using a high-resolution laser photoemission electron microscope VII	Yoichi Kageyama	The University of Tokyo	Asato Onishi	岡崎 浩三
60	202306-GNBXX-0093	カルシウム挿入グラフェンの電子格子相互作用の研究	一ノ倉 聖	東京工業大学	中村 達哉 徳田 啓	Study of electron-phonon interaction in Ca-intercalated graphene	Satoru Ichinokura	Tokyo Institute of Technology	Tatsuya Nakamura Tokuda Kei	岡崎 浩三
61	202306-GNBXX-0101	ディラック線ノード超伝導体ZeP2-xSexにおける超伝導ギャップの直接観測	井野 明洋	久留米工業大学	出浦 主雅 (広島大学) 西岡 幸美 (広島大学) 木村 昭夫 (広島大学)	Direct observation of superconducting gap in a Dirac nodal-line superconductor ZeP2-xSex	Akihiro Ino	Kurume Institute of Technology	kazumasa ideura Yukimi Nishioka akio kimura	岡崎 浩三
62	202305-GNBXX-0081	量子ホール系におけるトポロジカルDNPの研究	福田 昭	兵庫医科大学		Study of topological DNP in quantum Hall system	Akira Fukuda	Hyogo College of Medicine		量子物質ナノ構造ラボ運営委員会 (橋坂昌幸)
63	202305-GNBXX-0083	宙吊りグラフェン素子の作製と伝導測定	原 正大	熊本大学	堤 康二郎	Fabrication and transport measurement of suspended graphene devices	Masahiro Hara	Kumamoto University	Tsutsumi Kojiro	量子物質ナノ構造ラボ運営委員会 (橋坂昌幸)
64	202306-GNBXX-0126	MA2BOy(M-1201)酸化物のホール係数測定	神戸 士郎	山形大学	魏 毓良 吉永 幸弘 大竹 開智 今井 大雅 岡 承程 高橋 祐稀	Hall coefficient measurement of MA2BOy(M-1201) oxides	Shiro Kambe	Graduate School of Science and Engineering, Yamagata University	Wei Yuliang Yukihiro Yoshinaga Kaichi Otake Taiga Imai YAN CHENG CHENG Takahashi Yuki	量子物質ナノ構造ラボ運営委員会 (橋坂昌幸)
65	202310-GNBXX-0144	アルゴンイオン照射による酸化チタンナノシートにおける欠陥生成	原 正大	熊本大学	黒木 玲央	Defect generation in titanium oxide nanosheets by Ar ion irradiation	Masahiro Hara	Kumamoto University	Kurogi Reo	量子物質ナノ構造ラボ運営委員会 (橋坂昌幸)

物質合成・評価設備Gクラス / Materials Synthesis and Characterization G Class Research Project

No.	課題番号	課題名	氏名	所属	分担者	Title	Name	Organization	Member of research project	担当所員
-----	------	-----	----	----	-----	-------	------	--------------	----------------------------	------

1	202305-MCBXG-0053	低温で直線型三量体をもつRuX (X = P,As,Sb)の高温相局所構造解析	片山 尚幸	名古屋大学	小島 慶太	Local structure analysis of RuX (X = P,As,Sb) with linear trimer at low temperature in high temperature phase	Naoyuki Katayama	Nagoya University	Keita Kojima	物質合成室
2	202305-MCBXG-0102	フェロアキシシャル物質の物性開拓	木村 剛	東京大学	林田 健志 山岸 茂直 諸見里 真人 吉岡 知輝 永井 隆之 梶田 遙一	Physical properties of ferroaxial materials	Tsuyoshi Kimura	The University of Tokyo	Takeshi Hayashida Shigetada Yamagishi Masato Moromizato Tomoki Yoshioka Takayuki Nagai Yoichi Kajita	物質合成室
3	202306-MCBXG-0068	希土類硫化物Eu1-xGdxSの合成	脇倉 和平	岩手大学	小林 翔真	Synthesis of a rare-earth sulfide Eu1-xGdxS	Kazuhei Wakiya	Iwate University	Shoma Kobayashi	物質合成室
4	202305-MCBXG-0089	高いイオン伝導率を有する酸化物固体電解質の合成	矢島 健	名古屋大学	島 颯一	Synthesis of oxide solid electrolytes with high ionic conductivity	Takeshi Yajima	Nagoya University	Shima Souichi	X線測定室
5	202305-MCBXG-0097	高温高压水中の有機合成の多段反応装置による高効率化	秋月 信	東京大学	沖田 優美	Highly efficient organic synthesis in high temperature and high pressure water using a multi-stage reactor	Makoto Akizuki	The University of Tokyo	Yumi Okita	X線測定室
6	202305-MCBXG-0100	高温高压水中の有機反応に適した固体酸触媒の開発	秋月 信	東京大学	下沢 舞優	Development of solid acid catalysts suitable for organic reactions in high temperature and high pressure water	Makoto Akizuki	The University of Tokyo	Mayu Shimosawa	X線測定室
7	202306-MCBXG-0061	Co基ホイスラー合金におけるマルテンサイト変態材料の探索	重田 出	鹿児島大学	青島 英樹	Search for materials with the Martensitic transformation in Co-based Heusler alloys	Iduru Shigeta	Kagoshima University	Aoshima Hideki	X線測定室
8	202306-MCBXG-0077	反転対称心のない磁性絶縁体の磁気超構造の外場駆動	有馬 孝尚	The University of Tokyo	徳永 祐介 YAN ZHICHEN 鬼頭 俊介	Field-Effect on Nanometric Magnetic Objects in Noncentrosymmetric Magnetic Insulators	Taka-hisa Arima	The University of Tokyo	Yusuke Tokunaga ZHICHEN YAN Shunsuke Kitou	X線測定室
9	202306-MCBXG-0079	強誘電性ニオブ酸化物の構造解析	山本 文子	芝浦工業大学		Structural analysis of ferroelectric niobates	Ayako Yamamoto	Shibaura Institute of Technology		X線測定室
10	202306-MCBXG-0101	超伝導体・磁性体におけるトポロジカル量子相の探索	水上 雄太	東北大学	大野 綾太郎 東北大学 大学院生（前期・修士課程）	Search for topological quantum phases in superconductors and magnetic materials	Yuta Mizukami	Tohoku University	ryotaro ono Tohoku University	X線測定室
11	202304-MCBXG-0083	セラミックスナノ粒子の連続製造技術開発	陶 究	産業技術総合研究所		Development of continuous process for ceramics nanoparticles production	Kiwamu Sue	AIST		電子顕微鏡室
12	202306-MCBXG-0073	亜臨界水中におけるPLA樹脂のガス化に関する研究	布浦 鉄兵	東京大学環境安全研究センター	WU Fan	Gasification of PLA resin in subcritical water	Tepei Nunoura	Environmental Science Center, the University of Tokyo	WU FAN	電子顕微鏡室

13	202306-MCBXG-0103	トポロジカルな電子構造に基づく機能性材料の探索	酒井 明人	東京大学	王 陽明 Feng Zili 梶原 悠人 黒沢 駿一郎 小池 祐樹 段 之宜 松本 卓也 蘇 杭	Search for the functional material based on the topological electronic structure	Akito Sakai	The University of Tokyo	Yangming Wang Zili Feng yuto kajiwara Shunichiro Kurosawa Yuki Koike Zhiyi Duan Takuya Matsumoto Hang Su	電子顕微鏡室
14	202304-MCBXG-0080	(La0.1Nd0.9)1-x(Ca0.6Sr0.4)xFeO3-δ (0.1 ≤ x ≤ 0.9) の高温における磁性と熱電特性に関する研究	中津川 博	横浜国立大学		Magnetism and thermoelectric properties at high temperature in (La0.1Nd0.9)1-x(Ca0.6Sr0.4)xFeO3-δ (0.1 ≤ x ≤ 0.9)	Hiroshi Nakatsugawa	Yokohama National University		電磁気測定室
15	202305-MCBXG-0055	不純物ドーピングした金属酸化物膜および非晶質炭素膜における電気伝導特性の評価	村岡 祐治	岡山大学	中村 匠汰	Resistivity measurements of impurity doped transition metal oxide and amorphous carbon films	Yuji Muraoka	Okayama Univ.	Shota Nakamura	電磁気測定室
16	202305-MCBXG-0059	鉄系超伝導体に対するアニール効果の検証	栗原 綾佑	東京理科大学	矢口 宏 小峰 智弥 小暮 琉介 太田 知孝	Annealing effect on iron-based superconductors	Ryosuke Kurihara	Tokyo University of Science	Hiroshi Yaguchi Tomoya Komine Ryusuke Kogure Ota Tomotaka	電磁気測定室
17	202305-MCBXG-0060	ホイスラー化合物での反強磁性の研究	廣井 政彦	鹿児島大学	高本 翼	Study on antiferromagnetism in Heusler compounds	Masahiko HIROI	Kagoshima University	Tsubasa Takamoto	電磁気測定室
18	202305-MCBXG-0085	機械的に剥離したFe(Se,Te)薄膜の超伝導特性	飯田 和昌	日本大学		Superconducting properties of the mechanically exfoliated Fe(Se,Te) thin films	Kazumasa Iida	Nihon University		電磁気測定室
19	202306-MCBXG-0062	高スピンドープホイスラー合金の磁気特性のスピンドル理論による解析に関する研究	重田 出	鹿児島大学	青島 英樹	Study on analysis of magnetic properties for highly spin-polarized Heusler alloys by the spin fluctuation theory	Iduru Shigeta	Kagoshima University	Aoshima Hideki	電磁気測定室
20	202306-MCBXG-0067	アジ化物を用いて合成した準安定磁性体の物性	原口 祐哉	東京農工大学	若杉 和弘	Physical properties of metastable magnets synthesis via the Azide Route	Yuya Haraguchi	Tokyo University of Agriculture and Technology	wakasugi kazuhiko	電磁気測定室
21	202306-MCBXG-0070	低温で合成されたフラストレート磁性体の磁性	香取 浩子	東京農工大学	原口 祐哉 北村 昌大 伊藤 正明	Magnetism of frustrated magnetic materials synthesized at low temperatures	Hiroko Katori	Tokyo University of Agriculture and Technology	Yuya Haraguchi masahiro kitamura Masaaki Ito	電磁気測定室
22	202306-MCBXG-0091	MA2BOy(M-1201)酸化物の磁化率測定	神戸 士郎	山形大学	魏 毓良 吉永 幸弘 大竹 開智 今井 大雅 岡 承程 高橋 祐稀	Magnetic susceptibility measurement of MA2BOy(M-1201) oxides	Shiro Kambe	Graduate School of Science and Engineering, Yamagata University	Wei Yuliang Yukihiko Yoshinaga Kaichi Otake Taiga Imai YAN CHENG CHENG Takahashi Yuki	電磁気測定室
23	202306-MCBXG-0092	短距離秩序を有するパイロクロア型酸化物の物性	有馬 孝尚	東京大学	西田 祥太 鬼頭 俊介	Physical Properties of Pyrochlore Oxide Compounds with Short-Range Order	Taka-hisa Arima	The University of Tokyo	Shota Nishida Shunsuke Kitou	電磁気測定室
24	202306-MCBXG-0094	イオンミキシング制御した4d/5d遷移金属酸化物におけるスピン軌道結合磁性の観測	原口 祐哉	東京農工大学		Observation of spin-orbit coupled magnetism in the ion-mixing-controlled 4d/5d transition metal oxides	Yuya Haraguchi	Tokyo University of Agriculture and Technology		電磁気測定室

25	202305-MCBXG-0081	重希土類を含む充填スクテルダイト化合物の高圧合成と多極子物性	関根 ちひろ	室蘭工業大学	寺坂 聡志 長瀬 竜也 渡辺 陸人 尾崎 蒼空	High-pressure synthesis and multipole properties of filled skutterudite compounds containing heavy rare earths	Chihiro Sekine	Muroran Institute of Technology	Satoshi Terasaka Tatsuya Nagase Rikuto Watanabe Sora Ozaki	高圧合成室
26	202305-MCBXG-0084	アルミニウム含有鉱物への高圧下での希ガス取り込み機構の解明	飯塚 理子	早稲田大学		Incorporation of noble gases into new hexagonal aluminous phases under lower mantle condition	Riko Izuka-Oku	Waseda University		高圧合成室
27	202306-MCBXG-0066	高温高圧下におけるFe-S-H三元系における水素原子の占有サイトと水素誘起体積膨張係数の解明	鍵 裕之	東京大学	高野 将大	Site occupancy of hydrogen and hydrogen-induced volume expansion rate in Fe-S-H ternary system at high pressure and high temperature	Hiroyuki Kagi	The University of Tokyo	Masahiro Takano	高圧合成室
28	202306-MCBXG-0069	Phase Aの高温高圧合成	賀 雪菁	東京大学	鍵 裕之	High-pressure and high-temperature synthesis of phase A	XUEJING HE	The University of Tokyo	Hiroyuki Kagi	高圧合成室
29	202306-MCBXG-0093	発光中心多面体を有する無機蛍光体の高圧下における幾何学的変化と光学特性に関する研究	石垣 雅	東京大学	渡邊 美寿貴 (新潟大学)	Study on geometric changes and optical properties under high pressure of inorganic phosphors with luminescent center polyhedra	TADASHI ISHIGAKI	The University of Tokyo	Mizuki Watanabe	高圧合成室
30	202305-MCBXG-0096	亜臨界水と固体塩基触媒の組み合わせによる新規有機合成プロセスの開発	秋月 信	東京大学	王 一琦	Development of novel organic synthesis process with a combination of subcritical water and solid base catalyst	Makoto Akizuki	The University of Tokyo	Yiqi Wang	X線測定室 化学分析室
31	202305-MCBXG-0098	超臨界メタノールと固体塩基触媒を用いたバイオディーゼル燃料合成	秋月 信	東京大学	東郷 宣弘	Synthesis of biodiesel fuels in supercritical methanol using solid base catalysts	Makoto Akizuki	The University of Tokyo	Nobuhiro TOGO	X線測定室 化学分析室
32	202306-MCBXG-0065	高圧合成法を用いたハニカム化合物Ru(Br <sub>1-x</sub> I <sub>x</sub> ) <sub>3</sub> 単結晶の作製	今井 良宗	東北大学	佐藤 楓貴	High pressure synthesis of single crystals of honeycomb compounds Ru(Br <sub>1-x</sub> I <sub>x</sub> ) <sub>3</sub>	Yoshinori Imai	Tohoku university	Fuki Sato	X線測定室 高圧合成室
33	202306-MCBXG-0063	合金ナノ粒子のキャラクタリゼーション	佐々木 岳彦	東京大学	張 凱朝 徐 浩然 胡 寧睿	Characterization of alloy nanoparticles	Takehiko Sasaki	The University of Tokyo	KAICHAO ZHANG Haoran Xu Hu Ningrui	X線測定室 電子顕微鏡室 光学測定室
34	202306-MCBXG-0071	リグニンの有用化合物への変換を可能にする固体触媒及び反応条件の検討	布浦 鉄兵	東京大学環境安全研究センター	堂脇 大志	Study on solid catalysts and reaction conditions for lignin conversion into valuable chemicals	Teppey Nunoura	The University of Tokyo	Taishi Dowaki	化学分析室 X線測定室 電子顕微鏡室
35	202306-MCBXG-0074	高炉スラグ系改質材によるメッキ廃液からの重金属イオンの除去	布浦 鉄兵	東京大学環境安全研究センター	WANG Jiaqi	Removal of heavy metal ions from electroplating wastewater by blast furnace slag based modified materials	Teppey Nunoura	The University of Tokyo	WANG Jiaqi	化学分析室 X線測定室 電子顕微鏡室
36	202306-MCBXG-0064	遷移金属化合物の量体化近傍における電子状態の研究	平井 大悟郎	名古屋大学		Electronic states of transition metal compounds in the vicinity of molecular orbital crystallization	Daigorou Hirai	Nagoya University		高圧合成室 電磁気測定室
37	202305-MCBXG-0099	高温高圧水を利用したBaTiO <sub>3</sub> 微粒子の合成	秋月 信	東京大学		Synthesis of BaTiO <sub>3</sub> nanoparticles using hot compressed water	Makoto Akizuki	The University of Tokyo		電子顕微鏡室 X線測定室
38	202306-MCBXG-0076	ハニカム型磁性体の磁気熱輸送現象	有馬 孝尚	東京大学	上野 正人	Magneto-Thermal Transport in Honeycomb Magnets	Taka-hisa Arima	The University of Tokyo	Masato Ueno	電磁気測定室 X線測定室
39	202305-MCBXG-0090	新奇相転移を示すイリジウム酸化物の純良単結晶育成と基礎物性評価	松平 和之	九州工業大学		Growth of high-quality single crystals of iridium oxides exhibiting novel phase transitions and evaluation of their fundamental physical properties.	KAZUYUKI MATSUHIRA	Kyushu Institute of Technology		物質合成室 X線測定室

40	202305-MCBXG-0087	新規複合アニオン固体電解質の開発	矢島 健	名古屋大学	越田 耕平	Exploring novel mixed anion solid electrolytes	Takeshi Yajima	Nagoya University	Kouhei Koshita	物質合成室 X線測定室 高圧合成室
41	202305-MCBXG-0088	多段階合成による新規固体電解質の開発	矢島 健	名古屋大学	浜田 実久 島 颯一	Exploring novel solid electrolytes via multi-step reactions	Takeshi Yajima	Nagoya University	HAMADA MIKU Shima Souichi	物質合成室 X線測定室 高圧合成室
42	202305-MCBXG-0058	磁場誘起磁気多極子における電気磁気効果についての研究	阿部 伸行	日本大学	岩崎 義己	Study of magnetoelectric effect in magnetic field induced magnetic multipoles	Nobuyuki Abe	Nihon University	IWASAKI Yoshiki	物質合成室 X線測定室 電磁気測定室
43	202305-MCBXG-0056	キラル強誘電体の単結晶合成と評価	木村 健太	大阪公立大学		Single-crystal growth and characterization of chiral ferroelectrics	Kenta Kimura	Osaka Metropolitan University		物質合成室 電子顕微鏡室

物質合成・評価設備Uクラス / Materials Synthesis and Characterization U Class Research Project

No.	課題番号	課題名	氏名	所属	分担者	Title	Name	Organization	Member of research project	担当所員
1	202402-MCBXU-0112	Y型フェライトBaFe7O11における電荷秩序	和氣 剛	京都大学		Charge ordering in Y-type ferrite BaFe7O11	Takeshi Waki	Kyoto University		X線測定室
2	202309-MCBXU-0109	月資源現地利用を目指したレーザーによるアルミナ還元	高崎 大吾	東京大学	渡邊 真隆 峯松 涼 土屋 祐人	Laser alumina reduction toward utilization of lunar resources	Daigo Takasaki	The University of Tokyo	watanabe masataka Ryo Minematsu Tsuchiya Yuto	電子顕微鏡室
3	202309-MCBXU-0107	キラリティーの導入された有機無機ハイブリッドペロブスカイトハロゲン化銅物質における特異磁性の開拓	黄 柏融	東京工業大学		The development of unique magnetic properties in the chirality introduced organic-inorganic hybrid perovskites copper halides	Po-Jung Huang	Tokyo Institute of Technology		電磁気測定室
4	202309-MCBXU-0108	酸化還元活性分子の導入されたキラルな有機無機ハイブリッドペロブスカイトハロゲン化鉛物質における物性開拓	黄 柏融	東京工業大学		The development of unique properties in the redox-active-molecule-introduced chiral organic-inorganic hybrid perovskite lead halides	Po-Jung Huang	Tokyo Institute of Technology		電磁気測定室
5	202310-MCBXU-0110	欠陥を導入した酸化チタンナノシートの磁化測定	原 正大	熊本大学	黒木 玲央	Magnetization measurement of defect-induced titanium oxide nanosheets	Masahiro Hara	Kumamoto University	Kurogi Reo	電磁気測定室
6	202311-MCBXU-0111	電気推進機に搭載する熱電子カソードの耐食性評価	高崎 大吾	東京大学	藤森 蒼天 大日 勇海	Corrosion resistance evaluation of a thermionic cathode for electric propulsions	Daigo Takasaki	The University of Tokyo	Aoma Fujimori Isami Dainichi	光学測定室

国際超強磁場科学施設 / International MegaGauss Science Laboratory

No.	課題番号	課題名	氏名	所属	分担者	Title	Name	Organization	Member of research project	担当所員
1	202304-HMBXX-0056	パルス強磁場下におけるSrFeO3の異方的な超音波応答の観測	巖 正輝	理化学研究所		Observation of anisotropic ultrasonic response in SrFeO3 under pulsed high magnetic fields	Masaki Gen	RIKEN		金道 浩一
2	202305-HMBXX-0064	V2O3およびNiSナノ結晶の比熱測定	石渡 洋一	佐賀大学	赤瀬 慶祐 宮崎 駿	Heat capacity measurements of V2O3 and NiS nanocrystals	Yoichi Ishiwata	Saga University	Keisuke Akase Hayato Miyazaki	金道 浩一
3	202305-HMBXX-0078	カゴメ格子反強磁性フッ化物と不整合積層カルコゲナイドの強磁場磁化過程	道岡 千城	京都大学	吉永 公平	High field magnetization in Kagome-lattice antiferromagnetic fluorides and misfit layered chalcogenides	Michioka Chishiro	Kyoto University	Kohei YOSHINAGA	金道 浩一
4	202305-HMBXX-0079	重い電子系化合物が示す非従来型超伝導と量子臨界的挙動の相関	横山 淳	茨城大学	高橋 哲平	Relationship between unconventional superconductivity and quantum critical behavior in heavy-fermion compounds	Makoto Yokoyama	Ibaraki University	Teppeji Takahashi	金道 浩一

5	202305-HMBXX-0080	幾何学的フラストレート磁性体の強磁場磁化測定	菊池 彦光	福井大学		Magnetization measurements of the frustrated magnets	Hikomitsu Kikuchi	University of Fukui		金道 浩一
6	202305-HMBXX-0088	ラジカル系錯体における多様な量子スピンモデルの強磁場物性	山口 博則	大阪公立大学		High-field magnetic properties of various quantum spin models in radical-based complexes	Hironori Yamaguchi	Osaka Metropolitan University		金道 浩一
7	202306-HMBXX-0072	新しい硫化物フラストレート磁性体における強磁場物性	原口 祐哉	東京農工大学	北村 昌大	High Magnetic Field Properties in Sulfide Frustrate Magnets	Yuya Haraguchi	Tokyo University of Agriculture and Technology	masahiro kitamura	金道 浩一
8	202306-HMBXX-0074	トポロジカル近藤絶縁体YbB12と高压合成希土類ホウ化物R <sub>Bn</sub> (n=12, 66) の強磁場磁化と輸送特性	伊賀 文俊	茨城大学		Magnetic and transport properties in high fields of topological Kondo insulator YbB12 and novel rare earth borides R <sub>Bn</sub> (n=12, 66) produced by high pressure synthesis	Fumitoshi Iga	Ibaraki University		金道 浩一
9	202306-HMBXX-0085	有機超伝導体における高次ランダウ準位Abrikosov状態の観測	杉浦 栞理	東北大学 金属材料研究所	高橋 歩美	Abrikosov-like states of higher Landau levels in organic superconductor	Shiori Sugiura	Institute for Materials Research, Tohoku University	Ayumi Takahashi	金道 浩一
10	202309-HMBXX-0092	多元素ドーパLa <sub>0.7</sub> (Ba <sub>x</sub> CaySr <sub>z</sub> ) <sub>0.3</sub> MnO <sub>3</sub> 系における磁気熱量効果および異常光学応答の探索	赤木 暢	東北大学		Investigation of magneto-caloric effect and unusual photo response in multi-element doped La <sub>0.7</sub> (Ba <sub>x</sub> CaySr <sub>z</sub> ) <sub>0.3</sub> MnO <sub>3</sub>	Mitsuru Akaki	Tohoku University		金道 浩一
11	202304-HMBXX-0047	Explore the high-field magnetism and magnetic field induced exotic ferroelectric ordering in L-type Fe <sub>2</sub> (MoO <sub>4</sub> ) <sub>3</sub> ferrimagnetic sample.	Her Jim-Long	Division of Natural Science, Center for General Education, Chang Gung University		Explore the high-field magnetism and magnetic field induced exotic ferroelectric ordering in L-type Fe <sub>2</sub> (MoO <sub>4</sub> ) <sub>3</sub> ferrimagnetic sample.	Jim-Long Her	Division of Natural Science, Center for General Education, Chang Gung University		松田 康弘
12	202305-HMBXX-0049	Investigation of Sm-Co-B-based compounds with giant anisotropy field under ultrahigh magnetic field	Tozman Pelin	Functional Materials, Technical University of Darmstadt		Investigation of Sm-Co-B-based compounds with giant anisotropy field under ultrahigh magnetic field	Pelin Karanikolas Tozman	Functional Materials, Technical University of Darmstadt		松田 康弘
13	202305-HMBXX-0062	強磁場による分子軌道破壊と新規構造の開拓	平井 大悟郎	名古屋大学		Molecular orbital breaking and formation of novel crystal structures under high magnetic fields	Daigorou Hirai	Nagoya University		松田 康弘
14	202305-HMBXX-0065	Magnetostriction study of nematic transition and an entangled spin-orbital-lattice order in a 5d1-electron system	Islam Zahir	Argonne National Laboratory		Magnetostriction study of nematic transition and an entangled spin-orbital-lattice order in a 5d1-electron system	Zahir Islam	Argonne National Laboratory		松田 康弘
15	202305-HMBXX-0052	PPMSに取り付け可能な磁気冷凍セルを用いたサブケルビン温度域でのイメージング	志村 恭通	広島大学	渡邊 寛大 富田 光太郎 草ノ瀬 優香 (名古屋大学)	Imaging at sub-Kelvin temperature region by magnetic refrigeration cell attachable to PPMS	Yasuyuki Shimura	Hiroshima University	Kanta Watanabe Kotaro Tomita kusanose yuka (Nagoya University)	徳永 将史
16	202305-HMBXX-0076	希土類準結晶・近似結晶における磁気熱量効果	三宅 厚志	東北大学	出口 和彦 (名古屋大学)	Magnetocaloric effect measurements of rare-earths based quasicrystal and quasicrystal approximants	Atsushi Miyake	Tohoku University	Kazuhiko Deguchi (Nagoya University)	徳永 将史
17	202306-HMBXX-0071	UTe <sub>2</sub> とその関連物質の強磁場物性	三宅 厚志	東北大学	巖 正輝 (理化学研究所) 青木 大	High magnetic field properties in UTe <sub>2</sub> and its related materials	Atsushi Miyake	Tohoku University	Masaki Gen (RIKEN) Dai Aoki	徳永 将史
18	202306-HMBXX-0073	低温で合成されたフラストレート磁性体の強磁場下での物性	香取 浩子	東京農工大学	原口 祐哉 若杉 和弘 久米田 理桜	Physical properties of frustrated magnetic materials synthesized at low temperatures under high magnetic fields	Hiroko Katori	Tokyo University of Agriculture and Technology	Yuya Haraguchi wakasugi kazuhiko Rio Kumeda	徳永 将史

19	202309-HMBXX-0094	電子移動共役スピン転移を伴う分子結晶における磁場誘起分極スイッチング	呉 樹旗	九州大学先端物質化学研究所	鄭 文偉	Magnetic Field-Induced Polarization Switching in Molecular Crystals with the Electron Transfer Coupled Spin Transition	Shu-Qi Wu	Institute for Materials Chemistry and Engineering, Kyushu University	ZHENG WENWEI	徳永 将史
20	202311-HMBXX-0096	光磁気ドメイン発達過程のKerr効果顕微鏡観察	所 裕子	筑波大学	長島 俊太郎	Observation of development of magnetic domain in photo-induced magnetization using Kerr effect microscopy	Hiroko Tokoro	University of Tsukuba	Shuntaro Nagashima	徳永 将史
21	202401-HMBXX-0098	ハンダの超伝導状態における磁束トラップの観察	水口 佳一	東京都立大学	有馬 寛人	Observation of trapped magnetic flux in superconducting solder	Yoshikazu Mizuguchi	Tokyo Metropolitan University	Arima Hiroto	徳永 将史
22	202305-HMBXX-0051	金属超伝導体および強相関電子系の結晶育成と強磁場物性研究	小林 和	静岡大学	エスティアク アフメド 小林 和 大窪 悠太	Crystal growth and physical Properties at high magnetic fields in metallic superconductors and strongly correlated electron system	Kazu Kobayashi	Shizuoka University	Esteaque Ahmed Kazu Kobayashi Yuta Okubo	小濱 芳允
23	202305-HMBXX-0059	パルス強磁場下における CdCr2O4 の磁歪および比熱測定	巖 正輝	理化学研究所		Magnetostriction and heat capacity measurements on CdCr2O4 in pulsed high magnetic fields	Masaki Gen	RIKEN		小濱 芳允
24	202309-HMBXX-0093	カゴメ反強磁性体YCu3(OH)6.5Br2.5の1/9磁化プラトー状態	末次 祥大	京都大学		1/9 magnetization plateau state in kagome antiferromagnet YCu3(OH)6.5Br2.5	Shota Suetsugu	Kyoto University		小濱 芳允
25	202306-HMBXX-0081	超音波を軸とした複合物性測定による強相関電子系の強磁場中量子状態の探索	栗原 綾佑	東京理科大学	矢口 宏 小峰 智弥	Quantum states in strongly-correlated electron systems under high-magnetic fields by multiprobe measurements	Ryosuke Kurihara	Tokyo University of Science	Hiroshi Yaguchi Tomoya Komine	宮田 敦彦
26	202401-HMBXX-0099	パルス強磁場下における超音波測定を用いたウラン化合物の磁場誘起相の研究	柳澤 達也	北海道大学	清水 悠晴 (東北大学) 栗原 綾佑 (東京理科大学) 三宅 厚志 (東北大学) 青木 大 (東北大学) 日比野 瑠央 ウェイ ファンチュン 土田 健登	Magnetic field-induced phases of uranium compounds studied by ultrasonic measurements under pulsed high-magnetic fields	Tatsuya Yanagisawa	Hokkaido University	Yusei Shimizu (Tohoku University) Ryosuke Kurihara (Tokyo University of Science) Atsushi Miyake (Tohoku University) Dai Aoki (Tohoku University) Ruo Hibino FANCHUN WEI Kento Tsuchida	宮田 敦彦

大阪大学大学院理学研究科附属先端強磁場科学研究センター / Center for Advanced High Magnetic Field Science, Graduate School of Science, Osaka University

No.	課題番号	課題名	氏名	所属	分担者	Title	Name	Organization	Member of research project	担当所属
1	202305-HMOXX-0048	強磁性ホイスラー合金Ni2MnGaX(X= Cr, Fe)系合金の磁気的機能性の研究	左近 拓男	龍谷大学		Research on magnetic functionalities of Ni2MnGaX(X= Cr, Fe) type Heusler alloys	Takuo Sakon	Ryukoku University		萩原 政幸 (大阪大学)
2	202305-HMOXX-0050	パルス強磁場高圧下ESRシステムの改良	櫻井 敬博	神戸大学		Improvement of pulse high field high pressure ESR system	Takahiro Sakurai	Kobe University		萩原 政幸 (大阪大学)
3	202305-HMOXX-0054	マイクロ波加熱合成無機材料の強磁場物性	浅野 貴行	福井大学	I Putu Abdi Karya Muhammad Al Jalali 仲川 晃平	Magnetic properties of inorganic materials under a high magnetic field synthesized by microwave heating	Takayuki Asano	University of Fukui	I Putu Abdi Karya Muhammad Al Jalali Kohei Nakagawa	萩原 政幸 (大阪大学)

4	202305-HMOXX-0057	パルス強磁場用極低温実験装置の開発	野口 悟	大阪公立大学	前川 翔	Development of the cryostat for pulsed high magnetic field	Satoru Noguchi	Osaka Metropolitan University	Sho Maegawa	萩原 政幸 (大阪大学)
5	202305-HMOXX-0060	PtBi2における化学ドーピングによる超伝導増強の起源についての研究	工藤 一貴	大阪大学		Study on the origin of the enhanced superconductivity by chemical doping in PtBi2	Kazutaka Kudo	Osaka University		萩原 政幸 (大阪大学)
6	202305-HMOXX-0061	BaPt(As <sub>1-x</sub> Sb <sub>x</sub> )における超伝導転移温度の非単調なx依存性の起源についての研究	工藤 一貴	大阪大学		Study on the origin of the non-monotonic x dependence of the superconducting transition temperature in BaPt(As <sub>1-x</sub> Sb <sub>x</sub> )	Kazutaka Kudo	Osaka University		萩原 政幸 (大阪大学)
7	202305-HMOXX-0063	Sm化合物の強磁場磁化	竹内 徹也	大阪大学	大貫 惇睦 (東京都立大学)	High-Field Magnetization of Sm Compounds	Tetsuya Takeuchi	Osaka University	Yoshichika Onuki (Tokyo Metropolitan University)	萩原 政幸 (大阪大学)
8	202305-HMOXX-0083	非従来型フェロイック秩序を内包する磁性体の電気磁気特性評価	木村 健太	大阪公立大学	青木 一步	Magnetic and electrical characterization of magnetic materials with unconventional ferroic order	Kenta Kimura	Osaka Metropolitan University	Ippo Aoki	萩原 政幸 (大阪大学)
9	202306-HMOXX-0066	電気磁気反強磁性Cr <sub>2</sub> O <sub>3</sub> 薄膜の界面磁化検出	白土 優	大阪大学		Detection of interfacial magnetic moment in magnetoelectric Cr <sub>2</sub> O <sub>3</sub> thin film	Yu Shiratsuchi	Osaka University		萩原 政幸 (大阪大学)
10	202306-HMOXX-0067	カプセル蛋白質 (encapsulin from Pyrococcus furiosus) 内に合成した磁性ナノ粒子の磁気的性質	白土 優	大阪大学		Magnetic properties of magnetic nanoparticles synthesized in encapsulin from Pyrococcus furiosus	Yu Shiratsuchi	Osaka University		萩原 政幸 (大阪大学)
11	202306-HMOXX-0068	強いスピン軌道相互作用を活かした酸化物スピントロニクス	松野 丈夫	大阪大学	塩貝 純一 上田 浩平	Oxide spintronics utilizing strong spin-orbit coupling	Jobu Matsuno	Osaka University	Junichi Shiogai Kohei Ueda	萩原 政幸 (大阪大学)
12	202306-HMOXX-0069	層状磁性半導体の巨大磁気抵抗効果の研究	村川 寛	大阪大学		Research for the giant magnetoresistance in the layered magnetic semiconductors	Hiroshi Murakawa	Osaka University		萩原 政幸 (大阪大学)
13	202306-HMOXX-0082	鉄系母物質RFeAs <sub>1-x</sub> PxO (R=Pr, Nd) の磁気相図	宮坂 茂樹	兵庫県立大学		Magnetic phase diagram of RFeAs <sub>1-x</sub> PxO (R=Pr, Nd)	Shigeki Miyasaka	University of Hyogo		萩原 政幸 (大阪大学)
14	202306-HMOXX-0086	異種金属を含むハニカム格子反強磁性体 M <sub>1</sub> M <sub>2</sub> (pymca)3ClO <sub>4</sub> の磁性	本多 善太郎	埼玉大学		Magnetic properties of honeycomb lattice antiferromagnet M <sub>1</sub> M <sub>2</sub> (pymca)3ClO <sub>4</sub> containing two dissimilar metal ions	Zentaro Honda	Saitama University		萩原 政幸 (大阪大学)
15	202310-HMOXX-0095	非従来型超伝導体微細構造のパルス強磁場下輸送特性	掛谷 一弘	京都大学	北野 晴久 (青山学院大学) 本山 雄基 (青山学院大学)	Transport measurements on micro-structured unconventional superconductors under pulsed high magnetic fields	Itsuhiro Kakeya	Kyoto University	Haruhisa Kitano (Aoyama Gakuin University) Yuki Motoyama (Aoyama Gakuin University)	萩原 政幸 (大阪大学)

強磁場コラボラトリー / The High Magnetic Field Collaboratory

No.	課題番号	課題名	氏名	所属	分担者	Title	Name	Organization	Member of reseach project	担当所員
1	202305-HMCXX-0045	強磁場を用いたMn-Zn系合金のメタ磁性相転移の実験的調査	許 晶	東北大学	今富 大介	Investigation on metamagnetic transition behaviors of Mn-Zn alloys using high magnetic fields	Xiao Xu	Tohoku University	Daisuke Imatomi	徳永 将史
2	202212-HMCXX-0023	カゴメ磁性体において実現する新奇磁気状態の磁場制御とNMR測定による微視的機構解明	井原 慶彦	北海道大学		High-field control and NMR study of exotic magnetic states in kagome magnets	Yoshihiko Ihara	Hokkaido University		小濱 芳允
3	202211-HMBXX-0001	ラジカル系錯体における多様な量子スピンモデルの強磁場物性	山口 博則	大阪公立大学		High-field magnetic properties of various quantum spin models in radical-based complexes	Hironori Yamaguchi	Osaka Metropolitan University		萩原 政幸

留学研究課題 / External Research Project Long / Short-term

No.	課題番号	課題名	氏名	所属	分担者	Title	Name	Organization	Member of reseach project	担当所員
1	202211-VSBXL-0001	新規ケージドルシフェリンの光開裂定量計測	中野 智哉	群馬大学		Study for photocleavage of new caged luciferin	Nakano Tomoya	Gunma University		秋山 英文
2	202211-VSBXL-0002	青色波長領域における発光量絶対値測定系の校正	倉田 洋佑	群馬大学		Calibration of bio/chemiluminescence spectrometer with cooled charge-coupled device (CCD) detector at blue wavelengths	KURATA YOSUKE	GUNMA UNIVERSITY		秋山 英文
3	202211-VSBXL-0005	酵素環境下における AkaLumine-oxy 体の分光学的研究	大澤 敬太	群馬大学院理工学府		Spectroscopic Study of AkaLumine-oxy form in an Enzymatic Environment	Osawa Keita	Gunma University		秋山 英文
4	202211-VSBXL-0006	UVレーザー及びLED光源によるD-Luciferin光破壊条件の探索	松永 大輝	群馬大学		Study for photo-breaching condition of D-luciferin using UV laser and LED light	Hiroki Matsunaga	Gunma University		秋山 英文
5	202212-VSBXL-0003	レーザー光によるクマリンケージドルシフェリンの光開裂実験	今西 勇輔	群馬大学		Photocleavage of coumarin caged luciferin by laser irradiation	Yusuke Imanishi	Gunma University		秋山 英文
6	202305-VSBXS-0007	第一原理電子状態計算ソフトOpenMXのGPUとSIMDによる高速化とmodified-DNAへの応用	川井 弘之	新潟大学		GPU and SIMD acceleration for the first-principles electronic structure calculation software OpenMX and its application to modified-DNA	Hiroyuki Kawai	Niigata University		尾崎 泰助
7	202212-VSBXL-0004	超短パルスレーザー照射により誘起される微細構造変化の評価	高林 圭佑	秋田大学		Evaluation of structural changes induced by ultrashort pulsed laser	Keisuke Takabayashi	Akita University		小林 洋平

No.	課題名	氏名	所属	分担者 (共同研究者)	Title	Name	Organization	Member of research project	装置	ビームポート
1	4G-GPTAS (汎用3軸中性子分光器) IRT課題	佐藤 卓	東北大学	長谷 正司、 焔維 曾、 壁谷 典幸、 Piyawongwatthana Pharit、 三宅 厚志、 横山 淳、 石田 健浩、 金城 克樹、 村崎 遼、 那波 和宏、 Wu Hung-Cheng	IRT project of GPTAS	Taku Sato	Tohoku University	Masashi Hase, Chun Wai Tsang, Noriyuki Kabeya, Pharit Piyawongwatthana, Atsushi Miyake, Makoto Yokoyama, Takehiro Ishida, Katsuki Kinjo, Ryo Murasaki, Kazuhiro Nawa, Hung-Cheng Wu	GPTAS	4G
2	シクロヘキサン液体中における分子間相互作用 が電子分布に及ぼす影響	亀田 恭男	山形大学	強口 岬	Effect of intermolecular interaction on electron distribution of cyclohexane in the liquid state	Yasuo Kameda	Yamagata University	Misaki Kowaguchi	GPTAS	4G
3	特異な価数秩序を示すYbPdの最低温磁気構造解 析	光田 暁弘	九州大学	大山 研司、 富松 優花、 横枕 拓八、 田坂 啓悟、 中島 怜	Magnetic structure at lowest temperatures of exotic valence-ordered YbPd	Akihiro Mitsuda	Kyushu University	Kenji Ohoyama, Yuka Tomimatsu, Takuya Yokomakura, Keigo Tasaka, Ryo Nakashima	GPTAS	4G
4	Ce(Co,Rh)In5の磁性と超伝導発現機構の関係	古川 はづき	お茶の水女子大学	鈴木 萌香、 Foley Edward	Magnetism and Superconductivity in Ce(Co,Rh)In5	Hazuki Furukawa	Ochanomizu University	Moeka Suzuki, Edward Foley	GPTAS	4G
5	磁性イオンを持つリラクサー誘電体YbFeCoO4 における散漫散乱	左右田 稔	お茶の水女子大学	小野 友莉、 小林 星華	diffuse scattering in relaxor magnet YbFeCoO4	Minoru Soda	Ochanomizu University	Yuri Ono, Kirari Kobayashi	GPTAS	4G
6	金属間化合物MnPにおける1軸応力誘起される 巨大磁気応答を伴う原子配列再構成	満田 節生	東京理科大学	藤原 理賀、 玉造 博夢	Atomic array reconstruction with giant magnetic response induced by uniaxial stress in MnP	Setsuo Mitsuda	Tokyo University of Science	Masayoshi Fujihara, Hiromu Tamatsukuri	GPTAS	4G
7	フラストレート磁性体DyRu2Si2における次元 低下と異常な相転移ダイナミクス	田畑 吉計	京都大学	吉本 周玄	Dimensional reduction and extraordinary phase- transition dynamics in the frustrated magnet DyRu2Si2	Yoshikazu Tabata	Kyoto University	Subaru Yoshimoto	GPTAS	4G
8	Au72Si12.5Eu13.5近似結晶の臨界挙動	那波 和宏	東北大学	金城 克樹	Critical behavior of the quasicrystal approximant Au72Si12.5Eu13.5	Kazuhiro Nawa	Tohoku University	Katsuki Kinjo	GPTAS	4G
9	キタエフ模型候補物質Ru(Br,I)3の磁気構造	那波 和宏	東北大学	金城 克樹	Magnetic structure of Kitaev model candidate compound Ru(Br,I)3	Kazuhiro Nawa	Tohoku University	Katsuki Kinjo	GPTAS	4G
10	価数揺動希土類化合物における準弾性散乱の起 源の解明	筒井 智嗣	高輝度光科学研究 センター	小野 圭吾	Elucidation of the origin of the quasi-elastic scattering in a valence-fluctuating rare-earth compound	Satoshi Tsutsui	Japan Synchrotron Radiation Research Institute	Keigo Ono	GPTAS	4G
11	5G PONTAを用いた中性子散乱研究	中島 多朗	東京大学	高阪 勇輔、 秋光 純、 高橋 慎吾、 Larsen Simon、 寺田 典樹、 大熊 隆太郎、 植田 大地、 藤澤 唯太、 山田 林介、 Max Hirschberger、 Sebastian Esser、 齋藤 開	IRT project of PONTA	Taro Nakajima	The University of Tokyo	Yusuke Kousaka, Jun Akimitsu, Shingo Takahashi, Simon Larsen, Noriki Terada, Ryutarou Okuma, Daichi Ueta, Yuita Fujisawa, Rinsuke Yamada, Max Hirschberger, Sebastian Esser, Hiraku Saito	PONTA	5G
12	Tuning the spin configuration of the magnetic topological semimetal YbMnSb2 using uniaxial pressure	Bhoi Dilip Kumar	東京大学		Tuning the spin configuration of the magnetic topological semimetal YbMnSb2 using uniaxial pressure	Dilip Kumar Bhoi	The University of Tokyo		PONTA	5G
13	UPt2Ge2における電荷密度波と反強磁性の共存 状態の研究	今 布咲子	北海道大学	網塚 浩	Study on the coexistence of CDW and AFM in UPt2Ge2	Fusako Kon	Hokkaido University	Hiroshi Amitsuka	PONTA	5G
14	中性子散乱法によるフェリ磁性体NdAlSiの磁気 構造の検証	山田 林介	東京大学	石原 由貴	Verification of magnetic structure of ferrimagnetic NdAlSi by neutron scattering	Rinsuke Yamada	The University of Tokyo	Yuki Ishihara	PONTA	5G

15	NdRuSn3における量子スピン液体状態の探索	岩佐 和晃	茨城大学	熊田 隆伸、浦本 結稜、鈴木 貴太、告 華連、鈴木 陽太郎、浦本 結稜、黒澤 航海	Investigation of a quantum spin liquid state in NdRuSn3	Kazuaki Iwasa	Ibaraki University	Takanobu Kumada, Yui Uramoto, Kanta Suzumura, Karen Tsuge, Yotaro Suzuki, Yui Uramoto, Wataru Kurosawa	PONTA	5G
16	磁気強誘電性を示すMn3WO6の磁気構造研究	有馬 孝尚	東京大学	徳永 祐介、虎頭 大輔、鬼頭 俊介	Magnetic structure analysis of Mn3WO6 hosting spin-driven ferroelectricity	Taka-hisa Arima	The University of Tokyo	Yusuke Tokunaga, Daisuke Koto, Shunsuke Kitou	PONTA	5G
17	新規ウラン化合物UPt3Al5の磁気構造の探索2	本多 史憲	九州大学	広瀬 雄介	Magnetic structure study of an antiferromagnet UPt3Al5 using neutron diffraction - 2	Fuminori Honda	Kyushu University	Yusuke Hirose	PONTA	5G
18	巨大な異常ホール効果を示す反強磁性体の磁気構造解析	関 真一郎	東京大学	山内 健聖、井上 裕貴、北折 暁	Magnetic structure analysis of antiferromagnets with large anomalous Hall effect	Shinichiro Seki	The University of Tokyo	Kensei Yamauchi, Hiroki Inoue, Aki Kitaori	PONTA	5G
19	一軸応力下中性子弾性散乱による160Gd2PdSi3のsingle-q/multi-q磁気秩序の検証	齋藤 開	東京大学	小林 尚暉	Test for the single-q/multiple-q magnetic orders on 160Gd2PdSi3 by the elastic neutron scattering under the uniaxial stress	Hiraku Saito	The University of Tokyo	Naoki Kobayashi	PONTA	5G
20	一軸応力による正方格子遍歴磁性体 EuAl4 の磁気変調の制御	巖 正輝	理化学研究所		Uniaxial stress control of magnetic modulation in a square-lattice itinerant magnet EuAl4	Masaki Gen	RIKEN		PONTA	5G
21	巨大磁気熱量効果を示すHoB2の相転移の起源	寺田 典樹	物質材料研究機構	Larsen Simon	Origin of phase transitions in HoB2 with a giant magnetocaloric effect	Noriki Terada	National Institute for Materials Science	Simon Larsen	PONTA	5G
22	中性子回折によるLa5Mo4O16軌道整列の研究	飯田 一樹	総合科学研究機構	中尾 朗子、梶本 亮一	Neutron diffraction investigation on orbital order in La5Mo4O16	Kazuki Iida	Comprehensive Research Organization for Science and Society	Akiko Nakao, Ryoichi Kajimoto	PONTA	5G
23	6G TOPAN IRT課題	池田 陽一	東北大学	濱 綾太、黒澤 徹、Max Hirschberger、高橋 慎吾、Podlensnyak Andrey Aleksandrovich、Prokhnenko Oleksandr、筒井 智嗣、猪野 隆、清水 悠晴、宮崎 正範、北條 大輝、中野 愛弓、李 哲虎、岡田 始季、水口 佳一、小林 悟、藤田 全基、岩佐 和晃、南部 雄亮、谷口 貴紀、Tang Yifei、北澤 崇文、Seno Aji、Xie Peiao、Wang Tong、北沢 昂久、荒木 靖啓、竹本 朝、Zhao Hongfei、岡部 博孝、大亀 佑太、川又 雅広、鄭 家傑、梅本 好日古、高田 秀佐、二見 采樹、磯村 楓	IRT project of TOPAN	Yoichi Ikeda	Tohoku University	Ryota Itadaki, Tohru Kurosawa, Max Hirschberger, Shingo Takahashi, Andrey Aleksandrovich Podlensnyak, Oleksandr Prokhnenko, Satoshi Tsutsui, Takashi Ino, Yusei Shimizu, Masanori Miyazaki, Hiroki Hojo, Ayumi Nakano, Chul-Ho Lee, shiki okada, Yoshikazu Mizuguchi, Satoru Kobayashi, Masaki Fujita, Kazuaki Iwasa, Yusuke Nambu, Takanori Taniguchi, Yifei Tang, Takafumi Kitazawa, Seno Aji, Peiao Xie, Tong Wang, Takahisa Kitazawa, Nobuhiro Araki, Ashita Takemoto, Hongfei Zhao, Hiroataka Okabe, Yuta Oki, Masahiro Kawamata, Jiajie Zheng, Yoshihiko Umemoto, Shusuke Takada, Saiki Futami, Kaede Isomura	TOPAN	6G
24	Pressure dependence of the charge and spin density waves in La1.875Ba0.125-xSrxCuO4	WANG TONG	東北大学		Pressure dependence of the charge and spin density waves in La1.875Ba0.125-xSrxCuO4	Tong Wang	Tohoku University	Masaki Fujita, Takanori Taniguchi	TOPAN	6G
25	Incommensurate spin fluctuation on the triangular antiferromagnet: FeGa2S4	TANG YIFEI	東北大学	南部 雄亮	Incommensurate spin fluctuation on the triangular antiferromagnet: FeGa2S4	Yifei Tang	Tohoku University	Yusuke Nambu	TOPAN	6G
26	中性子回折実験によるLa2-xSrxCoO4 (0.6 < x < 1)の電荷秩序の観測	宮崎 正範	室蘭工業大学	藤村 佳紀、寺島 思唯、竹内 陸	Observation of charge ordering in La2-xSrxCoO4 (0.6 < x < 1) studied by neutron diffraction	Masanori Miyazaki	Muroran Institute of Techonogy	Yoshiki Fujimura, Kotoi Terashima, Riku Takeuchi	TOPAN	6G
27	塑性歪みを加えたPt3Fe反強磁性体における強磁性ドメインの磁気相関	小林 悟	岩手大学	Bekhbaatar Enkhmend、中野 愛弓、北條 大輝	Magnetic correlations of ferromagnetic domains in plastically strained Pt3Fe antiferromagnet	Satoru Kobayashi	Iwate University	Enkhmend Bekhbaatar, Ayumi Nakano, Hiroki Hojo	TOPAN	6G

28	Ce5Si3の磁気構造解析	小林 理気	琉球大学	前川 菜摘、富井 大海	Magnetic structure determination of Ce5Si3	Riki Kobayashi	University of the Ryukyus	Natsumi Maekawa, Hiromi Tomii	TOPAN	6G
29	フォノン分散測定による鉄マンガニ基恒弾性合金中の新規安定相の探索	池田 陽一	東北大学	藤田 全基、梅本 好日古	Search for new stable phases causing anomalous nonlinear phonon dispersion in an iron-manganese-based Elinvar alloy	Yoichi Ikeda	Tohoku University	Masaki Fujita, Yoshihiko Umemoto	TOPAN	6G
30	HERにおける量子物質の準粒子構造の研究	益田 隆嗣	東京大学	Kish Lazar, Shen Xiaoling, Shu Mingfang, Ma Jie, Zimmermann Valentin, 林田 翔平、小関 真、Igor Zaliznyak、姚 伟良、Zheludev Andrey、Syed Danish Nabi、浅井 晋一郎、Liu Zheyuan、菊地 帆高、魏 子駿	IRT project of HER	Takatsugu Masuda	The University of Tokyo	Lazar Kish, Xiaoling Shen, Mingfang Shu, Jie Ma, Valentin Zimmermann, Shohei Hayashida, Makoto Ozeki, Igor Zaliznyak, Weiliang Yao, Andrey Zheludev, Syed Danish Nabi, Shinichiro Asai, Zheyuan Liu, Hodaka Kikuchi, Zijun Wei	HER/HO DACA	C1-1
31	Incommensurate spin fluctuation on the triangular antiferromagnet: FeGa2S4	TANG YIFEI	東北大学	梅本 好日古、南部 雄亮	Incommensurate spin fluctuation on the triangular antiferromagnet: FeGa2S4	Yifei Tang	Tohoku University	Yoshihiko Umemoto, Yusuke Nambu	HER/HO DACA	C1-1
32	MnSiの変動電流下で駆動中の磁気スキルミオン格子のダイナミクス	奥山 大輔	高エネルギー加速器研究機構		Dynamics of the moving magnetic skyrmion lattice in MnSi under an alternative electric current flow	Daisuke Okuyama	High energy accelerator research organization		HER/HO DACA	C1-1
33	ワイル近藤半金属物質Ce3Rh4Sn13のケーブル構造相での磁気ゆらぎ	岩佐 和晃	茨城大学	熊田 隆伸、浦本 結稜、鈴木 貫太、告 華連、鈴木 陽太郎、浦本 結稜、黒澤 航海	Magnetic fluctuation in chiral structure phases of the Weyl-Kondo semimetal Ce3Rh4Sn13	Kazuaki Iwasa	Ibaraki University	Takanobu Kumada, Yui Uramoto, Kanta Suzumura, Karen Tsuge, Yotaro Suzuki, Yui Uramoto, Wataru Kurosawa	HER/HO DACA	C1-1
34	Nd3Co4Sn13の立方ロッド充填格子における束縛スピンの励起	岩佐 和晃	茨城大学	熊田 隆伸、浦本 結稜、鈴木 貫太、告 華連、鈴木 陽太郎、浦本 結稜、黒澤 航海	Bound spinon excitations in the cubic rod-packing lattice of Nd3Co4Sn13	Kazuaki Iwasa	Ibaraki University	Takanobu Kumada, Yui Uramoto, Kanta Suzumura, Karen Tsuge, Yotaro Suzuki, Yui Uramoto, Wataru Kurosawa	HER/HO DACA	C1-1
35	フラストレート磁性体RBaCo4O7におけるZ2ボルトックス秩序と準弾性散乱	左右田 稔	お茶の水女子大学		Z2-vortex ordering and quasi-elastic scattering in frustrated magnet RBaCo4O7	Minoru Soda	Ochanomizu University		HER/HO DACA	C1-1
36	2等辺三角格子イジング磁性体CoNb2O6のフニエ状態における磁気揺動	満田 節生	東京理科大学		Magnetic fluctuation at the Wannier point in isosceles triangular lattice Ising magnet CoNb2O6	Setsuo Mitsuda	Tokyo University of Science		HER/HO DACA	C1-1
37	磁場誘起量子臨界点近傍におけるキタエフ液体候補物質の磁気励起	益田 隆嗣	東京大学	金香紅、顧昱晨、李 源、浅井 晋一郎、Liu Zheyuan、菊地 帆高、魏 子駿	Magnetic excitations in a candidate Kitaev magnet near field-induced quantum criticality	Takatsugu Masuda	The University of Tokyo	Xianghong Jin, Yuchen Gu, Yuan Li, Shinichiro Asai, Zheyuan Liu, Hodaka Kikuchi, Zijun Wei	HER/HO DACA	C1-1
38	超低熱伝導Ag8SnSe6単結晶のフォノン分散	益田 隆嗣	東京大学	浅井 晋一郎、Liu Zheyuan、菊地 帆高、魏 子駿	Phonon dispersions of the Ag8SnSe6 single crystal with ultralow thermal conductivity	Takatsugu Masuda	The University of Tokyo	Shinichiro Asai, Zheyuan Liu, Hodaka Kikuchi, Zijun Wei	HER/HO DACA	C1-1
39	イルメナイト構造NiTiO3における外部磁場によるトポロジカル性の安定性の観測	菊地 帆高	東京大学	小関 真、益田 隆嗣、浅井 晋一郎、Liu Zheyuan、魏 子駿	Observation of topological stability on ilmenite NiTiO3 in magnetic field	Hodaka Kikuchi	The University of Tokyo	Makoto Ozeki, Takatsugu Masuda, Shinichiro Asai, Zheyuan Liu, Zijun Wei	HER/HO DACA	C1-1
40	Bi-2201系銅酸化物の超過剰ドーパ領域における磁気ゆらぎ	足立 匡	上智大学	小宮山 陽太、藤田 全基	Magnetic fluctuations in the heavily overdoped Bi-2201 cuprates	Tadashi Adachi	Sophia University	Yota Komiya, Masaki Fujita	HER/HO DACA	C1-1
41	無機有機ハイブリッド層状ペロブスカイト(C6H5CH2CH2NH3)2MnCl4のスピンの波	李 哲虎	産業技術総合研究所	Kim Ki-Yeon, Beddrich Lukas, Park Jitae, Oh In-Hwan	Spin wave investigations on the layered inorganic-organic hybrid perovskite (C6H5CH2CH2NH3)2MnCl4	Chul-Ho Lee	National Institute of Advanced Industrial Science and Technology	Ki-Yeon Kim, Lukas Beddrich, Jitae Park, In-Hwan Oh	HER/HO DACA	C1-1

42	SANS-U(二次元位置測定小角散乱装置)IRT課題	眞弓 皓一	東京大学	日高 正基、笠口 友隆、渡我部 りさ、清水 将裕、海老原 梨沙、中間 貴寛、龟谷 優樹、Kou Hao、温井 通介、石 棟、野々山 貴行、杉山 正明、難波 恵汰、呉羽 拓真、河野 紋佳、福本 颯太、宮崎 蒼生、菱田 真史、辻 優依、山田 悟史、土肥 侑也、橋本 慧、榎木 崇人、守島 健、井上 倫太郎、小田 達郎、Geonzon Lester	IRT project of SANS-U	Koichi Mayumi	The University of Tokyo	Masaki Hidaka, Tomotaka Oroguchi, Lisa Watakabe, Masahiro Shimizu, Risa Ebihara, Takahiro Nakama, Yuki Kametani, Hao Kou, Yosuke Nukui, Dong Shi, Takayuki Nonoyama, Masaaki Sugiyama, Keita Namba, Takuma Kureha, Ayaka Kawano, Sota Fukumoto, Aoi Miyazaki, Mafumi Hishida, Yui Tsuji, Norifumi Yamada, Yuya Doi, Kei Hashimoto, Takato Enoki, Ken Morishima, Rintaro Inoue, Tatsuro Oda, Lester Geonzon	SANS-U	C1-2
43	Investigating the in-situ structure-property of carrageenan gels and its mixtures using large deformation via stretching and small angle neutron scattering	Geonzon Lester	東京大学	榎木 崇人	Investigating the in-situ structure-property of carrageenan gels and its mixtures using large deformation via stretching and small angle neutron scattering	Lester Geonzon	The University of Tokyo	Takato Enoki	SANS-U	C1-2
44	Elucidating the effect of molecular weight on the hierarchical network structure of binary mixed carrageenan gel	Geonzon Lester	東京大学	榎木 崇人	Elucidating the effect of molecular weight on the hierarchical network structure of binary mixed carrageenan gel	Lester Geonzon	The University of Tokyo	Takato Enoki	SANS-U	C1-2
45	強磁性超伝導体における自発的磁束格子構造の研究	古川 はづき	お茶の水女子大学	植木 萌、伊藤 未希、Foley Edward	Spontaneous vortex phase in ferromagnetic superconductors	Hazuki Furukawa	Ochanomizu University	Moe Ueki, Miki Ito, Edward Foley	SANS-U	C1-2
46	ジェミニ型界面活性剤を添加したカチオン化ベシクルの中性子小角散乱による構造解析	吉村 倫一	奈良女子大学	高見 風夏、王 珊、金子 理香、矢田 詩歩	Structural Analysis of Gemini Surfactant Containing Cationized Vesicle Using Small-Angle Neutron Scattering	Tomokazu Yoshimura	Nara Women's University	Fuka Takami, Shan Wang, Rika Kaneko, Shiho Yada	SANS-U	C1-2
47	ポリオキシエチレンスルホン酸を親水基に有するセカンダリー界面活性剤がつくる泡沫の構造解析	吉村 倫一	奈良女子大学	岩瀬 裕希、高見 風夏、王 珊、金子 理香、矢田 詩歩	Structural Analysis of Foam Formed by Secondary Surfactant with Polyoxyethylene-Sulfonic Acid Group	Tomokazu Yoshimura	Nara Women's University	Hiroki Iwase, Fuka Takami, Shan Wang, Rika Kaneko, Shiho Yada	SANS-U	C1-2
48	逆転コントラスト同調中性子小角散乱法によるER-60のドメイン選択的構造解析	奥田 綾	京都大学	清水 将裕、坂本 璃月、笠口 友隆	Domain-selective structural analysis of the ER-60 using inverse contrast-matching small-angle neutron scattering	Aya Okuda	Kyoto University	Masahiro Shimizu, Ritsuki Sakamoto, Tomotaka Oroguchi	SANS-U	C1-2
49	時計タンパク質KaiA-KaiB-KaiC複合体におけるKaiAの動態の観測	守島 健	京都大学	坂本 璃月、井上 倫太郎	Observation of kinetics of clock protein KaiA in KaiA-KaiB-KaiC complex	Ken Morishima	Kyoto University	Ritsuki Sakamoto, Rintaro Inoue	SANS-U	C1-2
50	ドデカン酸カリウムとジグリセリン誘導体混合系の特異な表面張力の挙動と会合体特性の関係	安部 美季	奈良女子大学	三木 宏美、山田 悟史	Relationship between the peculiar surface tension behavior and aggregate properties of potassium dodecanoate and diglycerol derivative mixtures	Miki Abe	Nara Women's University	Hiroimi Miki, Norifumi Yamada	SANS-U	C1-2
51	異方的形状Fe3O4ナノ粒子の磁場誘起配列	小林 悟	岩手大学	Bekhbaatar Enkhmend、三上 翔也、及川 歩起	Field-induced assembly of anisotropic-shaped Fe3O4 nanoparticles	Satoru Kobayashi	Iwate University	Enkhmend Bekhbaatar, Shoya Mikami, Ibuki Oikawa	SANS-U	C1-2
52	コントラスト変調SANSによる環状高分子/クレイ粒子ナノコンポジット系の構造研究	小田 達郎	東京大学	眞弓 皓一、遠藤 仁	Study of the cross-linking structure of slide-ring polymer and clay nanocomposite systems by contrast variation SANS	Tatsuro Oda	The University of Tokyo	Koichi Mayumi, Hitoshi Endo	SANS-U	C1-2
53	マルチドメインタンパク質の柔軟な構造の解析	小田 隆	日本原子力研究開発機構	守島 健	Analysis of flexible structure of multi-domain protein	Takashi Oda	Japan Atomic Energy Agency	Ken Morishima	SANS-U	C1-2
54	小角中性子散乱測定を用いたポリエチレンの一軸変形挙動に与える延伸温度の影響の評価	木田 拓充	滋賀県立大学	鈴木 海渡、土肥 侑也	Influences of Temperature on Uniaxial Deformation Behavior of Polyethylene Solids Evaluated by SANS Measurement	Takumitsu Kida	The University of Shiga Prefecture	Kaito Suzuki, Yuya Doi	SANS-U	C1-2

55	スライドリング網目を有するイオンゲルの延伸中における異方的な網目構造変化	橋本 慧	岐阜大学	榎木 崇人	Anisotropy in strain-induced structural change of slide-ring network in ion gel	Kei Hashimoto	Gifu University	Takato Enoki	SANS-U	C1-2
56	マイクロエマルションの皮膚浸透における構造と皮膚水分量の影響	櫻木 美菜	崇城大学	篠田 翔大朗、中村 絵里佳	Influence of the water content of the skin and the microemulsion structure on the penetration mechanism	Mina Sakuragi	Sojo University	Shotaro Shinoda, Erika Nakamura	SANS-U	C1-2
57	星形高分子から成る過渡的網目における相分離構造の評価	片島 拓弥	東京大学	Li Xiang	Structural analysis of phase separation behavior in transient networks formed from star-shaped polymers	Takuya Katashima	The University of Tokyo	Xiang Li	SANS-U	C1-2
58	制汗機能を有するクロロヒドロキシアルミニウムの形成するナノ粒子およびゲルネットワークの構造解析	眞弓 皓一	東京大学	小野 真一、森垣 篤典、高林 輝、岩澤 広将、正岡 幸子	Structural analysis of hydrogels prepared from aluminum chlorohydroxy	Koichi Mayumi	The University of Tokyo	Masakazu Ono, Atsunori Morigaki, Hikaru Takabayashi, Hironobu Iwasawa, Sachiko Masaoka	SANS-U	C1-2
59	中性子散乱法によるアニオン-両性界面活性剤混合系の泡沫の構造解析	矢田 詩歩	東京理科大学	岩瀬 裕希、亀田 太朗、河田 結夏、松本 悠汰	Structural analysis of foam formed by mixed system of anionic surfactants and zwitterionic surfactant mixture using neutron scattering	Shiho Yada	Tokyo University of Science	Hiroki Iwase, Taro Kameda, Yuna Kawata, Yuta Matsumoto	SANS-U	C1-2
60	中性子散乱法による二次元状ポリスチレン溶液構造の研究	西島 杏実	東京大学		Study of the solution-state structure of two-dimensional polystyrene by small angle neutron scattering	Ami Nishijima	The University of Tokyo		SANS-U	C1-2
61	中性子散乱法による人工高分子イオンチャネル疎水領域の水和量の決定	西村 智貴	信州大学	小坂 峻史	Determination of hydration of the hydrophobic layer of the artificial macromolecular ion channels by neutron scattering	Tomoki Nishimura	Shinshu University	Shunji Kosaka	SANS-U	C1-2
62	重合条件を変えたときの重合誘起ガラス化とその近傍での不均一性の研究	鈴木 祥仁	大阪公立大学	土肥 侑也	Polymerization-induced vitrification and heterogeneity at the vicinity of vitrification	Yasuhito Suzuki	Osaka Metropolitan University	Yuya Doi	SANS-U	C1-2
63	中性子・X線散乱法を利用したpHを変化させた牛乳内のカゼインミセル構造変化の研究	高木 秀彰	高エネルギー加速器研究機構		A study on the structural changes of bovine casein micelles in milk using neutron and X-ray scatterings	Hideaki Takagi	High energy accelerator research organization		SANS-U	C1-2
64	イオン液体の陽イオン環構造が寄与する錯形成平衡の研究	高椋 利幸	佐賀大学	種熊 知紗、勝山 美空、佐々木 魁斗	Study on Effects of Ring Structure of Ionic Liquid Cation on Metal Complex Formation	Toshiyuki Takamuku	Saga University	Chisa Higuma, Miku Katsuyama, Kaito Sasaki	SANS-U	C1-2
65	ポリイオンコンプレックスベシクルの構造解析	高橋 倫太郎	名古屋大学		Structural analysis of polyion complex vesicles	Rintaro Takahashi	Nagoya University		SANS-U	C1-2
66	カテナン型高分子の希薄溶液中における拡がりの評価	高野 敦志	名古屋大学	井田 彪吾、伊藤 正浩、草野 杏佳、北原 綾音	Evaluation of Chain Dimension of Catenated polymer in Dilute Solution	Atsushi Takano	Nagoya University	Hyougo Ida, Masahiro Ito, Kyoka Kusano, Ayane Kitahara	SANS-U	C1-2
67	新しいコントラストを用いた小角中性子散乱法によるポリオレフィン相分離構造・界面構造の可視化とその制御	三田 一樹	総合科学研究機構		Visualization and control of polyolefin phase separation structure and interfacial structure by small-angle neutron scattering using new contrast	Kazuki Mita	Comprehensive Research Organization for Science and Society		SANS-U	C1-2
68	超高分子量イオンゲルの絡み合い網目の構造解析	廣井 卓思	芝浦工業大学	玉手 亮多	Structural analysis of entanglement networks of ultrahigh molecular weight ion gels	Takashi Hiroi	Shibaura Institute of Technology	Ryota Tamate	SANS-U	C1-2
69	磁場センサータンパク質の中性子小角散乱解析	新井 栄揮	量子科学技術研究開発機構		Small angle neutron scattering analysis of magnetoreceptor protein	Shigeki Arai	National Institutes for Quantum Science and Technology		SANS-U	C1-2

70	中性子小角散乱による変性状態の蛋白質の構造解析	藤原 悟	量子科学技術研究開発機構	茶竹 俊行	Sstructural analysis of proteins in denatured states by small-angle neutron scattering	Satoru Fujiwara	National Institutes for Quantum Science and Technology	Toshiyuki Chatake	SANS-U	C1-2
71	空間反転対称性の破れた超伝導体のヘリカル磁束格子の観測	古川 はづき	お茶の水女子大学	伊藤 未希、植木 萌	Herical vortex phase on non-centrosymmetric superconductors	Hazuki Furukawa	Ochanomizu University	Miki Ito, Moe Ueki	SANS-U	C1-2
72	側鎖基に適度な分岐を有するポリ(4-アルキルスチレン)/ポリイソプレンブレンドの小角中性子散乱測定による相溶性評価	土肥 侑也	名古屋大学	鈴木 海渡	Miscibility evaluation of blends of poly(4-alkylstyrene) with moderately branched side groups and polyisoprene by small angle neutron scattering measurements	Yuya Doi	Nagoya University	Kaito Suzuki, Yuya Doi	SANS-U	C1-2
73	ポリスチレン-b-ポリアクリル酸ブチルの相挙動に関する研究	山本 勝宏	名古屋工業大学		Phase Behavior of Polystyrene-b-poly(n-butyl acrylate)	Katsuhiro Yamamoto	Nagoya Institute of Technology		SANS-U	C1-2
74	アルコール添加によるタンパク質の変性に対する温度効果	高椋 利幸	佐賀大学	種熊 知紗、勝山 美空、佐々木 魁斗	Temperature Effects on Protein Denaturation by Adding Alcohols	Toshiyuki Takamuku	Saga University	Chisa Higuma, Miku Katsuyama, Kaito Sasaki	SANS-U	C1-2
75	iNSE (中性子スピネコー分光器)IRT課題	小田 達郎	東京大学	眞弓 皓一、Geonzon Lester	IRT project of iNSE	Tatsuro Oda	The University of Tokyo	Koichi Mayumi, Lester Geonzon	iNSE	C2-3-1
76	Elaborating the nano spatiotemporal dynamics of carrageenan gels and their mixtures using neutron spin echo	Geonzon Lester	東京大学		Elaborating the nano spatiotemporal dynamics of carrageenan gels and their mixtures using neutron spin echo	Lester Geonzon	The University of Tokyo		iNSE	C2-3-1
77	中性子スピネコー法による環状高分子/クレイナノコンポジット系のダイナミクス研究	小田 達郎	東京大学	眞弓 皓一、遠藤 仁	Dynamics study of the slide-ring polymer and clay nanocomposite systems by neutron spin echo spectroscopy	Tatsuro Oda	The University of Tokyo	Koichi Mayumi, Hitoshi Endo	iNSE	C2-3-1
78	勾配磁場RFを用いた広帯域波長対応 $\pi/2$ スピンプリッパーの開発	小田 達郎	東京大学		Development of a broad band $\pi/2$ spin flipper with a gradient field RF	Tatsuro Oda	The University of Tokyo		iNSE	C2-3-1
79	塩が誘起する有機溶媒水溶液の2次元流体的な臨界挙動	眞包 浩一朗	同志社大学	笠原 健司、大久保 直樹	2D-Ising like critical behavior in mixtures of water/organic solvent/antagonistic salt	Koichiro Sadakane	Doshisha University	Kenji Kasahara, Naoki Okubo	iNSE	C2-3-1
80	界面活性剤が誘起する液-液相分離のメカニズムの解明	眞包 浩一朗	同志社大学		Phase separation induced by surfactants	Koichiro Sadakane	Doshisha University		iNSE	C2-3-1
81	AGNES (高分解能パルス冷中性子分光器)IRT課題	山室 修	東京大学	遠藤 大成、廣井 慧、小林 健太郎、西岡 伸悟、矢口 寛、Zhang Menghan、泉 謙一、田路 智也、西岡 海人、佐藤 駿、秋葉 宙、大政 義典	IRT project of AGNES	Osamu Yamamuro	The University of Tokyo	Taisei Endo, Satoshi Hiroi, Kentaro Kobayashi, Shingo Nishioka, Hiroshi Yaguchi, Menghan Zhang, Kenichi Izumi, Tomoya Taji, Kaito Nishioka, Shun Sato, Hiroshi Akiba, Yoshinori Ohmasa	AGNES	C3-1-1
82	新規層状ハイドロペロブスカイトにおけるアンモニウムイオンダイナミクスの解明	Zhu Tong	京都大学		Investigation of Ammonium Dynamics in New Layered Halide Perovskites	Tong Zhu	Kyoto University		AGNES	C3-1-1
83	過塩素酸ナトリウムのエチレングリコール-水混合溶液のダイナミクス	吉田 亨次	福岡大学	上廣 誠也、川井田 拓弥、永井 哲郎	Dynamics of ethyleneglycol-water solution of NaClO4	Koji Yoshida	Fukuoka University	Seiya Uehiro, Takumi Kawaida, Tetsuro Nagai	AGNES	C3-1-1
84	疎水性溶媒中に生成する水クラスターのダイナミクスの解明	岡 弘樹	大阪大学	山室 修、秋葉 宙	Elucidation of the dynamics of water clusters generated in hydrophobic solvents	Kouki Oka	Tohoku University	Osamu Yamamuro, Hiroshi Akiba	AGNES	C3-1-1
85	水が非晶質アミロペクチンの分子ダイナミクスに及ぼす影響	川井 清司	広島大学	山田 武、曾我部 知史、望月 匠峰、加賀 谷 勇生	Effect of water on the molecular dynamics of amorphous amylopectin	Kiyoshi Kawai	Hiroshima University	Takeshi Yamada, Tomochika Sogabe, Takumi Mochizuki, Yuki Kagaya	AGNES	C3-1-1
86	エポキシネットワークの架橋密度が副緩和挙動に与える影響	眞弓 皓一	東京大学	花房 明宏、山室 修、秋葉 宙	Molecular origin of viscoelastic sub-relaxation in epoxy resins with different cross-linking densities	Koichi Mayumi	The University of Tokyo	Akihiro Hanafusa, Osamu Yamamuro, Hiroshi Akiba	AGNES	C3-1-1

87	アモルファスおよび結晶メタンハイドレートのダイナミクスに関する研究	秋葉 宙	東京大学	Zhang Menghan、山室 修	Dynamics of methane in amorphous and crystalline methane hydrate	Hiroshi Akiba	The University of Tokyo	Menghan Zhang, Osamu Yamamuro	AGNES	C3-1-1
88	中性子散乱法によるレジン含有ゴムのダイナミクスと破壊耐性の研究	菊地 龍弥	住友ゴム工業株式会社	幸泉 旭彦、塩沢 友美	Study of dynamics and fracture resistance of resin-containing rubber by neutron scattering	Tatsuya Kikuchi	Sumitomo Rubber Industries, Ltd.	Akihiko Koizumi, Tomomi Shiozawa	AGNES	C3-1-1
89	チョコレート成熟過程における油脂の相分離と結晶多形に関する非干渉性準弾性中性子散乱による研究	金子 文俊	大阪大学		Incoherent Quasi-Elastic Neutron Scattering of fats during Chocolate Aging process				AGNES	C3-1-1
90	中性子準弾性散乱法による硫化物ガラス電解質の研究	尾原 幸治	島根大学	廣井 慧、小林 健太郎	Neutron Quasi Elastic Scattering Study of Glassy Sulfide Electrolytes	Koji Ohara	Shimane University	Satoshi Hiroi, Kentaro Kobayashi	AGNES	C3-1-1
91	出土琥珀のボソンピーク測定	山口 繁生	元興寺文化財研究所		Observation of the boson peak in excavated amber.	Shigeo Yamaguchi	Gangoji institute for research of cultural property		AGNES	C3-1-1
92	ミセル内の分子運動に対するアルコール添加の影響	根本 文也	防衛大学校		Effect of additive alcohols on molecular motion in micelles	Fumiya Nemoto	National Defense Academy		AGNES	C3-1-1
93	MINE (京大複合研:多層膜中性子干渉計・反射率計) IRT課題	日野 正裕	京都大学	藤谷 龍澄、田崎 誠司、山岡 賢司、樋口 嵩、小田 達郎	MINE (Multilayer neutron interferometer and reflectometer)	Masahiro Hino	Kyoto University	Ryuto Fujitani, Seiji Tasaki, Kenji Yamaoka, Takashi Higuchi, Tatsuro Oda	MINE	C3-1-2-2
94	BGaN中性子半導体イメージングセンサーに向けた中性子検出特性評価	中野 貴之	静岡大学	安藤 光佑、櫻井 辰大	Neutron detection characteristics for B GaN neutron semiconductor imaging sensor	Takayuki Nakano	Shizuoka University	Kosuke Ando, Tatsuhiro Sakurai	MINE	C3-1-2-2
95	中性子基礎物理実験のためのデバイス開発	北口 雅暁	名古屋大学	藤家 拓大、南部 太郎	Development of neutron devices for fundamental physics	Masaaki Kitaguchi	Nagoya University	Takuhiko Fujjie, Taro Nambu	MINE	C3-1-2-2
96	自立駆動形薄膜半導体中性子検出素子の特性解明	奥野 泰希	理化学研究所		Characterization of Self-Driven Thin-Film Semiconductor Neutron Detection Devices	Yasuki Okuno	RIKEN		MINE	C3-1-2-2
97	中性子反射率MINEによる人工耐水素脆化合金多層膜[Fe/TiN]の膜構造の同定	山田 雅子	高エネルギー加速器研究機構	日野 正裕	Evaluation of the structure of bi-layers of Fe/TiN using the neutron reflectometer MINE	Masako Yamada	High energy accelerator research organization	Masahiro Hino	MINE	C3-1-2-2
98	超冷中性子スピン解析器の開発	川崎 真介	高エネルギー加速器研究機構	樋口 嵩、今城 想平、井出 郁央	Development of a Spin Analyzer for Ultra-Cold Neutrons	Shinsuke Kawasaki	High energy accelerator research organization	Takashi Higuchi, Sohei Imajo, Ikuo Ide	MINE	C3-1-2-2
99	多層膜中性子ミラーの高度化と集光デバイス開発	日野 正裕	京都大学	山岡 賢司	Development of multilayer neutron mirrors and focusing devices	Masahiro Hino	Kyoto University	Kenji Yamaoka	MINE	C3-1-2-2
100	中性子スピン干渉計への弱測定への適用	樋口 嵩	京都大学	藤谷 龍澄	Application of the weak measurement to a neutron spin interferometer	Takashi Higuchi	Kyoto University	Ryuto Fujitani	MINE	C3-1-2-2
101	中性子スピン干渉現象を用いた3次元偏極解析手法の開発	田崎 誠司	京都大学	藤谷 龍澄、鈴木 雄也	3D polarization analysis using resonance neutron spin interferometry	Seiji Tasaki	Kyoto University	Ryuto Fujitani, Takaya Suzuki	MINE	C3-1-2-2
102	反射型中性子タルボ・ロー干渉計による表面・界面構造評価手法の開発	關 義親	東北大学		Development of reflective Talbot-Lau interferometer for surface/interface structure analysis	Yoshichika Seki	Tohoku University		MINE	C3-1-2-2

103	T1-1 HQR IRT課題	大山 研司	茨城大学	伊倉 勇希、齋藤 皓太、浅野 貴行、桑原 慶太郎、宮地 優太、宇津野 魁杜、大橋 歩夢、中野 岳仁、熊田 隆伸、高橋 哲平、富士本 駿、横山 淳、海老澤 秀明、矢代 安澄、小泉 遼介、并能 楓、阿部 幸樹、黒梅 智子、富松 優花、小林 洋大、滝田 正勝、満田 節生、浦本 結稜、鈴木 貫太、告 華連、鈴木 陽太郎、浦本 結稜、黒澤 航海、會澤 幸希、川上 修汰、岩佐 和晃	IRT project of HQR	Kenji Ohoyama	Ibaraki University	Yuki Igura, Kohta Saito, Takayuki Asano, Keitaro Kuwahara, Yuta Miyachi, Kaito Utsuno, Ayumu Ohashi, Takehito Nakano, Takano Kumaeda, Teppei Takahashi, Hayao Fujimoto, Makoto Yokoyama, Hideki Ebisawa, Azumi Yashiro, Ryosuke Koizumi, Kaede Inoh, kouki abe, Tomoko Kuroume, Yuka Tomimatsu, Yodai Kobayashi, Masakatsu Takita, Setsuo Mitsuda, Yui Uramoto, Kanta Suzumura, Karen Tsuge, Yotaro Suzuki, Yui Uramoto, Wataru Kurosawa, Koki Aizawa, Shuta Kawakami, Kazuaki Iwasa	HQR	T1-1
104	AKANE (東北大金研：三軸型中性子分光器) IRT課題	谷口 貴紀	東北大学	山本 孟、時田 桂吾、岡野 洗明、松本 綾香、中川 鉄馬、朝日 透、小宮山 陽太、Saha Suvayan, Yan Pandu Akbar Mochammad, Agung Nugroho Agustinus, 藤田 全基、南部 雄亮、池田 陽一、川本 陽、Tang Yifei、北澤 崇文、Xie Peiao, Pang Xiaoqi, Wang Tong、北沢 昂久、荒木 靖啓、竹本 朝、Zhao Hongfei、岡部 博孝、大亀 佑太、川又 雅広、鄭 家傑、梅本 好日古、高田 秀佐、二見 采樹、北山 慎之介、磯村 楓	IRT project of AKANE	Takanori Taniguchi	Tohoku University	Hajime Yamamoto, Keigo Tokita, Komei Okano, Ayaka Matsumoto, Kenta Nakagawa, Toru Asahi, Yota Komiyama, Suvayan Saha, Mochammad Yan Pandu Akbar, Agustinus Agung Nugroho, Masaki Fujita, Yusuke Nambu, Yoichi Ikeda, Yo Kawamoto, Yifei Tang, Takafumi Kitazawa, Peiao Xie, Xiaoqi Pang, Tong Wang, Takahisa Kitazawa, Nobuhiro Araki, Ashita Takemoto, hongfei Zhao, Hiroataka Okabe, Yuta Oki, Masahiro Kawamata, Jiajie Zheng, Yoshiniko Umamoto, Shusuke Takada, Saiki Futami, Shinnosuke Kitayama, Kaede Isomura	AKANE	T1-2
105	Pressure dependence of the charge and spin density waves in La1.875Ba0.125-xSrxCuO4	WANG TONG	東北大学	竹本 朝、藤田 全基、谷口 貴紀	Pressure dependence of the charge and spin density waves in La1.875Ba0.125-xSrxCuO4	Tong Wang	Tohoku University	Ashita Takemoto, Masaki Fujita, Takanori Taniguchi	AKANE	T1-2
106	中性子を用いたNd3+-LaAlO3結晶における双晶ドメインの構造解析	井出 郁央	名古屋大学	南部 太郎	Structure analysis of twin domains in Nd3+-LaAlO3 crystal using neutrons	Ikuo Ide	Nagoya University	Taro Nambu	AKANE	T1-2
107	分子性キラル磁性体L酒石酸銅の低温磁気構造の研究	山口 明	兵庫県立大学	藤田 涉、明松 凜也	Study on magnetic structure of a molecular-based chiral magnet, copper L-tartrate at low temperatures	Akira Yamaguchi	University of Hyogo	Wataru Fujita, Rinya Akematsu	AKANE	T1-2
108	擬一次元かつカイラルな結晶構造をもつ六方晶La3FeGaS7における磁気励起	山根 悠	兵庫県立大学	日坂 誠、名古屋 太一	Magnetic Excitations in a Hexagonal La3FeGaS7 with a quasi-one-dimensional and chiral crystal structure	Yu Yamane	University of Hyogo	Makoto Hisaka, Taichi Nagoya	AKANE	T1-2
109	逐次転移を示すYbCu4Auの秩序変数の決定	谷口 貴紀	東北大学	藤田 全基、Xie Peiao、岡部 博孝、高田 秀佐、磯村 楓	The neutron determination of the order parameters in YbCu4Au	Takanori Taniguchi	Tohoku University	Masaki Fujita, Peiao Xie, Hiroataka Okabe, Shusuke Takada, Kaede Isomura	AKANE	T1-2
110	中性子散乱法によるNd系バイクロア酸化物の磁気秩序状態の研究	渡邊 功雄	理化学研究所	Shakuur Abdan	Neutron Defraction Study on Magnetic Properties of Nd-Based Pyrochlore Oxides	Isao Watanabe	RIKEN	Shakuur Abdan	AKANE	T1-2

111	T1-3 HERMES IRT課題	南部 雄亮	東北大学	川西 祥平、楊 楊、Wei Zefeng、Zhu Tong、筒井 智嗣、Avdeev Maxim、Nilsen Goeran Jan、杉山 和正、藤田 尚行、上野 美穂、藤尾 亮汰、笹原 悠輝、佐藤 眞直、樹下 まゆ、川又 透、吉村 徳之、藤田 全基、川本 陽、Tang Yifei、北澤 崇文、Xie Peiao、Pang Xiaoqi、Wang Tong、北沢 昂久、荒木 靖啓、竹本 朝、Zhao Hongfei、岡部 博孝、大亀 佑太、川又 雅広、鄭 家傑、梅本 好日古、高田 秀佐、二見 采樹、北山 慎之介、磯村 楓	IRT project of HERMES	Yusuke Nambu	Tohoku University	Shohei Kawanishi, Yang Yang, Zefeng Wei, Tong Zhu, Satoshi Tsutsui, Maxim Avdeev, Goeran Jan Nilsen, Kazumasa Sugiyama, Takayuki Fujitani, Miho Ueno, Ryota Fujio, Yuki Sasahara, Masugu Sato, Mayu Morita, Toru Kawamata, Noriyuki Yoshimura, Masaki Fujita, Yo Kawamoto, Yifei Tang, Takafumi Kitazawa, Peiao Xie, Xiaoqi Pang, Tong Wang, Takahisa Kitazawa, Nobuhiro Araki, Ashita Takemoto, Hongfei Zhao, Hirotsuka Okabe, Yuta Oki, Masahiro Kawamata, Jiajie Zheng, Yoshihiko Umemoto, Shusuke Takada, Saiki Futami, Shinosuke Kitayama, Kaede Isomura	HERMES	T1-3
112	Au65Ga21Dy14近似結晶の磁気構造	Labib FARID	東京理科大学	那波 和宏	Magnetic structure of the Au65Ga21Dy14 1/1 approximant crystal	Farid Labib	Tokyo University of Science	Kazuhiro Nawa	HERMES	T1-3
113	中性子回折法による新規Li-P-S-C固体電解質の構造解析	SONG SUBIN	東京工業大学	平山 雅章、菅野 了次	Neutron diffraction structural analysis of Li-P-S-Cl solid electrolyte	Subin Song	Tokyo Institute of Technology	Masaaki Hirayama, Ryoji Kanno	HERMES	T1-3
114	アニオンダイマーを含む分子固体の構造・磁性研究	Zhu Tong	京都大学		Structural and Magnetic Investigation of Some Molecular Solids Containing Anion Dimers	Tong Zhu	Kyoto University		HERMES	T1-3
115	強磁場合成したホイスラー合金の規則度評価	三井 好古	鹿児島大学		Evaluation of atomic order of Heusler alloys prepared by in-magnetic-field annealing	Yoshifuru Mitsui	Kagoshima University		HERMES	T1-3
116	六方ペロブスカイト関連構造を持つ新規イオン伝導体の構造解析	八島 正知	東京工業大学	梅田 健成、作田 祐一、上野 那智、兼則 祐輔、齊藤 馨、李 嘉晨、松崎 航平、前田 凌、青木 望、藤井 孝太郎	Crystal Structure Analysis of Novel Ion-Conducting Hexagonal Perovskite-Related Materials	Masatomo Yashima	Tokyo Institute of Technology	Kensei Umeda, Yuichi Sakuda, Nachi Ueno, Yusuke Kanenori, Kei Saito, Jiachen Li, Kohei Matsuzaki, Ryo Maeda, Nozomi Aoki, Kotaro Fujii	HERMES	T1-3
117	SCNアニオンを内包する新規複合アニオン化合物の結晶構造	加藤 大地	京都大学	吉井 健人、川西 祥平	The crystal structure of a new mixed anion compound with SCN anion	Daichi Kato	Kyoto University	Kento Yoshii, Shohei Kawanishi	HERMES	T1-3
118	希土類ハニカム化合物TbPt6Al3の磁気構造	大石 遼平	広島大学		Magnetic structure of the honeycomb rare-earth compound TbPt6Al3	Ryohei Oishi	Hiroshima University		HERMES	T1-3
119	熱電材料143ジントル相の結晶構造解析	小野 圭吾	慶應義塾大学	山下 愛智、三浦 章、瀬下 亜里、渡邊 雄翔	Crystal structure analysis of 143-Zintl phase thermoelectric compounds	Keigo Ono	Keio University	Aichi Yamashita, Akira Miura, Asato Seshita, Yuto Watanabe	HERMES	T1-3
120	Cr置換SrV0.3Fe0.7O2.8の磁気構造	長瀬 鉄平	東京工業大学	岩本 将旺、山本 隆文	The magnetic structure of Cr substituted SrV0.3Fe0.7O2.8	Tepei Nagase	Tokyo Institute of Technology	Masaaki Iwamoto, Takafumi Yamamoto	HERMES	T1-3
121	Eu3T4Sn13 (T = Rh, Ir)のカイラル対称結晶構造相での反強磁気秩序	岩佐 和晃	茨城大学	熊田 隆伸、浦本 結稜、鈴木 貴太、告 華連、鈴木 陽太郎、浦本 結稜、黒澤 航海	Antiferromagnetic ordered states in chiral structure phases of Eu3T4Sn13 (T = Rh, Ir)	Kazuaki Iwasa	Ibaraki University	Takanobu Kumada, Yui Uramoto, Kanta Suzumura, Karen Tsuge, Yotaro Suzuki, Yui Uramoto, Wataru Kurosawa	HERMES	T1-3
122	体積変化からみた超重電子系化合物YbCo2Zn20の価数転移の検証	志村 恭通	広島大学		Verification of the valence transition in the super-heavy fermion YbCo2Zn20 by volume change	Yasuyuki Shimura	Hiroshima University		HERMES	T1-3
123	ブリージングパイロクロア格子反強磁性体LiInCr4S8の中性子回折	浅井 晋一郎	東京大学	益田 隆嗣、Liu Zheyuan、菊地 帆高、魏子駿	Neutron diffraction on breathing pyrochlore magnet LiInCr4S8	Shinichiro Asai	The University of Tokyo	Takatsugu Masuda, Zheyuan Liu, Hodaka Kikuchi, Zijun Wei	HERMES	T1-3
124	FCCフラストレート磁性体TbInCu4の磁気構造解析	田畑 吉計	京都大学	吉本 周玄	Magnetic structure analysis of the FCC frustrated magnet TbInCu4	Yoshikazu Tabata	Kyoto University	Subaru Yoshimoto	HERMES	T1-3

125	酸塩化物イオン伝導体の結晶構造解析	藤井 孝太郎	東京工業大学	梅田 健成、作田 祐一、上野 那智、兼則 祐輔、齊藤 馨、李 嘉晨、松崎 航平、前田 凌、青木 望、八島 正知	Crystal Structure Analysis of Oxychloride Ionic Conductors	Kotaro Fujii	Tokyo Institute of Technology	Kensei Umeda, Yuichi Sakuda, Nachi Ueno, Yusuke Kanenori, Kei Saito, Jiachen Li, Kohei Matsuzaki, Ryo Maeda, Nozomi Aoki, Masatomo Yashima	HERMES	T1-3
126	量子臨界物質YbCu4Tの元素置換効果	谷口 貴紀	東北大学	藤田 全基	The elemental substitution study of quantum materials YbCu4T	Takanori Taniguchi	Tohoku University	Masaki Fujita	HERMES	T1-3
127	ホイスラー合金Ru2-xCr <sub>x</sub> Siの反強磁性状態	重田 出	鹿児島大学	瀧崎 員弘	Antiferromagnetic state of Heusler alloy Ru2-xCr <sub>x</sub> Si	Iduru Shigeta	Kagoshima University	Kazuhiro Fuchizaki	HERMES	T1-3
128	磁性半導体Yb三角格子の欠損系 Yb <sub>2</sub> Cu <sub>2</sub> nSn+3 における逐次相転移	鬼丸 孝博	広島大学	岡島 聡志	Successive phase transitions in a magnetic semiconductor Yb <sub>2</sub> Cu <sub>2</sub> nSn+3 with a deficient Yb triangle lattice	Takahiro Onimaru	Hiroshima University	Satoshi Okajima	HERMES	T1-3
129	新規プロトン伝導体の結晶構造解析	齊藤 馨	東京工業大学	梅田 健成、作田 祐一、上野 那智、兼則 祐輔、李 嘉晨、松崎 航平、前田 凌、青木 望、八島 正知、藤井 孝太郎	Crystal Structure Analysis of Novel Proton Conductors	Kei Saito	Tokyo Institute of Technology	Kensei Umeda, Yuichi Sakuda, Nachi Ueno, Yusuke Kanenori, Jiachen Li, Kohei Matsuzaki, Ryo Maeda, Nozomi Aoki, Masatomo Yashima, Kotaro Fujii	HERMES	T1-3
130	Er(Ho)Co <sub>2</sub> 系磁気冷凍材料の磁気構造	寺田 典樹	物質材料研究機構	Larsen Simon	Magnetic structures of magnetic refrigeration Er(Ho)Co <sub>2</sub> -based materials	Noriki Terada	National Institute for Materials Science	Simon Larsen	HERMES	T1-3
131	FONDER(中性子4軸回折装置)IRT課題	高橋 美和子	筑波大学	森 初果、出倉 駿、西岡 海人、辻本 吉廣、大胡田 龍輝、坂倉 輝俊、石川 喜久、小林 悟、野田 幸男	IRT proposal for FONDER (Neutron 4-circle diffractometer)	Miwako Takahashi	Tsukuba University	Hatsumi Mori, Shun Dekura, Kaito Nishioka, Yoshihiro Tsujimoto, Tatsuki Ogoda, Terutoshi Sakakura, Yoshihisa Ishikawa, Satoru Kobayashi, Yukio Noda	FONDER	T2-2
132	Quantitative Estimation of the DM vector in a Dresselhaus magnet	PANG XIAOQI	東北大学	川又 雅広、荒木 靖啓	Quantitative Estimation of the DM vector in a Dresselhaus magnet	Xiaoqi Pang	Tohoku University	Masahiro Kawamata, Nobuhiro Araki	FONDER	T2-2
133	一軸応力下におけるPt <sub>3</sub> Fe反強磁性体の磁気構造解析	小林 悟	岩手大学	Bekhbaatar Enkhmend、中野 愛弓、北條 大輝	Magnetic structural analysis of Pt <sub>3</sub> Fe antiferromagnet under uniaxial pressure	Satoru Kobayashi	Iwate University	Enkhmend Bekhbaatar, Ayumi Nakano, Hiroki Hojo	FONDER	T2-2
134	Tb <sub>0.5</sub> Gd <sub>0.5</sub> Mn <sub>2</sub> O <sub>5</sub> の等方的電気磁気効果の微視的機構解明	石井 祐太	東北大学		Microscopic mechanism of isotropic magneto-electric effect of Tb <sub>0.5</sub> Gd <sub>0.5</sub> Mn <sub>2</sub> O <sub>5</sub>	Yuta Ishii	Tohoku University		FONDER	T2-2
135	スピン1/2フラストレート正方格子磁性体 2VO <sub>5</sub> O <sub>4</sub> ·H <sub>2</sub> SO <sub>4</sub> ·nH <sub>2</sub> Oの結晶構造	那波 和宏	東北大学	村崎 遼	Crystal structure of the spin-1/2 frustrated square lattice magnet 2VO <sub>5</sub> O <sub>4</sub> ·H <sub>2</sub> SO <sub>4</sub> ·nH <sub>2</sub> O	Kazuhiro Nawa	Tohoku University	Ryo Murasaki	FONDER	T2-2
136	Fe-Ni-Cu合金における格子歪とインバー効果	高橋 美和子	筑波大学	大胡田 龍輝	Lattice deformation and the Invar effect in Fe-Ni-Cu alloy	Miwako Takahashi	Tsukuba University	Tatsuki Ogoda	FONDER	T2-2
137	ハイパーカゴメ格子における格子不整合磁気構造の解明	社本 真一	総合科学研究機構	Chang Lieh-Jeng	Incommensurate magnetic structure in a hyperkagome lattice	Shinichi Shamoto	Comprehensive Research Organization for Science and Society	Lieh-Jeng Chang	FONDER	T2-2
138	フラストレート磁性体BaFe <sub>12</sub> Se <sub>7</sub> O <sub>6</sub> の単結晶磁気構造解析	辻本 吉廣	物質材料研究機構		Single-crystal neutron diffraction study of a spin-frustrated antiferromagnet BaFe <sub>12</sub> Se <sub>7</sub> O <sub>6</sub>	Yoshihiro Tsujimoto	National Institute for Materials Science		FONDER	T2-2

## 2023年度 軌道放射物性研究施設 共同利用課題一覧 / Joint Research List of Synchrotron Radiation Research Project 2023

※実施課題一覧、所属は申請時のデータ

柏キャンパスE棟 / Laser and Synchrotron Radiation Laboratory in Kashiwa

No.	課題番号	課題名	氏名	所属	分担者 (共同研究者)	Title	Name	Organization	Member of research project	担当所員
1	202210-GNBXX-0004	自己組織化カゴメ格子Mn <sub>3</sub> C <sub>6</sub> O <sub>6</sub> の電子構造の観測	金井 要	東京理科大学	馬上 怜奈	Observation of electronic structure of self-assembled Kagome lattice Mn <sub>3</sub> C <sub>6</sub> O <sub>6</sub>	Kaname Kanai	Tokyo University of Science	Rena Moue	近藤 猛
2	202301-GNBXX-0057	ディラック半金属 $\alpha$ -Sn薄膜におけるトポジカル表面状態の評価	小林 正起	東京大学	武田 崇仁	Elucidation of surface topological states in Dirac semimetal $\alpha$ -Sn	Masaki Kobayashi	The University of Tokyo	Takahito Takeda	近藤 猛
3	202305-CMBXX-0043	レーザースピ角度光電子分光による表面電子状態の研究	矢治 光一郎	物質・材料研究機構	津田俊輔 ファンディン タン	SARPES studies of atomic layer materials at surface	Koichiro Yaji	National Institute for Materials Science	Shunsuke Tsuda PHAN DINH THAN	近藤 猛
4	202306-GNBXX-0097	炭化タングステン薄膜上グラフェンのスピン分解角度分解光電子分光	伊藤 孝寛	名古屋大学	乗松 航 Ni Yuanzhi 河野 健人 柳原 涼太郎	Spin- and angle-resolved photoemission spectroscopy of Graphene on WC thin film	Takahiro Ito	Nagoya University	Wataru Norimatsu Ni Yuanzhi Kento Kawano Ryotaro Sakakibara	近藤 猛
5	202306-GNBXX-0124	ハーフメタル強磁性体の時間分解スピン分解高分解能光電子分光	横谷 尚睦	岡山大学	東川 知樹	Time and spin-resolved high-resolution photoemission spectroscopy of half metallic ferromagnet	Takayoshi Yokoya	Okayama University	Tomoki Higashikawa	近藤 猛
6	202306-GNBXX-0133	ニッケル基板上的多層グラフェンの電子状態の研究	津田 俊輔	物質・材料研究機構	矢治 光一郎 ファンディン タン	Electronic structure of multilayer graphene on a Ni substrate	Shunsuke Tsuda	National Institute for Materials Science	Koichiro Yaji PHAN DINH THAN	近藤 猛
7	202310-GNBXX-0146	強磁性金属酸化物SrRuO <sub>3</sub> 薄膜における量子輸送特性の解明	小林 正起	東京大学	武田 崇仁	Unveiling quantum transport property of ferromagnetic metallic oxide SrRuO <sub>3</sub>	Masaki Kobayashi	The University of Tokyo	Takahito Takeda	近藤 猛
8	202311-GNBXX-0147	光電子スピン干渉を用いたアト秒光電子ダイナミクスへの研究	黒田 健太	広島大学	岩田 拓万 高佐 永遠	Study of attosecond photoemission dynamics through photoelectron spin interference	Kenta Kuroda	Hiroshima University	Takuma Iwata Towa Kosa	近藤 猛
9	所内	Investigation of magnetization response in the nearly half-metallic ferromagnet CoS <sub>2</sub> using spin- and angle-resolved photoemission spectroscopy	Changyong Kim	Seoul National University	Huh Soonsang (東京大学) 森 亮 (東京大学) 川口 海周 (東京大学)	Investigation of magnetization response in the nearly half-metallic ferromagnet CoS <sub>2</sub> using spin- and angle-resolved photoemission spectroscopy	Changyong Kim	Seoul National University	Huh Soonsang (The University of Tokyo) Ryo Mori (The University of Tokyo) Kaishu Kawaguchi (The University of Tokyo)	近藤 猛
10	所内	Investigation of spin propaty in quantum materials	Hugo Dil	PSI(Paul Scherre Institut)	森 亮 (東京大学) 川口 海周 (東京大学) 福島 優斗 (東京大学)	Investigation of spin propaty in quantum materials	Hugo Dil	PSI(Paul Scherre Institut)	Ryo Mori (The University of Tokyo) Kaishu Kawaguchi (The University of Tokyo) Yuto Fukushima (The University of Tokyo)	近藤 猛

## 1. 第一原理計算 / First-Principles Calculation of Materials Properties

No.	課題番号	課題名	氏名	所属	Title	Name	Organization
1	2023-Eb-0003	第一原理計算を用いた非調和フォノン特性データベースの構築	大西 正人	統計数理研究所	Construction of anharmonic phonon database with first-principles calculations	Masato Ohnishi	The Institute of Statistical Mathematics
2	2023-Ea-0004	量子論大規模計算による半導体薄膜成長とデバイス界面形成の微視的機構解明	押山 淳	名古屋大学未来材料・システム研究所	Clarification of Microscopic Mechanisms of Semiconductor Epitaxial Growth and Device-Interface Formation by Large-Scale Quantum-Theory-Based Computations	Atsushi Oshiyama	Institute of Materials and Systems for Sustainability
3	2023-Eb-0007	密度汎関数理論と機械学習法による不均一触媒の動的過程の理論的研究	森川 良忠	大阪大学 大学院工学研究科 物理学系専攻	Theoretical study on dynamical processes in heterogeneous catalysis using density functional theory and machine learning methods	Yoshitada Morikawa	Department of Precision Engineering, Graduate School of Engineering, Osaka University
4	2023-Ea-0007	密度汎関数理論と機械学習法による不均一触媒の動的過程の理論的研究	森川 良忠	大阪大学 大学院工学研究科 物理学系専攻	Theoretical study on dynamical processes in heterogeneous catalysis using density functional theory and machine learning methods	Yoshitada Morikawa	Department of Precision Engineering, Graduate School of Engineering, Osaka University
5	2023-Ea-0010	不規則固体界面の平衡/非平衡電気化学への展開	笠松 秀輔	山形大学学術研究院	Equilibrium/non-equilibrium electrochemistry of disordered solid-state interfaces	Shusuke Kasamatsu	Academic Assembly, Yamagata University
6	2023-Ca-0101	第一原理電子状態・輸送特性計算コードRSPACEの開発と高機能界面のデザイン	小野 倫也	神戸大学大学院工学研究科電気電子工学専攻	Development of first-principles calculation code RSPACE and design of highly functional interface	Tomoya Ono	Department of Electrical and Electronic Engineering, Graduate School of Engineering, Kobe University
7	2023-Eb-0009	第一原理計算に立脚したワイドギャップ半導体の電子状態解明:パワーデバイスから量子デバイスまで	松下 雄一郎	東京工業大学	Electronic structure of wide-gap semiconductors based on first-principles calculations: from power devices to quantum devices	Yu-ichiro Matsushita	Tokyo Institute of Technology
8	2023-Ca-0016	全電子混合基底法プログラムの改良と応用	大野 かおる	横浜国立大学大学院工学研究院	Improvement and application of all-electron mixed basis program	Kaoru Ohno	Graduate School of Engineering, Yokohama National University
9	2023-Ca-0099	分子性材料の構造探索と誘電特性予測	常行 真司	東京大学大学院理学系研究科物理学専攻	Structural exploration and prediction of dielectric properties of molecular materials	Shinji Tsuneyuki	Department of Physics, University of Tokyo
10	2023-Ca-0056	機械学習を利用したツイスト層状材料の大スケール熱輸送シミュレーション	堀見 淳一郎	東京大学工学系研究科	Large-scale simulations based on machine learning for thermal transport in twisted layered materials	Junichiro Shiomu	School of Engineering, The University of Tokyo
11	2023-Ca-0057	フォノン由来の負熱膨張材料の振動和近似計算と分子動力学計算	望月 泰英	東京工業大学物質理工学院	Quasi-harmonic approximated and molecular dynamic calculations for phonon-induced negative-thermal-expansion materials	Yasuhide Mochizuki	School of Materials and Chemical Technology, Tokyo Institute of Technology
12	2023-Ca-0084	機械学習ポテンシャルを用いた表面・界面・欠陥等の複雑構造における局所物性に関する解析	渡邊 聡	東京大学大学院工学系研究科マテリアル工学専攻	Analyses on local properties at complex structures such as surfaces, interfaces and defects via machine-learning potentials	Satoshi Watanabe	Department of Materials Engineering, School of Engineering, The University of Tokyo
13	2023-Ea-0011	巨大磁気熱量測定材料の計算機スクリーニング	トラン バ フン	東北大学	Computational screening of giant magnetocaloric materials	Hung Tran Ba	Tohoku University
14	2023-Ca-0135	ブロッホ波動関数のベリー位相を用いた物理量の第一原理計算手法開発と応用	石井 史之	金沢大学ナノマテリアル研究所	Development and applications of first-principles computational methods using Berry phase of Bloch wavefunctions	Fumiyuki Ishii	Kanazawa University
15	2023-Ca-0054	フラッシュメモリ応用を目指したa-SiN中のFloating State起因の新規点欠陥の理論的研究	白石 賢二	名古屋大学 未来材料・システム研究所	Theoretical Studies on New Types of Point Defects Originated from Floating States in a-SiN towards Flash Memories Applications	Kenji Shiraishi	Institute of Materials and Systems for Sustainability, Nagoya University
16	2023-Ca-0013	相平衡におけるフォノン効果	合田 義弘	東京工業大学物質理工学院材料系	Phonon effects in phase equilibria	Yoshihiro Gohda	Department of Materials Science and Engineering, Tokyo Institute of Technology
17	2023-Ca-0082	機械学習ポテンシャルと先進フォノン計算による熱物性の理解と予測	只野 央将	物質・材料研究機構	Elucidation and prediction of thermal properties of solids using machine-learning interatomic potentials integrated with advanced phonon calculation methods	Terumasa Tadano	National Institute for Materials Science
18	2023-D-0007	触媒性能向上を目指したペロブスカイト半導体光触媒の第一原理解析	天能 精一郎	神戸大学	First-principles analysis of perovskite semiconductors toward improving photocatalytic performance	Seichiro Ten-No	Kobe University
19	2022-D-0005	第一原理計算を用いた熱伝導度データベース作成	中村 和磨	九州工業大学	Construction of thermal conductivity database from first principles	Kazuma Nakamura	Kyushu Institute of Technology
20	2023-Cb-0006	電極表面吸着系の第一原理計算	杉野 修	東京大学物性研究所	First-principles calculation of adsorption on electrode surfaces	Osamu Sugino	Institute for Solid State Physics, University of Tokyo
21	2023-Cb-0046	ファンデルワールス磁性体における熱電効果の第一原理計算	石井 史之	金沢大学ナノマテリアル研究所	First-principles calculation of van der Waals magnet	Fumiyuki Ishii	Kanazawa University
22	2023-Ca-0059	第一原理計算による可視光型半導体光触媒の理論的研究	天能 精一郎	神戸大学	Theoretical study of visible-light-driven semiconductor photocatalysts using first-principles calculations	Seichiro Ten-No	Kobe University
23	2023-Ca-0063	リチウムイオン固体電解質材料の安定構造探索	山下 智樹	長岡技術科学大学技術研究院電気電子情報系	Crystal structure prediction of Li-ion solid electrolyte materials	Tomoki Yamashita	Nagaoka University of Technology
24	2023-Ca-0114	ナノグラフェン素子構造の外場応答	草部 浩一	兵庫県立大学大学院理学研究科	Response of nanographene device structures to external fields	Koichi Kusakabe	Graduate School of Science, University of Hyogo

25	2023-Ca-0005	多体波動関数理論による第一原理計算ソフトウェアの開発	越智 正之	大阪大学	Development of a first-principles calculation software for a many-body wave function theory	Masayuki Ochi	Osaka University
26	2023-Cb-0002	磁気異方性発現機構の電子論	合田 義弘	東京工業大学物質理工学院材料系	Electron theory of magnetocrystalline anisotropy	Yoshihiro Gohda	Department of Materials Science and Engineering, Tokyo Institute of Technology
27	2023-Ca-0051	電極の量子論	杉野 修	東京大学物性研究所	Quantum theory of electrode	Osamu Sugino	Institute for Solid State Physics, University of Tokyo
28	2023-Cb-0019	GaN MOSFET用のGaN/絶縁膜界面の第一原理計算による設計	白石 賢二	名古屋大学 未来材料・システム研究所	First Principles Design of GaN/Insulator Interface for GaN MOSFET	Kenji Shiraishi	Institute of Materials and Systems for Sustainability, Nagoya University
29	2023-Ca-0085	密度汎関数理論を用いた金属表面における分子吸着と反応の研究	濱田 幾太郎	大阪大学大学院工学研究科 物理学系専攻 精密工学コース	Density functional theory study of adsorption and reaction of molecules on metal surfaces	Ikutaro Hamada	Department of Precision Engineering, Graduate School of Engineering, Osaka University
30	2023-Ca-0122	HPCを基盤とした量子シミュレーション・実験解析・データ駆動科学の融合	星 健夫	核融合科学研究所研究部プラズマ量子プロセスユニット	HPC-based fusion of quantum simulation, experiment analysis and data-driven science	Takeo Hoshi	Plasma Quantum Processes Unit, Department of Research, National Institute for Fusion Science
31	2023-Ca-0025	2次のGW電子ホール相互作用核の開発と応用	野口 良史	静岡大学工学部	Development of second-order GW electron-hole interaction kernel	Yoshifumi Noguchi	Graduate School of Engineering, Shizuoka University
32	2023-Ca-0034	第一原理計算によるナノ物質の構造・機能の解明と予測	武次 徹也	北海道大学大学院理学研究院化学部門	Ab initio study on the structure and functions of nanomaterials	Tetsuya Taketsugu	Department of Chemistry, Faculty of Science, Hokkaido University
33	2023-Ca-0050	極限環境下における構造不規則系の構造と電子状態の第一原理計算	下藤 冬樹	熊本大学大学院先端科学研究部	First-Principles Molecular-Dynamics Study of Structural and Electronic Properties of Disordered Materials under Extreme Conditions	Fuyuki Shimajo	Department of Physics, Kumamoto University
34	2023-Ca-0089	有機半導体結晶における電子-フォノン結合を考慮した第一原理バンド計算	柳澤 将	琉球大学理学部物質地球科学科物理系	First-principles bandstructure calculation with electron-phonon interactions in organic semiconductor crystals	Susumu Yanagisawa	Department of Physics and Earth Sciences, Faculty of Science, University of the Ryukyus
35	2023-Ca-0017	機械学習力場を用いた多成分複雑系に対する熱伝導度計算II	島村 孝平	熊本大学大学院先端科学研究部	Thermal Conductivity calculation with machine-learning interatomic potential for multi-component heterogeneous materials II	Kohei Shimamura	Faculty of Advanced Science and Technology, Kumamoto University
36	2023-Ca-0115	原子層プロセスにおける表面反応解析	浜口 智志	大阪大学工学研究科	Surface reaction analyses for atomic layer processes	Satoshi Hamaguchi	Graduate School of Engineering, Osaka University
37	2023-Ca-0012	第一原理計算を用いた熱伝導度およびプラズマ振動データベース作成	中村 和磨	九州工業大学	Construction of thermal conductivity and plasma frequency database from first principles	Kazuma Nakamura	Kyushu Institute of Technology
38	2023-Ca-0037	反強磁性体における異常ホール効果の第一原理計算	山内 邦彦	大阪大学基礎工学研究科	First-principles calculation of anomalous Hall effect in antiferromagnets	Kunihiko Yamauchi	Graduate School of Engineering Science, Osaka University
39	2023-Ca-0049	燃料電池電極触媒とギ酸分解触媒の省貴金属化	坂口 紀史	北海道大学大学院工学研究院 附属エネルギー・マテリアル融合領域研究センター	Reduction of Rare Metals in Fuel Cell and Formic Acid Decomposition Catalysts	Norihito Sakaguchi	Center for Advanced Research of Energy and Materials, Faculty of Engineering, Hokkaido University
40	2023-Cb-0033	燃料電池電極触媒とギ酸分解触媒の省貴金属化	坂口 紀史	北海道大学大学院工学研究院 附属エネルギー・マテリアル融合領域研究センター	Reduction of Rare Metals in Fuel Cell and Formic Acid Decomposition Catalysts	Norihito Sakaguchi	Center for Advanced Research of Energy and Materials, Faculty of Engineering, Hokkaido University
41	2023-Cb-0021	ペロブスカイト半導体光触媒による人工光合成の第一原理解析	天能 精一郎	神戸大学	First-principles analysis of artificial photosynthesis using perovskite semiconductor photocatalysts	Seiichiro Ten-No	Kobe University
42	2023-Cb-0028	第一原理計算に基づく方法を用いた複雑構造における局所物性に関する解析	渡邊 聡	東京大学大学院工学系研究科マテリアル工学専攻	Analyses on local properties at complex structures via ab-initio-based methods	Satoshi Watanabe	Department of Materials Engineering, School of Engineering, The University of Tokyo
43	2023-Cb-0047	第一原理電子状態・輸送特性計算コードRSPACEの開発と高機能界面のデザイン	小野 倫也	神戸大学大学院工学研究科電気電子工学専攻	Development of first-principles calculation code RSPACE and design of highly functional interface	Tomoya Ono	Department of Electrical and Electronic Engineering, Graduate School of Engineering, Kobe University
44	2023-Ca-0129	大規模第一原理電気伝導計算法による量子伝導理論	小林 伸彦	筑波大学 数理物質系 物理学域	Quantum transport theory by large scale first-principles electron transport calculations	Nobuhiko Kobayashi	Department of Applied Physics, University of Tsukuba
45	2023-Ca-0038	鉄-白金合金におけるアト秒過渡吸収分光の第一原理的解析	佐藤 駿丞	筑波大学計算科学研究センター	First-principles analysis on attosecond transient absorption spectroscopy for FePt alloy	Shunsuke Sato	Center for Computational Sciences, University of Tsukuba
46	2023-Ca-0092	電極触媒の触媒発現機構および蓄電池電極材料の劣化機構の解明	大谷 実	筑波大学計算科学研究センター	Exploring the mechanism of catalytic activity and degradation of electrodes	Minoru Otani	Center for Computational Sciences, The University of Tsukuba
47	2023-Ca-0108	理論及び第一原理計算による効率的な電気化学触媒の設計	李 昊	東北大学材料科学高等研究所	Design of Effective Electrocatalysts by Theory and Ab Initio Computations	Hao Li	Advanced Institute for Materials Research (WPI-AIMR), Tohoku University
48	2023-Cb-0003	第一原理波動関数理論の高精度化およびソフトウェア開発	越智 正之	大阪大学	Improvement of accuracy and software development for the first-principles wave function theory	Masayuki Ochi	Osaka University
49	2023-Cb-0013	第一原理による粒界偏析構造解析と機能予測	幾原 雄一	東京大学大学院工学系研究科総合研究機構	Structural analysis and property prediction of grain-boundary segregation by first-principles calculations	Yuichi Ikuhara	Institute of Engineering Innovation, University of Tokyo

50	2023-Ca-0035	高機能スピントロニクス磁性材料の電子・磁気構造解析および準粒子自己無撞着GW法の並列化開発・応用	小田 竜樹	金沢大学理工研究域数物科学系	Analyses on electronic/magnetic structures in high-performance spintronics magnetic materials and parallelization development/application in quasi-particle self-consistent GW code	Tatsuki Oda	Faculty of Mathematics and Physics, Institute of Science and Engineering, Kanazawa University
51	2023-Cb-0018	密度汎関数理論を用いた金属表面における分子吸着と反応の研究	濱田 幾太郎	大阪大学大学院工学研究科 物理学系専攻 精密工学コース	Density functional theory study of adsorption and reaction of molecules on metal surfaces	Ikutaro Hamada	Department of Precision Engineering, Graduate School of Engineering, Osaka University
52	2023-Cb-0007	磁気的短距離秩序に依存した交換相互作用定数の第一原理計算	田中 友規	東京工業大学物質理工学院	First-principles calculations of exchange coupling constants dependent on magnetic short-range order	Tomonori Tanaka	School of Materials and Chemical Technology, Tokyo Institute of Technology
53	2023-Ca-0088	密度汎関数法と溶液理論を用いた電気化学反応の解析 5	春山 潤	理化学研究所開拓研究本部	Electrochemical reaction analysis using density functional calculation + implicit solvation model 5	Jun Haruyama	RIKEN Cluster for Pioneering Research
54	2023-Ca-0015	ナノ粒子および磁性材料表面・界面に関する第一原理的研究	立津 慶幸	名桜大学	Ab-initio research on nano particles, and surfaces and grain boundaries of magnetic materials	Yasutomi Tatetsu	Meio University
55	2023-Ca-0079	DFT-MDおよびNNP-MDによる固体酸化物触媒の機能解明	中山 哲	東京大学大学院工学系研究科化学システム工学専攻	DFT-MD and NNP-MD simulations for metal-oxide catalysis	Akira Nakayama	Department of Chemical System Engineering, The University of Tokyo
56	2023-Ca-0086	進化的アルゴリズムによる水素化物高温超伝導の探索	石河 孝洋	東京大学大学院理学系研究科物理学専攻	Search for high temperature superconductivity in hydrides	Takahiro Ishikawa	Department of Physics, The University of Tokyo
57	2023-Ca-0124	モット絶縁体のキャリアドーピング: 化学的トレンド	レービガー ハンネス	横浜国立大学 大学院工学研究科 物理学工学コース	Carrier doping of Mott insulators: chemical trends	Hannes Raebiger	Department Physics, Yokohama National University
58	2023-Ca-0008	第一原理計算による光熱変換原理の解明	江目 宏樹	山形大学	Study of the principle of photothermal conversion by ab initio calculations	Hiroki Gonome	Yamagata University
59	2023-Ca-0032	分子接合の第一原理計算伝導計算	大戸 達彦	名古屋大学大学院工学研究科	First-principles calculations for molecular junctions	Tatsuhiko Ohto	Graduate School of Engineering, Nagoya University
60	2023-Ca-0048	金属材料の高い耐食性を実現するセラミックス保護被膜の開発	國貞 雄治	北海道大学大学院工学研究院 附属エネルギー・マテリアル融合領域研究センター	Development of Ceramic Protective Coating for High Corrosion Resistance of Metallic Materials	Yuji Kunisada	Center for Advanced Research of Energy and Materials, Faculty of Engineering, Hokkaido University
61	2023-Ca-0131	第一原理計算を用いた2次元SiC構造における電子輸送特性研究	江上 喜幸	北海道大学大学院工学研究院	First-principles electron-transport study on 2-dimensional SiC materials	Yoshiyuki Egami	Faculty of Engineering, Hokkaido University
62	2023-Cb-0034	金属材料の高い耐食性を実現するセラミックス保護被膜の開発	國貞 雄治	北海道大学大学院工学研究院 附属エネルギー・マテリアル融合領域研究センター	Development of Ceramic Protective Coating for High Corrosion Resistance of Metallic Materials	Yuji Kunisada	Center for Advanced Research of Energy and Materials, Faculty of Engineering, Hokkaido University
63	2023-Ea-0009	第一原理計算に立脚したグリーンデバイスの提案: 材料探索からデバイス作製まで	松下 雄一郎	東京工業大学	Proposal for Free Devices Based on First-Principles Calculations: From Material Exploration to Device Fabrication	Yu-Ichiro Matsushita	Tokyo Institute of Technology
64	2023-Ca-0014	第一原理計算とニューラルネットワーク力場を併用した新規二次電池材料の解析	山田 淳夫	東京大学工学系研究科	Analysis of novel rechargeable battery materials using first-principles calculations and neural network force field	Atsuo Yamada	Faculty of Engineering, The University of Tokyo
65	2023-Cb-0052	第一原理計算による分子吸着した原子層状物質における電子輸送特性研究	江上 喜幸	北海道大学大学院工学研究院	First-principles study on electron transport properties in molecule-adsorbed atomic layered materials	Yoshiyuki Egami	Faculty of Engineering, Hokkaido University
66	2022-D-0007	プロトン互変異性伝導経路の第一原理NEB計算	森 初果	東京大学物性研究所	First-principles NEB calculations of proton tautomeric conduction pathways	Hatsumi Mori	The Institute for Solid State Physics, The University of Tokyo
67	2023-Ca-0061	フォノンモードに着目した固体電解質中のイオン伝導機構解析	藤井 進	九州大学エネルギー研究教育機構	Analysis of phonon-assisted ionic transport in solid electrolytes	Susumu Fujii	Kyushu University Platform of Inter-/Transdisciplinary Energy Research, Kyushu University
68	2023-Ca-0052	非調和フォノンデータベースを利用した熱機能材料の開発	大西 正人	統計数理研究所	Data-drive materials development using anharmonic phonon database	Masato Ohnishi	The Institute of Statistical Mathematics
69	2023-Cb-0023	GW近似における自己相互作用補正	野口 良史	静岡大学工学部	Self-interaction corrections in GW approximation	Yoshifumi Noguchi	Graduate School of Engineering, Shizuoka University
70	2023-Cb-0032	機械学習による反応性スパッタリングシミュレーション用原子間相互作用モデル構築	浜口 智志	大阪大学工学研究科	Development of atomic interaction models for reactive sputtering simulation by machine learning	Satoshi Hamaguchi	Graduate School of Engineering, Osaka University
71	2023-Cb-0029	第一原理計算に基づくK2NdNb5O15の安定構造探索および相転移機構の解析	安原 颯	東京工業大学	Stable Structure Exploration of K2NdNb5O15 and Phase Transition Mechanism Analysis Based on First-Principles Calculations	Sou Yasuhara	Tokyo Institute of Technology
72	2023-Cb-0040	第一原理計算と分子動力学計算による合金材料の力学特性解析	上村 直樹	京都先端科学大学ナガモリアクチュエータ研究所	Analysis of mechanical properties of alloy materials using first-principles and molecular dynamics calculations	Naoki Uemura	The Nagamori Institute of Actuators, Kyoto University of Advanced Science
73	2023-Cb-0041	高機能スピントロニクス磁性材料の電子構造・磁気異方性解析および準粒子自己無撞着GW法の並列化開発・応用	小田 竜樹	金沢大学理工研究域数物科学系	Analyses on electronic structure and magnetic anisotropy in high-performance spintronics magnetic materials and parallelization development/application in quasi-particle self-consistent GW code	Tatsuki Oda	Faculty of Mathematics and Physics, Institute of Science and Engineering, Kanazawa University
74	2023-Ca-0023	固体表面界面における構造的素励起の物性の研究	影島 博之	島根大学大学院自然科学研究科	Study on physical properties of structural elementary excitations at solid surfaces and interfaces	Hiroyuki Kageshima	Graduate School of Natural Science and Technology, Shimane University

75	2023-Ca-0064	バイオ系・ナノ系の光エネルギー変換過程の第一原理計算による解析	藤田 貴敏	量子科学技術研究開発機構	First-Principles Investigation of Energy-Conversion Processes in Biological and Material Systems	Takatoshi Fujita	National Institutes for Quantum Science and Technology
76	2023-Ca-0134	第一原理による界面の安定構造探索と機能特性	幾原 雄一	東京大学大学院工学系研究科総合研究機構	Exploring stable interface atomic structures and properties by first-principles calculations	Yuichi Ikuhara	Institute of Engineering Innovation, University of Tokyo
77	2023-Ca-0100	機械学習による担持酸化物単原子触媒のルイス酸度予測	沢邊 恭一	名古屋大学	Machine learning prediction of Lewis acidity of supported oxide single-atom catalysts	Kyochi Sawabe	Nagoya University
78	2023-Ca-0001	非層状物質の2次元構造	小野 頌太	東北大学金属材料研究所	Two-dimensional structures for non-layered materials	Shota Ono	Tohoku University
79	2023-Ca-0020	多パルスレーザー場による誘電体光吸収の第一原理シミュレーション	篠原 康	東京大学工学系研究科附属光量子科学研究センター	First-principles simulations for optical absorption of dielectrics by multi-pulse laser fields	Yasushi Shinohara	Photon Science Center, School of Engineering, the University of Tokyo
80	2023-Ca-0026	セメント系材料のナノ物性とCO <sub>2</sub> 固定に関する第一原理分子動力学シミュレーション	大村 訓史	広島工業大学 工学部	Nanoscale properties and CO <sub>2</sub> fixation of cement-based materials : ab initio molecular dynamics simulations	Satoshi Ohmura	Faculty of Engineering, Hiroshima Institute of Technology
81	2023-Ca-0044	二次元材料及基板のヘテロ界面での熱輸送	許 斌	東京大学大学院機械工学専攻	Thermal transport across heterojunction between 2D materials and substrate	Xu Bin	Department of Mechanical Engineering, The University of Tokyo
82	2023-Cb-0012	第一原理計算によるGaN中の点欠陥の研究	制野 かおり	九州工業大学大学院工学研究科物質工学研究系	First-principles study of defects in GaN	Kaori Seino	Department of Materials Science and Engineering, Kyushu Institute of Technology
83	2023-Ca-0107	全固体型イオン電池の電解質における中性分子の役割の探索	カンボスドスサントス イーゴン	東北大学	Exploring the Role of Neutral Molecules in All-solid-state Battery Electrolytes	Egon Campos Dos Santos	Tohoku University, Advanced Institute for materials research (AIMR)
84	2023-Ca-0127	機械学習を用いた環境発電用ストレッチャブル・エレクトレット材料の開発	鈴木 雄二	東京大学大学院工学系研究科機械工学専攻	Development of Stretchable Electret Materials for Energy Harvesting with the Aid of Machine Learning	Yuji Suzuki	Dept. of Mechanical Engineering, The University of Tokyo
85	2023-Ca-0036	分子薄膜表面における電子状態解析	二本 かおり	千葉大学	Electronic state analysis on molecular thin film surface	Kaori Niki	Chiba University
86	2023-Ca-0097	鉄系材料表面におけるアンモニア分解反応のモデル化	李 敏赫	東京大学大学院工学系研究科機械工学専攻	Modeling of the Ammonia Decomposition Reaction on Iron-based Material Surfaces	Minhyeok Lee	Department of Mechanical Engineering, The University of Tokyo
87	2023-Ca-0060	第一原理計算による有機強誘電体・圧電体の物性予測	石橋 章司	産業技術総合研究所	Prediction of properties of organic ferroelectrics and piezoelectrics by first-principles calculations	Shoji Ishibashi	National Institute of Advanced Industrial Science and Technology
88	2023-Cb-0050	有機半導体結晶における電子フォノン結合を考慮した第一原理バンド計算	柳澤 将	琉球大学理学部物質地球科学科物理系	First-principles bandstructure calculation with electron-phonon interactions in organic semiconductor crystals	Susumu Yanagisawa	Department of Physics and Earth Sciences, Faculty of Science, University of the Ryukyus
89	2023-Ca-0018	局所ベリー位相を用いた物性評価の第一原理コードの開発	山口 直也	金沢大学ナノマテリアル研究所	Development of First-principles Codes for Evaluation of Physical Properties Through Local Berry Phases	Naoya Yamaguchi	Nanomaterials Research Institute, Kanazawa University
90	2023-Ca-0113	第一原理計算による白金ナノ粒子の構造と反応の研究	佐々木 岳彦	東京大学 大学院新領域創成科学研究科	Study on structures and reactions of platinum nanoparticles	Takehiko Sasaki	Graduate School of Frontier Sciences, The University of Tokyo
91	2023-Cb-0020	機械学習に基づいた基盤上の二次元材料における輸送特性の大規模シミュレーションに関する研究	ソン シェ	東京大学 工学系研究科・総合研究機構	The study of transport properties in two-dimensional materials on substrates using large-scale simulation methods based on machine learning	Sun Jie	Department of Mechanical Engineering, The University of Tokyo
92	2023-Ca-0125	熱電応用に向けた遷移金属モノシリサイドの電子構造と伝導特性のKKR-CPA法による解析	ホ ゴック ナム	名古屋大学未来社会創造機構 マテリアルイノベーション研究所	Electronic and transport properties of transition metal monosilicides for thermoelectric applications: KKR-CPA calculations	Ngoc Nam Ho	Institute of Materials Innovation, Institutes of Innovation for Future Society, Nagoya University
93	2023-Ca-0133	Sub-3 nm金属酸化物ナノ粒子の第一原理計算	横 哲	東北大学材料科学高等研究所	First-principles calculations of sub-3 nm metal oxide particles	Akira Yoko	WPI-AIMR, Tohoku University
94	2023-Ca-0120	含水珪酸塩の混和・不混和転移	飯高 敏晃	理化学研究所	Miscible-Immiscible Transition of Hydrated Silicate Melt	Toshiaki Itaka	Riken
95	2023-Ca-0006	触媒基準エッチング法における酸化銅処理の除去機構	BUI VANPHO	大阪大学大学院工学研究科	Study on the removal mechanism of Copper Oxide processing in catalyst-referred etching method	Vanpho Bui	Graduate School of Engineering, Osaka University
96	2023-Ca-0029	第一原理分子動力学法に基づく軽金属合金の静的構造に関する機械学習を用いた研究	高良 明英	熊本大学技術部	Machine learning study on static structure of light metals alloys based on (ab initio) molecular dynamics	Akihide Koura	Technical Division, Kumamoto University
97	2023-Cb-0035	プロトン互変異性伝導経路の第一原理NEB計算(II)	森 初果	東京大学物性研究所	First-principles NEB calculations of proton tautomeric conduction pathways (II)	Hatsumi Mori	The Institute for Solid State Physics, The University of Tokyo
98	2023-D-0008	Embedding Green関数法によるCu(100)表面上CuPcのFano効果の数値的研究	濱本 雄治	大阪大学 大学院工学研究科 物理学系専攻	Numerical study of the Fano effect in CuPc adsorbed on the Cu(100) surface using the embedding Green function method	Yuji Hamamoto	Department of Precision Engineering, Osaka University
99	2023-Cb-0036	第一原理計算による酸素発生反応の理論的研究	辻 雄太	九州大学総合理工学研究院	Theoretical study of oxygen-evolution reactions by first-principles calculations	Yuta Tsuji	Faculty of Engineering Sciences, Kyushu University
100	2023-Eb-0002	磁気記録応用を目指した磁性ナノ粒子の大規模シミュレーション	トラン バン	東北大学	Large-scale simulation of magnetic nanoparticle toward magnetic recording applications	Hung Tran Ba	Tohoku University
101	2023-Ca-0028	照射損傷と格子間原子との相互作用の研究	大澤 一人	九州大学応用力学研究所	Study of interaction between radiation damage and interstitial atom	Kazuhiro Ohsawa	Research Institute for Applied Mechanics, Kyushu University

102	2023-Ca-0104	ガス過程帰帰による銀(111)表面上シリセント相の構造探索	濱本 雄治	大阪大学 大学院工学研究科 物理学系専攻	Structure search of the T phase in silicene on the Ag(111) surface by Gaussian process regression	Yuji Hamamoto	Department of Precision Engineering, Osaka University
103	2023-Ca-0109	第一原理NEB計算による無水分子性結晶中のプロトン互変異性に基づくプロトン伝導経路の解明	出倉 駿	東北大学多元物質科学研究所	Unveiling the proton conduction pathways based on proton tautomerism in anhydrous molecular crystals by first-principles NEB calculations	Shun Dekura	Institute of Multidisciplinary Research for Advanced Materials, Tohoku University
104	2023-Cb-0009	第一原理計算による光熱変換原理の解明	江目 宏樹	山形大学	Study of the principle of photothermal conversion by ab initio calculations	Hiroki Gonome	Yamagata University
105	2023-Ca-0027	金属間化合物の表面原子構造と化学的特性に関する第一原理計算	野澤 和生	鹿児島大学理学部物理科学科	First-principles study of surface atomic structure and chemical properties of intermetallic compounds	Kazuki Nozawa	Department of Physics and Astronomy, Kagoshima University
106	2023-Ca-0065	マテリアルズインフォマティクスによる触媒材料探索	原嶋 庸介	奈良先端科学技術大学院大学	Materials exploration using materials informatics	Yosuke Harashima	Nara Institute of Science and Technology
107	2023-Ca-0083	DFT計算とインフォマティクスによる固体触媒における反応解析	城塚 達也	茨城大学	Reaction Analysis in Solid Catalysts by DFT Calculations and Informatics	Tatsuya Joutsuka	Ibaraki University
108	2023-Cb-0039	金属間化合物の表面原子構造と化学的特性に関する第一原理計算	野澤 和生	鹿児島大学理学部物理科学科	First-principles study of surface atomic structure and chemical properties of intermetallic compounds	Kazuki Nozawa	Department of Physics and Astronomy, Kagoshima University
109	2023-Cb-0045	機械学習による担持酸化物単原子触媒のルイス酸度予測	沢邊 恭一	名古屋大学	Machine learning prediction of Lewis acidity of supported oxide single-atom catalysts	Kyoichi Sawabe	Nagoya University
110	2023-D-0004	プロトン互変異性伝導経路の第一原理NEB計算(I)	森 初果	東京大学物性研究所	First-principles NEB calculations of proton tautomeric conduction pathways(I)	Hatsumi Mori	The Institute for Solid State Physics, The University of Tokyo
111	2023-Ca-0009	酸化物系蛍光体における電子状態と圧電特性の評価	平田 研二	産業技術総合研究所	First-principles investigation of electronic state and piezoelectric property in oxide-based phosphor	Kenji Hirata	National Institute of Advanced Industrial Science and Technology
112	2023-Ca-0041	ダブルペロブスカイト表面における水分子の反応性に関する理論的研究	西館 数芽	岩手大学工学部	Theoretical study of the reactivity of HS <sub>2</sub> SO molecule on the double-perovskite	Kazume Nishidate	Faculty of Science and Engineering, IWATE University
113	2023-Ca-0126	グラフェンのキャリア輸送特性の研究	藤本 義隆	九州大学工学研究院	Transport study of graphene layers	Yoshitaka Fujimoto	Faculty of Engineering, Kyushu University
114	2023-Ba-0019	繰り込まれた電荷・スピン揺らぎの第一原理計算	明石 遼介	量子科学技術研究開発機構	Renormalized charge-spin fluctuations from first principles	Ryosuke Akashi	National Institutes for Quantum Science and Technology
115	2023-Ba-0071	トポロジカル絶縁体の表面・界面局所電子状態の浸み出しの評価	首藤 健一	横浜国立大学・工学部	leakage of surface/interfacial electrons of topological insulators	Ken-ichi Shudo	Yokohama Nat'l Univ.
116	2022-D-0006	ハイエントロピー合金と形状記憶合金の相平衡	御手洗 容子	東京大学新領域創成科学研究科	Phase equilibrium of high entropy alloys and shape memory alloys	Yoko Mitarai	Graduate School of Frontier Sciences, The University of Tokyo
117	2023-Ba-0009	カイラル物質のスピン流とカイラリティの第一原理計算	池田 浩章	立命館大学理工学部物理科学科	Ab initio calculations of spin currents and chirality in chiral materials	Hiroaki Ikeda	Department of Physics, Ritsumeikan University
118	2023-Ba-0013	第一原理計算によるC1化学のための触媒理論研究	辻 雄太	九州大学総合理工学研究院	First-principles theoretical catalytic studies for C1 chemistry	Yuta Tsuji	Faculty of Engineering Sciences, Kyushu University
119	2023-Ba-0051	原子層物質、有機物質、磁性材料のドーピングによる電子状態変化の研究	島田 敏宏	北海道大学 大学院工学研究院	Change in the electronic structure of atomic layered, organic and magnetic materials by doping	Toshihiro Shimada	Faculty of Engineering, Hokkaido University
120	2023-Ba-0053	半導体表面でのCO <sub>2</sub> 光還元における励起キャリア移動過程の解明	泉 康雄	千葉大学 大学院理学研究院	Excited carrier transfer processes in the CO <sub>2</sub> photo reduction at semiconductor surfaces	Yasuo Izumi	Graduate School of Science, Chiba University
121	2023-Ba-0065	表面ジラジカルの体系化に向けた理論的検討	多田 幸平	大阪大学 大学院基礎工学研究科 物質創成専攻化学工学領域	Theoretical investigation for systematizing surface diradical	Kohei Tada	Division of Chemical Engineering, Department of Materials Engineering Science, Graduate School of Engineering Science, Osaka University
122	2023-Cb-0005	グラフェンの電子輸送計算	藤本 義隆	九州大学工学研究院	First-principles calculations of electronic transport of graphene	Yoshitaka Fujimoto	Faculty of Engineering, Kyushu University
123	2023-Cb-0017	第一原理計算を用いた遷移金属化合物界面の光学特性調査	中村 和磨	九州工業大学	Ab initio calculations for optical property of transition-metal compound interface	Kazuma Nakamura	Kyushu Institute of Technology
124	2023-Cb-0027	As導入型有機元素材料の相安定性と電子状態に対する第一原理計算	出倉 駿	東北大学多元物質科学研究所	First-principles calculations for phase stabilities and electronic structures of As-incorporated organoelemental materials	Shun Dekura	Institute of Multidisciplinary Research for Advanced Materials, Tohoku University
125	2023-Ba-0005	新たなナノスケール表面界面の電子物性に関する理論的研究	小林 功佳	お茶の水女子大学理学部物理科学科	Theoretical study on electronic properties of new nanoscale surfaces and interfaces	Katsuyoshi Kobayashi	Department of Physics, Faculty of Science, Ochanomizu University
126	2023-Ba-0016	ハイエントロピー合金と形状記憶合金の相平衡	御手洗 容子	東京大学新領域創成科学研究科	Phase equilibrium of high entropy alloys and shape memory alloys	Yoko Mitarai	Graduate School of Frontier Sciences, The University of Tokyo

127	2023-Ba-0031	半導体表面上の新規インジウム超薄膜の電子構造と電気伝導物性	有賀 哲也	京都大学理学部研究科化学専攻	Electronic structure and conductivity of novel indium thin film on semiconductor surface	Aruga Tetsuya	Dept. Chem., School of Science, Kyoto University
128	2023-Ba-0034	ReO <sub>3</sub> の電子構造とフェルミ面	眞榮平 孝裕	琉球大学 理学部	Electronic Structure and Fermi surface of ReO <sub>3</sub>	Takahiro Maejira	Faculty of Science, University of the Ryukyus
129	2023-Ba-0047	第一原理バンド計算を用いた遷移金属化合物の電子相互作用の研究	榊原 寛史	鳥取大学大学院工学研究科	First-principles study of electron interactions in transition metal oxides	Hirofumi Sakakibara	Graduate School of Engineering, Tottori University
130	2023-Ba-0056	水素結合ネットワークを有する新規有機半導体における第一原理電子状態計算	出倉 駿	東北大学多元物質科学研究所	First-principles calculations on the electronic states of novel organic semiconductors with extended hydrogen-bonding networks	Shun Dekura	Institute of Multidisciplinary Research for Advanced Materials, Tohoku University
131	2023-Ba-0063	トポロジカル磁性体の安定性解析とトンネル伝導度の第一原理計算	見波 将	京都大学工学部研究科機械理工学専攻	First-principles study of stable interfacial structure analysis and magnetic tunnel conductance in topological magnets	Susumu Minami	Department of Mechanical Engineering and Science, Kyoto University
132	2023-Ba-0073	物質表面に対する電子ストレステンソル密度解析	福田 将大	東京大学物性研究所	Electronic stress tensor density analysis for material surfaces	Masahiro Fukuda	Institute for Solid State Physics, The University of Tokyo
133	2023-Bb-0015	ハイエントロピー合金と形状記憶合金の相平衡	御手洗 容子	東京大学新領域創成科学研究科	Phase equilibrium of high entropy alloys and shape memory alloys	Yoko Mitarai	Graduate School of Frontier Sciences, The University of Tokyo
134	2023-Ba-0022	第一原理計算による高エントロピー超伝導体のバンド構造の解析	白井 秀知	島根大学総合理工学部	First principles study on band structure of high entropy superconductors	Hidetomo Usui	Department of Physics and Materials Science, Shimane University
135	2023-Ba-0045	固体表面・界面、ナノ構造体の新規電子物性の探索と実現	福岡 毅	琉球大学理学部	Search and realization of novel electronic properties of surfaces and interfaces and of nanostructures	Takeshi Inaoka	Department of Physics and Earth Sciences, Faculty of Science, University of the Ryukyus
136	2023-Bb-0017	第一原理計算による高エントロピー超伝導体のバンド構造の解析	白井 秀知	島根大学総合理工学部	First principles study on band structure of high entropy superconductors	Hidetomo Usui	Department of Physics and Materials Science, Shimane University
137	2023-Bb-0001	第一原理計算を用いた磁気トンネル接合の設計と伝導度計算	田中 克大	東京大学大学院理学系研究科物理学専攻	First-principles study on designing magnetic tunnel junctions and calculating tunneling conductance	Katsuhiro Tanaka	Department of Physics, Graduate School of Science, University of Tokyo
138	2023-Bb-0004	超イオン導電体RbAg <sub>4</sub> Si <sub>5</sub> のイオン伝導メカニズム	田原 周太	中京大学教養教育研究院	Ionic conduction mechanism of superionic conductor RbAg <sub>4</sub> Si <sub>5</sub>	Shuta Tahara	Faculty of Liberal Arts and Sciences, Chukyo University
139	2023-Bb-0006	トポロジカル磁性体における磁気熱電効果の第一原理計算	見波 将	京都大学工学部研究科機械理工学専攻	First-principles study of magnetic thermoelectric effect in topological magnets	Susumu Minami	Department of Mechanical Engineering and Science, Kyoto University
140	2023-Bb-0008	フッ素樹脂表面に生成した水素を含む官能基のX線光電子分光スペクトルにおける化学シフト計算	大久保 雄司	大阪大学大学院工学研究科	Calculation of chemical shift of X-ray photoelectron binding energy of hydrogen-containing functional groups generated on fluoropolymer surface	Yuji Ohkubo	Graduate School of Engineering, Osaka University
141	2023-Bb-0028	電磁場と物質の相互作用の第一原理計算手法開発	加藤 洋生	東京大学量子科学研究所	Development of First Principles methods for Light-Matter Interaction	Hiroki Katow	Photon Science Center, the University of Tokyo
142	2023-Ba-0006	フッ素樹脂表面に生成した官能基のX線光電子分光スペクトルにおける化学シフト計算	大久保 雄司	大阪大学大学院工学研究科	Calculation of chemical shift of X-ray photoelectron binding energy of functional groups generated on fluoropolymer surface	Yuji Ohkubo	Graduate School of Engineering, Osaka University
143	2023-Ba-0041	二次元材料におけるナノスケール構造に基づくフォノン物性に関する研究	三澤 賢明	福岡工業大学工学部知能機械工学科	Phonon properties based on nanoscale structures in two-dimensional materials	Masaaki Misawa	Department of Intelligent Mechanical Engineering, Fukuoka Institute of Technology
144	2023-Ba-0069	イリジウム酸化物の格子熱伝導計算	河野 翔也	九州工業大学	Lattice thermal conductivity calculation of iridium oxide Ca <sub>5</sub> Ir <sub>3</sub> SO <sub>12</sub>	Shoya Kawano	Kyushu Institute of Technology
145	2023-Ba-0070	しわ構造を持つ機能性グラフェンシートの電子状態シミュレーション	有馬 健太	大阪大学 大学院 工学研究科	Simulation of electronic structures of functional graphene sheets with wrinkles	Kenta Arima	Graduate School of Engineering, Osaka University
146	2023-Bb-0009	ウルツァイト型LiGaO <sub>2</sub> の強誘電性発現機構の解明	安原 颯	東京工業大学	Investigation on a mechanism of Ferroelectricity in a wurtzite-type LiGaO <sub>2</sub>	Sou Yasuhara	Tokyo Institute of Technology
147	2023-Bb-0026	機能性グラフェンシート/半導体界面反応の解析	有馬 健太	大阪大学 大学院 工学研究科	Analysis of interface reaction between functional graphene and semiconductor surface	Kenta Arima	Graduate School of Engineering, Osaka University
148	2023-Ca-0117	Si(111)-r7xr3-In表面における超構造の第一原理計算(その2)	内田 和之	京都産業大学 理学部 物理科学科	First-principles Study on Superstructures of Si(111)-r7xr3-In Surface (PART II)	Kazuyuki Uchida	Department of Physics, Kyoto Sangyo University
149	2023-Ba-0055	異方的結晶構造を有する磁性材料の解析	小幡 正雄	金沢大学理工研究域	Analysis of magnetic materials with anisotropic crystal structures	Masao Obata	Institute of Science and Engineering, Kanazawa University
150	2023-Bb-0011	表面ベイン変形	小野 頌太	東北大学金属材料研究所	Surface Bain distortion	Shota Ono	Tohoku University
151	2023-Bb-0018	磁性形状記憶合金の第一原理計算	小幡 正雄	金沢大学理工研究域	First-principles investigation on magnetic shape memory alloy	Masao Obata	Institute of Science and Engineering, Kanazawa University
152	2023-Bb-0019	バイオガス直接供給による燃料電池の高効率化に向けた改質触媒の最適組成の探索	藤崎 貴也	島根大学 材料エネルギー学部	Search for optimal composition of reforming catalysts for high efficiency of fuel cells with direct biogas supply	Takaya Fujisaki	Faculty of materials for energy, Shimane university
153	2023-Bb-0021	ダイヤモンド材料の第一原理研究	Kadarisman Hana	Kanazawa University	First-principles calculation of diamond materials	Hana Kadarisman	Nanomaterials Research Institute, Kanazawa University
154	2023-Ba-0002	触媒インフォマティクスに向けたハイエントロピー合金の反応性評価	日沼 洋陽	産業技術総合研究所	Reactivity analysis of high entropy alloys for catalyst informatics	Yoyo Hinuma	National Institute of Advanced Industrial Science and Technology

155	2023-Ba-0015	水圏機能材料の電子状態	高橋 修	広島大学大学院理学研究科	Electronic structure of aqueous functional group materials	Osamu Takahashi	Graduate School of Science, Hiroshima University
156	2023-Ba-0025	シリカ melt 中のXeの圧縮挙動の解明	若林 大佑	高エネルギー加速器研究機構物質構造科学研究所	Compression behavior of xenon in silica melt	Daisuke Wakabayashi	Institute of Materials Structure Science, High Energy Accelerator Research Organization (KEK)
157	2023-Ba-0054	機械学習ポテンシャルの生成とそれによるダイヤモンド表面プロセスの解析	稲垣 耕司	大阪大学大学院工学研究科	Analyses of diamond surface processes by machine-learning based potentials	Kouji Inagaki	Graduate School of Engineering, Osaka University
158	2023-Ba-0001	金属表面上における有機金属構造体薄膜とそこに捕獲された原子・分子に対するDFT計算	塚原 規志	群馬工業高等専門学校	DFT calculations of the metal-organic film and atoms/molecules captured by the film on metal surfaces	Noriyuki Tsukahara	National Institute for Technology, Gunma College
159	2023-A-0001	新奇強誘電体LiGaO <sub>2</sub> への置換効果	安原 颯	東京工業大学	Investigation of substitution for a wurtzite-type ferroelectric material LiGaO <sub>2</sub>	Sou Yasuhara	Tokyo Institute of Technology
160	2023-A-0003	SnTe上の原子層 $\alpha$ -Snのバンド計算	秋山 了太	東京大学理学系研究科物理学専攻	Band calculations of atomic-layer $\alpha$ -Sn on SnTe	Ryota Akiyama	Department of Physics, The University of Tokyo
161	2023-A-0004	電磁場と物質の相互作用の第一原理計算手法開発	加藤 洋生	東京大学量子科学研究センター	Development of First Principles methods for Light-Matter Interaction	Hiroki Katow	Photon Science Center, the University of Tokyo
162	2023-A-0005	合金材料を対象としたVASPのベンチマークテスト	上村 直樹	京都先端科学大学ナガモリアクチュエータ研究所	A benchmark test using VASP for alloy materials	Naoki Uemura	The Nagamori Institute of Actuators, Kyoto University of Advanced Science
163	2023-A-0006	酸化物による水分解反応の理論的研究	山本 小夜子	九州大学	Theoretical study of water splitting reaction by oxides	Sayoko Yamamoto	Kyushu University
164	2023-A-0007	第一原理計算によるスピンデバイスの電子状態解析	海住 英生	慶應義塾大学	Electronic structure analysis of spin devices using first-principles calculation	Hideo Kajiu	Keio University
165	2023-A-0008	第一原理計算によるSi(111)-Inの表面超構造の相図の研究	福田 常男	大阪公立大学大学院工学研究科電子物理学専攻	First-principles Study of the Phase Diagram of Si(111)-In surface structures	Tuneo Fukuda	Depart. of Physics and Electronics, Graduate School of Eng., Osaka Metropolitan University
166	2023-A-0010	第一原理計算を用いたノンコリニア磁性体の物性開拓	田中 克大	東京大学大学院理学系研究科物理学専攻	Exploring physical properties of noncollinear magnets from first-principles	Katsuhiko Tanaka	Department of Physics, Graduate School of Science, University of Tokyo
167	2023-A-0012	単一成分分子性導体の固溶化・元素置換による電子構造変調効果の解明	横森 創	立教大学	Elucidation of electronic structure modulation effects of solid solution and element substitution in single-component molecular conductors	So Yokomori	Rikkyo University
168	2023-A-0013	無機高分子材料の第一原理分子動力学計算	本武 陽一	一橋大学大学院ソーシャル・データサイエンス研究科	Ab initio molecular dynamics study of inorganic polymer	Yoh-ichi Mototake	Faculty of Social Data Science, Hitotsubashi university
169	2023-A-0014	DFT計算を用いたナノセルロースの構造最適化	藤澤 秀次	東京大学農学生命科学研究科	Structure optimization of nanocellulose using DFT calculations	Shuji Fujisawa	Graduate School of Agricultural and Life Sciences, The University of Tokyo
170	2023-A-0015	自動微分を用いた目的の性質を持つハミルトニアンへの逆設計	乾 幸地	東京大学工学系研究科原子力国際専攻	Inverse design of Hamiltonians with target properties using automatic differentiation	Koji Inui	Department of Nuclear Engineering and Management, The University of Tokyo
171	2023-A-0016	金属触媒表面の分子吸着に関する理論的研究	翼 俊暢	九州大学総合理工学研究院	Theoretical study on molecular adsorption on metal catalyst surface	Toshinobu Tatsumi	Interdisciplinary Graduate School of Engineering Sciences, Kyushu University
172	2023-A-0017	二元系物質群に関するマテリアルズインフォマティクス基盤研究	草野 茜	九州大学大学院総合理工学研究院	Fundamental Materials Informatics Research on Binary Systems of Materials	Akane Kusano	Interdisciplinary Graduate School of Engineering Sciences, Kyushu University
173	2023-A-0021	第一原理計算による格子整合型磁気トンネル接合の電子状態解析	海住 英生	慶應義塾大学	Electronic structure analysis of lattice-matched magnetic tunnel junctions using first-principles calculation	Hideo Kajiu	Keio University
174	2023-A-0024	Ni表面上の単層ボロフェンの構造解析	中川 剛志	九州大学大学院総合理工学研究院	Structural analysis of single layer borophene on Ni surfaces	Takeshi Nakagawa	Interdisciplinary Graduate School of Engineering Sciences, Kyushu University
175	2023-A-0025	酸化物準結晶超薄膜の構造解析	柚原 淳司	名古屋大学	Structural analysis of oxide quasicrystal thin films	Junji Yuhara	Nagoya University

## 2. 強相関 / Strongly Correlated Quantum Systems

No.	課題番号	課題名	氏名	所属	Title	Name	Organization
1	2023-Ea-0008	人工ニューラルネットワークとテンソルネットワークの融合形式の開発と応用	野村 悠祐	東北大学金属材料研究所	Development and application of tensor neural network methods	Yusuke Nomura	Institute for Materials Research, Tohoku University
2	2023-Ea-0005	強相関量子多体系の長時間シミュレーション	今田 正俊	上智大学	Long-time simulation for strongly-correlated quantum systems	Masatoshi Imada	Faculty of Science and Engineering, Sophia University
3	2023-Eb-0005	データベースを活用した高温超伝導体に対する網羅的強相関第一原理計算	三澤 貴宏	東京大学物性研究所	Comprehensive ab initio investigation of high-Tc materials using database	Takahiro Misawa	Institute for Solid State Physics, The University of Tokyo
4	2023-Ea-0001	量子物質のための変分波動関数分光法の開発	山地 洋平	物質・材料研究機構	Development of variational-wave-function spectroscopy for quantum materials	Youhei Yamaji	National Institute for Materials Science
5	2023-D-0002	分子性固体(TMTTF) <sub>2</sub> PF <sub>6</sub> の圧力下の第一原理有効模型解析	三澤 貴宏	東京大学物性研究所	Analysis of $ab$ initio Hamiltonians for molecular solid (TMTTF) <sub>2</sub> PF <sub>6</sub> under pressure	Takahiro Misawa	Institute for Solid State Physics, The University of Tokyo
6	2023-D-0005	テンソル量子リザーブローピングによるスクランプリング速度の大規模解析	求 幸年	東京大学大学院工学系研究科	Large-scale analysis of scrambling rate by tensor quantum reservoir probing	Yukitoshi Motome	Department of Applied Physics, The University of Tokyo

7	2023-D-0006	機械学習ポテンシャルによるスピン電荷結合ダイナミクスの数値解析	求 幸年	東京大学大学院工学系研究科	Numerical study of spin-charge coupled dynamics by machine learning potentials	Yukitoshi Motome	Department of Applied Physics, The University of Tokyo
8	2023-Ca-0066	強相関トポロジカル物性の理論的解明と機械学習への応用	求 幸年	東京大学大学院工学系研究科	Theoretical study of strongly correlated topological phenomena and its application to machine learning	Yukitoshi Motome	Department of Applied Physics, The University of Tokyo
9	2023-Ca-0033	フラストレート磁性体における多体トポロジカル相	井戸 康太	東京大学物性研究所	Many-body topological phases in frustrated magnets	Kota Ido	Institute for Solid State Physics, The University of Tokyo
10	2023-Cb-0014	強相関トポロジカル物性の理論的解明と機械学習への応用	求 幸年	東京大学大学院工学系研究科	Theoretical study of strongly correlated topological phenomena and its application to machine learning	Yukitoshi Motome	Department of Applied Physics, The University of Tokyo
11	2023-Ca-0068	第一原理計算と量子多体計算による多バンド少数キャリア系の電子・フォノン状態と超伝導	大野 義章	新潟大学	Electronic and phonon states and superconductivity of multi-band low-carrier systems based on first-principles and quantum many-body calculations	Yoshiaki Ono	Niigata University
12	2023-Ca-0112	スピン・電荷・格子自由度が織りなす新奇磁気秩序相の研究	諏訪 秀磨	東京大学大学院理学系研究科物理学専攻	Novel magnetic phases emerging from spin-charge-lattice couplings	Hidemaro Suwa	Department of Physics, The University of Tokyo
13	2023-Ca-0132	ボソン系の量子計算法開発と、量子多体系の非時間順序相関	手塚 真樹	京都大学大学院理学研究科物理学・宇宙物理学専攻	Development of quantum computation for bosonic systems and out-of-time-ordered correlators for quantum many-body systems	Masaki Tezuka	Department of Physics, Kyoto University
14	2023-Cb-0022	強相関電子系で発現する多体トポロジカル相	井戸 康太	東京大学物性研究所	Many-body topological phases in strongly correlated electron systems	Kota Ido	Institute for Solid State Physics, The University of Tokyo
15	2023-Ca-0010	二次元準周期タイリング上ハバード模型の磁性	古賀 昌久	東京工業大学	Magnetism for the half-filled Hubbard model on the two-dimensional quasiperiodic tilings	Akihisa Koga	Tokyo Institute of Technology
16	2023-Ca-0022	ダイマー相関が強い一次元モット絶縁体の光励起過渡吸収スペクトル	遠山 貴己	東京理科大学先進工学部理工学系	Photoinduced transient absorption spectrum in one-dimensional Mott insulator with strong dimer correlation	Takami Tohyama	Department of Applied Physics, Tokyo University of Science
17	2023-Ca-0062	テルビウムおよびトリウムイオンに創出する3チャンネル近藤効果の研究	堀田 貴嗣	東京都立大学理学研究科物理学専攻	Research of Three-Channel Kondo Effect Emerging from Tb and Tm Ions	Takashi Hotta	Department of Physics, Graduate School of Science, Tokyo Metropolitan University
18	2023-Ca-0021	強相関電子系における非線形応答	ピーターズ ロバート	京都大学	nonlinear response in strongly correlated materials	Robert Peters	Kyoto University
19	2023-Cb-0026	多成分フェルミ粒子系のDMFTによる強磁性秩序の解析	古賀 昌久	東京工業大学	Analyzing Ferromagnetic Order in Multi-Component Fermionic Systems using DMFT	Akihisa Koga	Tokyo Institute of Technology
20	2023-Ca-0119	ニッケル酸化物超伝導体における非従来型超伝導の研究	黒木 和彦	大阪大学	Studies on unconventional superconductivity in nickelates	Kazuhiro Kuroki	Osaka University
21	2023-Ca-0105	キタエフ量子スピン液体におけるバイソンの励起の実時間ダイナミクス	那須 誠治	東北大学	Real-time dynamics of vison excitations in Kitaev spin liquids	Joji Nasu	Tohoku University
22	2023-Ca-0071	スピン軌道相互作用系・強相関系における光誘起非平衡電子状態に関する理論研究	望月 雅人	早稲田大学先進理工学部応用物理学科	Theoretical study on photoinduced nonequilibrium electron states in spin-orbit coupling systems and strongly correlated electron systems	Masahito Mochizuki	Waseda university
23	2023-Ca-0106	高伝導性オリゴマー型伝導体単結晶の電子構造解析	藤野 智子	東京大学物性研究所	Electronic structures for highly conducting oligomer conductors in single crystals	Tomoko Fujino	Institute for Solid State Physics, The University of Tokyo
24	2023-Ba-0042	多スケール時空仮説に基づく量子多体計算	品岡 寛	埼玉大学理学部物理学科	Many-body quantum simulations based on multi-scale space-time ansatz	Hiroshi Shinaoka	Department of Physics, Saitama University
25	2023-Ba-0066	光電場駆動された量子系の非平衡ダイナミクス	小野 淳	東北大学大学院理学研究科	Nonequilibrium dynamics in quantum systems driven by optical electric fields	Atsushi Ono	Department of Physics, Tohoku University
26	2023-Cb-0004	ニューラルネットワークを用いた相関量子物質の非平衡ダイナミクス	ピーターズ ロバート	京都大学	Nonequilibrium dynamics of correlated quantum matter using neural networks	Robert Peters	Kyoto University
27	2023-Ba-0023	固体物質におけるBCS-BECクロスオーバーの理論的研究	渡部 洋	日本大学生産工学部	Theoretical study of BCS-BEC crossover in solid-state materials	Hiroshi Watanabe	College of Industrial Technology, Nihon University
28	2023-Ba-0017	有機ディラック電子系において電子相関が誘起するトポロジカル秩序と空間反転対称性の破れ	小林 晃人	名古屋大学 大学院理学研究科	Electron correlation-induced topological order and spatial inversion symmetry breaking in organic Dirac electron systems	Akito Kobayashi	Graduate School of Science, Nagoya University
29	2023-Ca-0080	非共線磁気構造の電流駆動による創発電場の数値計算	賀川 史敬	東京工業大学	Numerical calculation of emergent electric field induced by current-driven non-collinear magnetic structure	Fumitaka Kagawa	Tokyo Institute of Technology
30	2023-Ba-0014	絶縁体的基底状態を有する希土類酸化物の強結合ハミルトニアン構成と誘電関数の決定	牧野 哲征	福井大学遠赤外線域開発研究センター	Construction of ab-initio tight-binding Hamiltonian and determination of dielectric functions of rare-earth monoxides having insulating ground states	Takayuki Makino	Research Center for Development of Far-Infrared Region, University of Fukui
31	2023-Ba-0033	強相関電子系における高温超伝導機構の研究	柳沢 孝	産業技術総合研究所	Research on the mechanism of high-temperature superconductivity in strongly correlated electron systems	Takashi Yanagisawa	National Institute of Advanced Industrial Science and Technology
32	2023-Ba-0052	弱結合理論によるホイスラー化合物の熱電性能に関する理論的研究	西口 和孝	神戸大学大学院システム情報学研究科	Theoretical study of thermoelectric properties in Heusler compounds using weak-coupling approaches	Kazutaka Nishiguchi	Graduate School of System Informatics, Kobe University
33	2023-Ba-0030	人工積層系におけるバンドエンジニアリングと電子相関効果	苅宿 俊風	物材機構	Band engineering and electron correlation effects in artificially stacked systems	Toshikazu Kariyado	NIMS
34	2023-Bb-0025	強相関電子系における高温超伝導機構の研究	柳沢 孝	産業技術総合研究所	Numerical study of the mechanism of high-temperature superconductivity in strongly correlated electron systems	Takashi Yanagisawa	National Institute of Advanced Industrial Science and Technology

35	2023-Bb-0020	トポロジカル物質Pr <sub>2</sub> Ir <sub>2</sub> O <sub>7</sub> の実験結果の解釈のためのモデルハミルトニアン構築	島田 敏宏	北海道大学 大学院工学研究院	Construction of model Hamiltonian to interpret experimental results of topological Pr <sub>2</sub> Ir <sub>2</sub> O <sub>7</sub>	Toshihiro Shimada	Faculty of Engineering, Hokkaido University
36	2023-D-0009	多成分フェルミ粒子系のDMFTによる強磁性秩序の解析	古賀 昌久	東京工業大学	Analyzing Ferromagnetic Order in Multi-Component Fermionic Systems using DMFT	Akihisa Koga	Tokyo Institute of Technology
3. 巨視系の協同現象 / Cooperative Phenomena in Complex, Macroscopic Systems							
No.	課題番号	課題名	氏名	所属	Title	Name	Organization
1	2023-Ea-0012	テンソルネットワーク表現に基づく古典ランダムスピン系の研究	川島 直輝	東京大学物性研究所	Tensor-Network Study of Classical Random Spin Systems	Naoki Kawashima	Institute for Solid State Physics, University of Tokyo
2	2023-Ea-0002	全原子・粗視化力場によるソフトマターの分子シミュレーション	篠田 渉	岡山大学異分野基礎科学研究所	Molecular Simulation of Soft Materials using All-Atom and Coarse-Grained Force Field	Wataru Shinoda	Okayama University, Research Institute for Interdisciplinary Science
3	2023-Eb-0001	超音波キャビテーションの分子動力学シミュレーション	浅野 優太	高度情報科学技術研究機構計算科学技術部	Molecular dynamics simulation of ultrasound cavitation	Yuta Asano	Research Organization for Information Science and Technology
4	2023-Eb-0006	テンソルネットワーク表現に基づく古典ランダムスピン系の研究	川島 直輝	東京大学物性研究所	Tensor-Network Study of Classical Random Spin Systems	Naoki Kawashima	Institute for Solid State Physics, University of Tokyo
5	2023-Eb-0004	全原子・粗視化力場によるソフトマターの分子シミュレーション	篠田 渉	岡山大学異分野基礎科学研究所	Molecular Simulation of Soft Materials using All-Atom and Coarse-Grained Force Field	Wataru Shinoda	Okayama University, Research Institute for Interdisciplinary Science
6	2023-Ea-0006	粗視化モデリングされた赤血球の動的性質の解析	渡辺 宙志	慶応義塾大学理工学部	Dynamic properties of coarse-grained modeled red blood cells	Hiroshi Watanabe	Faculty of Science and Technology, Keio University
7	2023-Ca-0019	蛋白質物性に強く関与するソフトモードの効率的サンプリングシミュレーション	北尾 彰朗	東京工業大学生命理工学院	Efficient sampling simulation of the soft modes significantly contribute to protein properties	Akio Kitao	Institute of Molecular and Cellular Biosciences, University of Tokyo
8	2023-Ca-0121	テンソルネットワークとサンプリングによる量子多体系のシミュレーション	藤堂 眞治	東京大学大学院理学系研究科物理学専攻	Simulation of quantum many-body systems by tensor network and sampling	Synge Todo	Department of Physics, University of Tokyo
9	2023-Ca-0069	フラストレート磁性体の有限温度物性の解明	大久保 毅	東京大学大学院理学系研究科知の物理学研究センター	Study on finite temperature properties of frustrated magnets	Tsuyoshi Okubo	Institute for Physics of Intelligence, The University of Tokyo
10	2023-Ca-0077	自己駆動粒子系が示すマイクロ相分離の解析	中野 裕義	東京大学物性研究所	Analysis of microphase separation in active particle systems with self-propulsion	Hiroyoshi Nakano	The Institute for Solid State Physics, The University of Tokyo
11	2023-Ca-0007	ガラス形成物質におけるJohari-Goldstein緩和に関する研究	荒木 武昭	京都大学大学院理学研究科物理学・宇宙物理学専攻	Study on Johari-Goldstein relaxation mode in glass-forming liquids	Takeaki Araki	Department of Physics, Kyoto University
12	2023-Ca-0067	熱流下相共存における準安定状態の定常性	中川 尚子	茨城大学理学部	Steady metastable states contained in heat conducting phase coexistence	Naoko Nakagawa	Department of Physics, Ibaraki University
13	2023-Ca-0042	量子スピン系の低エネルギー状態に関する数値的研究	中野 博生	兵庫県立大学大学院理学研究科	Numerical study on low-energy states of quantum spin systems	Hiroki Nakano	Graduate School of Science, University of Hyogo
14	2023-Cb-0049	テンソルネットワーク法によるハニカム格子量子スピン模型の研究	大久保 毅	東京大学大学院理学系研究科知の物理学研究センター	Tensor network study of quantum spin models on the honeycomb lattice.	Tsuyoshi Okubo	Institute for Physics of Intelligence, The University of Tokyo
15	2023-Ca-0031	両親媒性分子の自己組織化プロセスと構造制御	樋口 祐次	九州大学情報基盤研究開発センター	Self-assembly processes of amphiphilic molecules and their structural controls	Yuji Higuchi	Research Institute for Information Technology, Kyushu University
16	2023-Ca-0039	摩擦の物理	松川 宏	青山学院大学理工学部	Physics of Friction	Hiroshi Matsukawa	Faculty of Science and Engineering, Aoyama Gakuin University
17	2023-Ca-0111	複雑流動のマルチスケールシミュレーション	川勝 年洋	東北大学大学院理学研究科物理学専攻	Multiscale simulations for complex flows	Toshihiro Kawakatsu	Department of Physics, Faculty of Science, Tohoku University
18	2023-Cb-0031	酵素を合理的に高活性化させる普遍的手法の開発	新井 宗仁	東京大学大学院総合文化研究科	Development of a general method for rationally improving enzymatic activity	Munehito Arai	Graduate School of Arts and Sciences, The University of Tokyo
19	2023-Ca-0002	機械学習を用いた磁気スキルミオン探索	速水 賢	北海道大学大学院理学研究院	Search for magnetic skyrmion by machine learning	Satoru Hayami	Department of Physics, Hokkaido University
20	2023-Ca-0091	クロック異方性を持つカイラル磁性体における相転移	西川 宜彦	北里大学理学部物理学科	Phase transitions in a classical chiral magnet with a clock anisotropy	Yoshihiko Nishikawa	Department of Physics, School of Science, Kitasato University
21	2023-Ca-0095	ナノ多孔体中における高分子ダイナミクスの全原子分子動力学シミュレーション	細野 暢彦	東京大学大学院工学系研究科応用化学専攻	All-Atom Molecular Dynamics Simulation Study of Polymer Dynamics in Nanoporous Materials	Nobuhiko Hosono	Department of Applied Chemistry, Graduate School of Engineering, The University of Tokyo
22	2023-Cb-0042	鉄系超伝導体における等電子ドーピング効果の理論研究	Jeschke Harald	岡山大学異分野基礎科学研究所	Theoretical study of isoelectronic doping effects in iron-based superconductors	Harald Jeschke	Research Institute for Interdisciplinary Science Okayama University
23	2023-Cb-0016	レヴィウォークするアクティブブラウン粒子系の相分離現象	中野 裕義	東京大学物性研究所	Phase separation of active Brownian particles with Levy walks	Hiroyoshi Nakano	The Institute for Solid State Physics, The University of Tokyo
24	2023-Ca-0081	マクロな物体の動摩擦	大槻 道夫	大阪大学基礎工学研究科	Dynamic friction of macroscopic objects	Michio Otsuki	Graduate school of engineering science

25	2023-Ca-0043	スピンドラー系の新しい磁化プラトー	坂井 徹	兵庫県立大学大学院理学研究科	Novel Magnetization PLateau of the Spin Ladder System	Toru Sakai	Graduate School of Science, University of Hyogo
26	2023-Ca-0093	伸長流動下における多環状鎖の非平衡ダイナミクス	村島 隆浩	東北大学大学院理学研究科	Nonequilibrium dynamics of multicyclic chains under elongational flow	Takahiro Murashima	東北大学大学院理学研究科
27	2023-Ea-0003	超音波キャビテーションの大規模分子動力学シミュレーション	浅野 優太	高度情報科学技術研究機構計算科学技術部	Large-scale molecular dynamics simulation of ultrasonic cavitation	Yuta Asano	Research Organization for Information Science and Technology
28	2023-Ca-0128	センサー材料のためのトモグラフィを基盤とする量子混合計算シミュレーション	水上 渉	大阪大学 量子情報・量子生命研究センター	Quantum-classical hybrid simulations for sensor materials based on quantum state tomography	Wataru Mizukami	Center for Quantum Information and Quantum Biology
29	2023-Cb-0015	半導体界面での熱輸送機構解明	許 斌	東京大学大学院機械工学専攻	Elucidating the Thermal Transport Mechanisms at Semiconductor Interfaces	Xu Bin	Department of Mechanical Engineering, The University of Tokyo
30	2023-Ca-0087	プラストレートした量子磁性体に対する熱ゆらぎの効果	下川 統久朗	沖縄科学技術大学院大学	Thermal effects on quantum frustrated magnetisms	Tokuro Shimokawa	Okinawa Institute of Science and Technology Graduate University
31	2023-Ca-0055	異方の相互作用を持つ蜂の巣格子Kitaev- $\Gamma$ モデルの動的性質2	鈴木 隆史	兵庫県立大学 大学院工学研究科	Dynamical properties of the extended Kitaev- $\Gamma$ model on a honeycomb lattice 2	Takafumi Suzuki	Graduate School of Engineering, University of Hyogo
32	2023-Ca-0076	機械学習を活用した多層CNT紡績系の最適ナノ構造と潜在引張強度の発見	山本 剛	東北大学大学院工学研究科・航空宇宙工学専攻	Machine learning-assisted high-throughput molecular dynamics simulation of high-performance CNT yarn structure	Go Yamamoto	Department of Aerospace Engineering, Tohoku University
33	2023-Cb-0048	不規則系における熱輸送解析	塩見 淳一郎	東京大学工学系研究科	Analysis of thermal transport in disordered systems	Junichiro Shimi	School of Engineering, The University of Tokyo
34	2023-Ca-0072	電極との界面に電気二重層を形成するイオン液体の電位応答ダイナミクスの解析	福井 賢一	大阪大学大学院基礎工学研究科	Analyses on the Potential-dependent Dynamics of Ionic Liquid Forming Electric Double Layer Facing the Electrodes	Ken-ichi Fukui	Graduate School of Engineering Science, Osaka University
35	2023-Cb-0001	二次元強磁性ダイマー系のスピンネマティック相	坂井 徹	兵庫県立大学大学院理学研究科	Spin Nematic Phase of 2D Ferromagnetic Dimer Systems	Toru Sakai	Graduate School of Science, University of Hyogo
36	2023-Ca-0058	ガウス過程回帰を用いたゆらぎの緩和解析の改良	尾関 之康	電気通信大学情報理工学研究科	Improvement of analysis for relaxation of fluctuations by the use of Gauss process regression	Yukiyasu Ozeki	Department of Applied Physics and Chemistry, The University of Electro-Communications
37	2023-Ca-0075	ゆらぎ交換近似法を用いたインタカレートFeSe超伝導体の理論研究	Jeschke Harald	岡山大学異分野基礎科学研究所	Fluctuation exchange approximation for superconductivity in FeSe intercalates	Harald Jeschke	Research Institute for Interdisciplinary Science Okayama University
38	2023-Ca-0096	分子動力学法を用いた熱硬化性樹脂の微視的損傷解析	大矢 豊大	東京理科大学先進工学部	Molecular dynamics study of microscopic damage in thermosetting polymers	Yutaka Oya	Faculty of Advanced Engineering, Tokyo University of Science
39	2023-Cb-0030	ガウス過程回帰を用いた揺らぎの緩和解析の改良 II	尾関 之康	電気通信大学情報理工学研究科	Improvement of analysis for relaxation of fluctuations by the use of Gauss process regression II	Yukiyasu Ozeki	Department of Applied Physics and Chemistry, The University of Electro-Communications
40	2023-Cb-0051	層間架橋結合による多層CNTのトポジカル欠陥感受性の低減	山本 剛	東北大学大学院工学研究科・航空宇宙工学専攻	Decreasing Topological Defects Sensitivity in Multi-Walled Carbon Nanotubes Through Interwall Coupling	Go Yamamoto	Department of Aerospace Engineering, Tohoku University
41	2023-Cb-0056	センサー材料のためのトモグラフィを基盤とする量子混合計算シミュレーション	水上 渉	大阪大学 量子情報・量子生命研究センター	Quantum-classical hybrid simulations for sensor materials based on quantum state tomography	Wataru Mizukami	Center for Quantum Information and Quantum Biology
42	2023-Cb-0037	量子スピン液体におけるマヨラナゼロモードの生成と制御	那須 誠治	東北大学	Creation and manipulation of Majorana zero mode in quantum spin liquids	Joji Nasu	Tohoku University
43	2023-Ca-0123	創薬に向けた新規タンパク質の合理的設計	新井 宗仁	東京大学大学院総合文化研究科	Rational design of novel proteins for drug discovery	Munehito Arai	Graduate School of Arts and Sciences, The University of Tokyo
44	2023-Cb-0044	リン脂質二重膜上の水分子の回転拡散	樋口 祐次	九州大学情報基盤研究開発センター	Rotational diffusion of water molecules on phospholipid bilayers	Yuji Higuchi	Research Institute for Information Technology, Kyushu University
45	2023-Ca-0118	高分子架橋ネットワーク系のトポロジー構造解析による物性メカニズムの解明	萩田 克美	防衛大学校応用科学群応用物理学科	Physical properties of crosslinked polymer networks through network topology analysis	Katsumi Hagita	Department of Applied Physics, School of Applied Sciences, National Defense Academy
46	2023-Ca-0047	ハニカム格子スピン系におけるフラストレーションとランダムネス	安田 千寿	琉球大学理学部	Frustration and randomness in the honeycomb-lattice spin systems	Chitoshi Yasuda	Department of Physics and Earth Sciences, University of the Ryukyus
47	2023-Cb-0053	プラストレートした量子磁性体に対する熱ゆらぎの効果	下川 統久朗	沖縄科学技術大学院大学	Thermal effects on quantum frustrated magnets	Tokuro Shimokawa	Okinawa Institute of Science and Technology Graduate University
48	2023-Cb-0025	ランダム位相状態を用いた有限温度計算法の一般変分波動関数への拡張	飯高 敏晃	理化学研究所	Extension of finite temperature calculation with random-phase states to general variational wave functions	Toshiaki Itaka	Riken
49	2023-Ca-0102	テンソルデータ解析におけるテンソルネットワークの活用	原田 健自	京都大学大学院情報学研究所	Application of tensor networks in tensor data analysis	Kenji Harada	Graduate school of Informatics, Kyoto University
50	2023-Ca-0116	クロマチン分子モデルの分子動力学による研究	福島 孝治	東京大学大学院総合文化研究科	Molecular dynamics study of Chromatin molecular model	Koji Hukushima	Department of Basic Science, The University of Tokyo

51	2023-Ca-0045	パーシステント図を用いた錯イオン回転による超イオン伝導機構の解明	佐藤 能平	東北大学材料科学高等研究所	The Mechanism Study of Superionic Conduction Induced by Complex Ion Rotation Using Persistent Diagram	Ryuhei Sato	Advanced Institute for Materials Research, Tohoku University
52	2023-Ca-0110	Ground state and dynamical properties of the $SJ_{11}J_{2KS}$ -Heisenberg model on the square lattice	ゴウケ マティアス	沖縄科学技術大学院大学	Ground state and dynamical properties of the $SJ_{11}J_{2KS}$ -Heisenberg model on the square lattice	Matthias Gohlke	Okinawa Institute of Science and Technology Graduate University
53	2023-Cb-0038	フラストレート磁性体における新奇秩序	川村 光	神戸大学分子フォトサイエンス研究センター	Novel order in frustrated magnets	Hikaru Kawamura	Molecular Photoscience Research Center, Kobe University
54	2023-Ca-0024	準結晶と近似結晶における超伝導特性の比較	竹森 那由多	大阪大学 理学研究科	Comparison of superconducting properties in quasicrystals and approximant crystals	Nayuta Takemori	Graduate School of Science, Osaka University
55	2023-Ca-0103	フラストレート磁性体における新奇秩序	川村 光	神戸大学分子フォトサイエンス研究センター	Novel order in frustrated magnets	Hikaru Kawamura	Molecular Photoscience Research Center, Kobe University
56	2023-Ba-0029	ボンド重み付きテンソルネットワークくりこみ群による臨界現象の解析	森田 悟史	慶應義塾大学大学院理工学研究科	Study of critical phenomena by the bond-weighted tensor renormalization group method	Satoshi Morita	Faculty of Science and Technology, Keio University
57	2023-Ba-0003	行列のパーマネント計算を用いた自由ボゾン系における量子エンタングルメントダイナミクスの研究	金子 隆威	上智大学 理工学部 機能創造理工学科	Study of quantum entanglement dynamics in free boson systems by computing the matrix permanent	Ryui Kaneko	Department of Engineering and Applied Sciences, Faculty of Science and Technology, Sophia University
58	2023-Ba-0007	1次元フラストレート量子スピンの数値的研究	飛田 和男	埼玉大学大学院理工学研究科物質科学部門	Numerical Study of One Dimensional Frustrated Quantum Spin Systems	Kazuo Hida	Division of Material Science, Graduate School of Science and Engineering, Saitama University
59	2023-Ba-0035	臨界現象のテンソルネットワークに基づく有限サイズケーリング	押川 正毅	東京大学物性研究所	Tensor-network-based finite-size scaling of critical phenomena	Masaki Oshikawa	Institute for Solid State Physics, University of Tokyo
60	2023-Ba-0036	強相関・多自由度系における新奇超伝導現象の理論提案	角田 峻太郎	東京大学大学院総合文化研究科	Theoretical proposals of novel superconducting phenomena in strongly correlated systems with multi degrees of freedom	Shuntaro Sumita	Department of Basic Science, The University of Tokyo
61	2023-Ba-0039	空間的に非一様な超伝導超流動のボソン励起	正木 祐輔	東北大学	Bosonic excitation in spatially non-uniform superconductors and superfluids	Yusuke Masaki	Tohoku University
62	2023-Ba-0050	2次元量子アクティブ粒子の新モデルの数値シミュレーション	羽田野 直道	東京大学生産技術研究所	Numerical Simulation of A Novel Model of Two-Dimensional Quantum Active Particle	Naomichi Hatano	Institute of Industrial Science, The University of Tokyo
63	2023-Ba-0060	ブリージングカゴメ反強磁性体における磁場誘起カイラリティ	青山 和司	大阪大学大学院理学研究科宇宙地球専攻	Field-induced chirality in breathing-kagome antiferromagnets	Kazushi Aoyama	Department of Earth and Space Science, Graduate School of Science, Osaka University
64	2023-Ba-0062	測定誘起臨界現象の安定性に対する数値的研究	藤 陽平	東京大学工学系研究科物理工学専攻	Numerical study for stability of measurement-induced critical phenomena	Yohei Fuji	Department of Applied Physics, University of Tokyo
65	2023-Ba-0064	TRHEPDによるSb/Biヘテロ構造におけるトポロジカル相転移の解明	高山 あかり	早稲田大学	Topological phase transition in Sb/Bi heterostructure studied by TRHEPD	Akari Takayama	Waseda University
66	2023-Bb-0002	変分モンテカルロ法による多層型ピスマス系超伝導体の有効モデルの基底状態探索	金子 隆威	上智大学 理工学部 機能創造理工学科	Variational Monte Carlo study of ground-state properties in effective models for Bi-based multilayered superconductors	Ryui Kaneko	Department of Engineering and Applied Sciences, Faculty of Science and Technology, Sophia University
67	2023-Ba-0011	高分子鎖の伸長下における分子ダイナミクス	眞弓 皓一	東京大学物性研究所	Molecular Dynamics of Polymer Chain under Deformation	Koichi Mayumi	Institute for Solid State Physics, The University of Tokyo
68	2023-Ba-0028	ソフトマテリアルの秩序構造とそのダイナミクス、光学的性質の計算	福田 順一	九州大学 大学院理学研究院	Calculation of ordered structures, dynamics and optical properties of soft materials	Jun-ichi Fukuda	Faculty of Science, Kyushu University
69	2023-Ba-0061	量子開放系の緩和過程の解析	白井 達彦	早稲田大学高等研究所	Relaxation process in open quantum systems	Tatsuhiko Shirai	Waseda Institute for Advanced Study, Waseda University
70	2023-Ca-0078	幾何学的に荒れた炭酸カルシウム結晶表面へのイオン性高分子吸着構造の大規模メタダイナミクス計算研究	灘 浩樹	鳥取大学	A Large-Scale Metadynamics Simulation Study on the Binding Conformations of Ionic Polymers at a Geometrically Rough Surface of Calcium Carbonate Crystal	Hiroki Nada	Tottori University
71	2023-Ba-0010	強誘電性ネマチック液晶の発現機構	荒木 武昭	京都大学大学院理学研究科物理学・宇宙物理学専攻	Physical origin of forming ferroelectric nematic phase	Takeaki Araki	Department of Physics, Kyoto University
72	2023-Ba-0038	磁気構造に起因する摩擦力を通じた摩擦の微視的メカニズムの考察	小松 尚登	滋賀大学データサイエンス・AIイノベーション研究推進センター	Consideration on the microscopic mechanism of the friction by the frictional force caused by magnetic structures	Hisato Komatsu	Data Science and AI Innovation Research Promotion Center, Shiga University
73	2023-Ba-0067	局在電子・格子結合系の光誘起量子もつれ生成ダイナミクス	石田 邦夫	宇都宮大学工学部	Photoinduced entanglement generation dynamics in electron-phonon systems	Kunio Ishida	School of Engineering, Utsunomiya University
74	2023-Bb-0012	ソフトマテリアルの秩序構造とそのダイナミクス、光学的性質の計算	福田 順一	九州大学 大学院理学研究院	Calculation of ordered structures, dynamics and optical properties of soft materials	Jun-ichi Fukuda	Faculty of Science, Kyushu University
75	2023-Bb-0029	コロイドゲルのトポロジーと力学物性	荒木 武昭	京都大学大学院理学研究科物理学・宇宙物理学専攻	Topological and mechanical properties of colloidal gels	Takeaki Araki	Department of Physics, Kyoto University
76	2023-Bb-0007	非球形微粒子系における構造形成	寺尾 貴道	岐阜大学工学部	Structural formation of non-spherical colloidal particles	Takamichi Terao	Faculty of Engineering, Gifu University
77	2023-Bb-0023	トポロジカル絶縁体薄膜における表面と界面のスピンおよび電子状態の探索	森 亮	東京大学物性研究所	Investigation of spin and electronic structures in surface/interface of topological insulator thin films	Ryo Mori	Institute for Solid State Physics, The University of Tokyo
78	2023-Ba-0004	空間構造をもつ次元量子スピンの数値的研究	利根川 孝	神戸大学大学院理学研究科	Numerical Study of the One-Dimensional Quantum Spin Systems	Takashi Tonegawa	Graduate School of Science, Kobe University
79	2023-Ba-0012	生物発光基質類似体の吸収・蛍光スペクトル解析	樋山 みやび	群馬大学	Theoretical study for absorption and fluorescence spectra of firefly bioluminescence substrate analogs	Miyabi Hiyama	Gunma University

80	2023-Ba-0037	カゴメ格子系のq=0状態上のマグノン分散関係に対するジャロシンスキー-守谷ベクトルの方向の影響	福元 好志	東京理科大学	Impact of direction of the Dzyaloshinskii-Moriya vector on the magnon dispersion of the q=0 state in Kagome-lattice systems	Fukumoto Yoshiyuki	Tokyo University of Science
81	2023-Ba-0049	機械学習による相図予測手法開発	田村 亮	国立研究開発法人 物質・材料研究機構	Development of prediction method for phase diagrams by machine learning	Ryo Tamura	National Institute for Materials Science
82	2023-Bb-0016	空気分子含有水から成長する水結晶形の大規模分子動力学シミュレーション研究	灘 浩樹	鳥取大学	A Large-Scale Molecular Dynamics Simulation Study on the Shape of an Ice Crystal Grown from Water Including Air Molecules	Hiroki Nada	Tottori University
83	2023-Bb-0022	ハイゼンベルグ反強磁性体のスピノン演算子表示に基づく動的構造因子の数値的研究	福元 好志	東京理科大学	Numerical study of dynamical structure factors based on spinon operator representation of Heisenberg antiferromagnets	Fukumoto Yoshiyuki	Tokyo University of Science
84	2023-Ba-0043	機械学習を援用した適切な変換や射影の探索	道下 佳寛	理化学研究所	Machine-Learning-Assisted Exploration of Appropriate Transformation and Projections	Yoshihiro Michishita	Riken
85	2023-Ba-0020	転移学習を利用した不完全結晶構造超伝導体の転移温度予測	上原 政智	横浜国立大学	Prediction of Transition Temperatures for Superconductors with Imperfect Crystal Structures Using Transition Learning	Masatomo Uehara	Yokohama National University
86	2023-Ba-0027	非球形微粒子系における構造形成	寺尾 貴道	岐阜大学工学部	Structural formation of non-spherical colloidal particles	Takamichi Terao	Faculty of Engineering, Gifu University
87	2023-Bb-0014	深層学習による超伝導体転移温度予測とモデル解析によるフォノン状態密度推定	上原 政智	横浜国立大学	Superconductor transition temperature prediction by deep learning and phonon density of states estimation by model analysis	Masatomo Uehara	Yokohama National University
88	2023-Bb-0030	対称性のある測定下の量子系におけるダイナミクス	藤 陽平	東京大学工学系研究科物理学専攻	Dynamics of monitored quantum systems with symmetry	Yohei Fuji	Department of Applied Physics, University of Tokyo
89	2023-Bb-0027	局在電子・格子結合系の光誘起量子もつれ生成ダイナミクス	石田 邦夫	宇都宮大学工学部	Dynamics of photoinduced entanglement generation in electron-phonon systems	Kunio Ishida	School of Engineering, Utsunomiya University
90	2023-Ba-0018	量子スピン系の有限温度計算	森田 克洋	東京理科大学	Finite temperature calculations of quantum spin systems	Katsuhiko Morita	Tokyo university of science
91	2023-Ba-0044	反応力場を用いた蓄電固体ホモ・ヘテロ界面の分子動力学解析	小林 亮	名古屋工業大学	Molecular dynamics analyses of electrode-electrolyte interfaces using reactive potentials	Ryo Kobayashi	Nagoya Institute of Technology
92	2023-Bb-0005	空間構造をもつ一次元量子スピン系の数値的研究	利根川 孝	神戸大学大学院理学研究科	Numerical Study of the One-Dimensional Quantum Spin Systems	Takashi Tonegawa	Graduate School of Science, Kobe University
93	2023-Ba-0046	2次元ハバード型における多重Q秩序	内田 尚志	北海道科学大学	Multiple-Q orders in two-dimensional Hubbard models	Takashi Uchida	Hokkaido University of Science
94	2023-Ba-0040	ナノカーボン積層構造の分子動力学	小林 慶裕	大阪大学大学院工学研究科	Molecular dynamics simulation of nanocarbon stacking structure	Yoshihiro Kobayashi	Graduate School of Engineering, Osaka University
95	2023-Ba-0008	固有値ソルバの統合的インターフェースRokkoの開発と量子スピン系への応用	坂下 達哉	東京大学 理学系研究科	Development of integrated interface of eigensolvers Rokko and application to quantum spin systems	Tatsuya Sakashita	Graduate School of Science, The University of Tokyo
96	2023-Bb-0003	固有値ソルバの統合的インターフェースRokkoの開発と量子スピン系への応用	坂下 達哉	東京大学 理学系研究科	Development of integrated interface of eigensolvers Rokko and application to quantum spin systems	Tatsuya Sakashita	Graduate School of Science, The University of Tokyo
97	2023-A-0002	TiO2表面触媒の研究	李 艶君	大阪大学	Study of TiO2 surface catalysis	YanJun Li	Osaka University
98	2023-A-0011	スパースモデリングを用いた運動量密度の再構成手法の開発	櫻井 浩	群馬大学	Development of method for reconstruction of momentum density with a sparse modeling	Hiroshi Sakurai	Gunma University
99	2023-A-0018	Hyperuniform glass	ワン インチャオ	東京大学 先端科学技術研究センター	Hyperuniform glass	Yinqiao Wang	University of Tokyo, RCAST
100	2023-A-0019	粘着粒子系の圧縮降伏過程におけるボアの連結性の役割	館野 道雄	東京大学 先端科学技術研究センター	Impact of pore morphology on compressive yielding in sticky spheres	Michio Tateno	Research Center for Advanced Science and Technology, The University of Tokyo
101	2023-A-0020	ソフトマターの流体力学シミュレーション	ユアン ジャアシン	先端科学技術研究センター	Hydrodynamic Simulations of Soft Matter	Jiaxing Yuan	Research Center for Advanced Science and Technology, The University of Tokyo
102	2023-A-0023	MD-FEM連成解析手法の開発	村松 真由	慶應義塾大学	Development of a MD-FEM Coupling Analysis Method	Mayu Muramatsu	Keio University

## 2023年度 CCMSスパコン共用事業枠課題一覧 / Supercomputing Consortium for Computational Materials Science Project List of Supercomputer System 2023

※共同利用ではなく共用事業の実施課題一覧。所属は申請時のデータ

## 前期課題

No.	課題名	氏名	所属	Title	Name	Organization
1	第一原理計算による可視光型水素発生半導体光触媒の理論的研究	天能 精一郎	神戸大学大学院	Theoretical study of visible-light hydrogen-evolution semiconductor photocatalysts using first-principles calculations	Seiichiro Ten-no	Kobe University
2	KKRグリーン関数法を用いた磁性材料マップの作成	福島 鉄也	東京大学	Creating of magnetic material maps by KKR Green's function method	Tetsuya Fukushima	University of Tokyo
3	第一原理計算による磁性材料の研究	三宅 隆	産業技術総合研究所	First-principles study of magnetic materials	Takashi Miyake	National Institute of Advanced Industrial Science and Technology
4	計算機主導の新規高誘電率材料の探索	森分 博紀	ファインセラミックスセンター/ 東京工業大学	Computational Exploring of Novel high permittivity Materials	Hiroki Moriwake	Japan Fine Ceramics Center/Tokyo Institute of Technology
5	水素が構造材料の力学物性に与える影響の原子論的解析とデータ創出	尾方 成信	大阪大学	Atomistic analysis of hydrogen impact on mechanical properties of structural material and database construction	Shigenobu Ogata	Osaka University
6	計算機主導の新規強誘電性材料の探索	設楽 一希	ファインセラミックスセンター	Computational Exploring of Novel Ferroelectric Materials	Kazuki Shitara	Japan Fine Ceramics Center
7	全原子モデル自由エネルギー計算によるポリペプチドの溶媒溶解性の系統的評価	松林 伸幸	大阪大学大学院	Systematic evaluation of solubility of polypeptides in solvents by free energy calculation method using all-atom model	Nobuyuki Matubayasi	Osaka University
8	核の量子効果を含む第一原理シミュレーションによる燃料電池材料中でのプロトン移動に関する研究	島崎 智実	横浜市立大学	Theoretical study on proton transfer in fuel cell material based on first-principles method with nuclear quantum effect	Tomomi Shimazaki	Yokohama City University

## 後期課題

No.	課題名	氏名	所属	Title	Name	Organization
1	KKRグリーン関数法を用いた磁性材料マップの作成	福島 鉄也	産業技術総合研究所	Creating of magnetic material maps by KKR Green's function method	Tetsuya Fukushima	National Institute of Advanced Industrial Science and Technology
2	データ駆動手法による高誘電率材料開発	森分 博紀	ファインセラミックスセンター	Data-driven Exploration of High Dielectric Constant Materials	Hiroki Moriwake	Japan Fine Ceramics Center
3	大規模電子状態計算とデータ駆動手法による強誘電材料開発	設楽 一希	ファインセラミックスセンター	Computational and Data-driven Exploration of Ferroelectric Materials	Kazuki Shitara	Japan Fine Ceramics Center
4	磁性不規則合金のフォノン計算手法開発	大久保 忠勝	物質・材料研究機構	Phonon-calculation method for magnetic random alloys	Tadakatsu Ohkubo	National Institute for Materials Science

The Institute for Solid State Physics (ISSP), The University of Tokyo

---

Address 5-1-5 Kashiwanoha, Kashiwa, Chiba, 277-8581, Japan

Phone +81-4-7136-3207

Home Page <https://www.issp.u-tokyo.ac.jp>